

***PLANT-MEDIATED SYNTHESIS OF ZINC OXIDE NANOPARTICLES
USING EXTRACTS AND ISOLATED COMPOUNDS FROM SENECIO
SERRATULOIDES AND THEIR BIOLOGICAL ACTIVITY***


BY

NONHLANHLA JOYISA

2018

**Submitted in fulfilment of the academic requirements for the degree of Master of
Science in the School of Chemistry and Physics at the University of KwaZulu-Natal,
Durban**

**As the candidate's supervisor and co-supervisor, I have approved this dissertation for
submission**

Signed:  _____

Name: Dr Roshila Moodley

Date: 3/9/2018

Signed:  _____

Name: Dr Karin Pruessner

Date: 3/9/2018

ABSTRACT

Senecio serratuloides DC of the Asteraceae family is a medicinal plant used in South African traditional medicine for the treatment of skin diseases, sexually transmitted infections (STIs) and wounds. Despite the ethnomedicinal significance of the plant, a phytochemical investigation to determine the active components for future pharmacological developments has not been conducted. Nanotechnology is a promising field in the development of biocompatible metal nanoparticles from bio-resources. Zinc oxide nanoparticles (ZnONPs) are of great interest due to their wide range of applications in the field of biomedical sciences. Research on the exploitation of plant materials for the green synthesis of nanoparticles is increasing rapidly. The aim of this study was therefore to extract, isolate and identify secondary metabolites from *S. serratuloides*, to use the extracts and isolates as reducing agents in the synthesis of zinc oxide nanoparticles, and to compare the antioxidant, antibacterial and anti-quorum sensing activities of extracts, isolated compounds, freestanding and plant-derived zinc oxide nanoparticles.

The phytochemical investigation yielded one sesquiterpene (farnesylamine), five triterpenoids (sitosterol, α - and β -amyrin, stigmasterol and taraxerone) and two jacaranones (jacaranone and a mixture of jacaranone and methyl-2-(1-hydroxy-4-oxocyclohexyl)acetate). The synthesised zinc oxide nanoparticles were characterised using spectroscopic and microscopic techniques. Spherical zinc oxide nanoparticles were successfully synthesised but exhibited a wide size range. ZnONPs synthesised using jacaranones showed good antioxidant activity whilst ZnONPs synthesised using extracts of *S. serratuloides* showed moderate antioxidant activity.

The extracts, phytocompounds and nanoparticles were tested for antibacterial activity against three Gram-positive bacteria (*Pseudomonas aeruginosa*, *Staphylococcus aureus* and *Enterococcus faecalis*) and two Gram-negative bacteria (*Escherichia coli* and *Chromobacterium violaceum*). The extracts demonstrated promising antibacterial activity

against *Chromobacterium violaceum*. Amongst the isolated phytochemicals, jacaranones showed promising antibacterial activity against two Gram-positive bacteria, *Staphylococcus aureus* and *Enterococcus faecalis*, with good antibacterial activity against *Chromobacterium violaceum*. Nanoparticles did not possess antibacterial activity.

The isolated jacaranone, extracts and nanoparticles were further evaluated for quorum sensing inhibitory activity using a qualitative agar-overlay assay. The extracts showed promising anti-quorum sensing activity whilst the jacaranone showed good anti-quorum sensing activity. Nanoparticles did not show anti-quorum sensing activity. This can be attributed to freestanding nanoparticles not possessing activity against the bacterial strains tested and in plant-derived nanoparticles, the amount of the active compound capping particles could be too little to impart activity.

DECLARATION – PLAGIARISM

I, Nonhlanhla Joyisa declare that

1. The research reported in this thesis, except where otherwise indicated, is my original research.
2. This thesis has not been submitted for any degree or examination at any other university
3. This thesis does not contain other person/s data, pictures, graphs or other information, unless specifically acknowledged as being sourced from the other person/s.
4. This thesis does not contain other person/s writing, unless specifically acknowledged as being sourced from other researcher/s. Where other written sources have been quoted, then:
5. Their words have been re-written but the general information attributed to them has been referenced.
6. Where their exact words have been used, then their writing has been placed in italics and/or inside quotation marks, and referenced.
7. This thesis does not contain text, graphics or tables copied and pasted from the internet, unless specifically acknowledged, and the source being detailed in the thesis in the Reference section.

Signed: _____

PREFACE

The experimental work described in this thesis was carried out in the School of Chemistry and Physics at the University of KwaZulu-Natal, Durban, from June 2016 to February 2018 under the supervision of Dr Roshila Moodley and Dr Karin Pruessner.

These studies present original work by the author and have not otherwise been submitted in any form for any degree or diploma to any tertiary institution. Where use has been made of the work of others, it is duly acknowledged in the text.

Signed: _____

Name: _____

Date: _____

DEDICATION

Nothing in life can prepare us for the death of the loved one. Whether death results from a sudden accident or a sustained illness, it always catches us off-guard. I dedicate this study to the loving memory of my younger brother, Nhlakanipho Joyisa.

Revelation 21: 4

ACKNOWLEDGEMENTS

Firstly, I would like to thank God, Almighty for His guidance. I would also like to thank my family especially my mother, Thandazile Petronella Joyisa, my father, Vusumuzi David Mthembu, my grandmother, Fikelephi Alzinah Joyisa, my brother, Kwanele Ndudla Joyisa, and my favourite uncle, Wonder Joyisa, for their prayers, motivation and encouragement.

I would also like to convey my sincere appreciation to my supervisors, Dr R Moodley and Dr K Pruessner, who suggested the topic, helped me conceptualize it and reach the successful completion of this dissertation. I would also like to thank my mentor, Dr Nomfundo Mahlangeni, for continuous support throughout my research, for the knowledge and wisdom I gained from her expertise and her sacrificial giving of her time to the research.

I would also like to acknowledge the following individuals and organizations

- Dr. H. Y. Chenia and Farzana Mohamed, Discipline of Microbiology, for guiding me through the antimicrobial testing
- The technical team in the School of Chemistry and Physics at UKZN, Westville for their assistance
- Microscopy and microanalysis unit team for their equipment
- My colleagues in the natural products research group for moral support
- All my friends: Nyameka Diko, Nontokozo Msomi, Nelisiwe Shoji, Slungile Mhlongo, Andiswa Ntshela and Nomfundo Gabuza
- National Research Foundation (NRF) for financial support.

Lastly, I would like to specially thank my girlfriend, Lindiwe Noluthando Nkabane, for her love, encouragement and support.

Table of Contents

ABSTRACT.....	ii
DECLARATION – PLAGIARISM.....	iv
PREFACE.....	v
DEDICATION.....	vi
ACKNOWLEDGEMENTS.....	vii
ABBREVIATIONS.....	xi
LIST OF FIGURES.....	xiii
LIST OF TABLES.....	xv
CHAPTER ONE.....	1
1.1 Introduction.....	1
1.2 Problem Statement.....	3
1.3 Aims and Objectives of the Study.....	5
1.4 Outline of the Research Presented in this Thesis.....	6
CHAPTER 2.....	7
LITERATURE REVIEW.....	7
2.1 Use of Medicinal Plants in the Treatment of Skin Diseases.....	7
2.2 Pharmacological Activities of Medicinal Plants Applied to Skin Care.....	8
2.3 The Asteraceae Plant Family.....	9
2.3.1 The genus <i>Senecio</i>	10
2.3.2 <i>Senecio serratuloides</i> DC.....	10
2.4 Phytochemicals of <i>Senecio</i> Species.....	12
2.4.1 Flavonoids.....	13
2.4.2 Alkaloids.....	14
2.4.3 Triterpenoids.....	15
2.5 Introduction to Nanoparticles.....	15
2.5.1 Synthesis of nanoparticles.....	16
2.5.2 The physico-chemical synthesis of nanoparticles.....	18
2.5.3 Biological synthesis of nanoparticles.....	18
2.5.3.1 Medicinal plants used in the synthesis of nanoparticles.....	19
2.5.3.2 Phytochemicals used in the synthesis of nanoparticles.....	21
2.6.1 Phytochemical characterisation techniques.....	23
2.6.2 Chromatographic techniques.....	23
2.6.2.1 Thin-layer chromatography (TLC).....	24

2.6.2.2 Column chromatography (CC).....	24
2.6.3 Spectroscopic techniques	24
2.6.3.1 Fourier-transform infrared spectroscopy (FTIR)	25
2.6.3.2 Gas chromatography-mass spectrometry (GC-MS).....	25
2.6.3.3 Nuclear magnetic resonance (NMR) spectroscopy	26
2.7 Characterisation of Nanoparticles	27
2.7.1 Ultraviolet-visible (UV-Vis) spectroscopy	27
2.7.2 Powder X-ray diffraction (XRD)	28
2.7.3 Scanning electron microscopy (SEM) and energy-dispersive X-ray spectroscopy (EDX).....	30
2.8 Conventional Transmission Electron Microscopy (TEM)	31
2.8.1 Imaging in transmission electron microscopy (TEM).....	31
2.8.2 Selected area electron diffraction (SAED).....	33
2.9 Analytical Electron Microscopy (AEM)	34
2.10 Scanning Transmission Electron Microscopy (STEM)	35
2.11 Biological Activity	35
2.11.1 Antioxidant activity.....	36
2.11.3 Anti-quorum sensing activity	38
CHAPTER THREE	41
MATERIALS AND METHODS.....	41
3.1 Phytochemical Analysis of <i>Senecio serratuloides</i>	41
3.1.1 Collection of plant material.....	41
3.1.2 Extraction, isolation and purification of phytochemicals	41
3.1.3 Spectroscopic characterisation of extracted phytochemicals.....	43
3.2 Synthesis of zinc oxide nanoparticles (ZnONPs).....	44
3.2.1. Synthesis of freestanding zinc oxide nanoparticles (ZnONPs) using chemical synthesis	44
3.2.2. Synthesis of zinc oxide nanoparticles (ZnONPs) using plant material.....	45
3.3 Characterisation of Zinc Oxide Nanoparticles (ZnONPs)	45
3.3.1 Ultraviolet-visible (UV-Vis) spectroscopy and infrared (IR) spectroscopy	45
3.3.2 Scanning electron microscopy (SEM).....	46
3.3.3 X-ray diffraction (XRD).....	46
3.3.4 Transmission electron microscopy (TEM).....	46
3.4. Antioxidant activity.....	47
3.5 Antimicrobial Activity	47

3.5.1 Antibacterial activity	48
3.5.2 Quorum sensing inhibition (QSI) – agar overlay assay	48
CHAPTER FOUR.....	50
RESULTS AND DISCUSSION	50
4.1. Spectroscopic Data of Compounds	50
4.1.1 Identification of secondary metabolites isolated from <i>Senecio serratuloides</i>	53
4.2 Characterisation of Nanoparticles	57
4.2.1 Ultraviolet-visible (UV-Vis) spectroscopy	57
4.2.2 Fourier-transform infrared (FT-IR) spectroscopy	58
4.2.3 X-ray diffraction (XRD).....	59
4.2.4 Scanning electron microscopy (SEM).....	61
4.2.5 Transmission electron microscopy (TEM).....	63
4.3. Antioxidant Activity (DPPH Assay)	76
4.4 Antibacterial Activity	77
4.5 Anti-Quorum Sensing Activity	80
CHAPTER FIVE	83
SUMMARY AND CONCLUSIONS	83
RECOMMENDATIONS FOR FURTHER STUDY.....	84
REFERENCES	85
APPENDICES.....	105

ABBREVIATIONS

^{13}C -NMR	Carbon-13 nuclear magnetic resonance spectroscopy
^1H -NMR	proton nuclear magnetic resonance spectroscopy
CC	Column chromatography
COSY	Correlation spectroscopy
d	Doublet
DCM	Dichloromethane
dd	Doublet of doublets
DEPT	Distortionless enhancement by polarization transfer
DPPH	2,2-diphenyl-1-picrylhydrazyl
EDX	Energy-dispersive X-ray spectroscopy
EIMS	Electron impact mass spectroscopy
EtOAc	Ethyl acetate
FTIR	Fourier-transform infrared spectroscopy
GC-MS	Gas chromatography-mass spectrometry
HMBC	Heteronuclear multiple bond correlation
HRMS	High resolution mass spectroscopy
HSQC	Heteronuclear single quantum coherence
Hz	Hertz
IR	Infrared

m	Multiplet
MeOH	Methanol
NPs	Nanoparticles
QSI	Quorum sensing inhibition
s	Singlet
SAED	Selected area electron diffraction
SEM	Scanning electron microscopy
t	Triplet
TEM	Transmission electron microscopy
TLC	Thin layer chromatography
UV	Ultraviolet
XRD	X-ray diffraction

LIST OF FIGURES

Figure 2.1: Distribution of <i>Senecio serratuloides</i> DC in South Africa.....	11
Figure 2.2: <i>Senecio serratuloides</i> DC flowering plant	11
Figure 2.3: Basic structure of jacaranone	13
Figure 2.4: Chemical structure of pyrrolizidine alkaloid.....	14
Figure 2.5: Chemical structure of a pentacyclic triterpenoid.....	15
Figure 2.6: Techniques used in the synthesis of nanoparticles	17
Figure 2.7: Ultraviolet-visible spectrophotometer	28
Figure 2.8: Components of a powder X-ray diffractometer in θ -2 θ configuration.....	29
Figure 2.9: Principal design of a scanning electron microscope (SEM).....	31
Figure 2.10: Principal design of a transmission electron microscope	32
Figure 2.11: Beam path for imaging and SAED in the TEM and selected area electron pattern.	34
Figure 2.12: A typical quorum sensing system in Gram-negative bacteria.....	39
Figure 4.1: Chemical structures of compounds isolated from <i>Senecio serratuloides</i>	56
Figure 4.2: UV-Vis spectra of ZnONPs produced from aqueous and methanolic extracts of <i>S. serratuloides</i> as well as compound 6 (jacaranone), compound 7 (jacaranone and methyl-2-(1- hydroxy-4-oxocyclohexyl)acetate) and freestanding ZnONPs.....	57
Figure 4.3: FT-IR spectra of ZnO nanoparticles.....	59
Figure 4.4: XRD patterns of ZnONPs synthesised using aqueous extract (A), methanolic extract (B), the mixture of jacaranones (C) and jacaranone (D).....	60
Figure 4.5: SEM images of ZnONPs synthesised from aqueous extract (A), methanolic extract (B), jacaranone mixture (C), pure jacaranone (D) and freestanding ZnONPs (E).....	62
Figure 4.6: TEM images of freestanding ZnONPs	63
Figure 4.7: TEM images at low magnification and particle size distribution of ZnONPs	64
Figure 4.8: TEM images (a) low magnification (b) high magnification (inset SAED pattern) of ZnONPs synthesised with aqueous extract.....	66
Figure 4.9: Energy dispersive X-ray spectrum of ZnONPs synthesised from aqueous extract	67
Figure 4.10: TEM images (a) low magnification (b) high magnification (inset SAED pattern) of ZnONPs synthesised with methanolic extract	68
Figure 4.11: Energy-dispersive X-ray spectrum of ZnONPs synthesised from methanolic extract.....	69
Figure 4.12: TEM images (a) low magnification (b) high magnification (inset SAED pattern) of ZnONPs synthesised from the mixture of jacaranones	70
Figure 4.13: Energy dispersive X-ray spectrum of ZnONPs synthesised from the mixture of jacaranones.....	71
Figure 4.14: TEM images (a) low magnification (b) high magnification (inset SAED pattern) of ZnONPs synthesised from pure jacaranone.....	72
Figure 4.15: Energy dispersive X-ray spectrum of ZnONPs synthesised from pure jacaranone	73
Figure 4.16: TEM images (a) low magnification (b) high magnification (inset SAED pattern) of freestanding ZnONPs	74
Figure 4.17: Energy dispersive X-ray spectrum of freestanding ZnONP.....	75
Figure 4.18: Antioxidant activity of ZnONPs synthesised from the aqueous extract, methanolic extract, compound 6 (jacaranone) and compound 7 (mixture of jacaranones) by the DPPH radical scavenging assay	77

Figure 4.19: The quorum sensing inhibitory effect of the ZnONPs, compounds and crude extracts of <i>S .serratuloides</i> at 250 and 500 μ m.....	81
Figure 4.20: The quorum sensning inhibitory effect of the ZnO nanoparticles ((ZnONPs)....	82

LIST OF TABLES

Table 2.1: Traditional use of medicinal plants in skin care	8
Table 2.2: Phytocompounds used to synthesise nanoparticles and their biological activity ...	21
Table 4.1: Calculated d-spacing values using Braggs Law, $\lambda = 2.d \sin\theta$	61
Table 4.2: Antibacterial susceptibility profile of selected gram positive and gram-negative bacteria upon exposure to <i>S. serratuloides</i> phytocompounds, crude extracts and ZnONPs	79

CHAPTER ONE

1.1 Introduction

Traditional medicine is used globally to treat various ailments, and about 80 % of the people in African countries use traditional medicine to meet their primary health care needs (Oyebode *et al.*, 2016). Since ancient times, rural communities have relied on traditional medicine to treat a wide spectrum of diseases including infectious diseases. Most of these traditional remedies are still in use today, for example, the use of *Carica papaya* (pawpaw), *Arctostaphylos uva ursi* (bearberry) and *Vaccinium macrocarpon* (cranberry) to treat urinary infections (Head, 2008). Many common plants have medicinal value and are used for the treatment of various ailments, from skin to heart conditions, arthritis and infections. Examples of these plant species include *Aloe ferox* (bitter aloe), *Boophone disticha* (bushman poison), *Datura stramonium* (thornapple), *Harpagophytum procumbens* (devil's claw), *Hypericum perforatum* (St John's wort), *Sutherlandia frutescens* (cancer bush) and *Cinnamomum camphora* (camphor tree) (Chelliah, 2008, Cordier and Steenkamp, 2018, Reid *et al.*, 2018, Mavimbela *et al.*, 2018, Barnes *et al.*, 2018, Bano *et al.*, 2018).

These medicinal plants are also gaining popularity in western societies since the movement from synthetic to more natural sources of commercial products. The use of plants for medicinal purposes necessitates the isolation and identification of the active compounds which impart medicinal effects and the exploitation of their properties for other benefits. These active components, known as secondary metabolites, are organic compounds that are not crucial for growth and development of the plant but are required for the plant to survive in its environment (Scharf *et al.*, 2014). To date, over 100 000 secondary metabolites from plants have been isolated and characterised. Some have been implemented as active ingredients in commonly

used medications, and some have been used as starting materials in drug development (Rates, 2001). About 50 % of drugs that are clinically used in the world are derived from natural products and their derivatives, with 25 % being from higher plants (McChesney *et al.*, 2007). Common plant-derived drugs include Aspirin, which is a synthetic analogue of salicylic acid that was first isolated from the willow bark (Salicaceae) and caffeine, a stimulant which occurs naturally in *Coffea arabica* (Rubiaceae). Morphine is an analgesic that was initially isolated from *Papaver somniferum* (Papaveraceae). Taxol is a cancer chemotherapeutic agent which was extracted from *Taxus brevifolia* (Taxaceae). Quinine is used for malaria prophylaxis and was originally isolated from *Cinchona officinalis* (Rubiaceae). Betulinic acid is an anti-HIV compound isolated from the leaves of *Syzygium claviflorum* (Myrtaceae) (Ashihara and Crozier, 2001, Mahdi *et al.*, 2006, Weid *et al.*, 2004, Cragg and Newman, 2005, Bharadwaj *et al.*, 2018, Khan, 2017). These drugs are still commercially available and in use today.

The antibacterial activity of extracts and compounds isolated from various medicinal plants has been reported. Compounds belonging to different classes such as alkaloids, triterpenoids, flavonoids, phenolic acids, sterols, tannins, saponins and coumarins have been reported to possess antibacterial activity against a variety of pathogenic bacterial (Elisha *et al.*, 2017, Rekha *et al.*, 2017). Plant-derived drugs and secondary metabolites have the ability to either kill bacterial cells or prevent bacterial growth by targeting essential biochemical processes. However, the killing and inhibition of growth of bacterial cells is not enough since most diseases are mediated by quorum sensing (QS). Quorum sensing is a cell-to-cell communication pathway that enables bacterial populations to re-programme gene expression in a coordinated manner as a response to cell density (Adonizio *et al.*, 2006).

Currently, researchers and scientists are searching for novel plant-based compounds with mechanisms to inhibit bacterial cells from communicating with each other and coordinating their behaviour. This is also a consequence of the spreading of multi-drug resistant organisms.

Flavonoids isolated from medicinal plants such as *Psidium guajava* (Myrtaceae), *Senegalia nigrescens* (Fabaceae) and *Combretum albiflorum* (Combretaceae) have been reported to exhibit quorum sensing inhibition (Vasavi *et al.*, 2014, Bodede *et al.*, 2018, Vandeputte *et al.*, 2010).

Plant extracts and secondary metabolites from medicinal plants have also been exploited in the synthesis of nanoparticles as more cost-effective and eco-friendly reducing agents compared to toxic chemicals used in traditional chemical synthesis. It has been demonstrated that plant secondary metabolites such as terpenoids, alkaloids and flavonoids play an important role in the reduction of metal ions in solution to form nanoparticles and in stabilising them, i.e. decreasing or preventing agglomeration. The plant-mediated synthesis of gold (Au), silver (Ag), copper (Cu), selenium (Se), iron oxide (Fe₃O₄) and zinc(II) oxide (ZnO) nanoparticles has been reported (Kuppusamy *et al.*, 2016). Flavonoids such as quercetin, epicatechin, catechin, kaempferol and genistein have been used in the synthesis of gold and silver nanoparticles with particle sizes ranging from 10-70 nm (Satyavani *et al.*, 2011, Mittal *et al.*, 2014a, Raghavan *et al.*, 2015a). Since certain nanoparticles are also known to have biological activity such as antioxidant, antibacterial, anti-quorum sensing or antifungal activity, plant-derived nanoparticles have the potential to show even better activity due to synergistic effects.

1.2 Problem Statement

Skin diseases are among the common diseases in the world. The occurrence of skin diseases has increased over the years because of their association with Human Immunodeficiency Virus (HIV), Acquired Immune Deficiency Syndrome (AIDS) and diabetes mellitus (De Wet *et al.*, 2013). The dependence of rural communities on traditional remedies and medicinal plants for the treatment of skin diseases, sexual dysfunction, sexually transmitted infections (STIs) and

wound healing is primarily a function of economic and physical accessibility (Naidoo *et al.*, 2013). This reliance on traditional medicine can result in the decline of natural resources of commonly used medicinal plants (Cunningham, 1993). Therefore, the identification of other natural sources with medicinal benefits is necessary. One such plant is *Senecio serratuloides* DC which belongs in the Asteraceae family, and is commonly used by traditional healers in the treatment of wounds, burns, sores and STIs. No detailed phytochemical studies on *S. serratuloides* have been reported, despite its prominent role in South African traditional medicine.

Green chemistry is a promising field in the development of cost-effective, stable, reproducible, and biocompatible metal nanoparticles from bio-resources. Zinc oxide nanoparticles are of great interest due to their wide range of applications in the field of biomedical sciences, electronics, photocatalysis and optics. They have been reported to have ultraviolet filtering properties, antioxidant, anti-inflammatory, anticancer, antidiabetic and antibacterial properties (Mishra *et al.*, 2017, Patil *et al.*, 2014, Pandimurugan and Thambidurai, 2017, Gutha *et al.*, 2017, Nagajyothi *et al.*, 2015a, Hassan *et al.*, 2017, Rajakumar *et al.*, 2017). They can be used in wound dressings where the beneficial effects also include enhanced wound healing, faster re-epithelization and collagen deposition (Sudheesh Kumar *et al.*, 2012). These nanoparticles are also used in cosmetics such as sunscreens due to their ultraviolet filtering properties (Pandimurugan and Thambidurai, 2017).

Research on the exploitation of plant material for the green synthesis of nanoparticles is increasing rapidly due to its eco-friendliness, simplicity, cost-effectiveness, use of non-toxic chemicals, and one-step synthesis procedure. However, most studies use crude plant extracts containing many unidentified phytochemicals and the beneficial effects of these compounds are poorly understood. The route of utilising pure isolated phytochemicals has been unexplored and underexploited in the synthesis of nanoparticles. In this study, zinc oxide

nanoparticles were synthesised using extracts and pure isolated phytocompounds from the leaves of *S. serratuloides*. Zinc oxide nanoparticles and *S. serratuloides* were chosen due to their known beneficial effects in skin care and wound healing, due to the mechanisms of these properties not yet being understood and to test the hypothesis that synergistic effects might lead to improved properties.

1.3 Aims and Objectives of the Study

The aim of the study is to conduct a phytochemical investigation on the medicinal plant known as *Senecio serratuloides* DC. To determine the origin of the medicinal properties by isolating active compounds. To synthesise and characterise zinc oxide nanoparticle using the extracts and isolated secondary metabolites from the plant. Also, the antibacterial activities of crude plant extracts, secondary metabolites and nanoparticles were evaluated.

The research objectives were:

- To extract and isolate the secondary metabolites from different plants parts of the plants species, *Senecio serratuloides*.
- To isolated, identify and characterise the phytocompounds using spectroscopic techniques such as nuclear magnetic resonance (NMR) spectroscopy, infrared spectroscopy (IR), ultraviolet-visible spectroscopy (UV-Vis), and mass spectrometry (MS).
- To biosynthesise zinc oxide nanoparticles using extracts and secondary metabolites from *Senecio serratuloides* and to characterise these nanoparticles using IR, UV-Vis, X-ray diffraction (XRD), scanning electron microscopy (SEM), transmission electron

microscopy (TEM), energy-dispersive X-ray spectroscopy (EDX) and selected area electron diffraction (SAED).

- To test the crude plant extracts, secondary metabolites and synthesised nanoparticles for their biological activity using suitable assays (antioxidant, antibacterial and anti-quorum sensing).
- To compare the biological activity of plant-derived zinc oxide nanoparticles to freestanding ones, crude plant extracts and isolated phytochemicals.

1.4 Outline of the Research Presented in this Thesis

This thesis contains five chapters starting with Chapter 1 which is the introduction in the preceding section. Chapter 2 is a review of the literature related to this research. Chapter 3 highlights the materials and methods used in the phytochemical analysis of *Senecio serratuloides*, synthesis of nanoparticles and biological testing. Chapter 4 contains the results and discussion of the study. The research conclusions and future recommendations can be found in Chapter 5.

CHAPTER 2

LITERATURE REVIEW

This chapter focuses on the literature related to this research. The plant species, nanoparticles, biological testing and experimental techniques used in this study will be discussed hereunder.

2.1 Use of Medicinal Plants in the Treatment of Skin Diseases

The use of medicinal plants has been found to play a major role in the management and treatment of skin diseases, worldwide, contributing significantly to the primary health care of the population (Quave *et al.*, 2008, Agyare *et al.*, 2009, Abbasi *et al.*, 2010). In less developed and developing countries, traditional medicine is still the predominant means of health care in treating skin disorders (Mabona and Vuuren, 2013, Wyk *et al.*, 2008). African traditional herbalists employ infusion and decoction methods in preparing medicinal plant remedies (Dlova and Ollengo, 2018). A number of medicinal plants used traditionally for the treatment of skin disorders have been documented over the years (Table 2.1).

Table 2.1: Traditional use of medicinal plants in skin care

Scientific name	Family	Ailment	Reference
<i>Bombax buonopozense</i>	Bombacaceae	Decoction of leaves used for the treatment of microbial skin infections.	(Borokini and Omotayo, 2010)
<i>Acalypha wilkesiana</i>	Euphorbiaceae	Leaves are eaten as vegetable to treat skin infections in children.	(Borokini and Omotayo, 2010)
<i>Warburgia salutaris</i>	Canellaceae	Ointments made from pounded leaves and stalks, mixed with bark and fat are used against skin complaints.	(Maroyi, 2013)
<i>Ixillirion tataricum</i>	Amaryllidaceae	Paste made from flowering shoots used to wash skin abscesses and for disinfection of wounds.	(Baharvand-Ahmadi <i>et al.</i> , 2015)
<i>Sanguisorba minor</i>	Rosaceae	Boiled raw fruit is used to disinfect skin wounds.	(Baharvand-Ahmadi <i>et al.</i> , 2015)
<i>Verbascum agrimonifolium</i>	Scropholariaceae	Boiled leaves or flowers used in microbial wound infections.	(Baharvand-Ahmadi <i>et al.</i> , 2015)
<i>Aloe ferox</i>	Aloaceae	Leaves and roots applied topically or taken orally to treat dermatitis, acne, skin cancer, burns and psoriasis.	(Loots <i>et al.</i> , 2007)
<i>Olea europaea L. subsp. africana</i>	Oleaceae	Oil is applied to treat skin damage, such as contact dermatitis, atopic dermatitis, eczema, psoriasis, thermal and radiation burns, and aging.	(Aburjai and Natsheh, 2003)
<i>Terminalia sericea</i>	Combretaceae	Leaves used as an antibiotic for wounds.	(Wyk <i>et al.</i> , 1997)
<i>Ximenia americana</i>	Olacaceae	Crushed roots and sap applied to rashes, ringworm infections and skin ulcers.	(Ogunleye and Ibitoye, 2003)

2.2 Pharmacological Activities of Medicinal Plants Applied to Skin Care

Many environmental factors cause inflammation of the skin; sunlight in particular is a factor responsible for inflammatory skin disorders and skin diseases (Katiyar, 2005). Plants and their secondary metabolites can exhibit biological activities such as antioxidant, anti-inflammatory and anti-tyrosinase activities which are associated with skin care or assist in wound-healing. People in rural communities rely on medicinal plants for their primary health care needs including the treatment of different ailments, skin diseases and wound healing (Rupesh *et al.*, 2011). Antioxidants from plants inhibit the initiation of oxidative reactions and repair or

prevent oxidative damage to the cells of the body (Mohamed *et al.*, 2009). Pharmacological studies have revealed numerous plants with good antioxidant activity including *Acokanthera oppositifolia*, *Aloe ferox*, *Bauhinia bowkeri*, *Sutherlandia frutescens*, *Terminalia sericea* and *Trichilia dregeana* (Lall and Kishore, 2014).

Previous studies have also shown wound healing properties in medicinal plants such as *Grewia occidentalis*, *Terminalia sericea*, *Cissus quadrangularis*, *Ricinus communis*, *Malva parvifolia* and *Gunnera perpensa* (Mabona and Vuuren, 2013). Plants from the Asteraceae family, such as *Bidens pilosa* Linn. and *Bidens bipinnata* Lin, are used by people of the Limpopo Province, South Africa to treat skin diseases and to promote wound healing. These plants were also reported to possess antioxidant and antibacterial activities (Lall and Kishore, 2014, Bartolome *et al.*, 2013).

2.3 The Asteraceae Plant Family

The plant family Asteraceae, also known as composite, aster, daisy or sunflower family, has 1600–1700 genera containing 24000–30000 different species. Many plants in this family are herbaceous, but a significant number are also shrubs, vines or trees. They are characterised by their clusters of yellow flower heads, which appear as a single flower from a distance. Plants in this family are used commercially in the manufacture of many products such as cooking oil, sweetening agents, coffee substitutes, herbal teas and sunflower seeds. The family has a worldwide distribution, from the polar regions to the tropics, colonising a wide variety of habitats (Moreira-Muñoz and Muñoz-Schick, 2007). It is most common in the xeric or arid environments and in lower temperature latitudes. The genus *Senecio* is one of the largest flowering plants of this family (Moreira-Muñoz and Muñoz-Schick, 2007).

2.3.1 The genus *Senecio*

The genus *Senecio* comprises about 1100 species, often used in Asia, South America and Africa as a food source and in traditional medicine as ‘bush teas’ (Barnes *et al.*, 2007), anti-emetics and anti-inflammatories (Ali *et al.*, 2018). Other traditional uses may include the treatment of amenorrhoea, menopausal neurosis, leucorrhoea, flu, diarrhoea, eczema, asthma, bronchitis, blood purification for skin eruptions, stomach ache and burns (Kumar and Mathela, 2018).

The species are known to produce secondary metabolites including alkaloids, saponins, sesquiterpenoids, phenols, flavonoids and semiquinones (Mandi’c *et al.*, 2011). The genus is particularly known for its pyrrolizidine alkaloid constituents (Barnes *et al.*, 2007). This makes the species very interesting for further phytochemical investigations and leads for future drug development.

2.3.2 *Senecio serratuloides* DC

Senecio serratuloides DC, also known as the “two day cure” or “umsukumbili” in isiZulu, is one of the popular medicinal plants from the genus *Senecio* (Gould *et al.*, 2015). It is widespread throughout South Africa (Fig 2.1) including the Eastern Cape, KwaZulu-Natal and Limpopo (Wet and Ngubane, 2014). *Senecio serratuloides* is a small tree or woody herb that grows up to a meter high with leaves up to 60 mm long with serrated margins. It is easily recognised by its small dark yellow flowers (Fig 2.2) and inhabits sandstone slopes in grasslands (Abbott *et al.*, 2009).

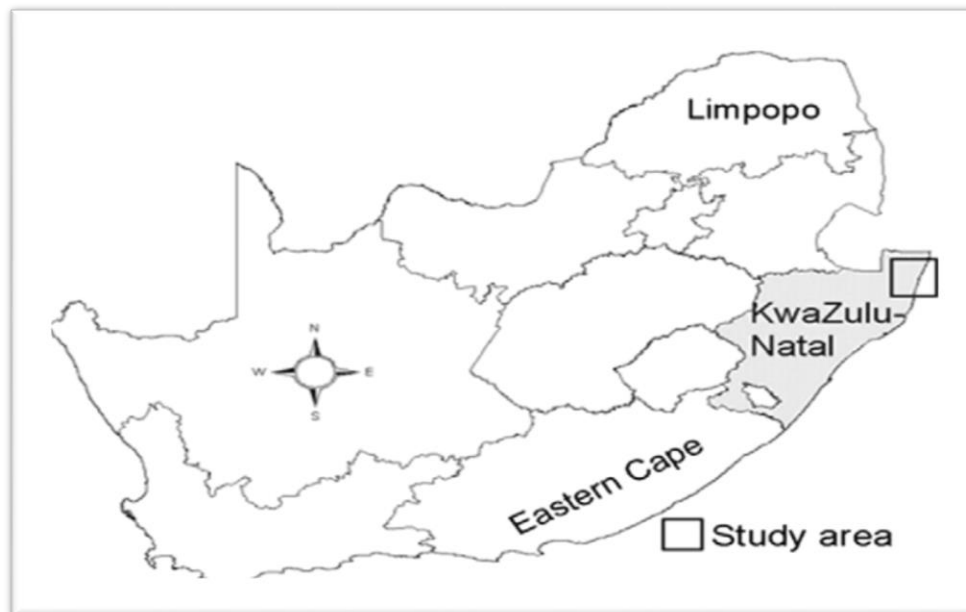


Figure 2.1: Distribution of *Senecio serratuloides* DC in South Africa



Figure 2.2: *Senecio serratuloides* DC flowering plant

Senecio serratuloides has a wide variety of applications in traditional medicine. Freshly dried and burnt leaves are applied directly on the affected area to aid wound healing (Gould, 2015). Crushed leaves are used to heal sores, cuts and burns (Kuete, 2014b). Powdered leaves are used to treat swollen gums and chest pains (Fawole *et al.*, 2010a). A hot water infusion of the leaves is taken orally to treat swelling and headaches (Taylor *et al.*, 2003). A boiled mixture of leaves the and *Hypoxis hemerocallide* (corn) is used to cure internal and external sores of sexually transmitted infections (STIs) such as gonorrhoea (De Wet *et al.*, 2012). The rural communities of Northern Maputaland use the heated leaves of *Ranunculus multifidus* with the whole plant of *S. serratuloides* to cleanse the blood during pregnancy, infertility and to ease labour pains (de Wet and Ngubane, 2014). The extracts of *S. serratuloides* leaves were reported to possess anti-inflammatory, antioxidant, anticholinesterase, anticancer and antifungal activities (Fawole *et al.*, 2010a, Kuete, 2014a, Madzinga *et al.*, 2018).

2.4 Phytocompounds of *Senecio* Species

Living organisms produce a variety of chemical substances that are termed natural products and can be divided into primary metabolites and secondary metabolites. Primary metabolites are common to all life forms. In addition, medicinal plants produce compounds which are less widely distributed known as secondary metabolites. These secondary metabolites have particular functions such as defence against predators hence their pharmacological action that can be used for medicinal purposes (Barnes *et al.*, 2007). Among the most prevalent of secondary metabolites are alkaloids, terpenoids and phenols (Saxena *et al.*, 2013). In the *Senecio* species, secondary metabolites include jacaranones (Arias *et al.*, 2017b), alkaloids, flavones (Wang *et al.*, 2013) and terpenes (Kumar and Mathela, 2018). In the Himalayan region, numerous *Senecio* species have been reported to have constituents such as

eudesmolides, germacrene D, β -pinene, β -caryophyllene, β -longipinene, cuprenene, zingiberene, curcumene and carotol (Kumar and Mathela, 2018).

2.4.1 Jacaranones

Jacaranones are organic compound with the formula $C_9H_{10}O_4$; it is a derivative of benzoquinone with a hydroxyl group and methyl ester. It is easily identified with bright yellow crystals. Jacaranones are a class of secondary metabolites exhibiting pharmacological and biological activities. The methanolic extracts from the plant *Jacaranda caucana* (Bignoniaceae) were found to have activity against P-388 lymphocytic leukemia. The compound responsible for the activity is a benzoquinone called jacaranone (Fig 2.3) (Ogura *et al.*, 1976). Since then, this compound has been isolated from numerous species belonging to the family Asteraceae (Jakupovic *et al.*, 1987, Mandić *et al.*, 2011, Wang *et al.*, 2013). Jacaranones that have been isolated from the genus *Senecio* include jacaranone glucoside (Tian *et al.*, 2009, Tian *et al.*, 2006), jacaranone ethyl ester, jacaranone methyl ester, and senecio lactone (Tian *et al.*, 2009).

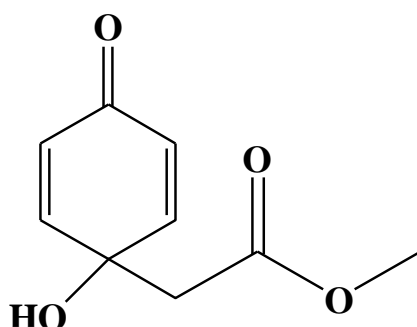


Figure 2.3: Basic structure of jacaranone

2.4.2 Alkaloids

Alkaloids (Fig 2.4) are compounds of low molecular weight which form approximately 20% of all plant based secondary metabolites (Kauri and Arora, 2015), thus making them the largest secondary metabolite class with 5500 known alkaloids. Alkaloids are usually colourless with a bitter taste (Harborne, 1973). They contain heterocyclic nitrogen atoms (Saxena *et al.*, 2013). The numerous classes of alkaloids include isoquinoline, quinolone, pyridine-piperidine and pyrrolidine-pyridine. Alkaloids were first isolated from medicinal plants in the nineteenth century. These compounds together with their synthetic derivatives are used as basic medicinal agents for their bactericidal, antispasmodic and analgesic effects (Stary, 1998). Numerous species in the genus *Senecio* are rich in pyrrolizidine alkaloids exhibiting carcinogenic, hepatotoxic, antitumor and mutagenic activities (El-Shazly, 2002). Pyrrolizidine alkaloids are classified based on their structure, and include those with a saturated nucleus (non-toxic) and those with an unsaturated nucleus (toxic) (Barnes *et al.*, 2007).

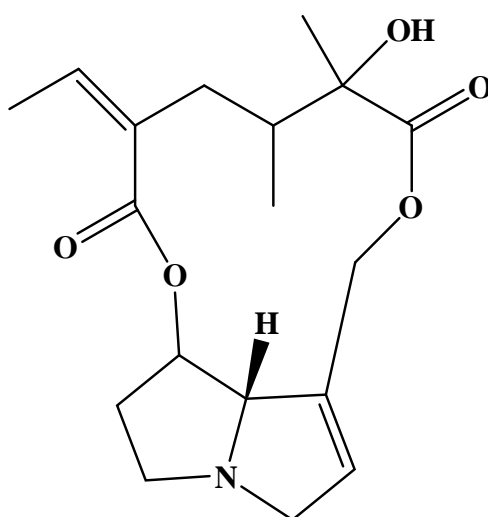


Figure 2.4: Chemical structure of pyrrolizidine alkaloid

2.4.3 Triterpenoids

Triterpenoids are natural products containing a carbon skeleton based on six isoprene units and derived biosynthetically from the cyclic C_{30} hydrocarbon, squalene (Fig 2.5). They are crystalline and colourless with high melting points. These compounds are a vastly diverse group including steroids, saponins and cardiac glycosides (Harborne, 1973, Okigbo *et al.*, 2009). In the genus *Senecio*, several triterpenoids have been isolated including sitosterol, stigmasterol and lupeol (Abdo *et al.*, 1992, Torres *et al.*, 1992).

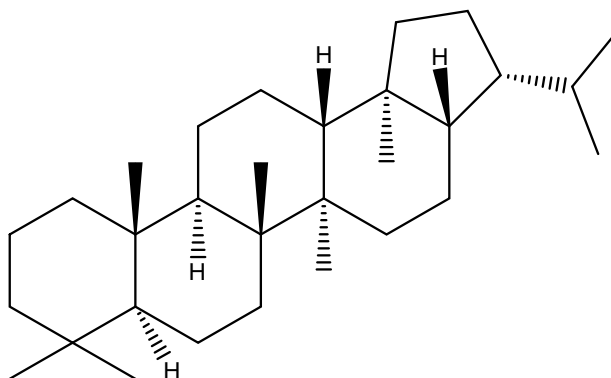


Figure 2.5: Chemical structure of a pentacyclic triterpenoid

2.5 Introduction to Nanoparticles

Nanotechnology is an interesting and promising approach in a variety of disciplines ranging from material science, mechanics and electronics to biomedical research and drug delivery. Nanoparticles (NPs) are solid colloids or particulate matter with a size of less than 100 nm in at least one dimension (Mohanraj and Chen, 2006). They can be produced from various materials and in different shapes, such as nanotriangles, nanorods, nanotubes, nanospheres, nanowires and nanohexagons, depending on the material, synthesis route and conditions (Dhillon *et al.*, 2012). The properties depend on size and shape. Therefore, synthesis conditions need to be optimised to control size and shape.

Nanoparticles have generated great interest in biomedicine due to their extremely small size and large surface-to-volume ratio, which leads to physical and chemical properties different from their bulk counterparts (Raghavan *et al.*, 2015b). The therapeutic potential of NPs is highly effective in treating diseases such as cancer due to their size being comparable to those of biological entities (Mittal *et al.*, 2014b).

Synthesis of metal or metal oxide NPs using whole plants or plants extracts is gaining importance due to the usage of less toxic chemicals, simplicity, eco-friendliness, ease of scaling up, cost-effectiveness and one step synthesis methods (Sundrarajan *et al.*, 2015). Nanoparticles can be synthesised using different plant parts including leaves, roots and flowers and biological materials such as algae, bacteria or fungi. Nanoparticles are known to be bio-safe, non-toxic and biocompatible and have been used as drug carriers, incorporated in cosmetics and fillings in medical materials (Mirzaei and Darroudi, 2017).

2.5.1 Synthesis of nanoparticles

Nanoparticles can be synthesised via chemical, physical and biological techniques (Dhillon *et al.*, 2012). These techniques can either be characterised as “top-down” or as “bottom-up” approaches (Fig 2.6). In top-down synthesis, the production of NPs is by size reduction from a bulk starting material. In the bottom-up synthesis, NPs are produced by joining smaller entities, such as molecules, atoms and smaller particles (Mittal *et al.*, 2013). The biological approach has been extensively reported in literature. This approach uses different organisms such as plants or microorganisms and their secondary metabolites as reducing and capping agents in the synthesis of NPs (Dhillon *et al.*, 2012, Gericke and Pinches, 2006, Sanghi and Verma, 2010).

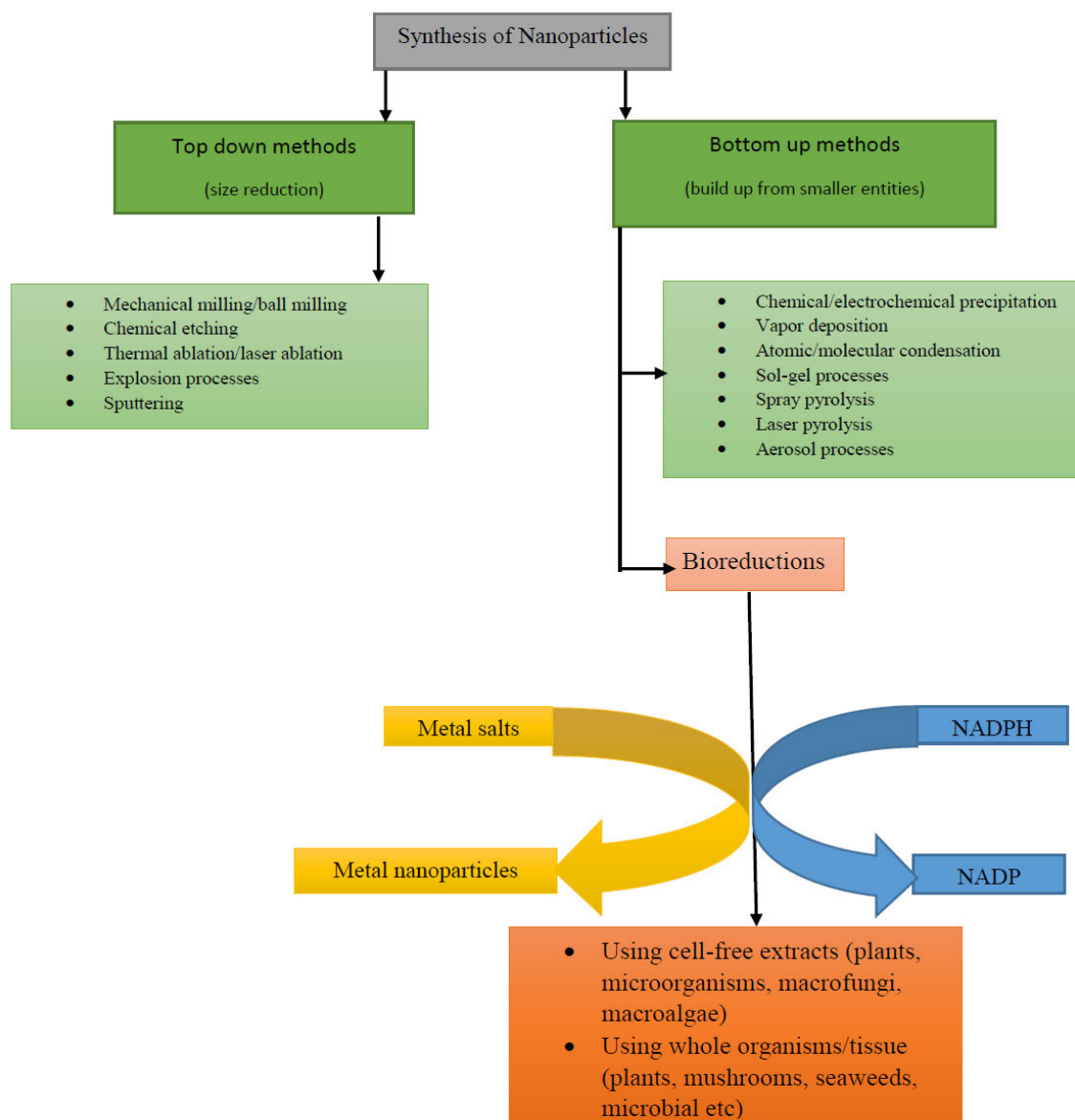


Figure 2.6: Techniques used in the synthesis of nanoparticles

2.5.2 The physico-chemical synthesis of nanoparticles

Various physical methods can be used for the synthesis of metallic NPs, such as lithography, vapor phase, pyrolysis and attrition (Li *et al.*, 1999). These methods have advantages and disadvantages. Physical methods often require expensive equipment and are difficult to scale up, but the generated NPs tend to have good mono-dispersity and low amounts of impurities (Mallick *et al.*, 2004). The chemical methods of NP synthesis are generally cheaper and easier to scale up. These methods involve reducing agents such as potassium bitartrate, sodium borohydride, hydrazine or methoxypolyethylene glycol to precipitate NPs from a salt solution (Li *et al.*, 1999, Mallick *et al.*, 2004). However, there are health and environmental concerns regarding the chemical synthesis of NPs. The NPs generated using this route may be contaminated by precursors and the use of toxic chemicals during synthesis is an environmental problem. In addition, the surface of NPs may absorb these toxic species resulting in adverse effects in bio-medical applications (Mallick *et al.*, 2004).

2.5.3 Biological synthesis of nanoparticles

There is a necessity to develop low cost, high yield, environmentally benign, non-toxic and biocompatible methods for the synthesis of metal and metal oxide NPs. Therefore, the synthesis of NPs by biological approaches has gained importance. Biological resources such as plants, plant products, bacteria, yeast, fungi, viruses, algae and actinomycetes have the ability to act as reducing and capping agents in the synthesis of NPs (Sastry *et al.*, 2003). These methods involve the use of biological and biodegradable compounds instead of toxic reagents conventionally used in nanomaterial synthesis. The biological methods used in microbial synthesis methods have been widely reported (Dhillon *et al.*, 2012). These methods are readily scalable and environmentally benign but often expensive.

Plant-mediated synthesis, on the other hand, involves the use of plant parts such as leaves, roots, flowers, seeds or stems. The method is readily scalable and environmentally benign with the added advantage of being economically feasible.

2.5.3.1 Medicinal plants used in the synthesis of nanoparticles

As a result of global environmental problems, there has been a growing need to use ‘greener’ processes in chemistry and chemical technology (Sathishkumar *et al.*, 2018b). Therefore, techniques using natural compounds such as sugars, vitamins and other phytochemicals have been considered and tested (Kharissova *et al.*, 2013). The use of plant extracts in the synthesis of NPs is cost-effective and can be scaled up easily, thus it can be used as a valuable and economic alternative for a significant production of metal NPs (Iravani, 2011).

Some plant-based metal and metal oxide NPs can exhibit exceptional anticancer, antimicrobial, antioxidant, immunomodulatory, antidiabetic and anti-inflammatory properties when medicinal plants containing biologically active secondary metabolites are used in the synthesis (Sathishkumar *et al.*, 2018b). Gold and silver are the most studied NPs for biomedical applications and in the developing interdisciplinary field of nanobiotechnology, due to their inertness in biological environments. The synthesis of silver and gold NPs from the tuber extract of *Dioscorea bulbifera* has been reported (Ghosh *et al.*, 2011). The combination of these NPs with antibiotics was found to have antibacterial activity against *Escherichia coli*, *Acinetobacter baumannii* and *Pseudomonas aeruginosa* (Ghosh *et al.*, 2012). The leaf extract of *Ocimum sanctum* was reported to reduce silver ions to NPs within 8 minutes (Mallikarjun *et al.*, 2011). These silver NPs were found to have antimicrobial activity against Gram-positive and Gram-negative microorganisms (Singhal *et al.*, 2011).

The biological activity of ‘green’ metal and metal oxide NPs other than silver and gold are less investigated although some potential has previously been demonstrated, for example, for zinc oxide NPs (ZnONPs). The leaf extracts of *Passiflora caerulea* (Passifloraceae) were used for the green synthesis of ZnONPs that were active against urinary tract infections (Santhoshkumar *et al.*, 2017). The ZnONPs synthesised using green tea leaves (*Camellia sinensis*) had good antimicrobial efficiency against some pathogenic bacteria and fungi (Senthilkumar and Sivakumar, 2014). Zinc oxide NPs grown using the roots of *Lathyrus sativus* by the alkaline precipitation method reduced oxidative stress and DNA damage (Panda *et al.*, 2017). The roots of *Polygala tenuifolia* have been reported in the synthesis of ZnONPs and demonstrated moderate antioxidant and excellent anti-inflammatory activity (Nagajyothi *et al.*, 2015b). Zinc oxide NPs synthesised using flower extracts of *Nyctanthes arbor-tristis* and *Anchusa italica* have been shown to possess antimicrobial activity and antifungal potential (Jamdagni *et al.*, 2016, Azizi *et al.*, 2016). *Eclipta alba*, a medicinal herb belonging to the plant family Asteraceae, has previously been reported in the synthesis of ZnONPs which showed enhanced antibacterial activity (Singh *et al.*, 2018). Zinc oxide NPs have also been reported as a novel anticancer approach in *in-vitro* and *in-vivo* studies (Fouche *et al.*, 2008). When the extracts of macro-algae, *Gracilaria edulis*, were utilised in the synthesis of ZnONPs, good anticancer activity against human prostate cancer cell lines was demonstrated (Priyadharshini *et al.*, 2014).

2.5.3.2 Phytocompounds used in the synthesis of nanoparticles

Phytocompounds such as phenols, alkaloids, terpenoids and flavonoids play an important role in the plant-mediated synthesis of nanoparticles. A crude plant extract contains many such compounds and the individual nature and efficacy against diseases is usually unknown. Isolated phytocompounds from such an extract, on the other hand, allow for individual studies of mechanisms of NP formation and comparison of biological activities.

Table 2.2: Phytocompounds used to synthesise nanoparticles and their biological activity

Phytocompound	Nanoparticles (NPs)	Biological activity	References
Catechin	SiO ₂ NPs	Protection against oxidative stress neuro-process	(Halevas <i>et al.</i> , 2016)
Anthocyanin	ZnONPs	Antidermatophytic activity	(Sujatha <i>et al.</i> , 2018)
Genistein	Au NPs	Anticancer activity	(Stolarczyk <i>et al.</i> , 2017)
Epicatechin	AgNPs	Anticancer activity	(Ikram <i>et al.</i> , 2018)
Luteolin	Ag NPs	Antimicrobial activity against <i>Bacillus subtilis</i>	(Nazeruddin <i>et al.</i> , 2014)
Quercetin and gallic acid	Ag-SeNPs	Antimicrobial and antioxidant activities	(Mittal <i>et al.</i> , 2014a)

Gallic acid, a phytocompound found in gallnuts, witch hazel and many other plants has been employed in the synthesis of bimetallic silver-selenium (Ag-Se) NPs with antioxidant, antimicrobial and anticancer activity (Mittal *et al.*, 2014a). Catechin has been reported to have activity against oxidative stress in the synthesis of silica oxide NPs (Halevas *et al.*, 2016). Genistein was reported to reduce gold ions to spherical gold NPs and found to have cytotoxic activity against cancer cells (Stolarczyk *et al.*, 2017).

The formation of the enol form of luteolin was reported as the reducing and stabilising agent in the synthesis of silver NPs. The synthesised silver NPs had antimicrobial activity against *B. subtilis* (Nazeruddin *et al.*, 2014). Quercetin, a well-known natural antioxidant, has been used in the synthesis of bimetallic silver-selenium (Ag-Se) NPs. The spherical Ag-Se NPs showed antibacterial, antioxidant and anticancer activity (Mittal *et al.*, 2014a).

Anthocyanins have been reported as reducing and capping agents in the synthesis of ZnONPs using *Cassia alata* leaves; the synthesised ZnONPs showed antidematophytic activity against *Epidermophyton floccosum* (Sujatha *et al.*, 2018). Flavonoids present in *Sageretia thea* have been reported to play a role in stabilising, reducing and capping, in the synthesis of ZnONPs; the synthesised ZnONPs demonstrated antimicrobial activity (Khalil *et al.*, 2017).

The potential of phytochemicals isolated from the Asteraceae family for the synthesis of metal oxide NPs is yet to be fully explored. Flavonoids are the only class of phytochemicals from this plant family that have been reported to be used for the synthesis of NPs. Flavonoid-mediated green nanoparticles have been reported in novel nanomedicine systems in the treatment of various diseases (Sathishkumar *et al.*, 2018a). Although flavonoid-mediated green nanomaterials are helpful in the treatment of various diseases and in the bio-reduction of metals into NPs, further studies using different classes of phytochemicals is needed to test their potential in biomedical applications. Considering the limited information available on the biosynthesis of ZnONPs using other phytochemicals, herein, we report on the jacaranone-mediated synthesis of ZnONPs using *Senecio serratuloides*.

2.6. Characterisation Techniques

2.6.1 Phytochemical characterisation techniques

The following phytochemical techniques have been employed to achieve the first objective of the study: extraction, isolation and characterisation of phytochemicals from *S. serratuloides*. Crude extracts from plant material are obtained by solvent extraction. Different classes of secondary metabolites are extracted depending on the polarity of the solvent used. The crude extract is then separated using organic solvents and column chromatography until pure phytochemicals are obtained. This is followed by structure elucidation and characterisation and identification.

2.6.2 Chromatographic techniques

Chromatographic techniques are used for the separation, identification and determination of components of complex mixtures found in natural products. Methods in chromatography make use of a stationary and mobile phase. The components of a mixture are passed through the stationary phase to a mobile phase; this process is called elution. Chromatographic separation depends on the differential distribution of various components of a mixture between the mobile and stationary phases. The different migration rates will lead to their separation over a period of time and distance. Chromatographic techniques have many applications such as analysis of environmental samples, checking the progress of a reaction, purification of bio-molecules such as proteins and separation of secondary metabolites from plant extracts. There are two basic chromatographic types that are commonly used in natural products research, namely, column chromatography (CC) and thin layer chromatography (TLC).

2.6.2.1 Thin-layer chromatography (TLC)

Thin layer chromatography (TLC) is one of the most inexpensive and simple techniques used to separate organic substances. The stationary phase is supported on a flat plate; the mobile phase then flows through the stationary phase by capillary action. This method is used for identification purposes and for determining the purity of components. The stationary phase is a powdered adsorbent fixed to an aluminium plate. The results obtained using TLC can inform the type of stationary phase to be used in column chromatography. It is a useful tool for determining the best solvent system for preparative separations of mixtures.

2.6.2.2 Column chromatography (CC)

Column chromatography (CC) uses a glass tube; the stationary phase is held in the tube and the mobile phase is forced through the tube by gravity. The stationary phase is fixed in the column; the most common stationary phase is silica gel. Silica gel is dissolved in a suitable solvent forming a slurry and transferred to the column; this process is called wet packing. The eluted fractions are then collected from the column into a receiving beaker and monitored by TLC.

2.6.3 Spectroscopic techniques

Spectroscopic techniques measure the spectrum produced when matter interacts with light or emits electromagnetic radiation. Spectrometry is used to measure the absorbance or emission of the radiation. The interaction might give rise to electronic excitations, such as ultraviolet, molecular vibrations such as infrared and nuclear spin orientations eg. NMR.

2.6.3.1 Fourier-transform infrared spectroscopy (FTIR)

Fourier-transform infrared spectroscopy (FTIR) is used to obtain an infrared spectrum of absorption or emission of a sample, also used for the identification of pure organic and inorganic compounds. The sample is exposed to different wavelengths of infrared light and the instrument measures which wavelengths are absorbed. The computer takes that raw absorption data and conducts a math process known as the Fourier-transform to generate a readable absorbance spectrum. The absorption bands on the spectrum provide information on the functional groups and the chemical structure of a molecule.

2.6.3.2 Gas chromatography-mass spectrometry (GC-MS)

In gas chromatography-mass spectrometry (GC-MS), the gas chromatograph works on separating volatile components in a sample into individual substances when heated. The heated gases are carried through a column with an inert gas such as helium. As the separated substances emerge from the column, they flow into the MS and get fragmented. The mass spectrometer measures the mass-to-charge ratio (m/z) of ions that have been produced from the sample. Most of the ions are singly charged ($z = 1$). There are different ionization sources for MS, one of the most commonly used is an electron impact source, where the molecules are bombarded with a high energy beam of electrons. This then results in the fragmentation of the molecule producing positive ions, negative ions and neutral species. The fragments are very helpful in identifying molecular species entering the spectrometer.

2.6.3.3 Nuclear magnetic resonance (NMR) spectroscopy

Nuclear magnetic resonance (NMR) spectroscopy is used in quality control and research for determining the content and purity of a sample as well as its molecular structure. Nuclear magnetic resonance spectroscopy can quantitatively analyse mixtures containing both known and unknown compounds; also used to determine the molecular conformation of a compound. The principle behind NMR is that many nuclei have spin and all nuclei are electrically charged. If an external magnetic field is applied, an energy transfer is possible between the base energy to a higher energy level, generally a single energy level. The energy transfer takes place at a wavelength that corresponds to radio frequencies (RF) and when the spin returns to its base level, energy is emitted at the same frequency. The signal that matches this transfer can be measured in different ways and processed to yield an NMR spectrum for the nucleus concerned.

The identity of chemical compounds can be determined by elucidating the detailed structural information obtained from one dimensional NMR (1D-NMR). The chemical shifts in ^{13}C -NMR are 0-250 ppm and those of ^1H -NMR are 0-13 ppm. The signals in ^{13}C -NMR appear as singlets because of the decoupling of the attached proton. The other 1D-NMR techniques are distortionless enhancement by polarisation transfer (DEPT 90) where only signals for quaternary and tertiary carbons can be seen and are positive, whereas in DEPT 135 signals are for tertiary, secondary and primary carbons and the signals for secondary carbons appear as negative. Two-dimensional ^1H , ^1H Correlation Spectroscopy (COSY) gives correlation signals between cross peaks with covalently bonded protons; these can be observed for distances up to three bonds away. The 2D-nuclear Overhauser enhancement spectroscopy (NOESY) represents interactions between proton nuclei that are 5\AA closer to each other in space (long-ranged correlations). The 2D-heteronuclear single quantum coherence (HSQC) spectroscopy shows correlations between a carbon and its protons; ^1H - ^{13}C one bond correlation. Correlations

of protons with more distant carbons are referred to as 2D-heteronuclear multiple bond correlation (HMBC) spectroscopy.

2.7 Characterisation of Nanoparticles

Nanoparticles are characterised by their chemical composition, shape, dispersity, size, surface area and surface charge (Jiang *et al.*, 2009). The techniques of characterising NPs include ultraviolet-visible spectroscopy (UV-Vis), Fourier-transform infrared spectroscopy (FTIR), dynamic light scattering (DLS), powder X-ray diffraction (XRD), scanning electron microscopy (SEM), transmission electron microscopy (TEM), energy-dispersive X-ray spectroscopy (EDX), and selected area electron diffraction (SAED) (Feldheim and Foss, 2002).

2.7.1 Ultraviolet-visible (UV-Vis) spectroscopy

Ultraviolet-visible (UV-Vis) spectroscopy is a technique used to measure the light that is absorbed and scattered by a sample. Fig 2.7 shows a typical UV-Vis spectrophotometer. A sample is placed between a light source (monochromator) and a photodetector. Tungsten lamps and deuterium (D₂) lamps are used to provide illumination across the UV-Vis spectrum. The intensity of a beam is measured before and after passing through the sample. The spectrum is background-corrected using a reference, which is a cuvette filled with only the used solvent to guarantee that spectral features from the solvent are not included in the sample extinction spectrum. Data is processed and plotted with respect to absorbance and wavelength. Ultraviolet-visible spectroscopy is a valuable tool for identifying, characterising, and studying NPs due to their optical properties that are sensitive to size, shape, concentration, agglomeration state and surface area. Nanoparticles made from metals oxide such as zinc oxide

strongly interact with specific wavelengths of light, and the unique optical properties of these materials are the foundation for the field of plasmonics (Mittal *et al.*, 2013).

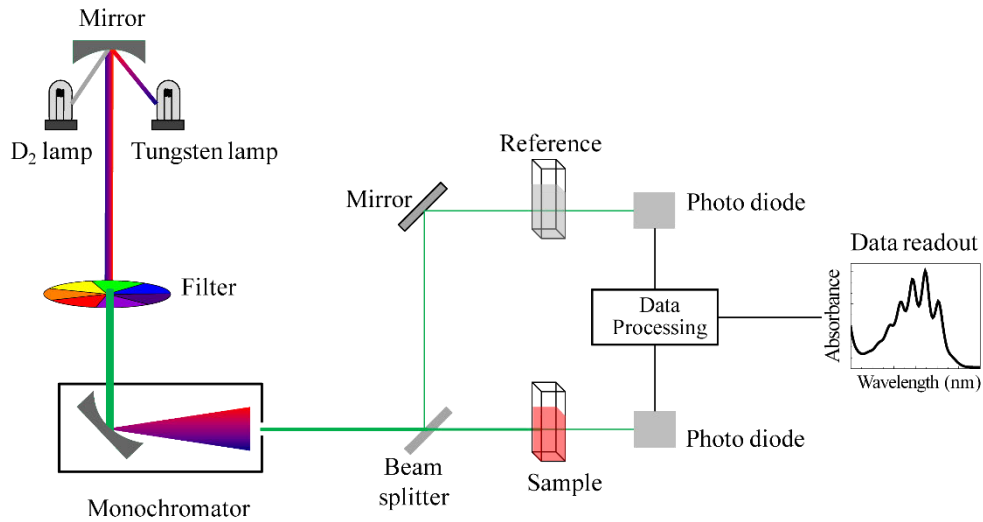


Figure 2.7: Ultraviolet-visible spectrophotometer

2.7.2 Powder X-ray diffraction (XRD)

Powder X-ray diffraction (XRD) is a technique applied in the phase identification and characterisation of a crystal structure. The structural information is obtained from the diffraction angle 2θ of X-rays interacting with the material (Cullity and Stock, 2001). Figure 2.8 shows the geometrical arrangement of components of a typical X-ray powder diffractometer. X-rays from the tube are incident on a powder sample, which may be set at any desired angle to the incident beam by rotation about an axis through the centre of the diffractometer circle. The X-ray detector is an ionization chamber or some form of counter which measures the intensity of the diffracted X-rays. It can also be rotated and set at any desired angular position. The powder sample is positioned so that its reflecting planes make particular angle θ with the incident beam, and X-ray detector is set at the corresponding angle 2θ . The intensity of the diffracted beam is then measured and its wavelength calculated from

the Bragg equation: $n\lambda = 2d \sin\theta$, describes the relationship between the wavelength of the incident X-rays, the incident angle of the beam and the spacing between the crystal lattice planes of atoms, is used to calculate lattice spacing and miller indices (hkl) depending on the phase.

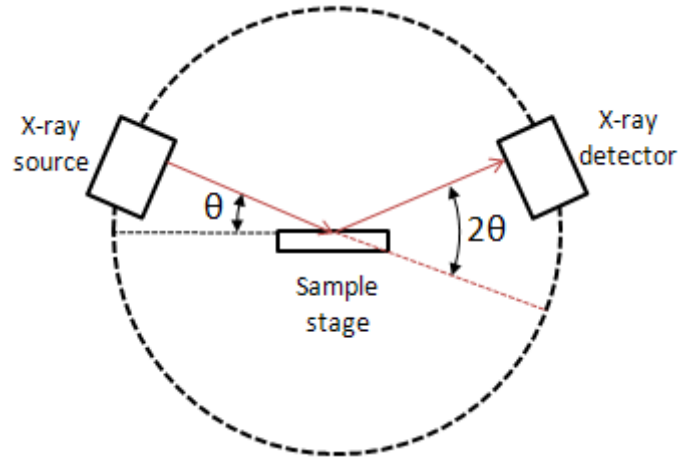


Figure 2.8: Components of a powder X-ray diffractometer in θ - 2θ configuration

The interplanar spacing d_{hkl} , measured at right angles to the planes, is a function both of the plane indices (hkl) and the lattice constants (a, b and c). The exact relation depends on the crystal system involved and for the hexagonal system takes on the relatively form

$$\text{Hexagonal } d_{123} = \frac{4}{3} \left(\frac{h^2 + k^2 + l^2}{a^2 + b^2 + c^2} \right)$$

In X-ray diffraction, Scherrer equation is used to determine the size of particles of crystals in the form of powder. The Scherrer equation can be written as: $T = \frac{K\lambda}{\beta \cos\theta}$

where: T is the mean size of the ordered (crystalline) domains, which may be smaller or equal to the grain size, K is a dimensionless shape factor, with a value close to unity. The shape factor has a typical value of about 0.9, but varies with the actual shape of the crystallite, λ is the X-ray wavelength, β is the line broadening at half the maximum intensity (FWHM), after subtracting the instrumental line broadening, in radians and θ is the Bragg angle.

2.7.3 Scanning electron microscopy (SEM) and energy-dispersive X-ray spectroscopy (EDX)

Scanning electron microscopy (SEM) is a technique used for the morphological and chemical characterisation at the nanometre to micrometre scale (Schaffer *et al.*, 2009). Images obtained from SEM can have a resolution down to the nanometre range. The three-dimensional appearance of the images is due to the large depth of field of the scanning electron microscope as well as to the shadow relief effect of the secondary electron contrast.

Scanning electron microscopy involves an electron optical system to produce an electron beam, a specimen stage to place the specimen, a secondary-electron (SE) detector to collect secondary electrons, a back-scattered detector (BSE) to collect back-scattered electrons, an image display unit and an operation system to perform various operations (Fig 2.9). The electron beam is focused on the sample and, with the help of scanning coils, scanned across the sample in a TV-like fashion. The interaction between beam and sample gives rise to a number of signals that can be used for characterisation, e.g. secondary electrons, backscattered electrons, characteristic X-rays, and Auger electrons. These signals are obtained from a certain emission volume within the sample and are used to extract information of the sample such as surface topography, composition and crystallography (Goldstein *et al.*, 1977).

For imaging, secondary and/or back-scattered electrons are used. Secondary electrons are electrons of the sample material that have been ejected due to the interaction with the beam. Back-scattered electrons are beam electrons that have been backscattered due to interaction with sample atoms. Secondary electron images (SEI) mostly show the topography of the sample, and in back-scattered electron images (BEI) the brightness of an image point depends on the average atomic number at that spot, i.e. it gives qualitative information of the elemental composition.

Some of the techniques used in conjunction with SEM include energy dispersive X-ray spectroscopy (EDX). In SEM, EDX is used to determine the local chemical composition of the sample. When a beam electron interacts with the sample, electron from lower shells in the sample can be ejected due to an energy transfer from the beam electron. The remaining hole in the electron structure is filled by an electron from a higher shell. The difference in energy is emitted as X-ray photon, which is characteristic for the element. The analysis of energy-dispersive X-ray spectra emitted from samples can yield both qualitative and quantitative elemental information.

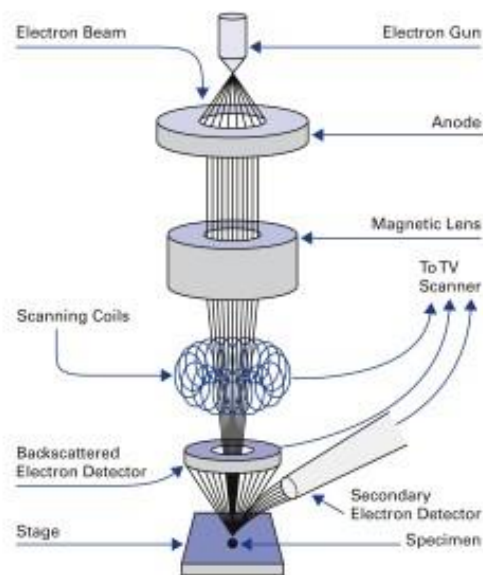


Figure 2.9: Principal design of a scanning electron microscope (SEM)

2.8 Conventional Transmission Electron Microscopy (TEM)

2.8.1 Imaging in transmission electron microscopy (TEM)

Transmission electron microscopy (TEM) is a technique similar to SEM, in that an electron beam is used to image a sample. In the case of TEM, the sample must be less than 100 nm thick

to be electron transparent (Schaffer *et al.*, 2009). For most techniques, the sample is illuminated by a parallel electron beam, which transmits the sample, and the image is collected below the sample.

In TEM (Fig. 2.10), a thermionic or a field-emission gun produces the electron beam, which is then accelerated towards the anode by the acceleration voltage used (typically 100-200 kV). A condenser lens focuses the beam onto the sample, which sits in the gap between the upper and lower pole piece of the objective lens. The objective lens produces a diffraction pattern of the sample, and different settings of the microscope allow imaging due to the interaction of primary and diffracted beams or recording the actual diffraction pattern. The image or diffraction pattern can be viewed on a fluorescent screen and recorded e.g. on photographic film or on a charge-coupled device (CCD) (Fultz and Howe, 2012). Contrast (different brightness of different sample areas) arises from different sample thicknesses, different average atomic numbers (Z) (mass-thickness contrast) and the crystallographic orientation of a crystalline sample (diffraction contrast).

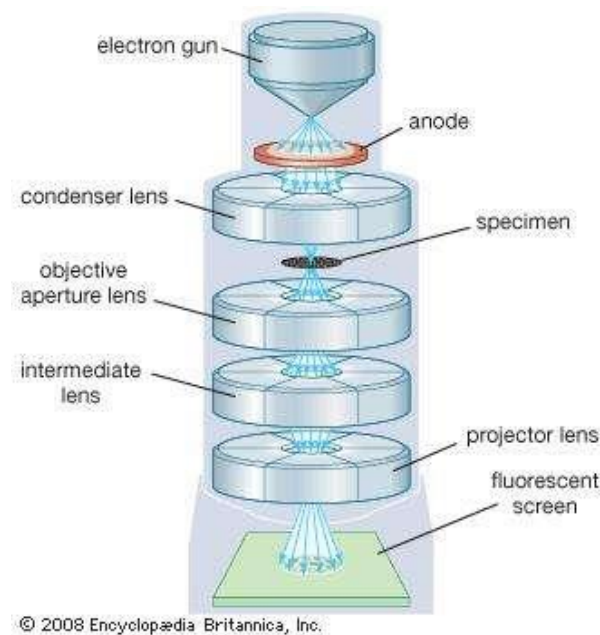


Figure 2.10: Principal design of a transmission electron microscope

2.8.2 Selected area electron diffraction (SAED)

Conventional TEM includes techniques such as selected area electron diffraction (SAED), which is used to identify phases and characterise crystal structures. Fig 2.11 shows a diagram of the beam path in SAED mode. The intermediate lens is focused on the back focal plane of the objective lens. The transmitted beam and diffracted beams are imaged on the fluorescent screen. An aperture positioned in the image plane of the objective lens is used to confine the beam to a selected area of the specimen. In SAED the electrons are treated as wave-like, rather than particle-like in normal TEM, because the wavelength of high energy electrons is a few thousandths of a nanometer, and the spacing between atoms in a solid is about a hundred times larger, the atoms act as a diffraction grating to the electrons, which are diffracted (Cullity and Stock, 2001). Some fraction of them will be scattered to particular angles, determined by the crystal structure of the sample. As a result, the image observed on the TEM will be a series of spots, selected area diffraction pattern (Fig 2.11), each spot corresponding to a specific diffraction condition of the sample's crystal structure. If the sample is tilted, the same crystal will stay under illumination, but different diffraction conditions will be activated, and different diffraction spots will appear. It is called selected area because the user can easily choose from which area of the sample to obtain the diffraction pattern. The patterns are a projection of the reciprocal lattice, with lattice reflections showing as sharp diffraction spots. By tilting a crystalline sample to low-index zone axes, SAD patterns can be used to identify crystal structures and measure lattice parameters. This technique is similar to X-ray diffraction in that a diffraction pattern is formed following Bragg's law. In SAED, the selected area can be much smaller though and the Bragg condition is not as strict as in XRD due to the limited thickness of the sample.

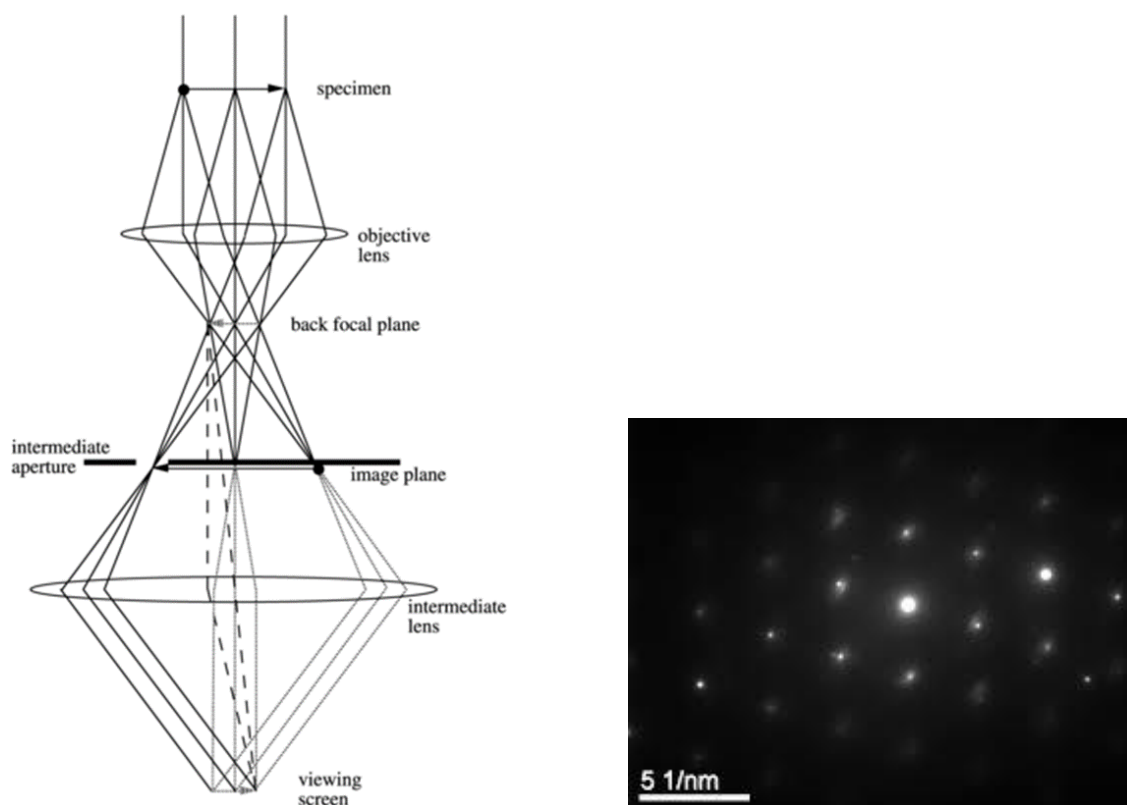


Figure 2.11: Beam path for imaging and SAED in the TEM and selected area electron pattern.

2.9 Analytical Electron Microscopy (AEM)

Analytical electron microscopy (AEM) includes all technique that use secondary signals from the specimen produced by electron transitions due to the interaction with the electron beam, to give chemical information about the specimen (Williams and Carter, 2009). This includes energy-dispersive electron spectroscopy (EDS) and electron-energy loss spectroscopy (EELS) including the mapping techniques that use one of both of those signals (Fultz and Howe, 2013). Both EDS and EELS involve an energy transfer between beam and sample electrons. A beam electron can knock an inner shell electron from the sample out of position ionising the atom. The hole will be filled with an electron from a higher shell. The discrete energy difference between the two shells is emitted as an X-ray. The energy of that X-ray is characteristic for the sample atom and can be analysed.

The mechanism is the same as in the SEM. During this process, the incident electron loses energy, which is transferred to the emitted sample electron. This energy loss in the primary beam can also be analysed and is characteristic for the sample atoms. In addition, information on local chemistry and structure can be obtained from features in EELS spectra caused by plasmon excitations and core electron excitations (Fultz and Howe, 2013). Characteristic X-rays and energy losses can be used to determine the qualitative and quantitative concentration of elements in the sample.

2.10 Scanning Transmission Electron Microscopy (STEM)

In scanning transmission electron microscopy (STEM), the sample is not illuminated by a parallel beam but a focused, convergent beam of $\sim 1\text{--}10\text{ \AA}$ diameter, is moved in a television-style raster pattern across the specimen. In synchronisation with the raster scan, various data from the specimen are acquired, such as emitted EDX and EELS signals. Transmitted electrons are detected with a moveable detector at the bottom of the microscope column. The STEM mode of operation is especially useful for spectroscopy work, since it permits the acquisition of a “chemical map” of the sample, which shows the spatial distribution of elements.

2.11 Biological Activity

The antioxidant activity of the selected compounds isolated *S. serratuloides* and synthesised ZnONPs was determined by the 2,2-diphenyl- β picrylhydrazyl (DPPH) assay. The antimicrobial activity was determined using antibacterial susceptibility testing using Gram-positive and Gram-negative bacterial strains and anti-quorum sensing activity was determined by qualitative agar-overlay well-diffusion assay.

2.11.1 Antioxidant activity

Reactive oxygen species (ROS) are significant signal transduction mediators that regulate cell differentiation, gene expression, apoptosis and immune activation (Ikeda *et al.*, 2008). However, when these free radicals accumulate excessively and for longer periods of time, they cause chronic oxidative damage and other adverse effects on cells as well as biomolecules (Prabhakar, 2016). Antioxidants are essentially substances that are capable of reacting with ROS producing less harmful species. A large number of secondary metabolites found in plants are antioxidants.

The most common method of assessing plants and compounds for antioxidant activity is the 2,2-diphenyl- β picrylhydrazyl (DPPH) assay. It is fast, easy and inexpensive. It involves the use of a free radical, DPPH, which is purple in colour. The odd electron on the free radical has a strong absorption maximum at 517 nm. The activity of a compound leads to decolourisation from purple to yellow as the DPPH is consumed. The reaction is monitored using a spectrophotometer.

Fawole et al. (2010b) evaluated the antioxidant effect of the methanolic leave extract of leaves from *S. serratuloides* by determining its DPPH radical scavenging activity. The extract showed good radical scavenging activity compared to the positive control, ascorbic acid. The EC₅₀ values of the leaf extract and ascorbic acid were 10.40 and 5.06 $\mu\text{g mL}^{-1}$, respectively.

2.11.2 Anti-bacterial activity

Antibacterial activity is known as the action by which bacterial growth is destroyed or inhibited. It is also described as a function of the surface area in contact with the microorganisms (Wahab *et al.*, 2010). Antibacterial agents are selective concentration drugs capable of damaging or inhibiting bacterial growth and they are not harmful to the host. These

compounds act as chemo-therapeutic agents for the treatment or prevention of bacterial infections. An antibacterial agent is considered as bactericidal if it kills bacteria or as bacteriostatic if it inhibits their growth (Wahab *et al.*, 2010). Methods such as agar well diffusion, broth dilution and disk diffusion have been adopted for the assessment and investigation of antibacterial activity *in-vitro* (Premanathan *et al.*, 2011).

An agar well diffusion method was employed in antibacterial activities of ZnONPs against three multiple drug resistant bacterial strains such as *S. aureus* (ATCC-6538), *E. coli* (ATCC-15224) and *K. pneumonia* (ATCC-4619) using roots extracts of *Linum usitatissimum* (Abbasi *et al.*, 2017). The agar diffusion method is the most frequently used method and has been standardised as an official method for detecting bacteriostatic activity. Dobrucka and Długaszewska (2016) reported on the biosynthesis of ZnONPs using *Trifolium pratense* flower extracts and their antibacterial activity against clinical and standard strains of *S. aureus* and *P. aeruginosa* and standard strain of *E. coli*.

Gram-negative bacteria such as *Escherichia coli*, *Pseudomonas aeruginosa* and *Chromobacterium violaceum* have two cell membranes, an outer membrane and a plasma membrane with a thin layer of peptidoglycan (Wheat *et al.*, 1963, Dahl *et al.*, 1989) with a thickness of 7–8 nm. Whereas Gram-positive bacteria such as *Enterococcus faecalis*, *Staphylococcus aureus* and *Bacillus anthracis* have one cytoplasmic membrane with a multilayer of peptidoglycan polymer and a thicker cell wall of 20–80 nm (Dahl *et al.*, 1989).

Zinc oxide NPs capped with medicinal plants exhibit greater antimicrobial effects against Gram-negative bacteria regardless of their resistance level compared to Gram-positive bacteria (Emami-Karvani and Chehrazi, 2011). Unlike most antibiotics, ZnONPs do not attack a single target of the cell. The combination of the above-mentioned factors, targeting multiple components of a cell, makes treatment with ZnONPs an ideal alternative as a broad -spectrum antimicrobial.

2.11.3 Anti-quorum sensing activity

At low cell density, bacteria behave as a single cellular organism. They achieve their communication by production, diffusion, sensing and response to a small signalling molecules called autoinducers (Koh *et al.*, 2013). Autoinducers are produced and diffuse out of the cell causing the bacteria to behave in a multicellular type, until their population density reaches a threshold level. The produced autoinducers enable bacterial populations to re-programme gene expression in a coordinated fashion. This process is called quorum sensing (Nazzaro *et al.*, 2013). Bacteria use two quorum sensing classes; one used by Gram-negative bacteria and one used by Gram-positive bacteria. Those used by Gram-negative bacteria are the more common ones. The diagram in Figure 2.12 presents a typical quorum sensing molecular signalling network of Gram-negative bacteria. Gram-negative bacteria produce acylated homoserine lactone (AHL) as autoinducers, which are synthesised by a LuxI-type enzyme (autoinducer synthase). The autoinducers are produced at low cell density. When the signal levels reach a specified threshold level, the signal synthase is activated, increasing the production of autoinducers. The autoinducers then bind to cognate receptors forming an autoinducer receptor complex which leads to quorum sensing gene expression.

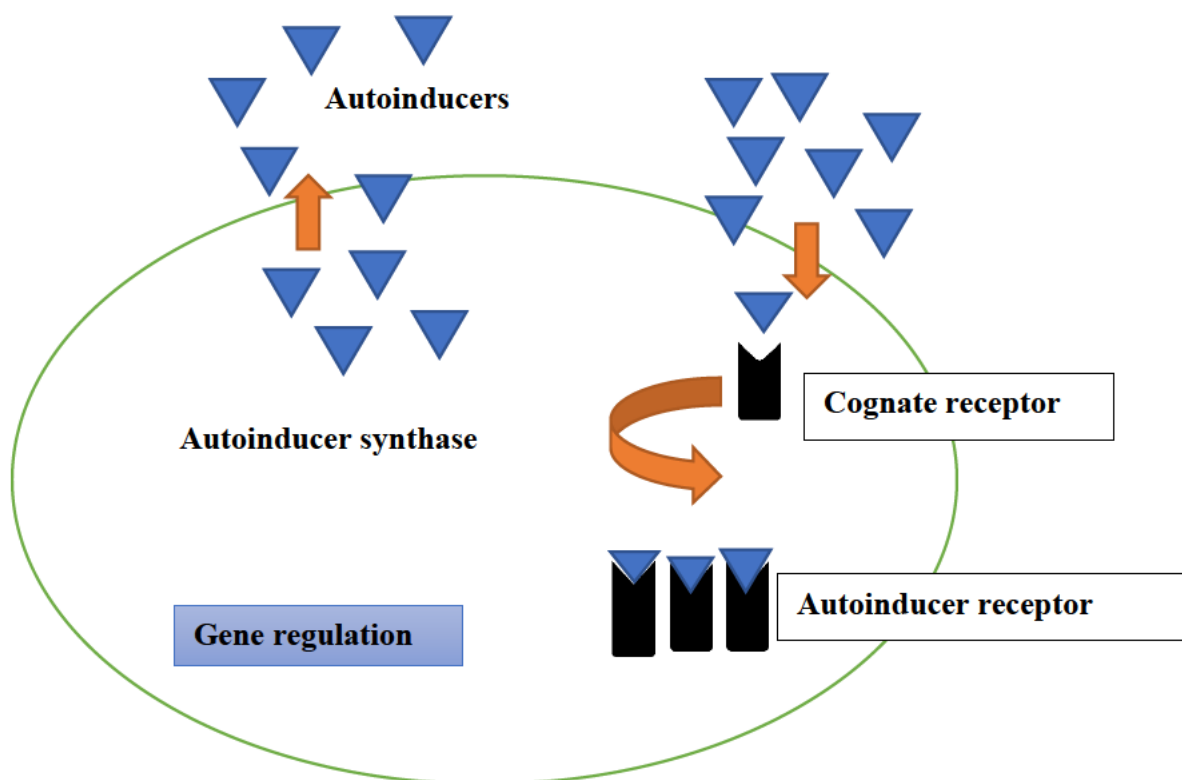


Figure 2.12: A typical quorum sensing system in Gram-negative bacteria

The emergence of antibiotic-resistant bacteria necessitates an alternative approach to control bacterial infections. About 65 % of infectious diseases are linked to quorum sensing systems to coordinate their virulence expression (Kalia, 2013). Currently, there is increased interest in the discovery of natural quorum sensing inhibitors that can interrupt quorum sensing by repressing signal generation and blocking signal receptors, thereby providing an alternative approach to the control of microbial pathogenesis. Nanotechnology is also seen as a promising approach to design antimicrobial and quorum sensing antagonists. Nanomaterials have been reported to have the potential to tackle bacterial diseases by attenuating quorum sensing, inhibiting biofilms and reducing cell viability (Huh and Kwon, 2011, Allaker and Ren, 2008, Fernandes *et al.*, 2010).

Zinc oxide NPs have been reported to have potential anti-virulence activity against *Pseudomonas aeruginosa* infections and inhibit biofilm formation. The study also indicated that ZnONPs activated the expression levels of a quorum sensing-related operon and transcriptional regulators of *P. aeruginosa* (Lee *et al.*, 2014). Plant-mediated synthesis of metal or metal oxide NPs have been employed in the discovery of novel anti-quorum sensing compounds and biofilm inhibitors. Extracts from *Cymbopogon citratus* and *Sargassum polyphyllum* have been used in the green synthesis of silver NPs. The synthesised NPs enhanced anti-quorum sensing activity against *S. aureus* and *C. violaceum* CV026 and prevented biofilm formation (Mirzaei and Darroudi, 2017, Arunkumar *et al.*, 2014).

Plant extracts and phytocompound have been reported as quorum sensing antagonist against the Gram-negative bacterium, *Chromobacterium violaceum* ATCC 12472, which responds to quorum sensing regulated gene expression by producing the pigment, violacein (Nazzaro *et al.*, 2013). *Malus domestica* (apple) demonstrated quorum sensing inhibitory activity against *Chromobacterium violaceum* due to the presence of hydroxycinnamic acids, rutin and epicatechin (Fratianni *et al.*, 2011). A possible mechanism for the anti-quorum sensing activity of phytocompounds could be the similarity of their skeletal structures to those of quorum sensing signal compounds and their ability to disrupt signal receptors. This necessitates the phytochemical investigation of other medicinal plants and to identify their potential in quorum sensing inhibition.

The present study discusses the isolation of phytocompounds from *Senecio serratuloides*, synthesis of ZnONPs using isolated phytocompounds and their antimicrobial and anti-quorum sensing activities.

CHAPTER THREE

MATERIALS AND METHODS

This chapter focuses on the materials and methods used in the phytochemical analysis, synthesis of freestanding ZnONPs and ZnONPs synthesised using extracts and isolated compounds from *S. serratuloides* as well as the testing of their biological activities.

3.1 Phytochemical Analysis of *Senecio serratuloides*

3.1.1 Collection of plant material

Leaves and stem bark of *S. serratuloides* were purchased at the Muthi market, Warwick Avenue, Durban, in June 2016. They were collected by a traditional healer, Mr TW Nhlenko, who gave more information on traditional uses and benefits of the plant. The plant was identified and authenticated by the taxonomist, Dr Syd Ramdhani (School of Life Sciences, University of KwaZulu-Natal, Westville, South Africa). A voucher specimen, NJoyisa 01, was deposited at the ward Herbarium, University of KwaZulu-Natal.

3.1.2 Extraction, isolation and purification of phytocompounds

The leaves and stem bark of *S. serratuloides* were separated, dried and crushed to a fine powder using a mill. Leaves (1350 g) and stem bark (950 g) were sequentially extracted using n-hexane, dichloromethane (DCM), ethyl acetate (EtOAc) and methanol (MeOH) by maceration and continuous shaking on an orbital shaker at room temperature for three days. A rotary evaporator was used to concentrate the extracts that were monitored or profiled using TLC, and those with similar TLC profiles were combined based on their retention factor (Rf).

The hexane extract from leaves (17.4 g) was fractionated using column chromatography (CC) with a hexane: EtOAc solvent system starting with 100% hexane that was stepped by 10% to 100% EtOAc. Four fractions of 80 mL were collected for each eluent step. Fractions 1 to 10 were combined to yield compound 1, a white oily liquid (44 mg). Fractions 21 to 40 were combined and further separated using a hexane: EtOAc (20:80, v/v) solvent system that was stepped to 100% EtOAc. Fourth fractions of 40 mL were collected for each eluent step. Compound 2, a white powder (55 mg), was obtained from fractions 17 to 25.

The DCM extract from leaves (10.2 g) were subjected to CC. A hexane: EtOAc solvent system starting with 10% EtOAc in hexane was used. This was stepped by 30% to 100% EtOAc. Fourth fractions of 80 mL were collected for each eluent step. Compound 3, a white powder (15.34 mg) was obtained in fraction 42. Fractions 54 to 59 yielded compound 4 as white needles (36.64 mg).

The hexane extract from the stem bark (3.4 g) was subjected to CC with a hexane: DCM: EtOAc solvent system, starting at 20% DCM in hexane that was stepped by 20% to 100% DCM then 20% EtOAc in DCM that was stepped by 20% to 100% EtOAc. Three fractions of 80 mL were collected for each eluent step resulting in thirty fractions. Fractions 4 and 5 were combined and further purified with 10% EtOAc in hexane in a small column to yield compound 5 which was a white powder (20.12 mg).

The MeOH extract from leaves (58.6 g) were dissolved in water and subjected to partitioning (in triplicate for each solvent) with equal volumes of DCM and EtOAc. The resulting combined DCM fraction (12.4 g) was subjected to CC and eluted using a hexane: EtOAc solvent system starting with 100% hexane that was stepped by 10% to 100% EtOAc. Four fractions of 80 mL were collected for each eluent step. Fractions 16 to 23 were combined to yield compound 6, as yellow crystals (80 mg).

The resulting combined EtOAc fraction (10.6 g) was subjected to CC and eluted using a hexane: EtOAc: MeOH solvent system. Initially, 30% EtOAc in hexane was used that was increased to 90% EtOAc by 20% increments. Finally, 100% EtOAc was used followed by addition of MeOH to 10% by 2% increments. Three fractions of 80 mL were collected for each eluent step. Fractions 11 to 35 were combined and purified to yield compound 7 which was a yellow oil (55 mg).

3.1.3 Spectroscopic characterisation of extracted phytochemicals

Isolated phytochemicals were characterised and identified by use of various analytical techniques such as IR spectroscopy using a Perkin Elmer Universal ATR spectrometer, UV-Vis Spectroscopy on a UV-Vis-NIR Shimadzu UV-3600 Spectrophotometer, GC-MS on an Agilent GC-MSD apparatus equipped with a DB-5SIL MS (30 m x 0.25 mm inner diameter, 0.25 μ m film thickness) fused silica capillary column. Helium (2 mL min⁻¹) was used as the carrier gas and EtOAc was used to dissolve the samples. The injector was kept at 250 °C whilst the transfer line was at 280 °C. The column temperature was held at 50 °C for 2 min, and then ramped up to 280 °C at 20 °C min⁻¹ where it was held for 15 min. NMR spectra were recorded using a Bruker Avance III 400 MHz spectrometer. Samples were dissolved in deuterated chloroform (CDCl₃) or deuterated methanol (MeOD) with tetramethylsilane (TMS) as internal standard.

3.2 Synthesis of zinc oxide nanoparticles (ZnONPs)

Zinc oxide NPs were prepared in two ways; chemical synthesis using sodium borohydride and green synthesis using plant material. The plant material included crude extracts and isolated secondary metabolites from the leaves and stem bark of *S. serratuloides*. Freestanding ZnONPs were chemically synthesised.

3.2.1. Synthesis of freestanding zinc oxide nanoparticles (ZnONPs) using chemical synthesis

The chemical synthesis was used for zinc salt reduction. The solution of $\text{Zn}(\text{NO}_3)_2$ (0.1 M) was reduced using sodium hydroxide (0.1 M). The strong reducing agent such sodium borohydride is normally used for synthesis of free standing ZnONPs, but this is a longer route. NaOH was used as a reducing agent for the present synthesis since this route is simple and faster. The reducing agent (NaOH) was added dropwise with constant stirring into zinc nitrate salt until the pH of the solution reached 11. After complete addition of NaOH, the reaction continued; the reaction was allowed to continue overnight. A white precipitate was collected after centrifugation of the solution at 5,000 rpm for 15 minutes. The precipitate (powder) was washed using distilled water to remove by-products. Finally, the materials were dried at 80°C, overnight.

3.2.2. Synthesis of zinc oxide nanoparticles (ZnONPs) using plant material

Dried leaves from *S. serratuloides* (10 g) were extracted with double distilled water on a hot plate at (60 °C) under constant stirring. The resultant aqueous extract was cooled and filtered using a Büchner funnel. The methanolic extract of *S. serratuloides* was prepared by extracting leaves extract with methanol in an orbital shaker for three days. Isolated compounds (6 and 7, 10 mg) were dissolved in MeOH (HPLC grade). This resulted in aqueous extract, methanolic extract and pure compounds dissolved in methanol. Zinc nitrate hexahydrate (14.874 g, 0.1 M) was added to each solution under constant stirring using a magnetic stirrer. Thereafter, a sodium hydroxide solution (0.1 M) was added dropwise to the solution under constant stirring until a pH of 11 was reached. The mixture was then allowed to settle overnight resulting in a yellow solution with white precipitate. The solution was centrifuged at 5.000 rpm for 15 minutes to separate NPs and supernatant, and the supernatant was discarded. The obtained NPs were washed three times using distilled water to remove by-products and contaminants. The NPs were dried at 80 °C, overnight.

3.3 Characterisation of Zinc Oxide Nanoparticles (ZnONPs)

3.3.1 Ultraviolet-visible (UV-Vis) spectroscopy and infrared (IR) spectroscopy

The obtained ZnONPs were characterised by UV-Vis Spectroscopy on a UV-1800 Shimadzu spectrophotometer in the range of 200- 500 nm with double distilled water as baseline using a 10 mm quartz cell. Infrared spectra were recorded using a Perkin Elmer Universal ATR spectrometer.

3.3.2 Scanning electron microscopy (SEM)

The ZnONPs were distributed on an aluminium stub using a sticky carbon tape and sputter-coated with gold for conductivity. The shape and particle size as well as the agglomeration of synthesised ZnONPs were characterised by SEM on a ZEISS LEO 1450.

3.3.3 X-ray diffraction (XRD)

A Bruker D8 Advance X-ray powder diffractometer with Cu K α radiation (wavelength 1.5406 Å) and operated at 10 kV and 30 mA was used to record the diffraction patterns and determine phase composition, and potential impurities. The diffractometer was run in $\theta/2\theta$ configuration. Bragg's law ($n\lambda = 2d \sin \theta$) was used to calculate lattice parameters and other interplanar spacings. Phases were identified by comparison with reference patterns from the JCPDS database. Miller indices were assigned accordingly.

3.3.4 Transmission electron microscopy (TEM)

A small amount of ZnONPs was dissolved in ethanol and sonicated for about 10 minutes to break up agglomerated particles. A drop of the solution was then deposited onto a lacey carbon coated copper grid and allowed to dry at room temperature. A JEOL TEM 2100 operated at an acceleration voltage of 200 kV was used to determine morphology, particle size distribution, elemental composition, phase composition, impurities, crystallinity and aggregation behaviour of the ZnONPs. The microscope is equipped with an EDX detector for chemical analysis and a STEM unit for spot analysis and elemental mapping. Selected area electron diffraction (SAED) was used to determine crystallinity and lattice spacing of the ZnONPs.

3.4. Antioxidant activity

The antioxidant activity of ZnONPs synthesised using extracts and isolated compounds from *S. serratuloides* was determined using the 2,2 diphenyl-1-picrylhydrazyl (DPPH) radical scavenging assay according to the method of Molyneux (2004) with modifications. Volumes of 150 µL of ZnONPs in methanolic solution were prepared at different concentrations (75, 125, 250, 500 and 1000 ppm). These were mixed with 2850 µL of methanolic DPPH solution (0.1 mM) which was prepared by dissolving 39.4 mg in 1000 mL of MeOH. The reaction mixtures were incubated in the dark for 30 minutes at room temperature. The absorbance of samples was measured with ascorbic acid as the standard at 517 nm using a UV spectrophotometer. The solution of DPPH and MeOH without the addition of NPs was used as a control. The percentage scavenging activity was calculated according to the following equation:

$$\% \text{ scavenging activity} = \frac{A_{bc}-A_{bs}}{A_{bc}} \times 100$$

Where A_{bc} = Absorbance of control, A_{bs} = Absorbance of sample.

3.5 Antimicrobial Activity

Bacterial strains of three Gram-negative bacteria (*Pseudomonas aeruginosa* ATCC 27853, *Escherichia coli* ATCC 35218 and *Chromobacterium violaceum* ATCC 12472) and two Gram-positive bacteria (*Staphylococcus aureus* ATCC 43300 and *Enterococcus faecalis* ATCC 51299) were used in this study. The bacteria were chosen due to the variety of properties they exhibit. *Pseudomonas aeruginosa* ATCC 27853 is a known multidrug resistant organism. *Escherichia coli* ATCC 35218 produces β -lactamase. *Chromobacterium violaceum* ATCC 12472 is a quorum sensing inhibitor indicator. *Staphylococcus aureus* ATCC 43300 is resistant to methicillin, and *Enterococcus faecalis* ATCC 51299 is resistant to vancomycin.

3.5.1 Antibacterial activity

The antibacterial activity of test samples (crude aqueous and MeOH extracts of *S. serratuloides* leaves, isolated compounds (compounds 6 and 7) and synthesised ZnONPs) was determined using the disc diffusion method. Blank discs (MAST, UK) were impregnated with 25 and 50 μL of test samples and allowed to dry. Bacterial isolates were grown overnight on Luria-Bertani (LB) agar plates, and the turbidity of cell suspensions was adjusted to be equivalent to that of a 0.5 McFarland standard. These bacteria were used to inoculate Mueller-Hinton (MH) agar plates by streaking swabs over the entire agar surface followed by the application of the respective test sample disc.

The plates were incubated for 21 h at 30 °C. Testing was done in duplicate and tetracycline (TE30) and ampicillin (AMP10) discs were used as standard antimicrobial controls. Zone diameters were measured and averaged. The following criteria were used to assign susceptibility or resistance to phytochemicals tested: Susceptible (S) ≥ 15 mm, Intermediate (I) = 11 – 14 mm, and Resistant (R) ≤ 10 mm. Criteria for assigning susceptibility or resistance to AMP10 were as follows: (S) ≥ 17 mm, (I) = 14–16 mm, (R) ≤ 13 mm, while those for TE30 were: (S) ≥ 19 mm, (I) 15–18 mm, (R) ≤ 14 mm.

3.5.2 Quorum sensing inhibition (QSI) – agar overlay assay

The anti-quorum sensing activity of test samples (crude aqueous and MeOH extracts of *S. serratuloides* leaves, isolated compounds (compounds 6 and 7) and synthesised ZnONPs) was determined using the pigmented biosensor strain *C. violaceum* ATCC 12472. Molten soft LB agar (5 mL, 0.3% w/v) was inoculated with 150 μL of *C. violaceum* ATCC 12472 and grown overnight in LB broth. The agar culture solution was poured over the surface of pre-warmed LB agar plates, immediately. Volumes of 25 and 50 μL of test samples were pipetted on sterile paper discs, dried and placed on the solidified agar.

The plates were incubated overnight at 30 °C and examined for violacein pigment production. Quorum sensing inhibition (QSI) was detected by the appearance of a colourless, opaque, but visible halo around the discs which indicated the loss of pigmentation. Purified halogenated furanone (10 and 20 $\mu\text{g mL}^{-1}$) was used as a known quorum sensing inhibitor, and DMSO was used as a control.

CHAPTER FOUR

RESULTS AND DISCUSSION

In this section results obtained from the phytochemical analysis, synthesis of ZnONPs using *Senecio serratuloides* DC extracts and isolated compounds and testing of their biological activity are reported and discussed.

4.1. Spectroscopic Data of Compounds

This section summarises the spectroscopic data obtained for the isolated compounds. The experimental spectra can be found in the appendix. The explanation for the identification of each compound follows the spectral data. The chemical structures of compounds isolated from *S. serratuloides* are presented in Figure 4.1.

Farnesyl amine (1): White crystals; m/z (rel %): 221 $[M]^+$, IR spectra (KBr) V_{\max} cm^{-1} ; 3436, 2916, 2848, 1713, 1462, 1377, 1047, 719; ^1H -NMR spectral data (400 MHz, CDCl_3) δ_{H} 5.11 (H-2, 6, 10), 2.07 (2H-1), 2.06 (2H-4), 2.05 (2H-9), 2.03 (2H-5), 1.69 (3H-12), 1.62 (3H-13, 3H-14, 3H-15), 1.28 (2H-8); ^{13}C -NMR spectral data (400 MHz, CDCl_3) δ_{C} 134.82 (C-3), 134.16 (C-7), 130.97 (C-11), 124.12 (C-6), 124.02 (C-10), 123.98 (C-2), 39.45 (C-1, 4), 29.42 (C-8), 27.99 (C-5), 26.48 (C-9), 25.41 (C-12), 17.39 (C-13), 15.75 (C-14), 15.71 (C-15).

β -Sitosterol (2): white crystalline powder; m/z (rel %): 414 $[M]^+$, IR spectra (KBr) V_{\max} cm^{-1} 3489, 3313, 2925, 2186, 2010, 1431, 1375, 1093, 1046, 697, 630; ^1H -NMR spectral data (400 MHz, CDCl_3) δ_{H} 5.35 (1H, m, H-5, $J = 6.4$ Hz), 3.52 (1H, m, H-3, $J = 4.7$ Hz), 0.95 (d, $J = 6.2$ Hz, H-19), 0.89 (t, $J = 7.1$ Hz, H-24), 0.86 (d, $J = 6.6$ Hz, H-26), 0.80 (d, $J = 6.6$ Hz, H-27), 0.71 (s, H-28), 1.03 (s, H-29). ^{13}C -NMR spectral data (400 MHz, CDCl_3) δ_{C} 140.76 (C-5), 121.72 (C-6), 71.82 (C-3), 56.063 (C-14), 56.775 (C-17), 50.142 (C-9), 33.95 (C-20), 39.782

(C-13), 42.32 (C-4), 39.78 (C-12), 36.148 (C-1), 19.39 (C-19), 11.92 (C-24), 11.86 (C-29), 21.08 (C-26), 19.03 (C-28), 19.87 (C-27).

Mixture of α and β -amyrin (3): white powder; m/z (rel %): 426 $[M]^+$, IR spectra (KBr) V_{\max} cm^{-1} ; 3423, 2895 and 2850, 1714, 1462, 1378, 1172, 1036, 995, 719; ^1H -NMR spectral data (400 MHz, CDCl_3) δ_{H} 5.15 (1H, t, $J = 3.5$ Hz, H-12), 3.19 (m, H-3), 1.03 (3H, d, $J = 1.01$ Hz), 0.97 (s, H-23), 0.96 (3H, s, H-26), 0.91 (3H, s, H-25), 0.87 (6H, s, H-29, 30), 0.83 (3H, s, H-18), 0.79 (3H, s, H-24), 0.75 (1H, d, $J = 1.8$ Hz).

The ^{13}C NMR spectral data (400 MHz, CDCl_3) δ_{C} 145.06 (C-13 β), 139.46 (C-13 α), 124.30 (C-12 α), 121.61 (C-12 β), 78.95 (C-3), 58.95 (C-5 α), 55.07 (C-5 β), 47.60 (C-9), 47.51 (C-9), 47.11 (C-18), 46.71 (C-19), 41.96 (C-14), 41.60 (C-14), 39.90 (C-4), 39.54 (C-4), 39.48 (C-8), 39.24 (C-8), 38.67 (C-1), 38.64 (C-10), 37.16 (C-22), 36.77 (C-21), 34.61 (C-29), 33.62 (C-29), 33.20 (C-7), 32.82 (C-17), 32.66 (C-20), 30.95 (C-20), 29.22 (C-23), 28.62 (C-23), 28.27 (C-28), 28.00 (C-28), 27.10 (C-2), 27.06 (C-16), 26.82 (C-15), 26.03 (C-27), 23.56 (C-30), 23.41 (C-11), 18.23 (C-6), 17.34 (C-26), 16.74 (C-25), 16.68 (C-24).

Stigmasterol (4): white needles; m/z (rel %): 412 $[M]^+$, IR spectra (KBr) V_{\max} cm^{-1} ; 3419, 2917, 2849, 1707, 1463, 1377, 1042, 719 ^1H -NMR spectral data (400 MHz, CDCl_3) δ_{H} 5.32 (1H, m, H-6), 5.10 (1H, dd, $J = 15.3, 8.0$ Hz, H-22), 5.02 (1H, dd, $J = 15.3, 8.0$ Hz, H-23), 3.50-3.47 (1H, m, H-3), 0.90 (3H, d, $J = 6.5$ Hz, Me-21), 0.89 (3H, d, $J = 6.6$ Hz, Me-26), 0.85 (3H, t, $J = 7.0$ Hz, Me-29), 0.82 (3H, d, $J = 6.5$ Hz, Me-27), 0.80 (3H, s, Me-19), 0.67 (3H, s, Me-18).

The ^{13}C -NMR spectral data (400 MHz, CDCl_3) δ_{C} 140.75 (C-5), 138.31 (C-22), 129.28 (C-23), 121.72 (C-6), 71.83 (C-3), 56.87 (C-14), 55.96 (C-17), 51.24 (C-24), 50.16 (C-9), 42.30 (C-13), 40.30 (C-4), 39.68 (C-20), 37.25 (C-12), 36.51 (C-1), 31.90 (C-10), 39.1 (C-8), 34.0 (C-

25), 31.66 (C-7), 29.70 (C-2), 28.92 (C-16), 28.92 (C-28), 26.07 (C-15), 24.36 (C-27), 22.69 (C-21), 21.08 (C-11), 19.03 (C-19), 18.89 (C-26), 12.25 (C-18), 12.05 (C-29).

Taraxerone (5): white powder; IR spectra (KBr) V_{\max} cm^{-1} 3405, 2850, 1707, 1463, 1385, 1176, 994, 719, 584; HR-ESI-MS at m/z 425.3776 $[\text{M}+\text{H}]^+$ (calculated, 425.3783). ^1H -NMR spectral data (400 MHz, CDCl_3) δ_{H} 5.52 (m, $J = 8.2$ Hz, H-15), 2.59 (dd, $J = 4.8, 18.9$ Hz, H-2), 2.57 (dd, $J = 7.0$), 2.34 (d, $J = 3.2$ Hz), 2.31 (d, $J = 8.9$ Hz), 2.09 (d, $J = 14.0$ Hz), 2.04 (d, $J = 6.4$ Hz), 1.92 (d, $J = 2.9$ Hz), 1.88 (d, $J = 3.0$ Hz), 1.85 (dd, $J = 3.4, 6.2$ Hz), 1.65 (d, $J = 4.7$ Hz), 1.59 (d, $J = 12.1$ Hz), 1.55 (d, $J = 8.9$ Hz), 1.01 (d, $J = 7.8$ Hz), 0.91 (s), 0.88 (s), 0.81 (s).

The ^{13}C -NMR spectral data (400 MHz, CDCl_3) δ_{C} 217.57 (C-3), 157.50 (C-14), 117.08 (C-15), 55.67 (C-5), 48.68 (C-18), 48.59 (C-9), 47.48 (C-4), 40.52 (C-19), 14.01 (C-29).

Jacaranone (6): yellow crystals; IR spectra (KBr) V_{\max} cm^{-1} ; 3254, 2957, 2929, 2661, 1866, 1731, 1664, 1611, 1439, 1377, 1278, 1222; HR-ESI-MS at m/z 205.0477 $[\text{M}+\text{Na}]^+$ (calculated, 205.0477); ^1H -NMR spectral data (400 MHz, CDCl_3) δ_{H} 2.67 (2H, s, CH_2 , H-7) 3.73 (3H, s, OMe, H-9) 6.18 (2H, d, $J = 10$ Hz, H-2, 6), 6.94 (2H, d, $J = 10$ Hz, H-3, 5); ^{13}C -NMR spectra data (400 MHz, CDCl_3) δ_{C} 184.94 (C-4), 128.32 (C-2, 6), 148.85 (C-3, 5), 67.34 (C-1), 43.30 (C-7), 171.30 (C-8), 52.33 (C-9).

Methyl-2-(1-hydroxy-4-oxocyclohexyl)acetate (7): yellow oil; IR spectra (KBr) V_{\max} cm^{-1} ; 3390, 2954, 1717, 1667, 1530, 1439, 1161, 1042, 861; HR-ESI-MS at m/z 391.1372 $[\text{M}+\text{Na}]^+$ (calcd, 391.1369); GC-MS at m/z (rel %): 182 and 186 $[\text{M}]^+$; ^1H -NMR spectral data (400 MHz, CDCl_3) δ_{H} 2.77 (2H, t, $J = 6.6$ Hz, H-3'b, 5'b), 1.73 (2H, t, $J = 4.5$ Hz, H-3'a, 5'a), 2.06 (2H, t, $J = 3.3$ Hz, H-2'a, 6'a), 2.10 (2H, t, $J = 6.3$ Hz, H-2'b, 6'b), 2.54 (2H, s, H-7'), 3.72 (3H, s, H-9').

The ^{13}C -NMR (400 MHz, CDCl_3) δ_{C} 211.28 (C-4'), 173.09 (C-8'), 68.33 (C-1'), 51.83 (C-9'), 44.43 (C-7'), 36.74 (C-3', 5'), 36.52 (C-2', 6').

4.1.1 Identification of secondary metabolites isolated from *Senecio serratuloides*

The ^1H and ^{13}C -NMR spectral assignments for compounds 1 to 4 were made by comparison of experimentally observed chemical shifts with literature data. The hexane extract from the leaves yielded farnesylamine (1), a sesquiterpene amine which is known to produce unbranched fatty acids derived from alkaloids. This compound has previously been detected in animal species such as ants of *Monomorium fieldi* Forel and was shown to inhibit pancreatic cancer. It was also isolated from *Vernonia auriculifera* (Kiplimo *et al.*, 2011, Jones *et al.*, 2003). β -sitosterol (2) has previously been isolated from *Ageratum conyzoides* (Kamboj and Saluja, 2011).

The DCM extract from the leaves yielded a mixture of α - and β -amyrin (3) and stigmasterol (4). Amyrins are pentacyclic triterpenoids that have previously been isolated from the stem bark of *Alstonia boonei* (Okoye *et al.*, 2014); they have been reported to have anti-inflammatory and antifungal activity (Vázquez *et al.*, 2012). Stigmasterol (4) is a phytosterol also isolated from other medicinal plants such as *Heteropogon contortus* and *Ageratum conyzoides* (Kamboj and Saluja, 2011, Kaur and Gupta, 2018).

The hexane extract from the stem bark yielded compound (5), which was isolated as a white powder. HR-ESI-MS showed a molecular ion peak at m/z 425.3776 $[\text{M}+\text{H}]^+$ (calculated 425.3783) which agrees with the molecular formula $\text{C}_{30}\text{H}_{48}\text{O}$. The IR spectrum showed a broad absorption band at 1707 cm^{-1} (C=O group) and 1463 cm^{-1} (C=C). The ^{13}C -NMR spectrum indicated thirty resonances that corresponds with pentacyclic triterpenes. The ^1H -NMR spectrum confirmed the presence of eight methyl groups, all of which were singlets (δ 0.81, (2 \times 0.89), 0.93, 1.04, (2 \times 1.06) and 1.12). The spectrum also showed a doublet of doublets at δ 5.55 ($J = 7.8, 2.7\text{ Hz}$, H-15) which was ascribed to the olefinic proton.

The DEPT experiments showed eight quaternary carbons, four methines, ten methylenes and eight methyl groups. The carbon signal at δ 217.57 (C-3) indicated the presence of a carbonyl group. The singlet at δ 157.50 and doublet at δ 117.08 was assigned to C-14 and C-15, respectively. This data together with NMR spectral data corresponded with that in the literature and confirmed compound 5 to be a taraxerone (Shiojima *et al.*, 1996).

Compound 6 was isolated from the MeOH extract of leaves as a yellow crystal with a mass of 80 mg. HR-ESI-MS showed a molecular ion peak at m/z 205.0477 $[M+Na]^+$ (calculated 205.0477), suggesting a molecular formula of $C_9H_{10}O_4$. The 1H -NMR spectrum shows doublet resonance at δ 6.18 (H-2, 6) and δ 6.94 (H-3, 5) with a coupling constant of $J = 10$ Hz, confirming the presence of a para-disubstituted cyclohexadiene ring. This was supported by the intensity of the carbon signal at δ 148.35 (C 2, 6) and δ 128.32 (C3, 5). The HMBC experiment showed correlations between vinyl protons (H-2, 6 and H-3, 5) and the carbonyl carbon at δ 184.94 (C-4) confirming a carbonyl group as one of the substituents on the ring. The HMBC experiment also showed the correlation between δ 67.34 (C-1) and the vinyl protons, suggesting a hydroxyl group as another substituent.

The carbon signal at δ 171.30 (C-8) suggested another carbonyl carbon and its correlation with methoxy protons at δ 3.75 (H-9) confirmed the presence of a methyl ester moiety. The position of the methyl ester was confirmed by the correlation between the carbonyl carbon (C-8) and the methylene protons at δ 2.67 (H-7) as well as the correlation between the quaternary carbon δ 67.34 (C-1) and the methylene protons.

The IR spectrum of compound 6 further confirmed the presence of a carbonyl group (absorption band at 1731 cm^{-1}) and hydroxyl group (3254 cm^{-1}).

The above-mentioned data together with that in literature confirmed compound 6 to be jacaranone. Jacaranones have previously been reported from plants such as the *Jacaranda* (Gachet et al., 2010), *Senecio* and *Delesseria* species (Yvin *et al.*, 1985).

Compound 7 was isolated from the MeOH extract of leaves as a yellow oil with a mass of 55 mg. HR-ESI-MS of compound 7 showed only one molecular ion peak at m/z 391.1372 $[M+Na]^+$ (calculated 391.1369), indicating a formula of $C_{18}H_{24}O_8$. However, GC-MS data showed two molecular ion peaks $[M+]$ at m/z 182.75 corresponding to $C_9H_{10}O_4$ and 185.40 corresponding to $C_9H_{14}O_4$. The ^{13}C -NMR spectrum confirmed the presence of eighteen carbons. DEPT experiments showed the presence of six quaternary carbons, four methines, six methylenes and two methyl groups. Resonances for jacaraone were observed in the NMR spectra. In addition, the chemical shift at δ_c 211 (C-4'), 36.74 (C-3', 5'), 36.52 (C-2', 6'), 68.33 (C-1') and the proton signals at δ_H 1.73 (2H, t, $J = 4.5$ Hz, H-3'a, 5'a), 2.77 (2H, t, $J = 6.6$ Hz, H-3'b, 5'b), 2.06 (2H, t, $J = 3.3$ Hz, H-2'a, 6'a), 2.10 (2H, t, $J = 6.3$ Hz, H-2'b, 6'b), confirm the presence of 4-oxo-cyclohexanone. The carbon signals at 173.09 (C-8') and 51.83 (C-9') confirm the presence of another carbonyl and methyl ester, respectively. Thus, compound 7 was identified as a mixture of jacaranone and methyl-2-(1-hydroxy-4-oxocyclohexyl)acetate. Attempts to further separate the two compounds were not successful. These two compounds have previously been isolated from *Senecio cleaveland* (Bohlmann *et al.*, 1981).

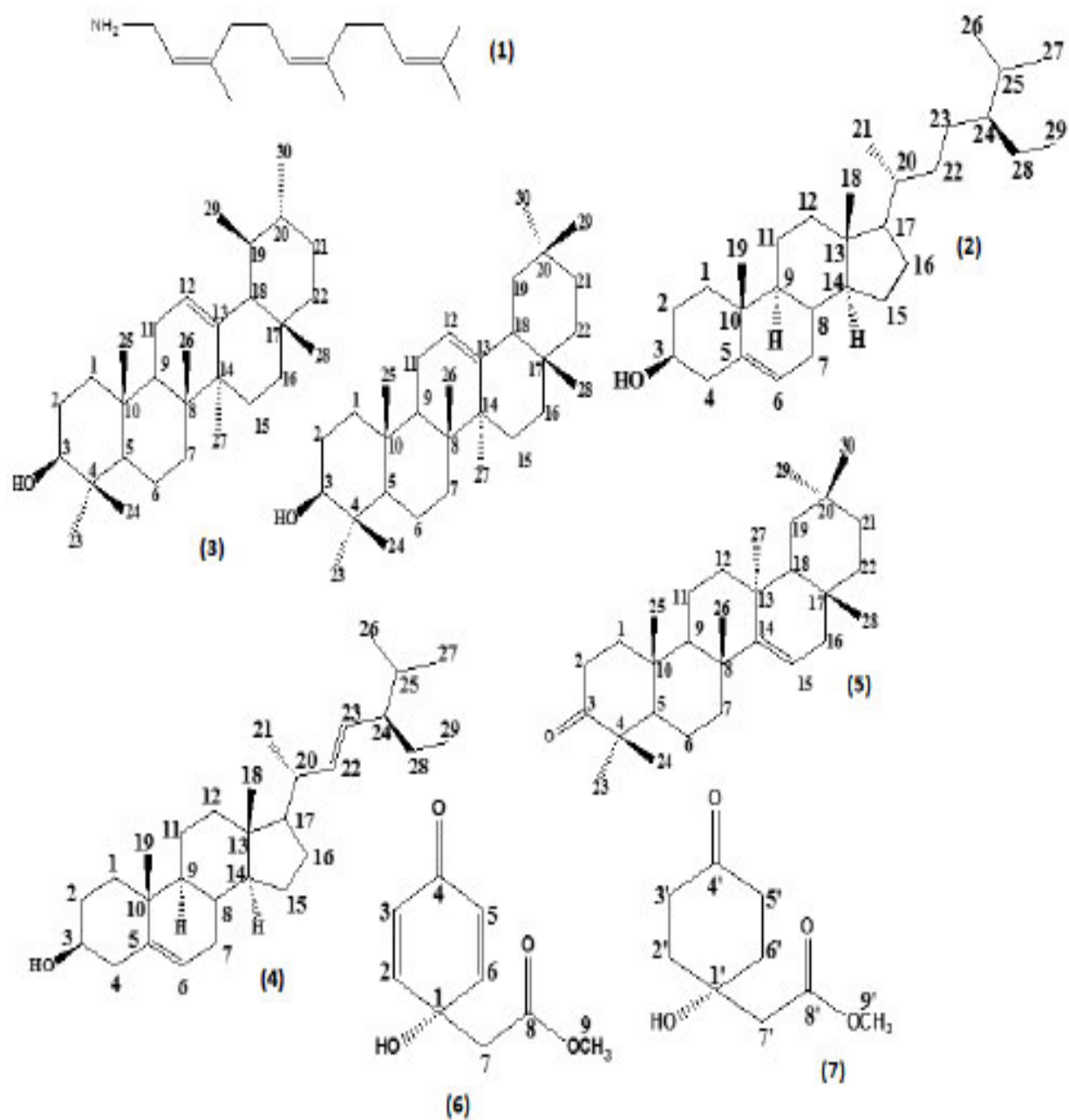


Figure 4.1: Chemical structures of compounds isolated from *Senecio serratuloides*

4.2 Characterisation of Nanoparticles

4.2.1 Ultraviolet-visible (UV-Vis) spectroscopy

The synthesis of ZnONPs was initially confirmed by visual inspection and observation of a colour change before and after reaction. The colour of the solution changed from light yellow to brown with a precipitate. It has been reported that the addition of plant extracts to aqueous zinc nitrate solution produces a colour change due to the surface plasmon resonance (SPR) of the formed ZnONPs (Manokari and Shekhawat, 2016). Surface plasmon resonance is the surface oscillation of high-density free electrons that occurs under irradiation with light. The colloidal solutions of NPs show differences in colour depending on their shape and size (Lee *et al.*, 2008, Stroyuk *et al.*, 2005).

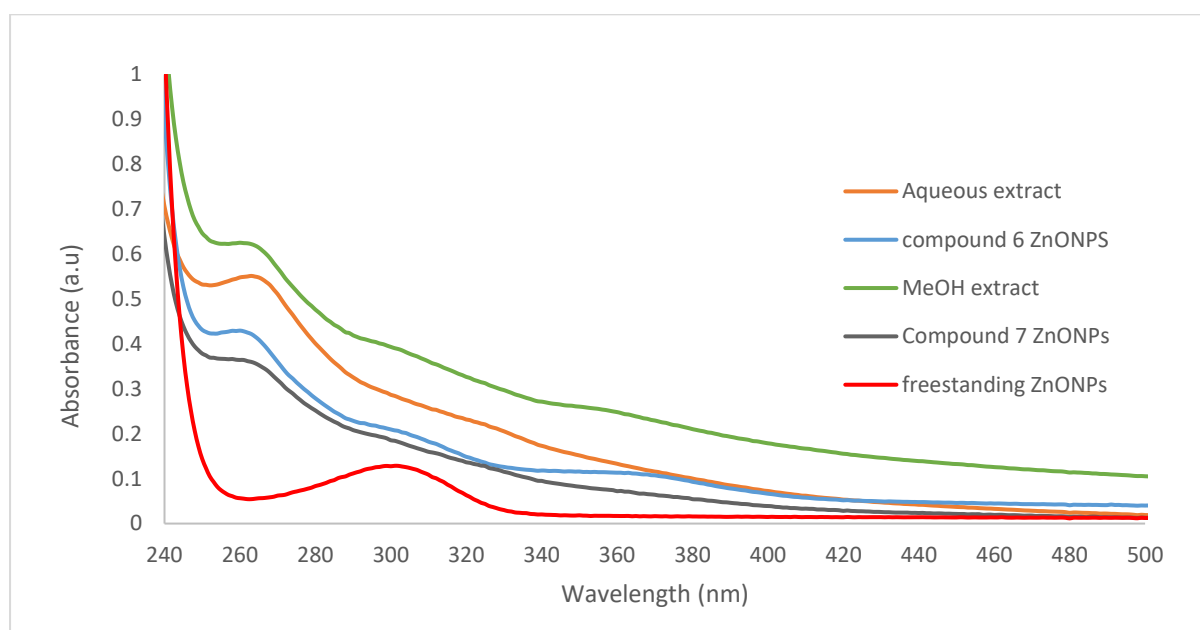


Figure 4.2: UV-Vis spectra of ZnONPs produced from aqueous and methanolic extracts of *S. serratuloides* as well as compound 6 (jacaranone), compound 7 (jacaranone and methyl-2-(1-hydroxy-4-oxocyclohexyl)acetate) and freestanding ZnONPs

UV-Vis was used to characterise and confirm the synthesis of ZnONPs. Zinc oxide NPs show a broad peak in the range of 200-700 nm. The synthesised ZnONPs from aqueous and methanolic extracts of leaves and compound 6 (jacaranone) and 7 (jacaranone and methyl-2-(1-hydroxy-4-oxocyclohexyl)acetate) of *S. serratuloides* exhibited an absorption peak between 262 and 267 nm. The freestanding ZnONPs had an absorption peak at 305 nm (Fig 4.2). The shift from shorter wavelengths for the plant-synthesised ZnONPs to longer wavelengths for the freestanding ZnONPs indicates an increase in size.

4.2.2 Fourier-transform infrared (FT-IR) spectroscopy

The FT-IR spectra of ZnONPs are shown in Figure 4.4 in the range of 300 to 4000 cm^{-1} . The peak at 416 cm^{-1} for the aqueous extract, at 455 cm^{-1} for methanolic extract, at 451 cm^{-1} for the mixture of jacaranones and at 470 cm^{-1} for jacaranone corresponds to ZnO stretching vibrations which confirm the presence of ZnONPs. The broad peak at 3321 cm^{-1} is due to the O-H stretching vibration of residual water molecules on remaining $\text{Zn}(\text{OH})_2$. The sharp peak at 2934 cm^{-1} is due to the stretching vibration of C-H (alkane) bonds, and the bands at 840- 865 cm^{-1} is due to the presence of CH_2 vibration bonds.

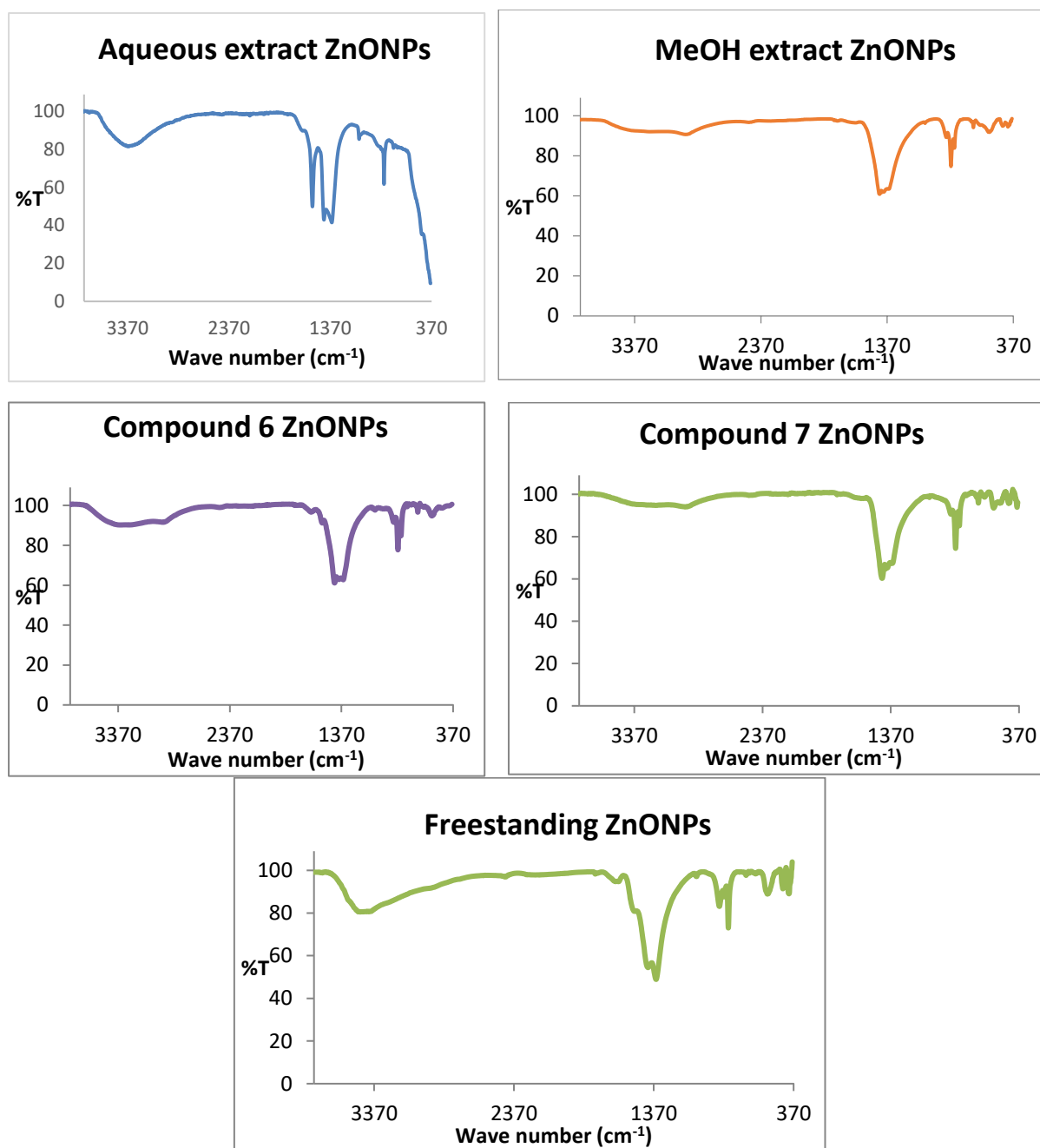


Figure 4.3: FT-IR spectra of ZnO nanoparticles

4.2.3 X-ray diffraction (XRD)

The XRD analysis of ZnONPs prepared from the aqueous extract (A), methanolic extract (B), mixture of jacaranones (C) and jacaranone (D) are shown in Figure 4.14. The XRD pattern shows distinctive diffraction peaks in the range between 30 and 80°. The observed reflections at 31.84, 34.74, 36.73, 47.76, 56.75, 62.83, 66.85, 68.46 and 69.60 degrees of 2 θ correspond

to (100), (022), (101), (102), (110), (103), (200), (112) and (201) crystal planes of the hexagonal ZnO (Wurtzite structure), respectively. They are in good agreement with the Joint Committee on Powder Diffraction Standards (JCPDS) card PDF no 36-1451 file for ZnO ($a = b = 3.249 \text{ \AA}$, $c = 5.206 \text{ \AA}$) with space group of $P6_3mc$. The observed peaks are sharp, which indicates that the formed ZnONP is well crystalline. Small peaks indicate the presence of small amounts of impurities for freestanding ZnONPs which might result from Zn(OH)_2 or from starting material. The crystallite size of ZnONPs calculated using the Scherrer formula for the (101) peak, with full width and half maximum (FWHM) of 0.323 was 0.26 nm which is in good agreement with the TEM results. The XRD results are in good agreement with the SAED patterns. Crystallite size of ZnONPs was calculated by Scherrer formula as follows:

$$D = \frac{0.9\lambda}{\beta \cdot \cos\theta}$$

Where D = crystallite size, $\lambda = 0.154 \text{ nm}$ for $\text{CuK}\alpha$, and β = FWHM (line width at half maximum)

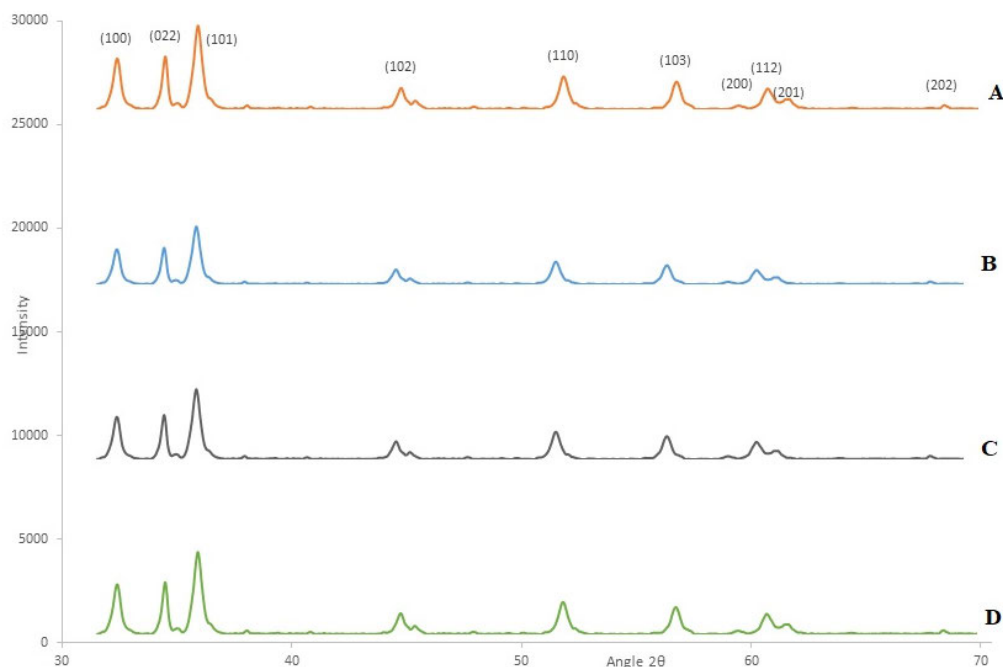


Figure 4.4: XRD patterns of ZnONPs synthesised using aqueous extract (A), methanolic extract (B), the mixture of jacaranones (C) and jacaranone (D).

Table 4.1: Calculated d-spacing values using Braggs Law, $\lambda = 2.d \sin\theta$

Nanoparticle	Experimental Calculated values		Reference with PDF no. 00-036-1451		
	2θ (°)	d-spacing (Å)	Intensity	d-spacing (Å)	(hkl)
ZnO	31.84	2.8070	57	2.8101	100
	34.74	2.5792	44	2.5890	002
	36.76	2.4439	100	2.4472	101
	47.76	1.9021	23	1.9080	102
	56.75	1.1602	32	1.6220	110

4.2.4 Scanning electron microscopy (SEM)

The SEM images of ZnONPs are shown in Figure 4.3. They show the surface morphology, size, shape and agglomeration of ZnONPs synthesised from aqueous extract (A), methanolic extract (B), mixture of jacaranones (C) and jacaranone (D). The lower magnification images of ZnONPs demonstrated that synthesised nanoparticles were almost spherical shaped and smooth surface is observed in ZnONPs synthesised using aqueous, methanol extracts and phytocompounds (A – D) compared to freestanding ZnONPs (E). They appear to be strongly agglomerated forming mostly spherical shapes in different size range. It is observed that ZnONPs synthesised from plant extracts and phytocompounds are mono-dispersed, homogeneously distributed and grown in moral density in nature, especially those synthesised from aqueous extracts (A).

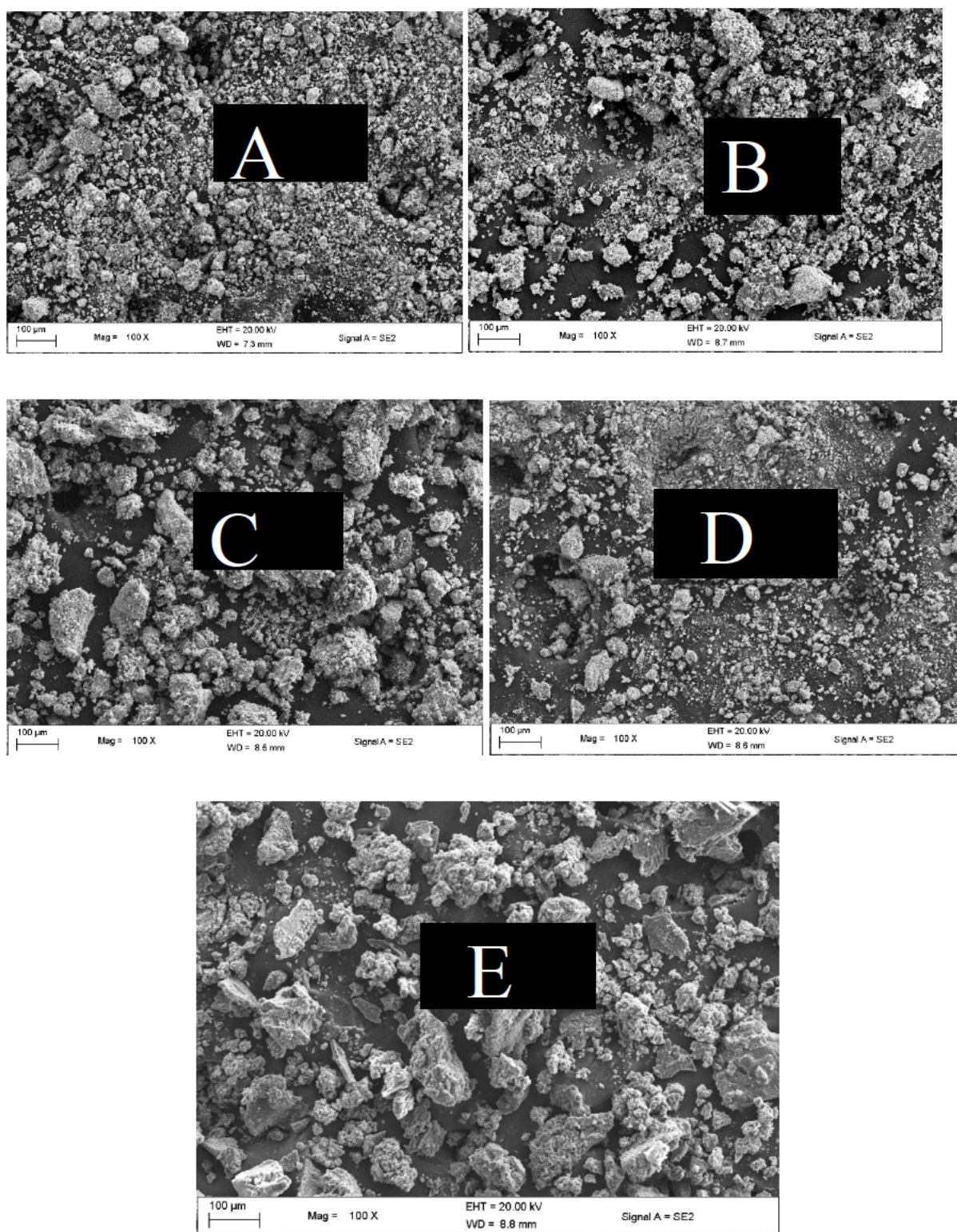


Figure 4.5: SEM images of ZnONPs synthesised from aqueous extract (A), methanolic extract (B), jacaranone mixture (C), pure jacaranone (D) and freestanding ZnONPs (E)

4.2.5 Transmission electron microscopy (TEM)

Figure 4.6 shows a TEM image of the freestanding ZnONPs. It can be seen that there is a large variation of sizes and shapes. Small spherical particles exist together with long thin bands, thin sheets and agglomerations of irregular shape.

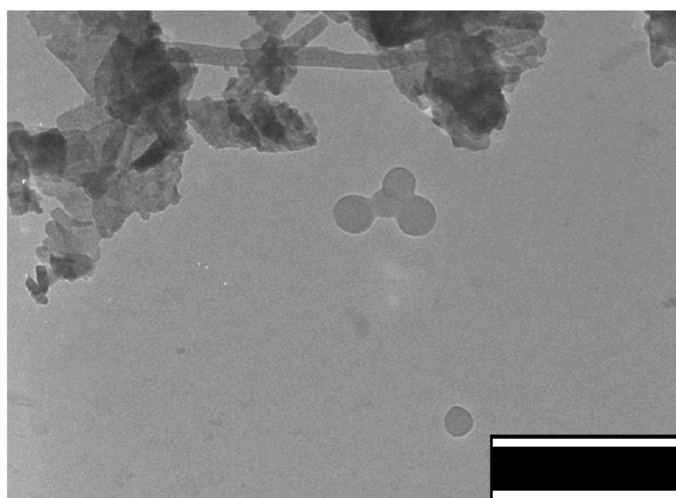


Figure 4.6: TEM images of freestanding ZnONPs

Figure 4.7 shows TEM images and particle size distributions of ZnONPs synthesised from aqueous extract (A), methanolic extract (B), mixture of jacaranones (C) and jacaranone (D). The synthesised ZnONPs were mostly spherical in shape with a large range of sizes. The medium particle size of ZnONPs was 18 nm for aqueous extracts, 15 nm for methanolic extract, 16 nm for the mixture of jacaranones and 18 nm for jacaranone. Given the dispersity of the particles and the presence of particles with different shapes that will be shown in the following, these numbers are probably not too significant though.

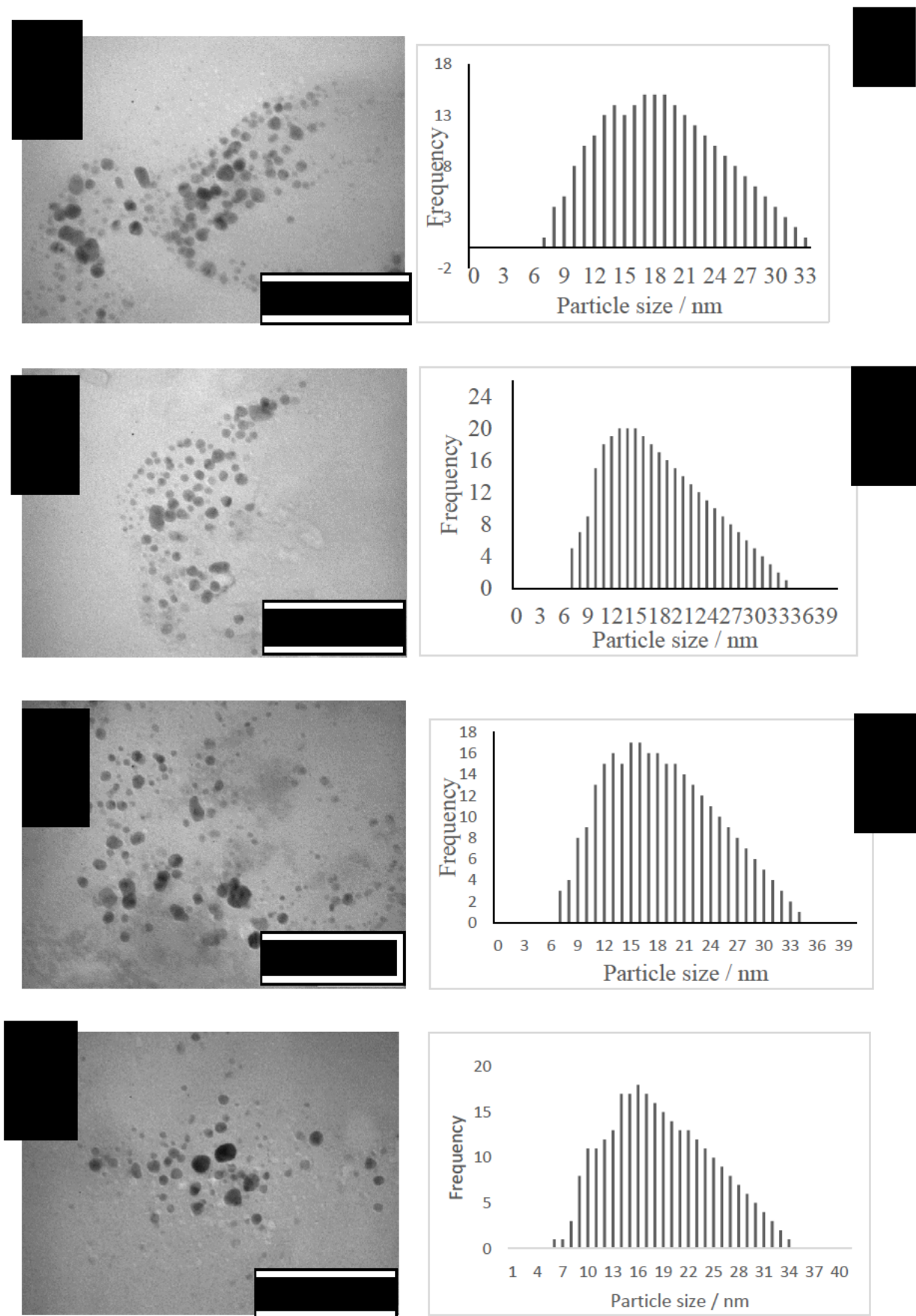


Figure 4.7: TEM images at low magnification and particle size distribution of ZnONPs

More TEM images and SAED patterns of the ZnONPs, some showing lattice fringes, are shown in Figure 4.8 for the aqueous extract, Figure 4.10 for the methanolic extract, Figure 4.12 for mixture of jacaranones, Figure 4.14 for pure jacaranone 4.16 for freestanding ZnONPs. The TEM images at higher resolution show that many of the synthesised ZnONPs are actually not spherical in shape but have irregular shapes and large thin plates. The observed lattice spacings of 0.25 nm, 0.26 nm, and 0.28 nm correspond to (101), (002), and (100) planes of hexagonal zinc oxide. The SAED patterns include some single-crystal patterns as well as some patterns from several crystallites. The sharpness of the peaks confirmed the presence of well crystalline ZnO in Wurtzite structure. The elemental composition of the NPs was determined by EDX. EDX spectra of ZnONPs synthesised from aqueous extract are shown in Figure 4.9, those from methanolic extracts in Figure 4.11, those from the mixture of jacaranones in Figure 4.13, those from jacaranone in Figure 4.15 and figure 4.17 for freestanding. The spectra look similar with Zn and O being the major constituents. The carbon (C) and copper (Cu) peaks are due to the carbon-coated copper grids that were used by to support the sample.

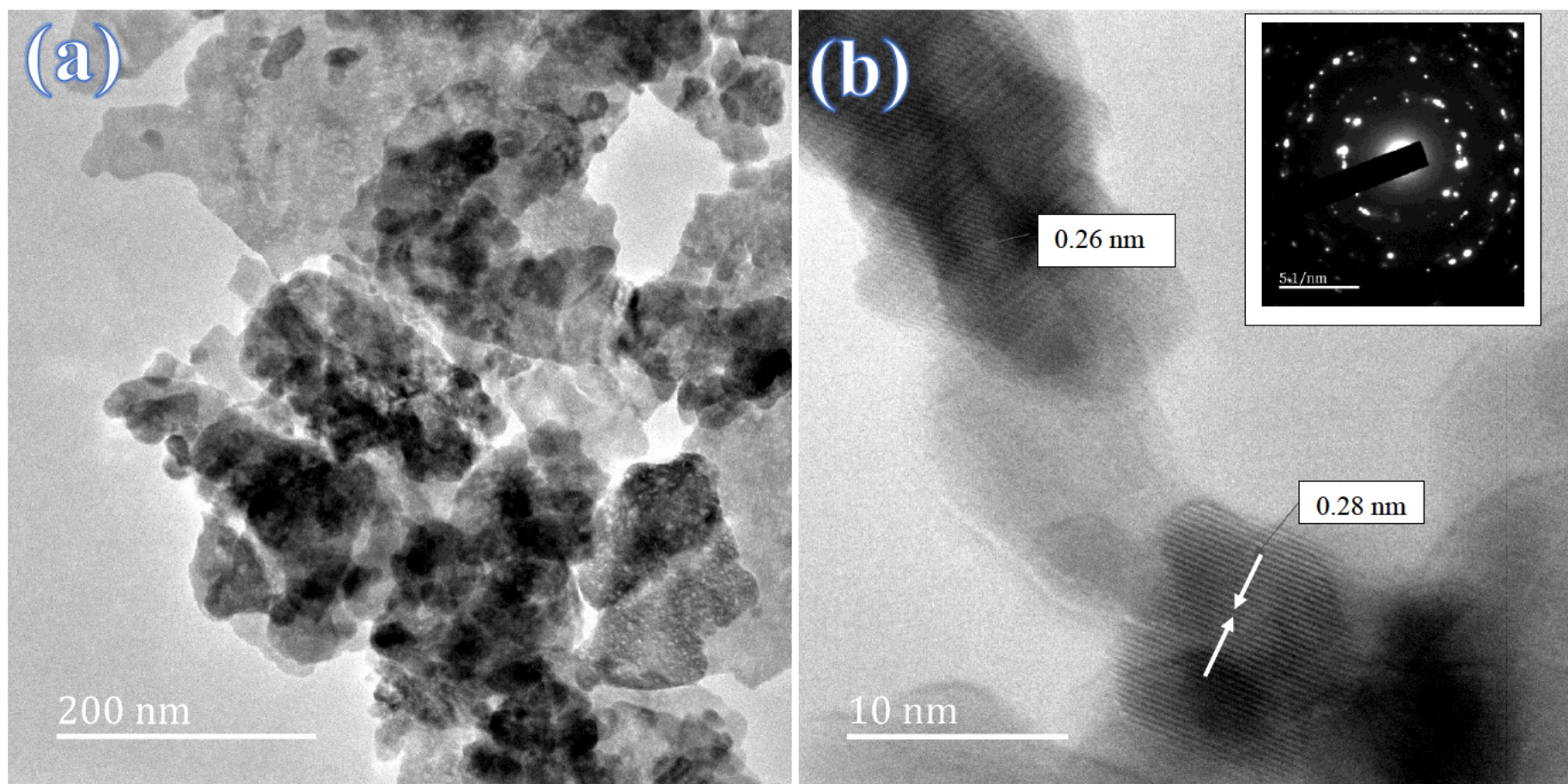
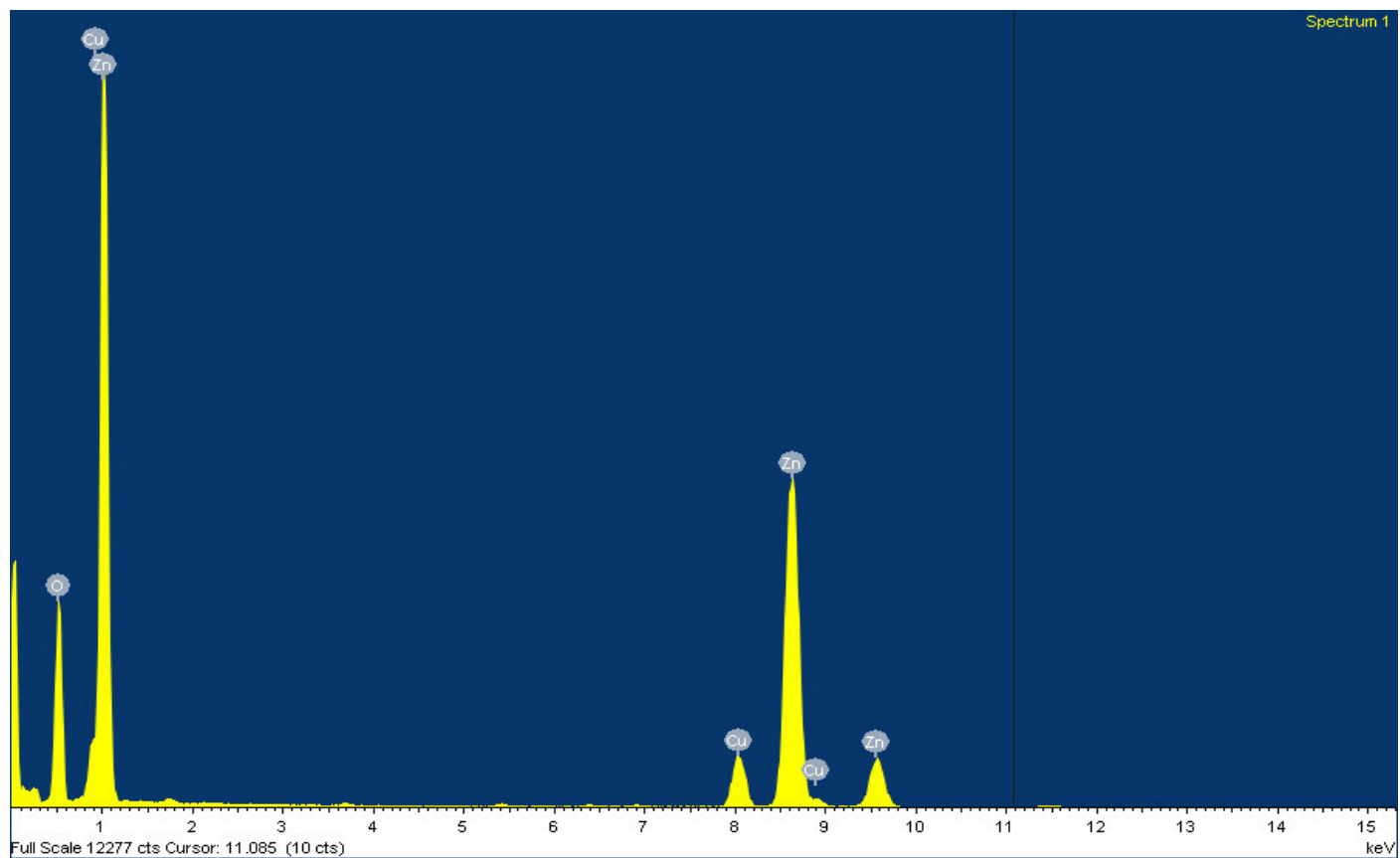


Figure 4.8: TEM images (a) low magnification (b) high magnification (inset SAED pattern) of ZnONPs synthesised with aqueous extract



Elements	Weight %	Atom%
C	1.79	6.08
O	19.29	46.61
Cu	9.25	5.75
Zn	67.28	40.56

Figure 4.9: Energy dispersive X-ray spectrum of ZnONPs synthesised from aqueous extract

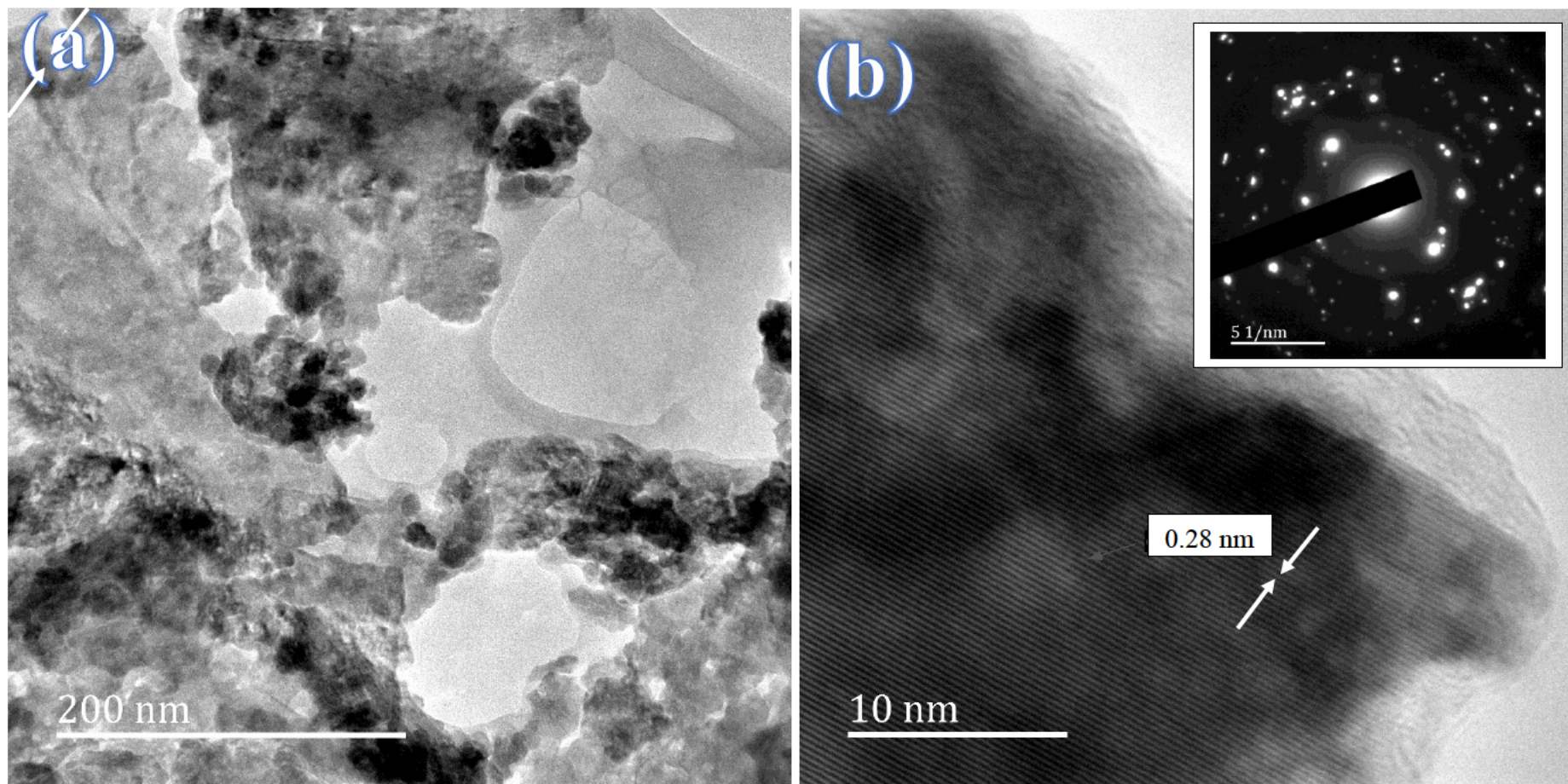
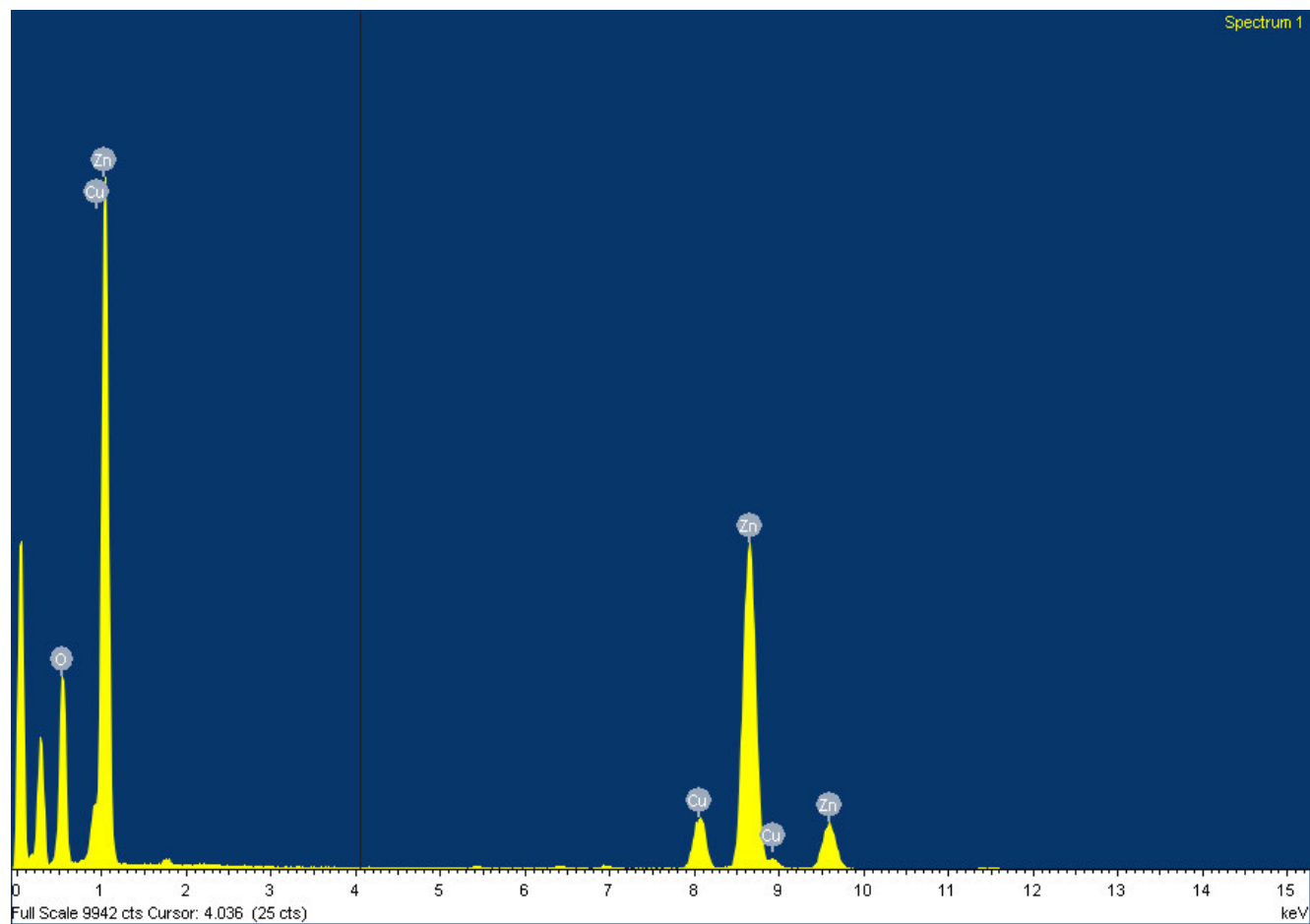


Figure 4.10: TEM images (a) low magnification (b) high magnification (inset SAED pattern) of ZnONPs synthesised with methanolic extract



Element	Weight%	Atomic%
C	13.88	35.14
Cu	8.61	4.12
O	17.86	32.29
Zn	59.24	27.55

Figure 4.11: Energy-dispersive X-ray spectrum of ZnONPs synthesised from methanolic extract

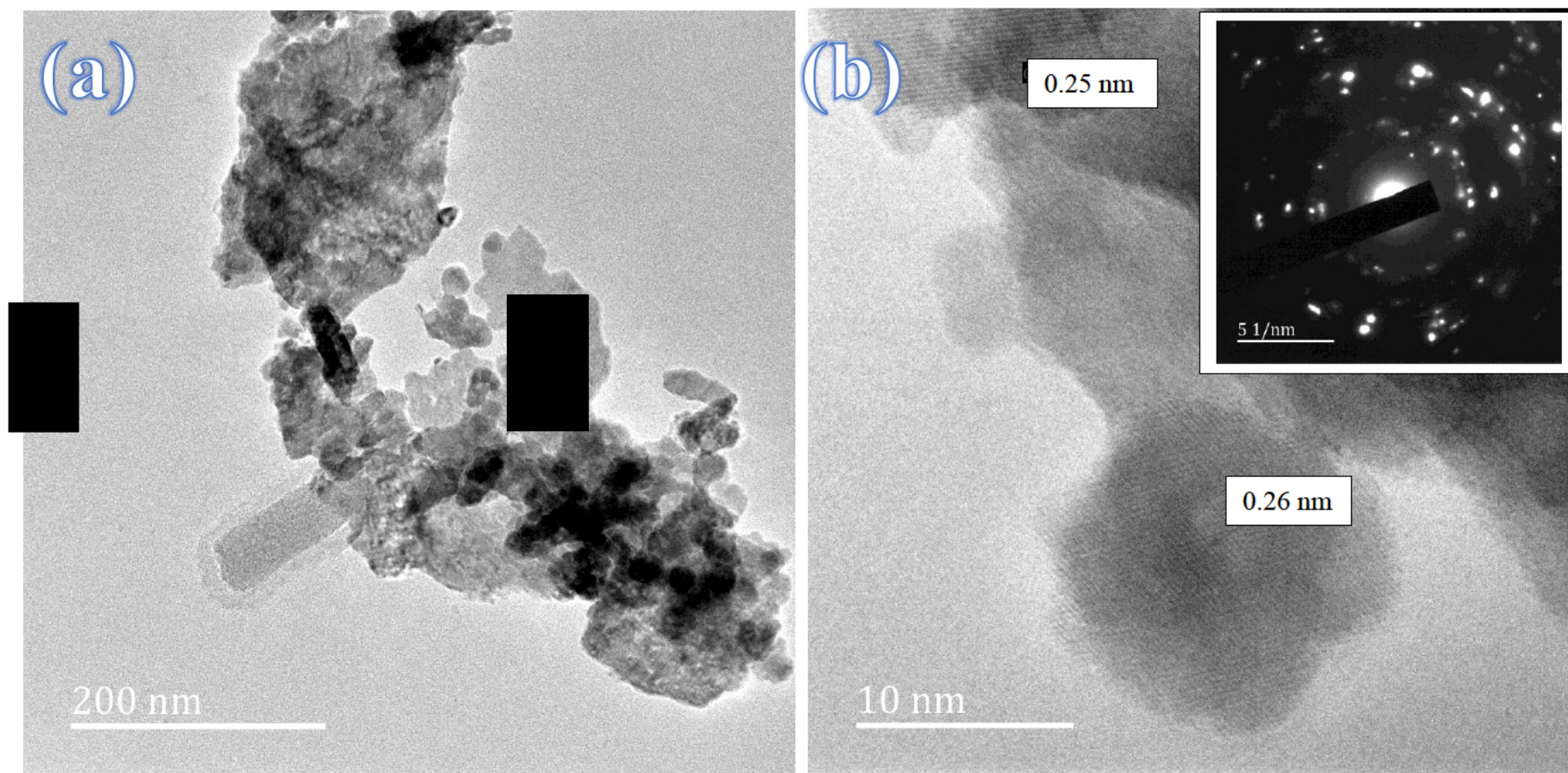
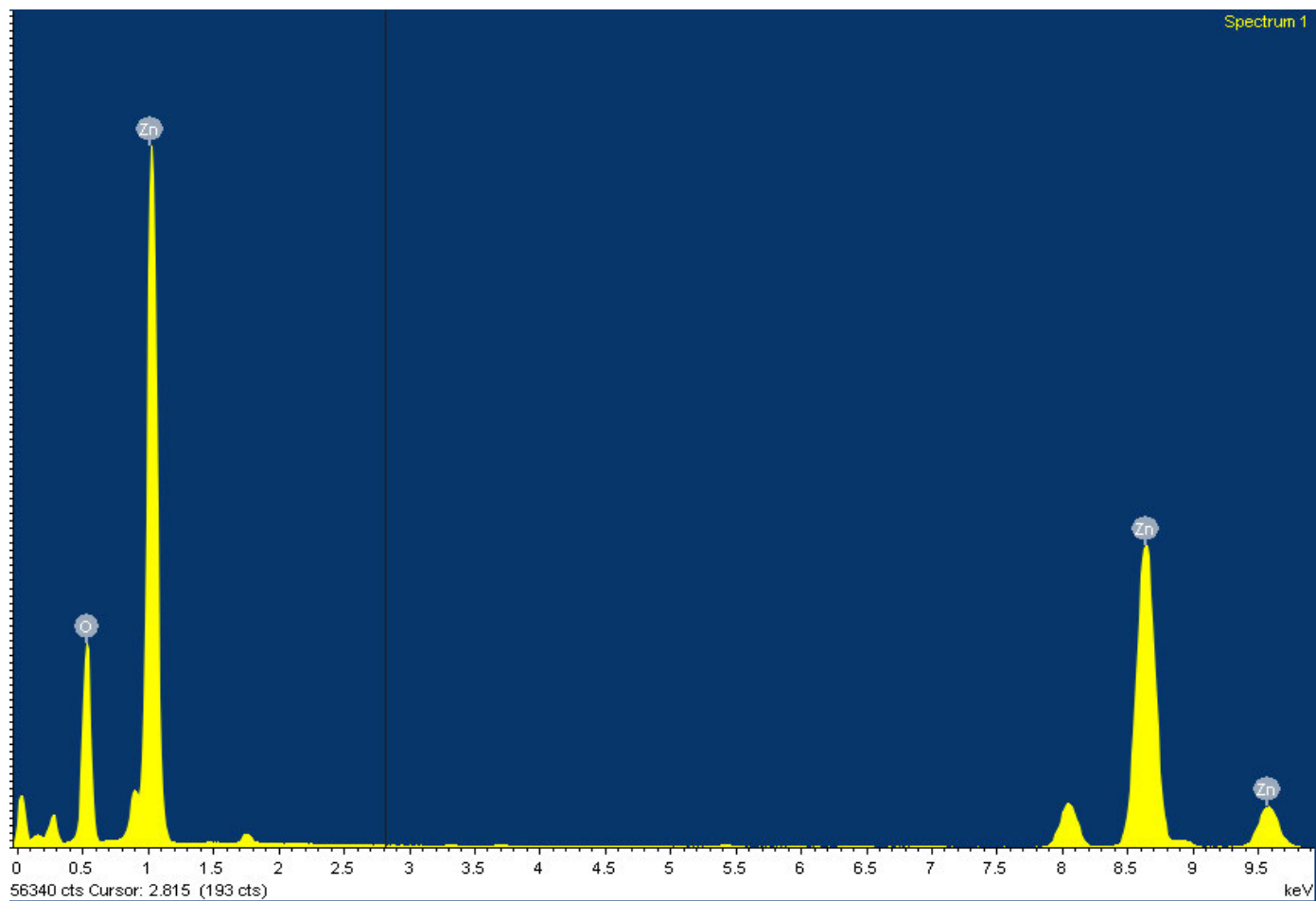


Figure 4.12: TEM images (a) low magnification (b) high magnification (inset SAED pattern) of ZnONPs synthesised from the mixture of jacaranones



Element	Weight%	Atomic%
C	3.47	10.53
Cu	8.40	4.82
O	20.62	46.99
Zn	64.22	35.85

Figure 4.13: Energy dispersive X-ray spectrum of ZnONPs synthesised from the mixture of jacaranones

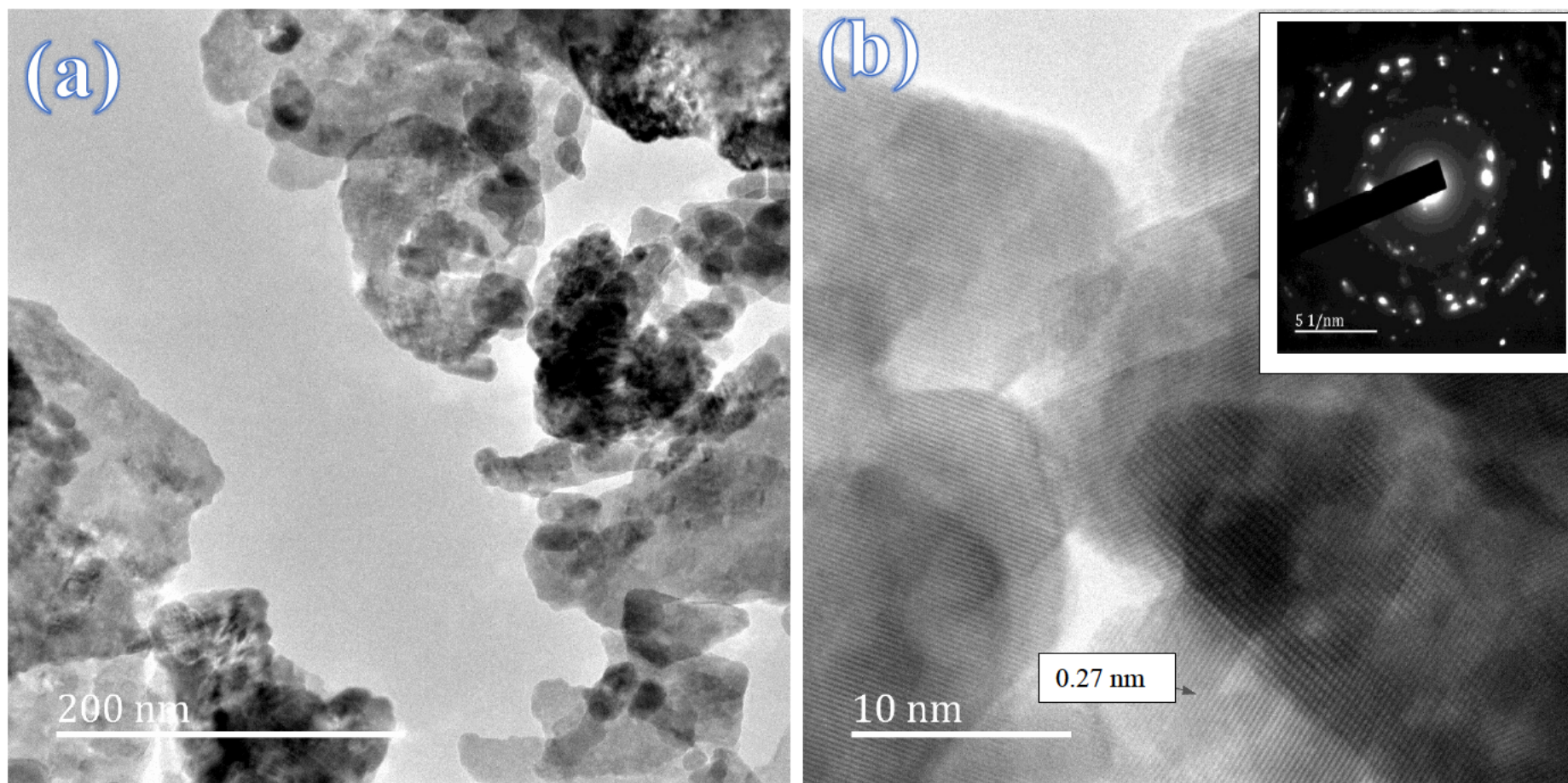
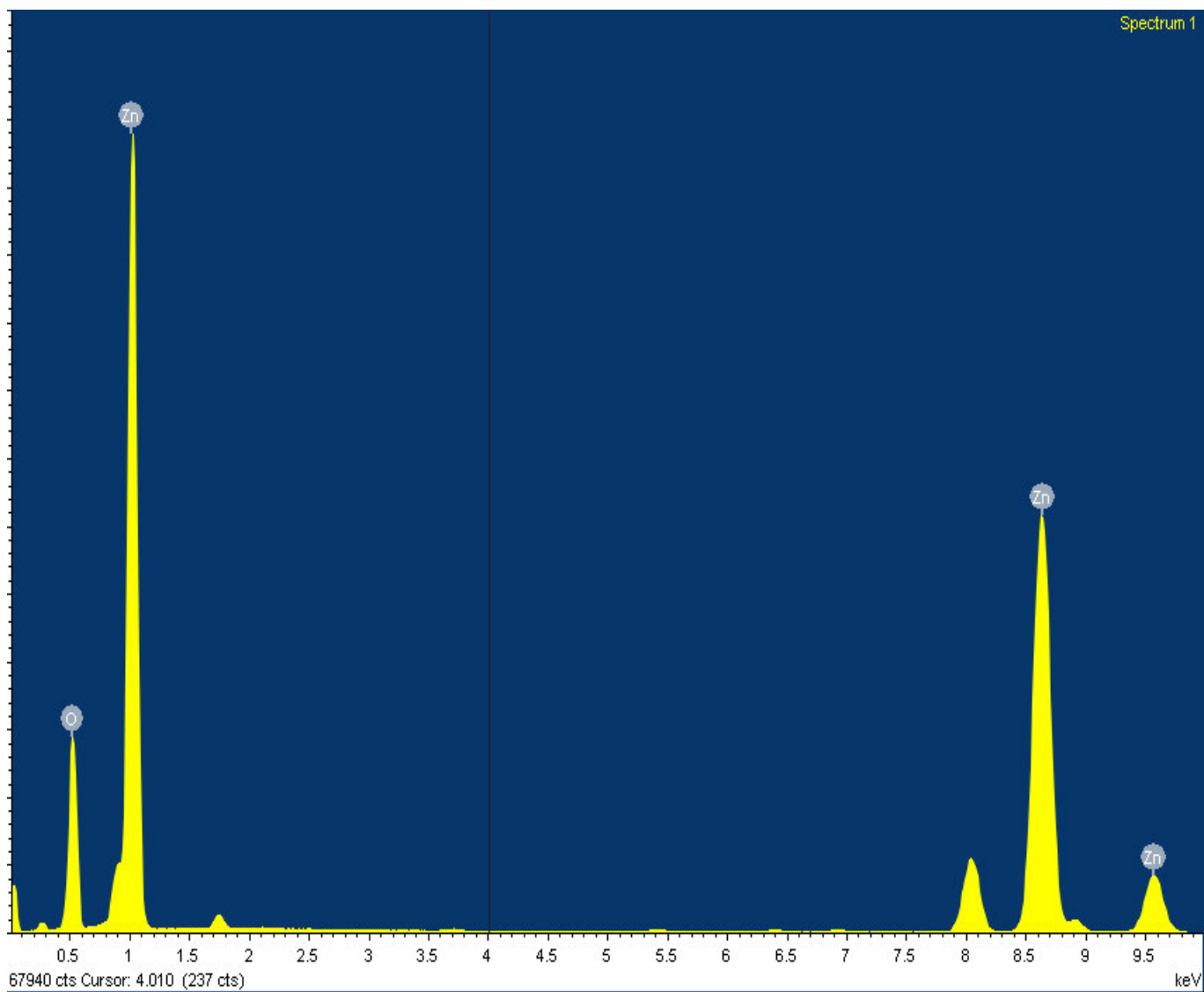


Figure 4.14: TEM images (a) low magnification (b) high magnification (inset SAED pattern) of ZnONPs synthesised from pure jacaranone



Element	Weight%	Atomic%
C	0.80	2.88
Cu	11.01	7.44
O	15.02	42.97
Zn	69.45	45.40

Figure 4.15: Energy dispersive X-ray spectrum of ZnONPs synthesised from pure jacaranone

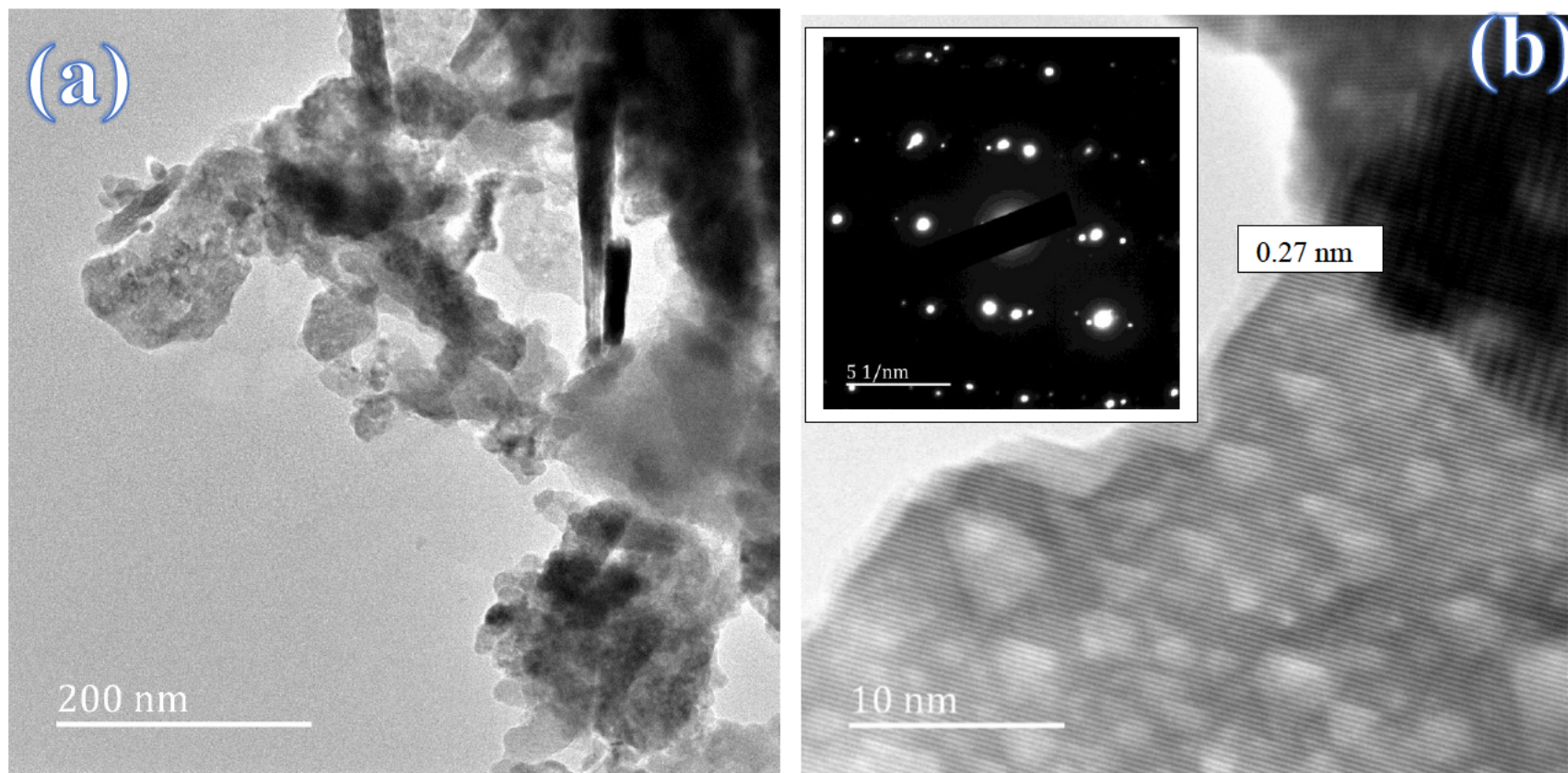
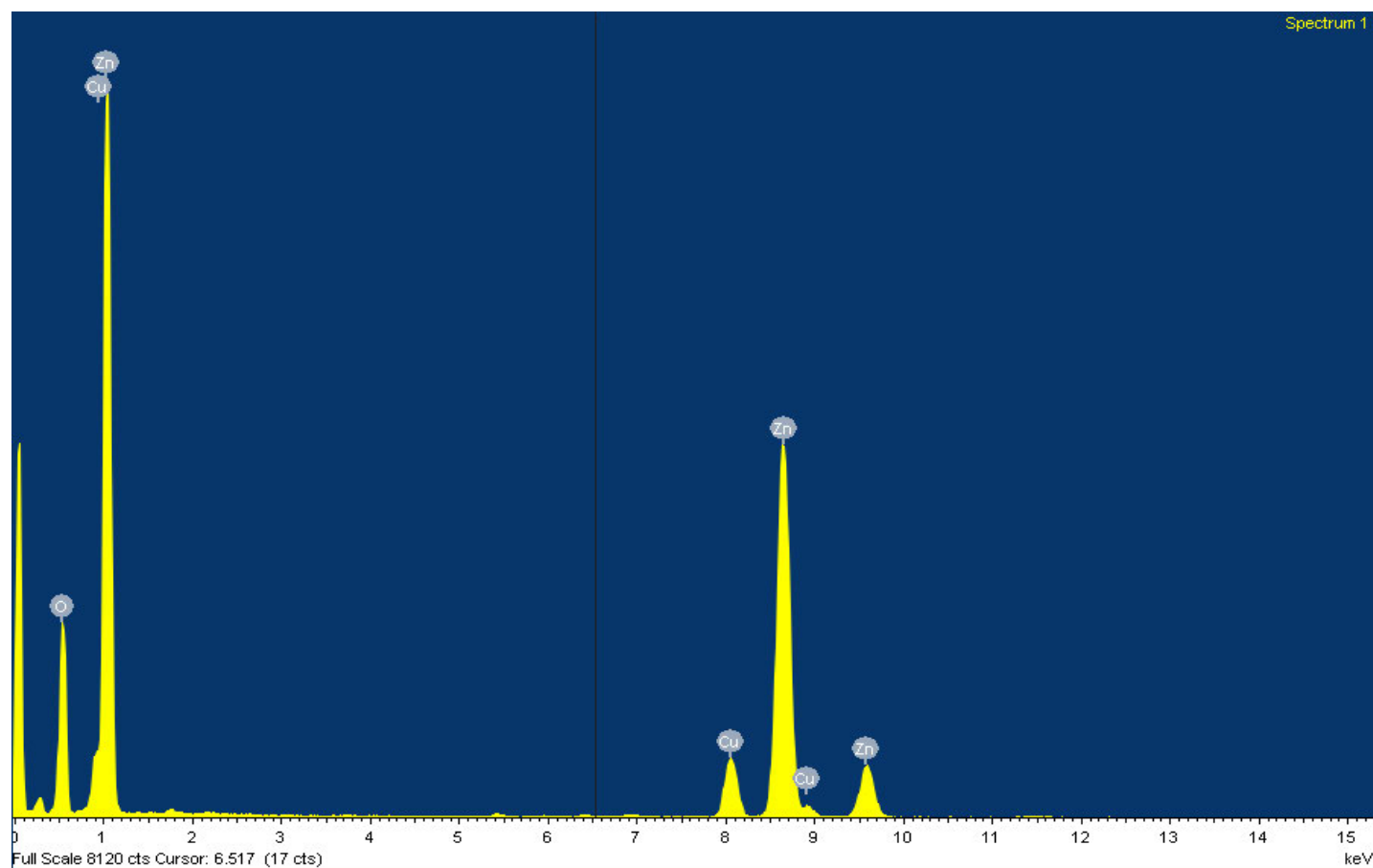


Figure 4.16: TEM images (a) low magnification (b) high magnification (inset SAED pattern) of freestanding ZnONPs



Element	Weight%	Atomic%
C	1.70	6.08
Cu	9.96	6.39
O	17.16	42.72
Zn	68.02	42.42

Figure 4.17: Energy dispersive X-ray spectrum of freestanding ZnONP

4.3. Antioxidant Activity (DPPH Assay)

The antioxidant activity of standard ascorbic acid and prepared ZnONPs, *S. serratuloides* extracts and pure compounds at different concentrations (75, 125, 250, 500 and 1000 ppm) are shown in Figure 4.18. The radical scavenging activity of ascorbic acid was significantly higher than that of all tested samples. The scavenging activity increases with an increase in concentration. Test samples show good activity at 500 ppm with scavenging activity of samples being in decreasing order of jacaranones > ZnONPs capped with compounds > extracts > ZnONPs capped with extract > freestanding ZnONPs. Jacaranones have previously been shown to demonstrate good antioxidant activity (Rana *et al.*, 2013). The chemical structure of jacaranones possess the -OC-CH(CH₂OH)-CH₂- moiety where the hydrogen may be easily donated to the DPPH radical to form DPPH-H, thus possess high scavenging activity compare to other compounds. The results revealed herein show ZnONPs capped with jacaranones isolated from *S. serratuloides* can be used as a source of antioxidants.

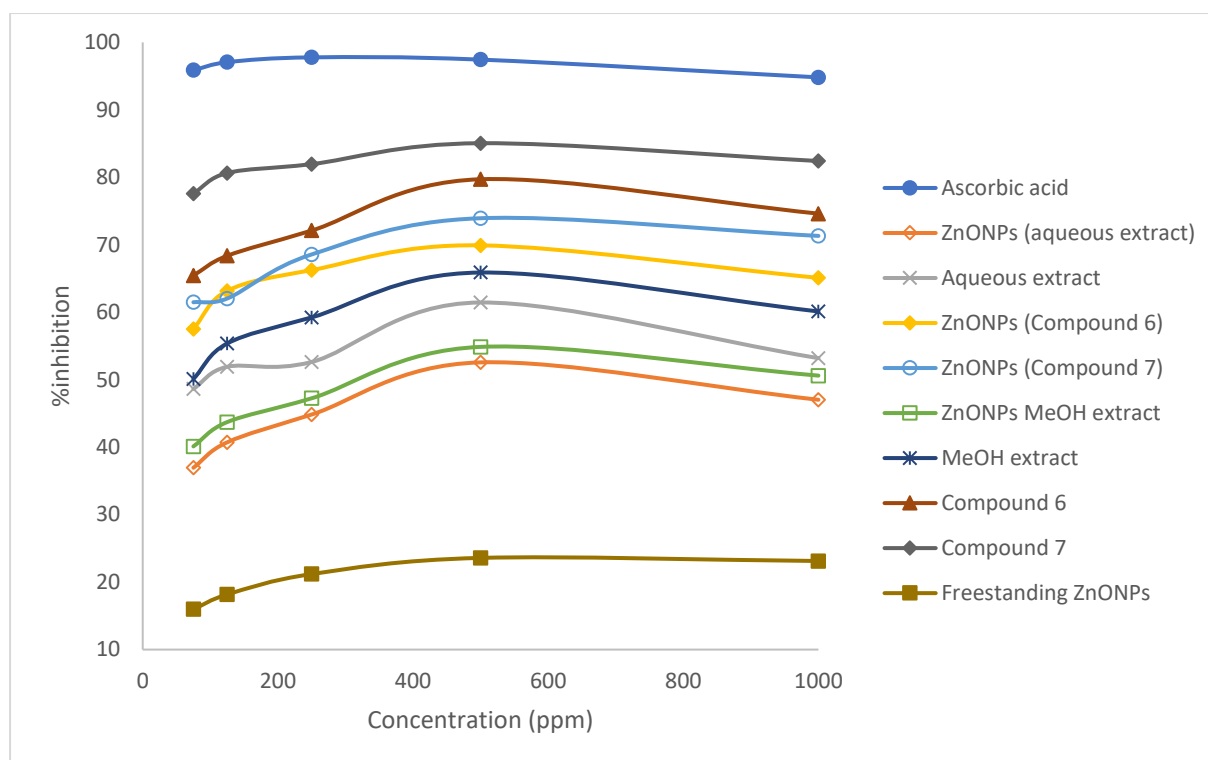


Figure 4.18: Antioxidant activity of ZnONPs synthesised from the aqueous extract, methanolic extract, compound 6 (jacaranone) and compound 7 (mixture of jacaranones) by the DPPH radical scavenging assay

4.4 Antibacterial Activity

The antibacterial activities of crude extracts and isolated compounds from *S. serratuloides* and synthesised ZnONPs are presented in Table 4.2. The MeOH extract from leaves (L-MeOH) and hexane extract from the stem bark (SB-Hex) showed promising antibacterial activity against *Chromobacterium violaceum* ATCC 12475. The hexane extract from leaves (L-Hex) and DCM extract from leaves (L-DCM) showed no antibacterial activity against any of the tested bacterial strains. Oleanolic acid, a pentacyclic triterpene, has a similar chemical structure to isolated compounds 3 (amyrins) and 5 (taraxerone). However, the amyrins and taraxerone showed no antibacterial activity unlike oleanolic acid. Triterpenoids including stigmasterol, ursolic acid and oleanolic acid have been reported to possess antibacterial activity (Cunha et al., 2007) (Yusuf et al., 2018).

In this study, the sesquiterpene (farnesylamine) and triterpenes (amyryns, sterols and taraxerone) showed low antibacterial activity against both Gram-positive and Gram-negative bacteria. The jacaranones were active against susceptible Gram-positive methicillin-resistant *S. aureus* ATCC 43300 and vancomycin resistant *Enterococcus faecalis* ATCC 51299 as well as susceptible Gram-negative quorum sensing inhibitor indicator *Chromobacterium violaceum* ATCC 12475. Jacaranones were the most active tested compounds with inhibition zones ranging from 12.5 to 18 mm. The results were in good agreement with literature, where synthetic jacaranones and their derivatives were reported to have good activity against both Gram-positive bacteria such as *Leuconostoc mesenteroides* ATCC 82932 and Gram-negative *Salmonella enteritidis* ATCC 13076 (Arias *et al.*, 2017a). The present study reports the antibacterial activity of a natural jacaranone against *Chromobacterium violaceum* ATCC 12475 for the first time. By making use of zone diameters, resistance was observed for ZnONPs synthesised from the MeOH extract of leaves and compound 7 (mixture of jacaranones) for all tested bacterial strains. ZnONPs synthesised from the mixture of jacaranones demonstrated promising antibacterial activity against *C. violaceum*, *S. aureus* and *P. aeruginosa*.

Table 4.2: Antibacterial susceptibility profile of selected gram positive and gram-negative bacteria upon exposure to *S. serratuloides* phytochemicals, crude extracts and ZnONPs

Test compound	Zone diameter (nm)									
	Gram-positive bacteria					Gram-negative bacteria				
	<i>Sa</i>		<i>Pa</i>		<i>Ef</i>		<i>Cv</i>		<i>Ec</i>	
	ATCC 51299		ATCC 27853		ATCC 51299		ATCC 12472		ATCC 35218	
	Concentration (µg)									
	200	500	200	500	200	500	200	500	200	500
L-Hex	0	0	0	0	0	0	0	0	0	0
SB-Hex	0	0	0	0	0	0	0	13	0	0
L-DCM	0	0	0	0	0	0	0	0	0	0
L-MeOH	0	0	0	0	0	0	12	12	0	0
Farnesylamine	0	0	0	0	0	0	0	0	0	0
Sitosterol	0	0	0	0	0	0	0	0	0	0
Amyrins	0	0	0	0	0	0	0	0	0	0
Stigmasterol	0	0	0	0	0	0	0	0	0	0
Taraxerone	0	0	0	0	0	0	0	0	0	0
Jacaranone	0	6.5	0	0	0	11	12.5	16.5	0	0
Jacaranones	6	8	0	0	9	14	13	18	0	0
Aqueous extract	0	0	0	0	0	0	0	0	0	0
Aqueous extract ZnONPs	0	0	0	0	0	0	0	0	0	0
MeOH extract ZnONPs	0	0	0	0	0	0	0	9	0	0
Compound 6 ZnONPs	0	0	0	0	0	0	0	0	0	0
Compound 7 ZnONPs	0	9	0	9.5	0	0	9	11	0	0
Freestanding ZnONPs	0	0	0	0	0	0	0	0	0	0
(AMP10)	0		0		20		0		0	
(TE30)	19		15		23		23		23	

Hexane extract from leaves (L-Hex), hexane extract from stem bark (SB-Hex), DCM extract from leaves (L-DCM), MeOH extract from leaves (L-MeOH), compound 6 (jacaranone) and compound 7 (mixture of jacaranones). AMP10 (Ampicillin at 10 µg per disc) and TE30 (Tetracycline at 30 µg per disc).

The ability of pure compounds to prevent the growth of bacteria was found to be more effective than that of crude extracts and ZnONPs. The highest efficiency of preventing the growth was observed for *C. violaceum*. The antimicrobial activity was concentration dependent. An increase in concentration resulted in an increase in activity as can be expected.

4.5 Anti-Quorum Sensing Activity

The inhibitory effect of crude extracts, isolated compounds from *S. serratuloides* and ZnONPs in comparison with the quorum sensing inhibitor control (furanone) on violacein production by *Chromobacterium violaceum* ATCC 12475 assessed at 250 and 500 µg is presented in (Fig 4.19). A clear zone (opaque halos) indicates no growth of bacteria and inhibition of violacein. The larger colourless halos show quorum sensing inhibition (QSI). The opaque halos of the hexane extract from the stem bark (SB-Hex) showed higher QSI compared to taraxerone (compound 5) isolated from this extract. The hexane extract from leaves (L-Hex) and compound 1 (farnesylamine) obtained from this extract as well as the DCM extract from leaves (L-DCM) demonstrated no QSI. The MeOH xtract from leaves (L-MeOH) exhibited moderate QSI whilst the cpmounds obtained fromm this extract, compound 6 (jacaranone) and compound 7 (mixture of jacaranones), demonstrated good QSI at both 250 and 500 µg, with increased growth inhibition zone diameters at 500 µg. Compound 6 (jacaranone) showed strong QSI, with zone diameters ranging from 13 to 15 mm. Compound 7 (mixture of jacaranones) exhibited strong QSI, with zone diameters ranging from 12 to 16 mm.

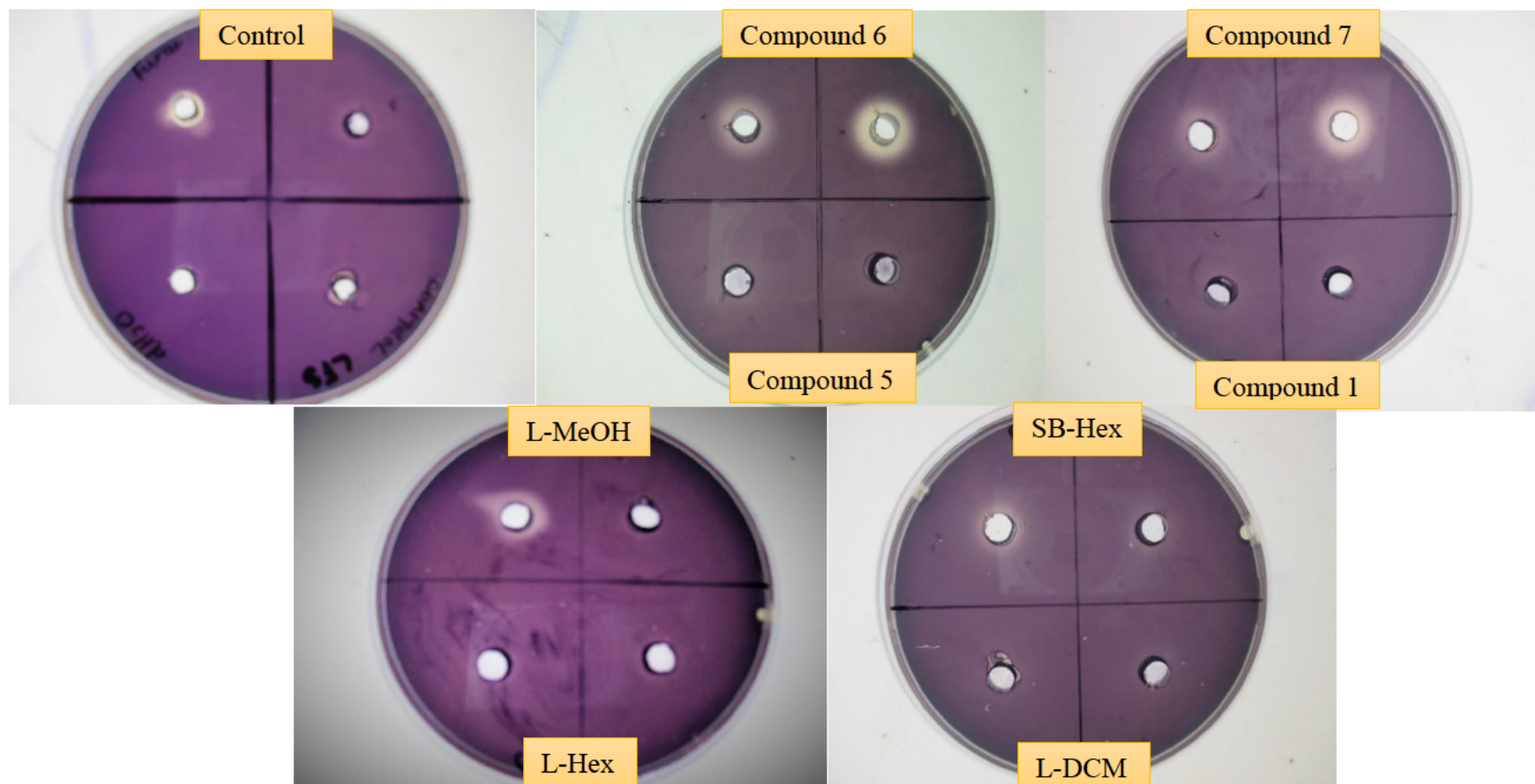


Figure 4.19: The quorum sensing inhibitory effect of the ZnONPs, compounds and crude extracts of *S. serratuloides* at 250 and 500 μm

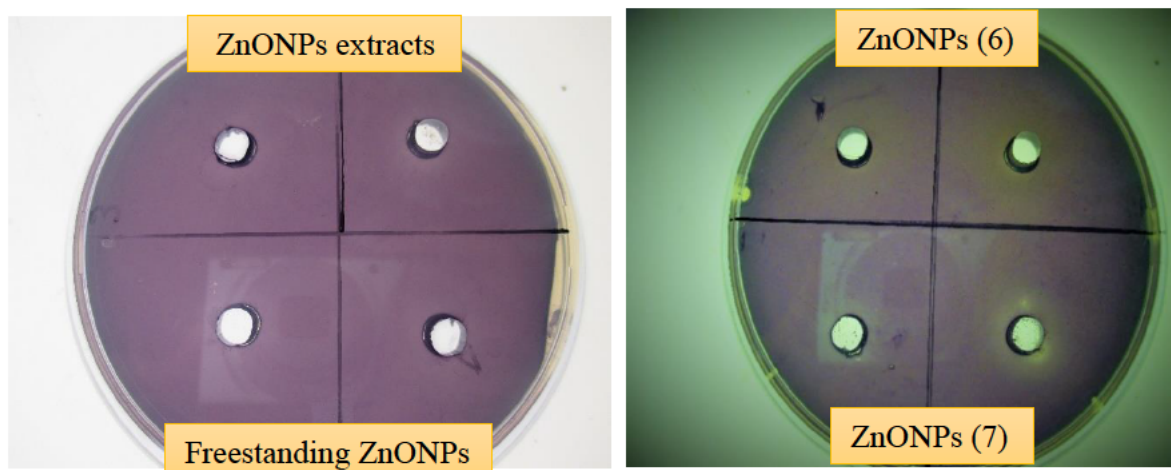


Figure 4.20: The quorum sensing inhibitory effect of the ZnO nanoparticles ((ZnONPs)

Freestanding ZnONPs and ZnONPs capped with crude extracts showed no QSI (Fig 4.20). ZnONPs capped with compound 6 (jacaranone, ZnONPs (6)) and compound 7 (mixture of jacaranones, ZnONPs (7)) demonstrated promising QSI. The pure jacaranone displayed the potential to be a novel therapeutic agent, which might be important in reducing virulence and pathogenicity of drug-resistant bacteria. The increasing order for QSI was freestanding ZnONPs = ZnONPs capped with crude extracts < ZnONPs capped with compounds < crude extracts < pure compounds (jacaranones).

CHAPTER FIVE

SUMMARY AND CONCLUSIONS

Eight secondary metabolites from *S. serratuloides* were obtained from extracts of the plant; five were successfully isolated and two were obtained as mixtures. They included a sesquiterpene (farnesylamine), two sterols (stigmsterol and β -sitosterol), three pentacyclic triterpenes (a mixture of α - and β -amyrin and taraxerone) and two jacaranones (jacaranone and a mixture of jacaranone and methyl-2-(1-hydroxy-4-oxocyclohexyl)acetate).

The crude extract of *S. serratuloides* and isolated phytochemicals showed antibacterial activity against *Staphylococcus aureus* ATCC 43300, *Enterococcus faecalis* ATCC 51299 and *Chromobacterium violaceum* ATCC 12472 bacterial strains. Agar overlay assays were done to test for anti-quorum sensing activity of *S. serratuloides* and selected phytochemicals. The result of the present study suggest that *S. serratuloides* extracts and phytochemicals such as jacaranone and methyl-2-(1-hydroxy-4-oxocyclohexyl)acetate have the ability to reduce virulence and to be used as anti-pathogenicity agents. It can be concluded that *S. serratuloides* produces quorum sensing compounds (jacaranones) that can be used to defect quorum sensing pathogens.

ZnONPs with a variety of sizes and shapes were successfully synthesised by a one-step precipitation method using extracts and secondary metabolites isolated from *Senecio serratuloides*. The average particle size of spherical particles was between of 10 and 30 nm. XRD and SAED confirmed the NP phase to be crystalline ZnO in the hexagonal Wurtzite structure. Impurities were minimal. The study shows that jacaranones (isolated compounds) and extracts of *S. serratuloides* act as a reducing and capping agent in the synthesis of ZnONPs. ZnONPs synthesised using jacaranones showed good antioxidant activity whilst ZnONPs synthesised using extracts of *S. serratuloides* showed moderate antioxidant activity.

This is the first study to examine *S. serratuloides* crude extracts, pure compounds (jacaranones) and ZnONPs capped with phytocompounds for anti-quorum sensing activity. The study revealed the potential of *S. serratuloides* extracts, capped ZnONPs and pure compounds as anti-virulence therapy approach to help in combatting the problem of multidrug-resistant bacteria.

RECOMMENDATIONS FOR FURTHER STUDY

Future work should focus on the quantitative analysis of anti-quorum sensing activity, modulation of quorum sensing activity using other biosensor systems such as *Agrobacterium tumefaciens* strains and using other plants and different classes of phytocompounds to further investigate phytocompounds as quorum sensing antagonist and test their anti-pathogenic efficacy in an experimental animal model.

Also, *Senecio serratuloides* extracts, isolated compounds, metal or metal oxide capped nanoparticles can be screened for antidiabetic and anticancer activity. Synthesis and characterisation of other metal or metal oxide nanoparticles using *Senecio serratuloides* extracts and isolated compounds can be conducted. Computational studies can be undertaken on the phytocompounds isolated from *Senecio serratuloides*.

REFERENCES

- ABBASI, A., KHAN, A., AHMAD, M., ZAFAR, M., JAHAN, S. and SULTANA, S. 2010. Ethnopharmacological application of medicinal plants to cure skin diseases and in folk cosmetics among the tribal communities of North-West Frontier Province, Pakistan. *Journal of Ethnopharmacology*, 128, 322–335.
- ABBASI, B. H., ANJUM, S. and HANO, C. 2017. Differential effects of in vitro cultures of *Linum usitatissimum* L.(Flax) on biosynthesis, stability, antibacterial and antileishmanial activities of zinc oxide nanoparticles: a mechanistic approach. *Royal Society of Chemistry Advances*, 7, 15931-15943.
- ABBOTT, A. T. D., ARCHER, C., ARCHER, R. H., BALKWILL, K., BARKER, N. P., BAYER, B. M., BERGH, N. G., BERRINGTON, W. and BESTER, S. P. 2009. *Red list of South African Plants 2009*, Pretoria, South African National Biodiversity Institute.
- ABDO, S., BERNARDI, M. D., MARINONI, G., MELLERIO, G., SAMANIEGO, S., VIDARI, G. and FINZI, P. V. 1992. Furanoeremophilanes and other constituents from *Senecio canescens*. *Phytochemistry*, 31, 3937-41.
- ABURJAI, T. and NATSHEH, F. 2003. Plants used in cosmetics. *Phytotherapy Research*, 17, 987–1000.
- ADONIZIO, A. L., DOWNUM, K., BENNETT, B. C. and MATHEE, K. 2006. Anti-quorum sensing activity of medicinal plants in southern Florida. *Journal of Ethnopharmacology*, 105, 427-435.
- AGYARE, C., ASASE, A., LICHTENBERG, M., NIEHUES, M., DETERS, A. and HENSEL, A. 2009. An ethnopharmacological survey and in vitro confirmation of ethnopharmacological use of medicinal plants used for wound healing in Bosomtwi-Atwima-Kwanwoma area, Ghana. *Journal of Ethnopharmacology*, 125, 393–403.

- ALI, S. I., GOPALAKRISHNAN, B. and VENKATESALU, V. 2018. Evaluation of larvicidal activity of *Senecio laetus* Edgew. against the malarial vector, *Anopheles stephensi*, dengue vector, *Aedes aegypti* and Bancroftian filariasis vector, *Culex quinquefasciatus*. *South African Journal of Botany*, 114, 117–125.
- ALLAKER, R. P. and REN, G. 2008. Potential impact of nanotechnology on the control of infectious diseases. *Transactions of the Royal Society of Tropical Medicine and Hygiene*, 102, 1-2.
- ARIAS, M. L., POVEDA, R. and CABEZAS, J. A. 2017. Synthesis and Determination of antibacterial activity of jacaranone and synthetic analogs. *International Journal of Multidisciplinary and Current Research*, 5, 918-924.
- ARUNKUMAR, M., SUHASHINI, K., MAHESH, N. and RAVIKUMAR, R. 2014. Quorum quenching and antibacterial activity of silver nanoparticles synthesized from *Sargassum polyphyllum*. *Bangladesh Journal of Pharmacology*, 9, 54-59.
- ASHIHARA, H. and CROZIER, A. 2001. Caffeine: a well known but little mentioned compound in plant science. *Trends in Plant Science*, 6, 407-413.
- AZIZI, S., MOHAMAD, R., BAHADORAN, A., BAYAT, S., RAHIM, R. A., ARIFF, A. and SAAD, W. Z. 2016. Effect of annealing temperature on antimicrobial and structural properties of bio-synthesized zinc oxide nanoparticles using flower extract of *Anchusa italica*. *Journal of Photochemistry and Photobiology : Biology*, 161, 441-449.
- BAHARVAND-AHMADI, B., BAHMANI, M., NAGHDI, N., KOUROSH SAKI, BAHARVAND-AHMADI, S. and RAFIEIAN-KOPAEI, M. 2015. Medicinal plants used to treat infectious and non-infectious diseases of skin and skin appendages in city of Urmia, northwest Iran. *Der Pharmacia Lettre*, 7, 189-196.

- BANO, S., REHMAN, H., AKHTAR, F., IQBAL, A., KHANUM, K. and USMANGHANI, K. 2018. Comparative acute oral toxicity study of cartinovex plus verses anti-arthritis Devil's Claw in mice. *RADS Journal of Pharmacy and Pharmaceutical Sciences*, 6, 02-06.
- BARNES, J., ANDERSON, L. A. and PHILLIPSON, J. D. 2007. Herbal Medicine, third edition, *Royal Pharmaceutical Society of Great Britain*.
- BARNES, J., BARBER, N., WHEATLEY, D., SHARPE, D. and WILLIAMSON, E. 2018. A prospective, open, uncontrolled study of a standardised extract of St John's wort (*Hypericum perforatum*) as an aid in smoking cessation. *Journal of Stroke*, 13, 57.
- BARTOLOME, A. P., VILLASEÑOR, I. M. and YANG, W.-C. 2013. *Bidens pilosa* L.(Asteraceae): botanical properties, traditional uses, phytochemistry, and pharmacology. *Evidence-Based Complementary and Alternative Medicine*, 2013, 340215
- BHARADWAJ, K. C., GUPTA, T. and SINGH, R. M. 2018. Alkaloid group of *Cinchona officinalis*: structural, synthetic, and medicinal aspects. *Synthesis of Medicinal Agents from Plants*. Elsevier, Amsterdam, Netherlands, 205-227.
- BODEDE, O., SHAIK, S., CHENIA, H., SINGH, P. and MOODLEY, R. 2018. Quorum sensing inhibitory potential and in silico molecular docking of flavonoids and novel terpenoids from *Senegalia nigrescens*. *Journal of Ethnopharmacology*, 216, 134-146.
- BOHLMANN, F., ZDERO, C., KING, R. M. and ROBINSON, H. 1981. The first acetylenic monoterpene and other constituents from *Senecio clevelandii*. *Phytochemistry*, 20, 2425-2427.
- BOROKINI, T. I. and OMOTAYO, F. O. 2010. Phytochemical and ethnobotanical study of some selected medicinal plants from Nigeria. *Journal of Medicinal Plants Research*, 6, 1106-1118.

- CHELLIAH, D. A. 2008. Biological activity prediction of an ethno medicinal plant *Cinnamomum camphora* through bio-informatics. *Ethnobotanical leaflets*, 2008, 22.
- CORDIER, W. and STEENKAMP, V. 2018. Bulb extracts of *Boophone disticha* induce hepatotoxicity by perturbing growth, without significantly impacting cellular viability. *South African Journal of Botany*, 114, 1-8.
- CRAGG, G. M. and NEWMAN, D. J. 2005. Plants as a source of anti-cancer agents. *Journal of Ethnopharmacology*, 100, 72-79.
- CUNHA, L. C. S., E SILVA, M. L. A., FURTADO, N. A. C., VINHOLIS, A. H., MARTINS, C. H. G., DA SILVA FILHO, A. and CUNHA, W. R. 2007. Antibacterial activity of triterpene acids and semi-synthetic derivatives against oral pathogens. *Zeitschrift für Naturforschung C, Journal of Biosciences*, 62, 668-672.
- CUNNINGHAM, A. B. 1993. African medicinal plants: setting priorities at the interface between conservation and primary healthcare, people and plants working paper 1. Paris *United Nations Educational, Scientific and Cultural Organization*.
- DAHL, T. A., MIDDEN, W. and HARTMAN, P. E. 1989. Comparison of killing of gram-negative and gram-positive bacteria by pure singlet oxygen. *Journal of Bacteriology*, 171, 2188-2194.
- DE WET, H., NCIKI, S. and VAN VUUREN, S. F. 2013. Medicinal plants used for the treatment of various skin disorders by a rural community in Northern Maputaland, South Africa. *Journal of Ethnobiology and Ethnomedicine*, 9, 51.
- DE WET, H. and NGUBANE, S. C. 2014. Traditional herbal remedies used by women in a rural community in Northern Maputaland (South Africa) for the treatment of gynaecology and obstetric complaints. *South African Journal of Botany*, 94, 129-139.

- DE WET, H., NZAMA, V. N. and VAN VUUREN, S. 2012. Medicinal plants used for the treatment of sexually transmitted infections by lay people in Northern Maputaland, KwaZulu–Natal Province, South Africa. *South African Journal of Botany*, 78, 12-20.
- DHILLON, G. S., BRAR, S. K., KAUR, S. and VERMA, M. 2012. Green approach for nanoparticle biosynthesis by fungi: current trends and applications. *Critical Reviews in Biotechnology*, 32, 49-73.
- DLOVA, N. C. and OLLENGO, M. A. 2018. Traditional and ethnobotanic dermatology practices in Africa. *Clinics in Dermatology*, 36, 353-362.
- DOBRUCKA, R. and DŁUGASZEWSKA, J. 2016. Biosynthesis and antibacterial activity of ZnO nanoparticles using *Trifolium pratense* flower extract. *Saudi Journal of Biological Sciences*, 23, 517-523.
- EL-SHAZLY, A. 2002. Pyrrolizidine alkaloid profiles of some *Senecio* species from Egypt. *Zeitschrift für Naturforschung, Journal of Chemical Sciences*, 57, 429-433.
- ELISHA, I. L., BOTHA, F. S., MCGAW, L. J. and ELOFF, J. N. 2017. The antibacterial activity of extracts of nine plant species with good activity against *Escherichia coli* against five other bacteria and cytotoxicity of extracts. *BMC Complementary and Alternative Medicine*, 17, 133.
- EMAMI-KARVANI, Z. and CHEHRAZI, P. 2011. Antibacterial activity of ZnO nanoparticle on gram-positive and gram-negative bacteria. *African Journal of Microbiology Research*, 5, 1368-1373.
- FAWOLE, O., AMOO, S., NDHLALA, A., LIGHT, M., FINNIE, J. and VAN STADEN, J. 2010. Anti-inflammatory, anticholinesterase, antioxidant and phytochemical properties of medicinal plants used for pain-related ailments in South Africa. *Journal of Ethnopharmacology*, 127, 235-241.

- FELDHEIM, D. and FOSS, C. 2002. Metal nanoparticles: synthesis, characterization and applications, *Boca Raton, Florida: CRC Press, Taylor & Francis.*
- FERNANDES, R., ROY, V., WU, H.-C. and BENTLEY, W. E. 2010. Engineered biological nanofactories trigger quorum sensing response in targeted bacteria. *Nature nanotechnology*, 5, 213.
- FOUCHE, G., CRAGG, G. M., PILLAY, P., KOLESNIKOVA, N., MAHARAJ, V. J. and SENABE, J. 2008. In vitro anticancer screening of South African plants. *Journal of Ethnopharmacology*, 119, 455-461.
- FRATIANNI, F., COPPOLA, R. and NAZZARO, F. 2011. Phenolic composition and antimicrobial and antiquorum sensing activity of an ethanolic extract of peels from the apple cultivar *Annurca*. *Journal of Medicinal Food*, 14, 957-963.
- FULTZ, B. and HOWE, J. 2013. Neutron scattering in Transmission Electron Microscopy and diffractometry of materials, Graduate texts in physics. Springer, Berlin, Heidelberg
- FULTZ, B. and HOWE, J. M. 2012. Transmission Electron Microscopy and diffractometry of materials, fourth edition. Springer Science, Berlin Heidelberg.
- GACHET, M. S., KUNERT, O., KAISER, M., BRUN, R., MUNOZ, R. A., BAUER, R. and SCHÜHL, W. 2010. Jacaranone-derived glucosidic esters from *Jacaranda glabra* and their activity against *Plasmodium falciparum*. *Journal of Natural Products*, 73, 553-556.
- GERICKE, M. and PINCHES, A. 2006. Biological synthesis of metal nanoparticles *Hydrometallurgy*, 83, 132-140.
- GHOSH, S., PATIL, S., AHIRE, M., KITTURE, R., JABGUNDE, A. and KALE, S. 2011. Synthesis of gold nano-angisotrops using *Dioscorea bulbifera* tuber extract. *Journal of Nanomaterials*, 7, 483-496

- GHOSH, S., PATIL, S., AHIRE, M., KITTURE, R., KALE, S. and PARDESI, K. 2012. Synthesis of silver nanoparticles using *Dioscorea bulbifera* tuber extract and evaluation of its synergistic potential in combination with antimicrobial agents. *International Journal of Nanomedicine*, 7, 483-96.
- GOLDSTEIN, J., YAKOWITZ, H., NEWBURY, D., LIFSHIN, E., COLBY, J. and COLEMAN, J. 1977. Practical Scanning Electron Microscopy: Electron and ion microprobe analysis. Springer New York, Plenum Press.
- GOULD, A. N. 2015. *Senecio serratuloides* var. in wound healing: efficacy and mechanistic investigations in a porcine wound model. (PhD thesis), South Africa : Department of Health Sciences, University of Witwatersrand.
- GOULD, A. N., PENNY, C. B., PATEL, C. C. and CANDY, G. P. 2015. Enhanced cutaneous wound healing by *Senecio serratuloides* (Asteraceae/Compositae) in a pig model. *South African Journal of Botany*, 100, 63–68.
- GUTHA, Y., PATHAK, J. L., ZHANG, W., ZHANG, Y. and JIAO, X. 2017. Antibacterial and wound healing properties of chitosan/poly (vinyl alcohol)/zinc oxide beads (CS/PVA/ZnO). *International Journal of Biological Macromolecules*, 103, 234-241.
- HALEVAS, E., NDAY, C. and SALIFOLOU, A. 2016. Hybrid catechin silica nanoparticle influence on Cu (II) toxicity and morphological lesions in primary neuronal cells. *Journal of Inorganic Biochemistry*, 163, 240-249.
- HARBORNE, J. B. 1973. Phytochemical methods: A guide to modern techniques of plant analysis, second edition. London, Chapman and Hall Ltd.
- HASSAN, H. F. H., MANSOUR, A. M., ABO-YOUSSEF, A. M. H., ELSADEK, B. E. and MESSIHA, B. A. S. 2017. Zinc oxide nanoparticles as a novel anticancer approach; in vitro and in vivo evidence. *Clinical and Experimental Pharmacology and Physiology*, 44, 235-243.

- HEAD, K. A. 2008. Natural approaches to prevention and treatment of infections of the lower urinary tract. *Alternative Medicine Review*, 13, 227-245.
- HUH, A. J. and KWON, Y. J. 2011. "Nanoantibiotics": a new paradigm for treating infectious diseases using nanomaterials in the antibiotics resistant era. *Journal of Controlled Release*, 156, 128-145.
- IKEDA, Y., MURAKAMI, A. and OHIGASHI, H. 2008. Ursolic acid: An anti-and pro-inflammatory triterpenoid. *Molecular Nutrition and Food Research*, 52, 26-42.
- IKRAM, F., QAYOOM, A. and SHAH, M. R. 2018. Synthesis of epicatechin coated silver nanoparticles for selective recognition of gentamicin. *Sensors and Actuators B: Chemical*, 257, 897-905.
- IRAVANI, S. 2011. Green synthesis of metal nanoparticles using plants. *Green Chemistry*, 13, 2638–2650.
- JAKUPOVIC, J., CHAU-THI, T. V. and CASTRO, V. 1987. Cyclohexene derivatives from *Pseudogynoxys cunninghamii*. *Journal of Fitoterapia*, 58, 187-188
- JAMDAGNI, P., KHATRI, P. and RANA, J. S. 2016. Green synthesis of zinc oxide nanoparticles using flower extract of *Nyctanthes arbor-tristis* and their antifungal activity. *Journal of King Saud University - Science*, 30, 168-175
- JIANG, J., OBERDORSTER, G. and BISWAS, P. 2009. Characterization of size, surface change and agglomeration state of nanoparticle dispersions of toxicological studies. *Journal of Nanoparticle Research*, 11, 77-89.
- JONES, T. H., CLARK, D. A., HETERICK, B. E. and SNELLING, R. R. 2003. Farnesylamine from the Ant *Monomorium fieldi* Forel. *Journal of Natural Products*, 66, 325-326.
- KALIA, V. C. 2013. Quorum sensing inhibitors: an overview. *Biotechnology Advances*, 31, 224-245.

- KAMBOJ, A. and SALUJA, A. K. 2011. Isolation of stigmasterol and β -sitosterol from petroleum ether extract of aerial parts of *Ageratum conyzoides* (Asteraceae). *International Journal of Pharmacy and Pharmaceutical Sciences*, 3, 94-96.
- KATIIYAR, S. 2005. Silymarin and skin cancer prevention: anti-inflammatory, antioxidant and immunomodulatory effects (Review). *International Journal of Oncology*, 26, 139–176.
- KAUR, N. and GUPTA, R. C. 2018. High-Performance Thin-Layer Chromatography (HPTLC) of four sterols in a medicinally important grass species–*Heteropogon contortus* (L.) Beauv. *JPC-Journal of Planar Chromatography-Modern TLC*, 31, 143-149.
- KAURI, R. and ARORA, S. 2015. Alkaloids-important therapeutic secondary metabolites of plant origin *Journal of Critical Reviews*, 2, 1-8.
- KHALIL, A. T., OVAIS, M., ULLAH, I., ALI, M., SHINWARI, Z. K., KHAMLICH, S. and MAAZA, M. 2017. *Sageretia thea* (Osbeck.) mediated synthesis of zinc oxide nanoparticles and its biological applications. *Journal of Nanomedicine*, 12, 1767-1789.
- KHAN, A. S. 2017. Woody Plants with Possible Anti-HIV Activity. *Medicinally Important Trees*. Springer, International Publishing Switzerland.
- KHARISSOVA, O. V., DIAS, H. R., KHARISOV, B. I., PEREZ, B. O. and PEREZ, V. M. J. 2013. The greener synthesis of nanoparticles. *Trends in Biotechnology*, 31, 240-248.
- KIPLIMO, J. J., KOORBANALLY, N. A. and CHENIA, H. 2011. Triterpenoids from *Vernonia auriculifera* Hiern exhibit antimicrobial activity. *African Journal of Pharmacy and Pharmacology*, 5, 1150-1156.
- KOH, C.-L., SAM, C.-K., YIN, W.-F., TAN, L. Y., KRISHNAN, T., CHONG, Y. M. and CHAN, K.-G. 2013. Plant-derived natural products as sources of anti-quorum sensing compounds. *Sensors*, 13, 6217-6228.

- KUETE, V. 2014. Mutagenicity and carcinogenicity of african medicinal plants. *Toxicological Survey of African Medicinal Plants*. Elsevier. Jamestown, London 277-322
- KUMAR, V. and MATHELA, C. S. 2018. Chemical constituents of essential oils of *Himalayan Nepeta ciliaris* Benth. and *Senecio nudicaulis* Buch-Ham. Ex D. Don. *Journal of Essential Oil Research*, 30, 207-213.
- KUPPUSAMY, P., YUSOFF, M. M., MANIAM, G. P. and GOVINDAN, N. 2016. Biosynthesis of metallic nanoparticles using plant derivatives and their new avenues in pharmacological applications—An updated report. *Saudi Pharmaceutical Journal*, 24, 473-484.
- LALL, N. and KISHORE, N. 2014. Are plants used for skin care in South Africa fully explored? *Journal of Ethnopharmacology*, 153, 61-84.
- LEE, J.-H., KIM, Y.-G., CHO, M. H. and LEE, J. 2014. ZnO nanoparticles inhibit *Pseudomonas aeruginosa* biofilm formation and virulence factor production. *Microbiological Research*, 169, 888-896.
- LEE, M.-K., KIM, T. G., KIM, W. and SUNG, Y.-M. 2008. Surface plasmon resonance (SPR) electron and energy transfer in noble metal– zinc oxide composite nanocrystals. *The Journal of Physical Chemistry*, 112, 10079-10082.
- LI, Y., DUAN, X., QIAN, Y., LI, Y. and LIAO, H. 1999. Nanocrystalline silver particles: synthesis. *Colloids and Surfaces B: Biointerfaces*, 209, 347-349.
- LOOTS, D., WESTHUIZEN, F. and BOTES, L. 2007. *Aloe ferox* leaf gel phytochemical content, antioxidant capacity, and possible health benefits. *Journal of Agricultural and Food Chemistry*, 55, 6891–6896.
- MABONA, U. and VUUREN, S. V. 2013. Southern African medicinal plants used to treat skin diseases. *South African Journal of Botany*, 87, 175–193.

- MADZINGA, M., KRITZINGER, Q. and LALL, N. 2018. Medicinal plants used in the treatment of superficial skin infections from traditional medicine to herbal soap formulations. *Medicinal Plants for Holistic Health and Well-Being*. Elsevier, Academic Press, 255-275.
- MAHDI, J., MAHDI, A., MAHDI, A. and BOWEN, I. 2006. The historical analysis of aspirin discovery, its relation to the willow tree and antiproliferative and anticancer potential. *Journal of Cell Proliferation*, 39, 147-155.
- MALLICK, K., WITCOMB, M. and SCURELL, M. 2004. Polymer stabilized silver nanoparticles: A photochemical synthesis route. *Journal of Materials Science*, 39, 4459-4463.
- MALLIKARJUN, K., NARSIMHA, G., DILLIP, G., PRAVEEN, B., SHREEDHAR, B. and LARSHMI, S. 2011. Green synthesis of silver nanoparticles using *Ocimum* leaf extract and their characterization. *Digest Journal of Nanomaterials Biostructures*, 6, 181-6.
- MANDIĆ, B. M., GOĐEVAC, D. M., LJUBODRAG V. VUJISIĆ, TRIFUNOVIĆ, S. S., TESEVIĆ, V. V., VAJS, V. V. and MILOSAVLJEVIĆ, S. M. 2011. Semiquinol and phenol compounds from seven *Senecio* species. *Chemical Papers*, 65, 90-92.
- MANOKARI, M. and SHEKHAWAT, M. S. 2016. Synthesis of Zinc oxide nanoparticles from *Clitoria ternatea* L. extracts: a green approach. *World Scientific News*, 52, 216-227.
- MAROYI, A. 2013. *Warburgia salutaris* (Bertol. f.) Chiov.: A multi-use ethnomedicinal plant species. *Journal of Medicinal Plants Research*, 7, 53-60.
- MAVIMBELA, T., VERMAAK, I., CHEN, W. and VILJOEN, A. 2018. Rapid quality control of *Sutherlandia frutescens* leaf material through the quantification of SU1 using vibrational spectroscopy in conjunction with chemometric data analysis. *Phytochemistry Letters*, 25, 184-190.

- MCCHESNEY, J. D., VENKATARAMAN, S. K. and HENRI, J. T. 2007. Plant natural products: Back to the future or into extinction? *Phytochemistry*, 68, 2015-2022.
- MIRZAEI, H. and DARROUDI, M. 2017. Zinc oxide nanoparticles: biological synthesis and biomedical applications. *Ceramics International*, 43, 907-914.
- MISHRA, P. K., MISHRA, H., EKIELSKI, A., TALEGAONKAR, S. and VAIDYA, B. 2017. Zinc oxide nanoparticles: a promising nanomaterial for biomedical applications. *Drug Discovery Today*, 22, 1825-1834.
- MITTAL, A., CHISTI, Y. and BANERJEE, U. 2013. Synthesis of metallic nanoparticles using plant extracts. *Biotechnology Advances*, 31, 346-356 .
- MITTAL, A. K., KUMAR, S. and BANERJEE, U. C. 2014. Quercetin and gallic acid mediated synthesis of bimetallic (silver and selenium) nanoparticles and their antitumor and antimicrobial potential. *Journal of Colloid and Interface Science*, 431, 194-199.
- MOHAMED, I., EL-NUR, B., CHOUDHARY, M. and KHAN, S. 2009. Bioactive natural products from two Sudanese medicinal plants *Diospyros Mespiliformis* and *Croton zambesicus*. *Records of Natural Products*, 3, 198–203.
- MOHANRAJ, V. and CHEN, Y. 2006. Nanoparticles – A Review. *Tropical Journal of Pharmaceutical Research*, 5, 651-573.
- MOLYNEUX, P. 2004. The use of the stable free radical diphenylpicrylhydrazyl (DPPH) for estimating antioxidant activity. *Songklanakarin Journal of Science and Technology*, 26, 211-219.
- MOREIRA-MUÑOZ, A. and MUÑOZ-SCHICK, M. 2007. Classification, diversity, and distribution of *Chilean Asteraceae*: implications for biogeography and conservation. *Diversity and Distributions*, 13, 818–828.

- NAGAJYOTHI, P. C., CHA, S. J., YANG, I. J., SREEKANTH, T. V. M., KIM, K. J. and SHIN, H. M. 2015. Antioxidant and anti-inflammatory activities of zinc oxide nanoparticles synthesized using *Polygala tenuifolia* root extract. *Journal of Photochemistry and Photobiology B: Biology*, 146, 10-17.
- NAIDOO, D., VAN VUUREN, S. F., VAN ZYL, R. L. and DE WET, H. 2013. Plants traditionally used individually and in combination to treat sexually transmitted infections in Northern Maputaland, South Africa: Antimicrobial activity and cytotoxicity. *Journal of Ethnopharmacology*, 149, 656-667.
- NAZERUDDIN, G., PRASAD, N., PRASAD, S., SHAIKH, Y., WAGHMARE, S. and ADHYAPAK, P. 2014. *Coriandrum sativum* seed extract assisted in situ green synthesis of silver nanoparticle and its anti-microbial activity. *Industrial Crops and Products*, 60, 212-216.
- NAZZARO, F., FRATIANNI, F. and COPPOLA, R. 2013. Quorum sensing and phytochemicals. *International Journal of Molecular Sciences*, 14, 12607-12619.
- OGUNLEYE, D. and IBITOYE, S. 2003. Studies of antimicrobial activity and chemical constituents of *Ximenia americana*. *Tropical Journal of Pharmaceutical Research*, 2, 239-241.
- OGURA, M., CORDELL, G. A. and FARNSWORTH, N. R. 1976. Potential anticancer agents III. Jacaranone, a novel phytoquinoid from *Jacaranda caucana*. *Journal of Natural Products*, 39, 255-257.
- OKIGBO, R. N., ANUAGASI, C. L. and AMADI, J. E. 2009. Advances in selected medicinal and aromatic plants indigenous to Africa. *Journal of Medicinal Plants Research*, 3, 86-95.

- OKOYE, N. N., AJAGHAKU, D. L., OKEKE, H. N., ILODIGWE, E. E., NWORU, C. S. and OKOYE, F. B. C. 2014. Beta-Amyrin and alpha-amyrin acetate isolated from the stem bark of *Alstonia boonei* display profound anti-inflammatory activity. *Pharmaceutical Biology*, 52, 1478-1486.
- OYEBODE, O., KANDALA, N.-B., CHILTON, P. J. and LILFORD, R. J. 2016. Use of traditional medicine in middle-income countries: a WHO-SAGE study. *Health Policy and Planning*, 31, 984-991.
- PANDA, K. K., GOLARI, D., VENUGOPAL, A., ACHARY, V. M. M., PHAOMEI, G., PARINANDI, N. L., SAHU, H. K. and PANDA, B. B. 2017. Green Synthesized Zinc Oxide (ZnO) Nanoparticles Induce Oxidative Stress and DNA Damage in *Lathyrus sativus* L. Root Bioassay System. *Journal of Antioxidants*, 6, 35.
- PANDIMURUGAN, R. and THAMBIDURAI, S. 2017. UV protection and antibacterial properties of seaweed capped ZnO nanoparticles coated cotton fabrics. *International Journal of Biological Macromolecules*, 105, 788-795.
- PATIL, R. S., KOKATE, M. R., SHINDE, D. V., KOLEKAR, S. S. and HAN, S. H. 2014. Synthesis and enhancement of photocatalytic activities of ZnO by silver nanoparticles. *Spectrochimica Acta Part A: Molecular and Biomolecular Spectroscopy*, 122, 113-117.
- PRABHAKAR, P. K. 2016. Pathophysiology of Secondary Complications of Diabetes Mellitus *Asian Journal of Pharmaceutical and Clinical Research*, 9, 32-36.
- PREMANATHAN, M., KARTHIKEYAN, K., JEYASUBRAMANIAN, K. and MANIVANNAN, G. 2011. Selective toxicity of ZnO nanoparticles toward Gram-positive bacteria and cancer cells by apoptosis through lipid peroxidation. *Nanomedicine: Nanotechnology, Biology and Medicine*, 7, 184-192.

- PRIYADHARSHINI, R. I., PRASANNARAJ, G., GEETHA, N. and VENKATACHALAM, P. 2014. Microwave-mediated extracellular synthesis of metallic silver and zinc oxide nanoparticles using macro-algae (*Gracilaria edulis*) extracts and its anticancer activity against human PC3 cell lines. *Applied Biochemistry and Biotechnology*, 174, 2777-2790.
- QUAVE, C., PIERONI, A. and BENNETT, B. 2008. Dermatological remedies in the traditional pharmacopoeia of *Vulture-Alto Bradano*, inland southern Italy. *Journal of Ethnobiology and Ethnomedicine*, 4, 5.
- RAGHAVAN, B. S., KONDATH, S., ANANTANARAYANAN, R. and RAJARAM, R. 2015. Kaempferol mediated synthesis of gold nanoparticles and their cytotoxic effects on MCF-7 cancer cell line. *Process Biochemistry*, 50, 1966-1976.
- RAJAKUMAR, G., THIRUVENGADAM, M., MYDHILI, G., GOMATHI, T. and CHUNG, I.-M. 2017. Green approach for synthesis of zinc oxide nanoparticles from *Andrographis paniculata* leaf extract and evaluation of their antioxidant, anti-diabetic, and anti-inflammatory activities. *Bioprocess and Biosystems Engineering*, 1-10.
- RANA, A., BHANGALIA, S. and SINGH, H. P. 2013. A new phenylethanoid glucoside from *Jacaranda mimosifolia*. *Natural Product Research*, 27, 1167-1173.
- RATES, S. M. K. 2001. Plants as source of drugs. *Toxicon*, 39, 603-613.
- REID, A.-M., OOSTHUIZEN, C. B., FIBRICH, B. D., TWILLEY, D., LAMBRECHTS, I. A., DE CANHA, M. N., RADEMAN, S. and LALL, N. 2018. Traditional medicine: The ancient roots of modern practice. *Medicinal Plants for Holistic Health and Well-Being*. Elsevier, Academic Press, 1-11 .
- REKHA, P., VASAVI, H., VIPIN, C., SAPTAMI, K. and ARUN, A. 2017. A medicinal herb *Cassia alata* attenuates quorum sensing in *Chromobacterium violaceum* and *Pseudomonas aeruginosa*. *Letters in Applied Microbiology*, 64, 231-238.

- RUPESH, T., NITIKA, J., RAGHVENDRA, P. and SARDUL, S. 2011. Practices in wound healing studies of plants. *Evidence Based Complementary and Alternative Medicine*, 2011, 438056
- SANGHI, R. and VERMA, P. 2010. Microbes are green and eco-friendly nanofactories. *Green Chemistry for Environmental Sustainability*, 15, 315-39.
- SANTHOSHKUMAR, J., KUMAR, S. V. and RAJESHKUMAR, S. 2017. Synthesis of zinc oxide nanoparticles using plant leaf extract against urinary tract infection pathogen. *Resource-Efficient Technologies*, 3, 459-465.
- SASTRY, M., AHMAD, A., KHAN, M. and KUMAR, R. 2003. Biosynthesis of metal nanoparticles using fungi and actinomycetes. *Current Science*, 85, 162-170.
- SATHISHKUMAR, P., GU, F. L., ZHAN, Q., PALVANNAN, T. and MOHD YUSOFF, A. R. 2018. Flavonoids mediated 'Green' nanomaterials: A novel nanomedicine system to treat various diseases – Current trends and future perspective. *Materials Letters*, 210, 26-30.
- SATYAVANI, K., GURUDEEBAN, S., RAMANATHAN, T. and BALASUBRAMANIAN, T. 2011. Biomedical potential of silver nanoparticles synthesized from calli cells of *Citrullus colocynthis* (L.) Schrad. *Journal of Nanobiotechnology*, 9, 43.
- SAXENA, M., SAXENA, J., NEMA, R., SINGH, D. and GUPTA, A. 2013. Phytochemistry of medicinal plants. *Journal of Pharmacognosy and Phytochemistry*, 1.
- SCHAFFER, B., HOHENESTER, U., TRUGLER, A. and HOFER, F. 2009. High resolution surface plasmon imaging of gold nanoparticles by energy -filtered transmission electron microscopy. *Physical Review*, 79.
- SCHARF, D. H., HEINEKAMP, T. and BRAKHAGE, A. A. 2014. Human and plant fungal pathogens: the role of secondary metabolites. *PLoS pathogens*, 10, e1003859.

- SENTHILKUMAR, S. and SIVAKUMAR, T. 2014. Green tea (*Camellia sinensis*) mediated synthesis of zinc oxide (ZNO) nanoparticles and studies on their antimicrobial activities. *International Journal of Pharmacy and Pharmaceutical Science*, 6, 461-465.
- SHIOJIMA, K., SUZUKI, H., KODERA, N., AGETA, H., CHANG, H.-C. and CHEN, Y.-P. 1996. Composite constituents: thirty-nine triterpenoids including two novel compounds from *Ixeris chinensis*. *Chemical and Pharmaceutical Bulletin*, 44, 509-514.
- SINGH, A. K., PAL, P., GUPTA, V., YADAV, T. P., GUPTA, V. and SINGH, S. P. 2018. Green synthesis, characterization and antimicrobial activity of zinc oxide quantum dots using *Eclipta alba*. *Materials Chemistry and Physics*, 203, 40-48.
- SINGHAL, G., BHAVESH, R., KASARIYA, K., SHARMA, A. and SINGH, R. 2011. Biosynthesis of silver nanoparticles using *Ocimum sanctum* (Tulsi) leaf extract and screening its antimicrobial activity. *Journal of Nanoparticle Research*, 13, 2981-8.
- STARY, F. 1998. The natural guide to medicinal herbs, and plants. Tiger Books International, Wallingford, United Kingdom.
- STOLARCZYK, E. U., STOLARCZYK, K., ŁASZCZ, M., KUBISZEWSKI, M., MARUSZAK, W., OLEJARZ, W. and BRYK, D. 2017. Synthesis and characterization of genistein conjugated with gold nanoparticles and the study of their cytotoxic properties. *European Journal of Pharmaceutical Sciences*, 96, 176-185.
- STROYUK, A., SHVALAGIN, V. and KUCHMII, S. Y. 2005. Photochemical synthesis and optical properties of binary and ternary metal–semiconductor composites based on zinc oxide nanoparticles. *Journal of Photochemistry and Photobiology A: Chemistry*, 173, 185-194.

- SUDHEESH KUMAR, P., LAKSHMANAN, V.-K., ANILKUMAR, T., RAMYA, C., RESHMI, P., UNNIKRISHNAN, A., NAIR, S. V. and JAYAKUMAR, R. 2012. Flexible and microporous chitosan hydrogel/nano ZnO composite bandages for wound dressing: in vitro and in vivo evaluation. *ACS Applied Materials and Interfaces*, 4, 2618-2629.
- SUJATHA, J., ASOKAN, S. and RAJESHKUMAR, S. 2018. Antidermatophytic activity of green synthesised zinc oxide nanoparticles using *Cassia alata* leaves. *The Journal of Microbiology, Biotechnology and Food Sciences*, 7, 348.
- SUNDRARAJAN, M., AMBIKA, S. and BHARATHI, K. 2015. Plant-extract mediated synthesis of ZnO nanoparticles using *Pongamia pinnata* and their activity against pathogenic bacteria. *Advanced Powder Technology*, 26, 1294-1299.
- TAYLOR, J. L. S., ELGORASHI, E. E., MAES, A., VAN GORP, U., DE KIMPE, N., VAN STADEN, J. and VERSCHAEVE, L. 2003. Investigating the safety of plants used in South African traditional medicine: Testing for genotoxicity in the micronucleus and alkaline comet assays. *Environmental and Molecular Mutagenesis*, 42, 144-154.
- TIAN, X.-Y., WANG, Y.-H., YANG, Q.-Y., LIU, X., FANG, W.-S. and YUA, S.-S. 2006. Jacaranone glycosides from *Senecio scandens*. *Journal of Asian Natural Products Research*, 8, 125–132.
- TIAN, X.-Y., WANG, Y.-H., YANG, Q.-Y., YU, S.-S. and FANG, W.-S. 2009. Jacaranone analogs from *Senecio scandens*. *Journal of Asian Natural Products Research*, 11, 63–68.
- TORRES, P., CHINCHILLA, R. and GRANDE, M. 1992. Triterpenes from *Senecio linifolius* *Studia Chimica*, 17, 53-57.

- VANDEPUTTE, O. M., KIENDREBEOGO, M., RAJAONSON, S., DIALLO, B., MOL, A., EL JAZIRI, M. and BAUCHER, M. 2010. Identification of catechin as one of the flavonoids from *Combretum albiflorum* bark extract that reduces the production of quorum-sensing-controlled virulence factors in *Pseudomonas aeruginosa* PAO1. *Applied and Environmental Microbiology*, 76, 243-253.
- VASAVI, H. S., ARUN, A. B. and REKHA, P. D. 2014. Anti-quorum sensing activity of *Psidium guajava* L. flavonoids against *Chromobacterium violaceum* and *Pseudomonas aeruginosa* PAO1. *Microbiology and Immunology*, 58, 286-293.
- VÁZQUEZ, L. H., PALAZON, J. and NAVARRO-OCAÑA, A. 2012. The Pentacyclic Triterpenes α - β amyrins: A review of sources and biological activities. *Phytochemicals-A Global Perspective of Their Role in Nutrition and Health*, 23
- WAHAB, R., KIM, Y.-S., MISHRA, A., YUN, S.-I. and SHIN, H.-S. 2010. Formation of ZnO micro-flowers prepared via solution process and their antibacterial activity. *Nanoscale Research Letters*, 5, 1675.
- WANG, D., HUANG, L. and CHEN, S. 2013. *Senecio scandens* Buch.-Ham.: A review on its ethnopharmacology, phytochemistry, pharmacology, and toxicity. *Journal of Ethnopharmacology*, 149, 1-23.
- WEID, M., ZIEGLER, J. and KUTCHAN, T. M. 2004. The roles of latex and the vascular bundle in morphine biosynthesis in the opium poppy, *Papaver somniferum*. *Proceedings of the National Academy of Sciences of the United States of America*, 101, 13957-13962.
- WET, H. D. and NGUBANE, S. C. 2014. Traditional herbal remedies used by women in a rural community in northern Maputaland (South Africa) for the treatment of gynaecology and obstetric complaints. *South African Journal of Botany*, 94, 129–139.

- WHEAT, R. W., ROLLINS, E., LEATHERWOOD, J. and BARNES, R. 1963. Studies on the cell wall of *Chromobacterium violaceum*: the separation of lipopolysaccharide and mucopeptide by phenol extraction of whole cells. *Journal of Biological Chemistry*, 238, 26-29.
- WILLIAMS, D. B. and CARTER, C. B. 2009. Transmission Electron Microscopy, A textbook for materials science, New York, Springer.
- WYK, B. V., OUDTSHOORN, B. V. and GERICKE, N. 1997. Medicinal Plants of South Africa, second edition, South Africa Briza Publications
- WYK, B. V., WET, H. D. and HEERDEN, F. V. 2008. An ethnobotanical survey of medicinal plants in south-eastern Karoo, South Africa. *South African Journal of Botany*, 74, 696–704.
- YUSUF, A. J., ABDULLAHI, M. I., ALEKU, G. A., IBRAHIM, I. A., ALEBIOSU, C. O., YAHAYA, M., ADAMU, H. W., SANUSI, A., MAILAFIYA, M. M. and ABUBAKAR, H. 2018. Antimicrobial activity of stigmasterol from the stem bark of *Neocarya macrophylla*. *Journal of Medicinal Plants for Economic Development*, 2, 1-5.
- YVIN, J. C., CHEVOLOT, L., CHEVOLOT-MAGUEUR, A. M. and COCHARD, J. C. 1985. First isolation of jacaranone from an alga, *Delesseria sanguinea*: A metamorphosis inducer of pecten larvae. *Journal of Natural Products*, 48, 814-816.

APPENDIX

Supporting information consisting the NMR, IR, UV and MS data.

Compound 1- farnesylamine

Compound 2- β -sitosterol

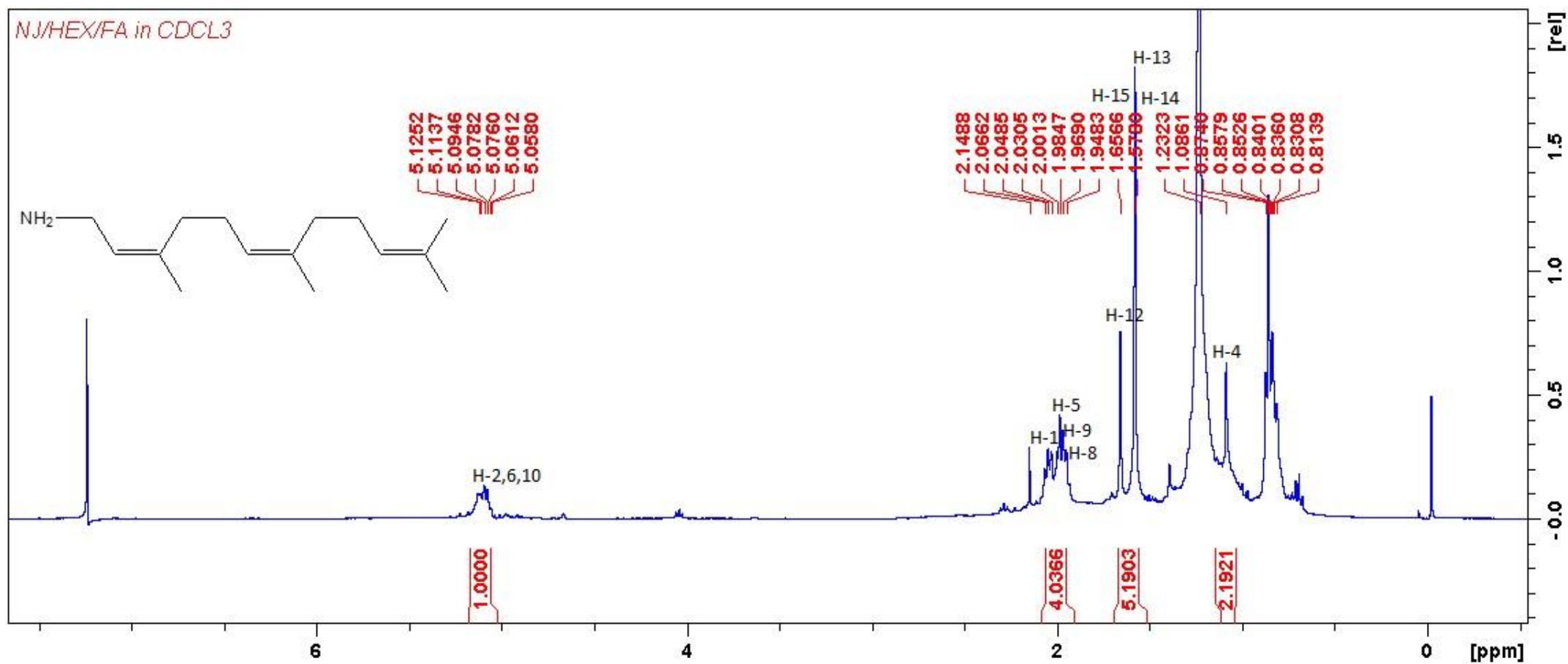
Compound 3- α - β amyrin

Compound 4- stigmasterol

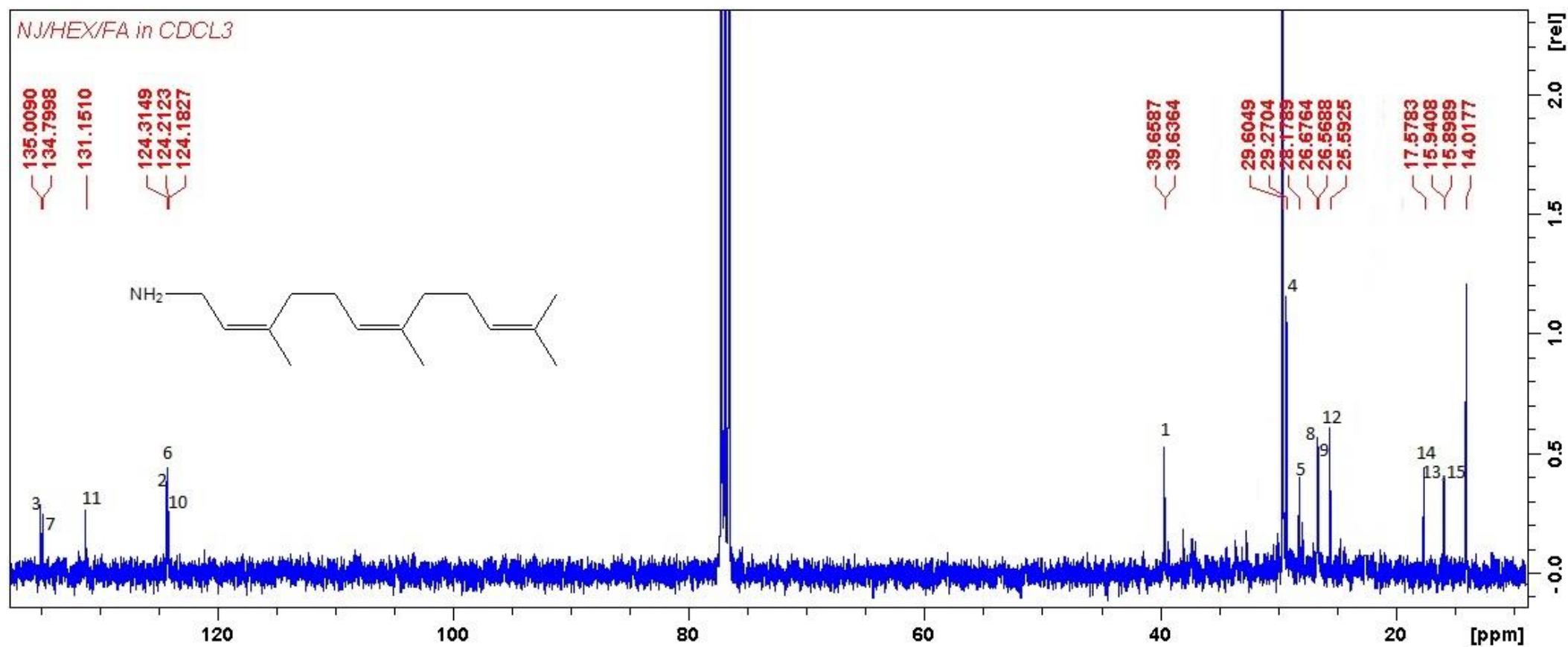
Compound 5- taraxerone

Compound 6- jacaranone

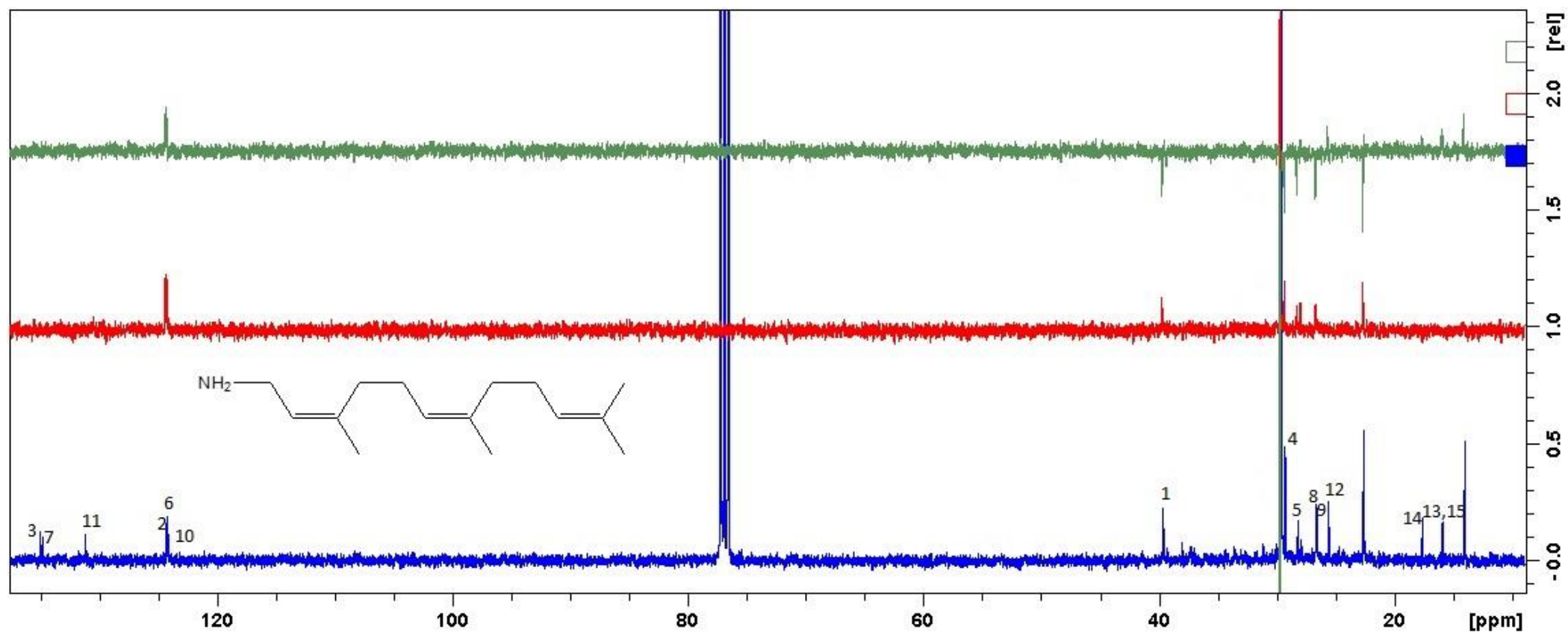
Compound 7- jacaranone methyl ester and methyl-1-hydroxy-4 oxocyclohexylacetate



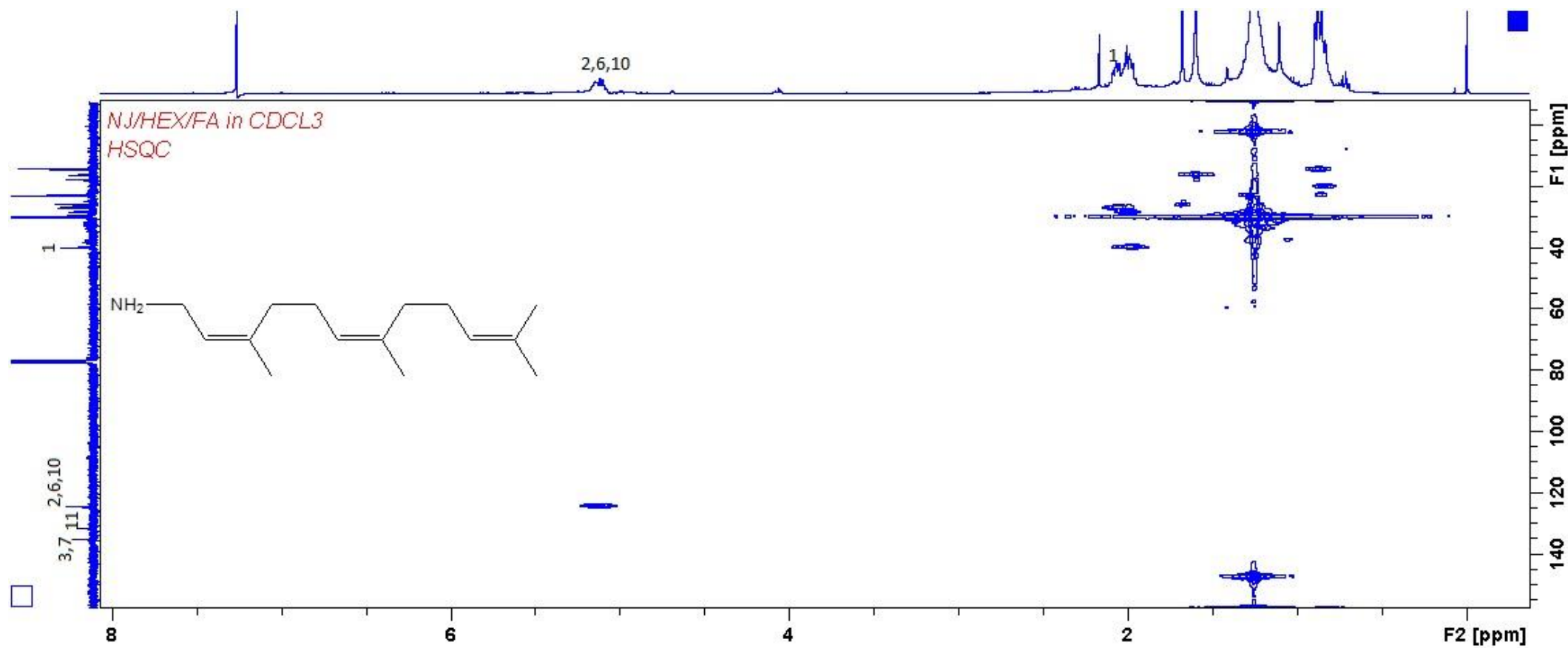
¹H NMR spectrum of farnesylamine



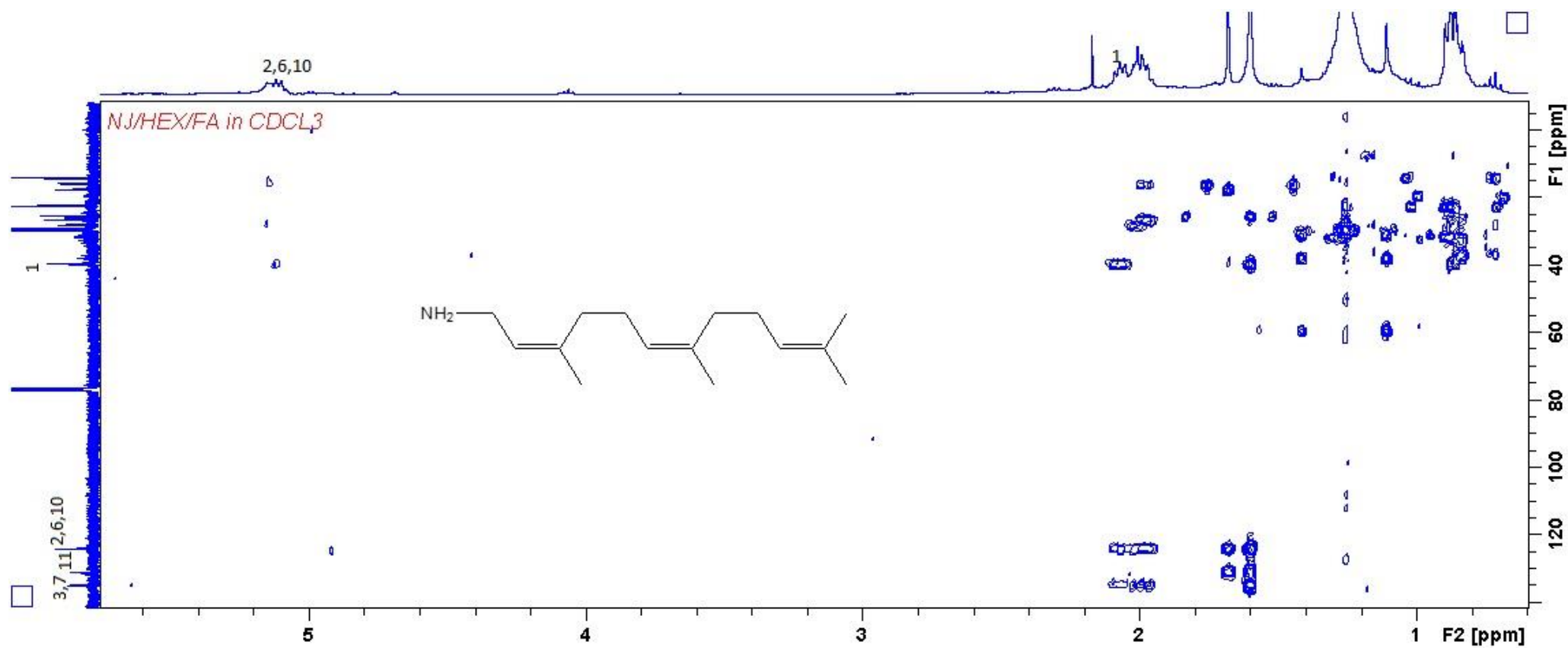
^{13}C NMR spectrum of farnesylamine



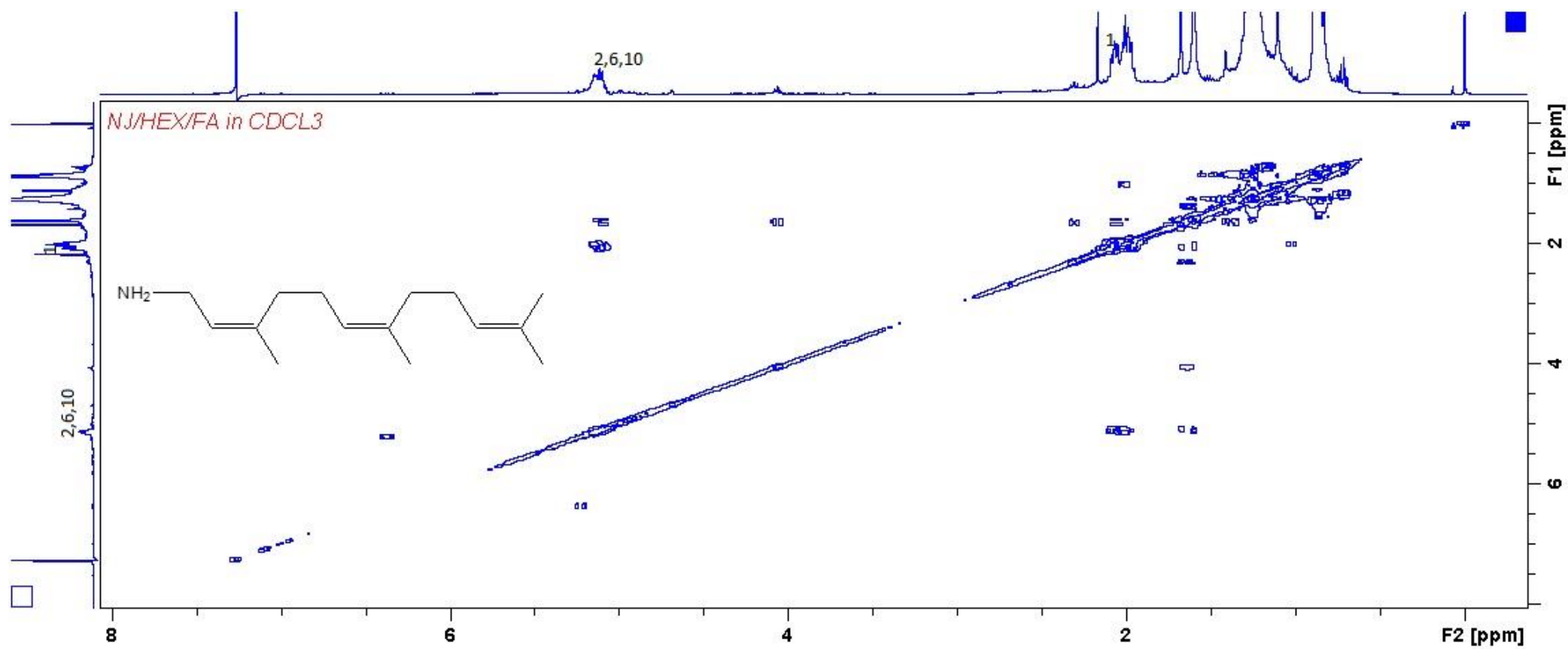
DEPT spectrum of farnesylamine



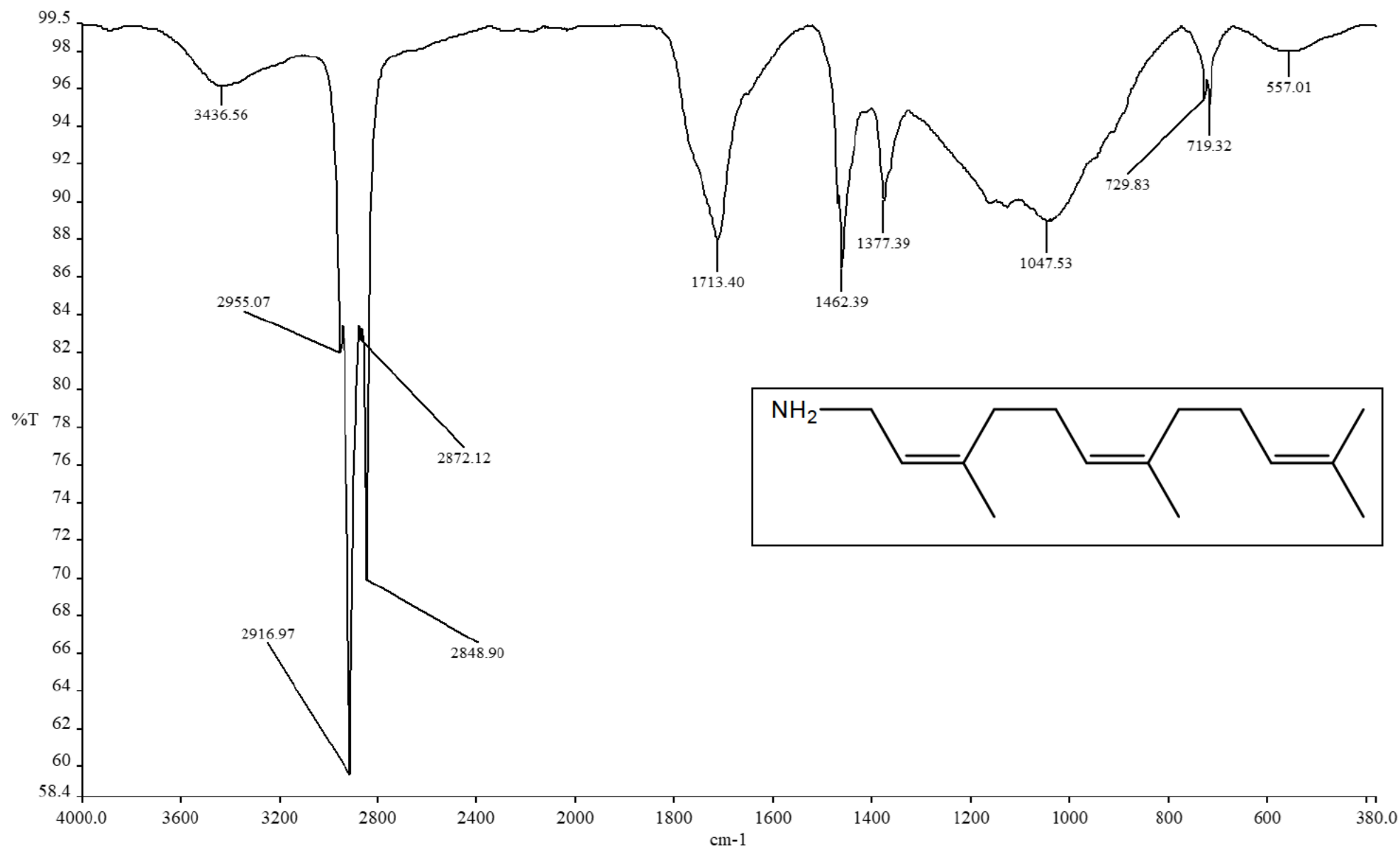
HSQC spectrum of farnesylamine



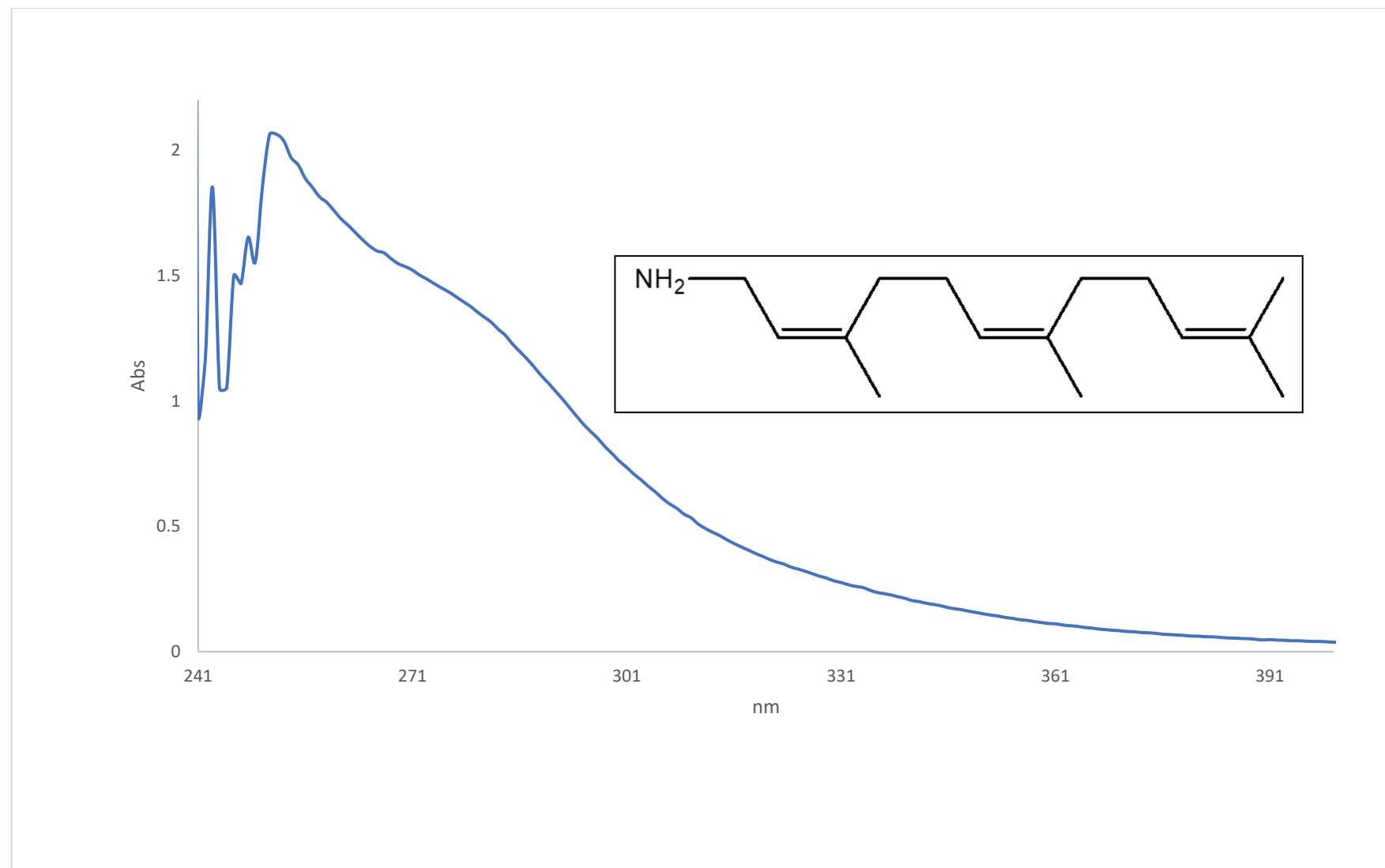
HMBC spectrum of farnesylamine



COSY spectrum of farnesylamine

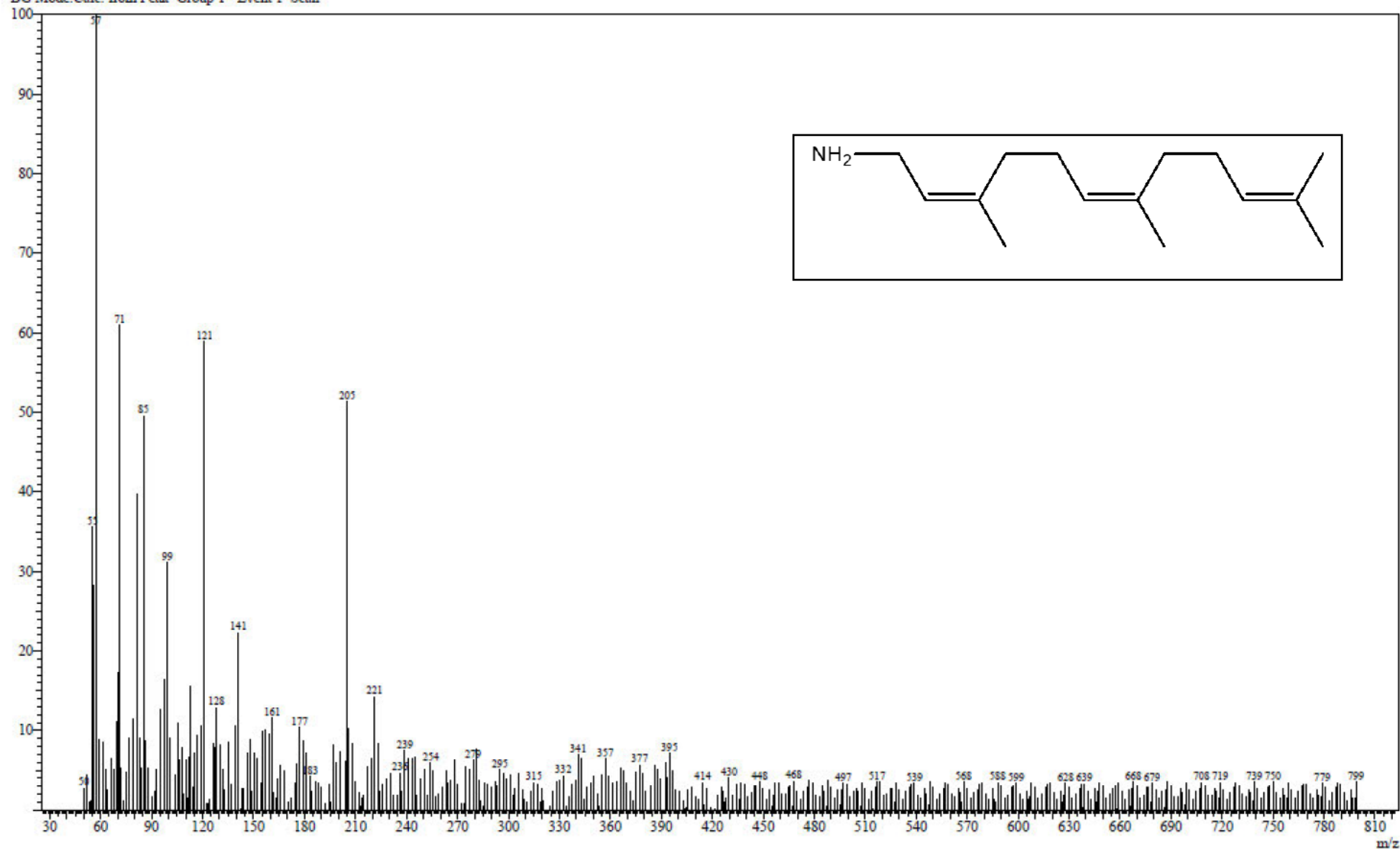


IR spectrum of farnesylamine

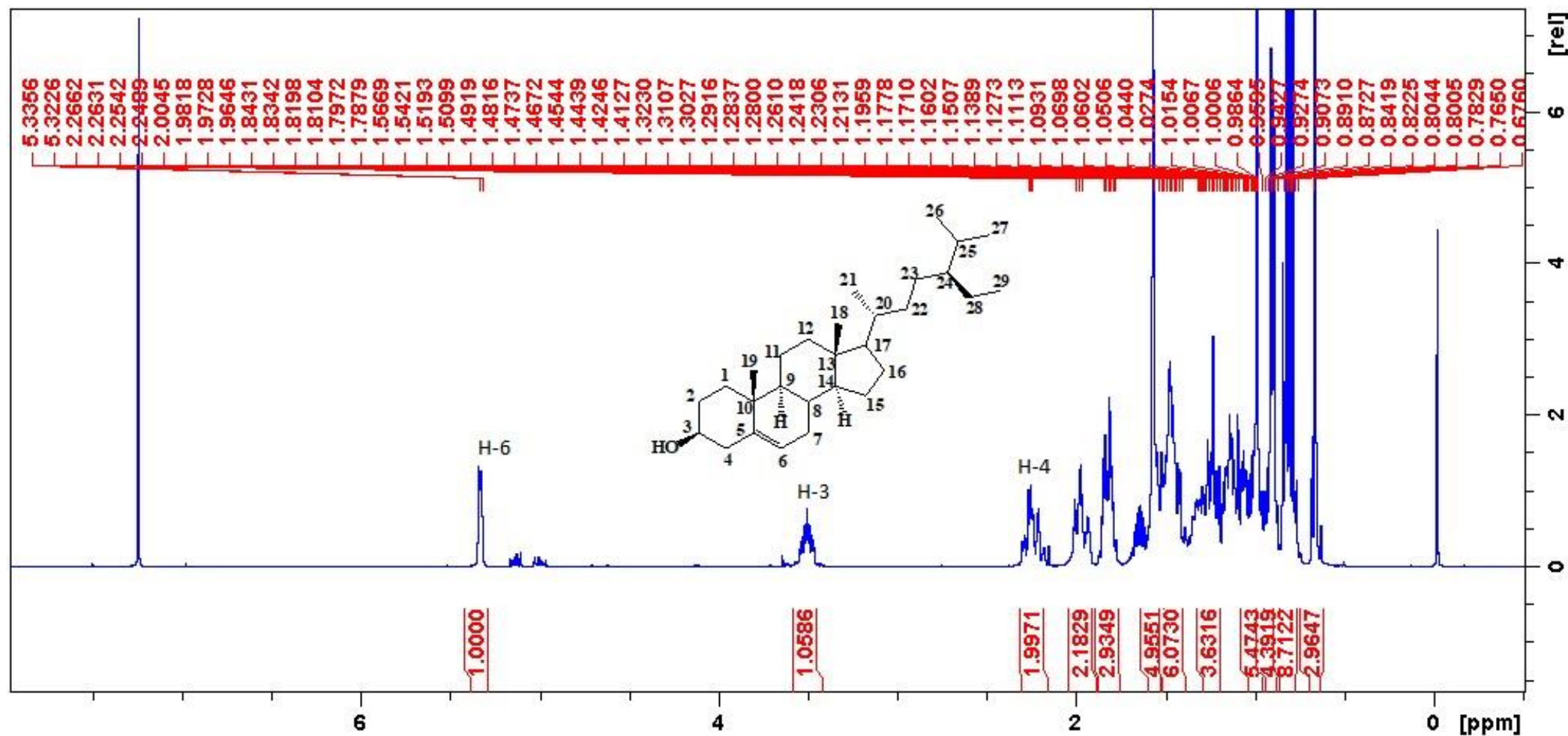


UV spectrum of farnesylamine

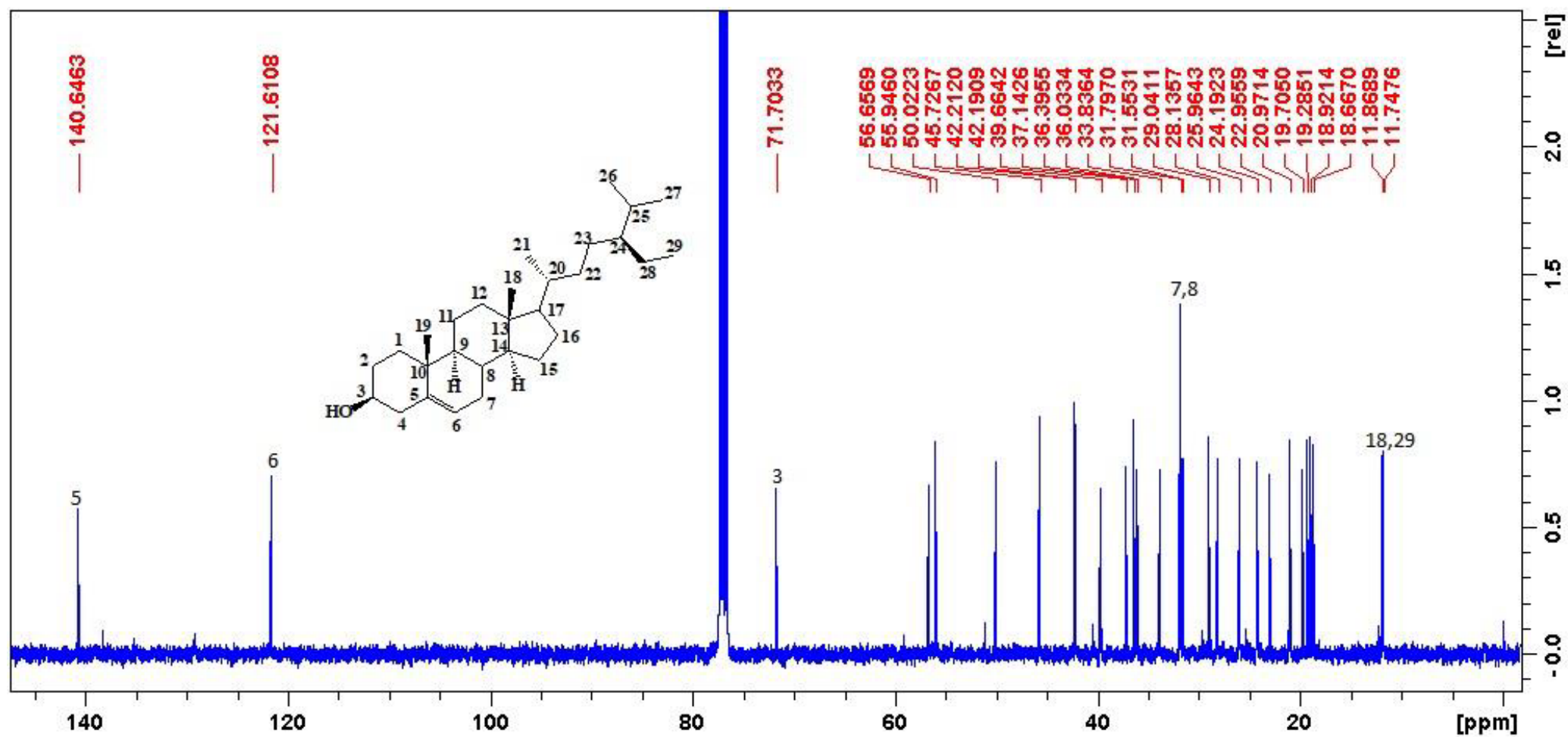
Line#:65 R.Time:26.845(Scan#:4470)
MassPeaks:453
RawMode:Averaged 26.840-26.850(4469-4471) BasePeak:57(21332)
BG Mode:Calc. from Peak Group 1 - Event 1 Scan



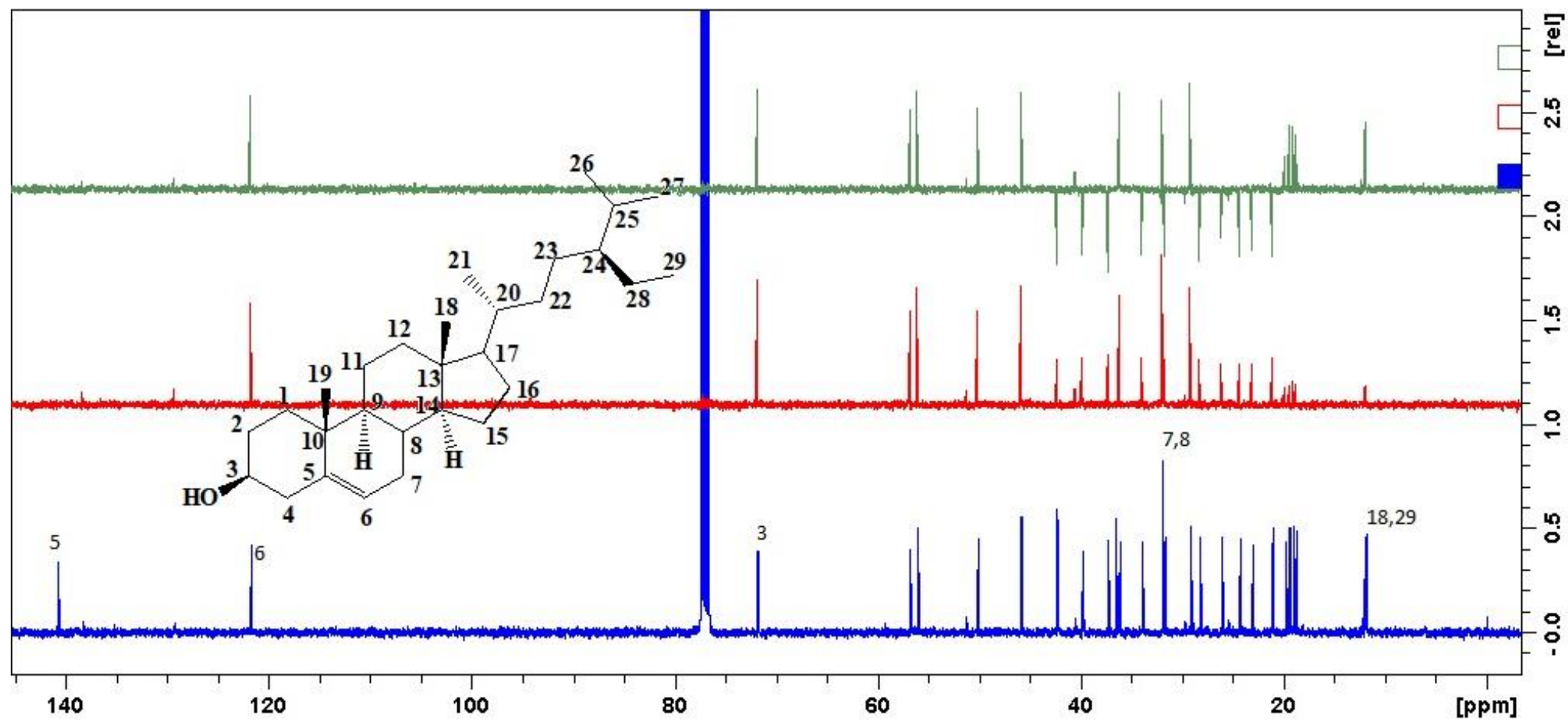
Mass spectrum of farnesylamine



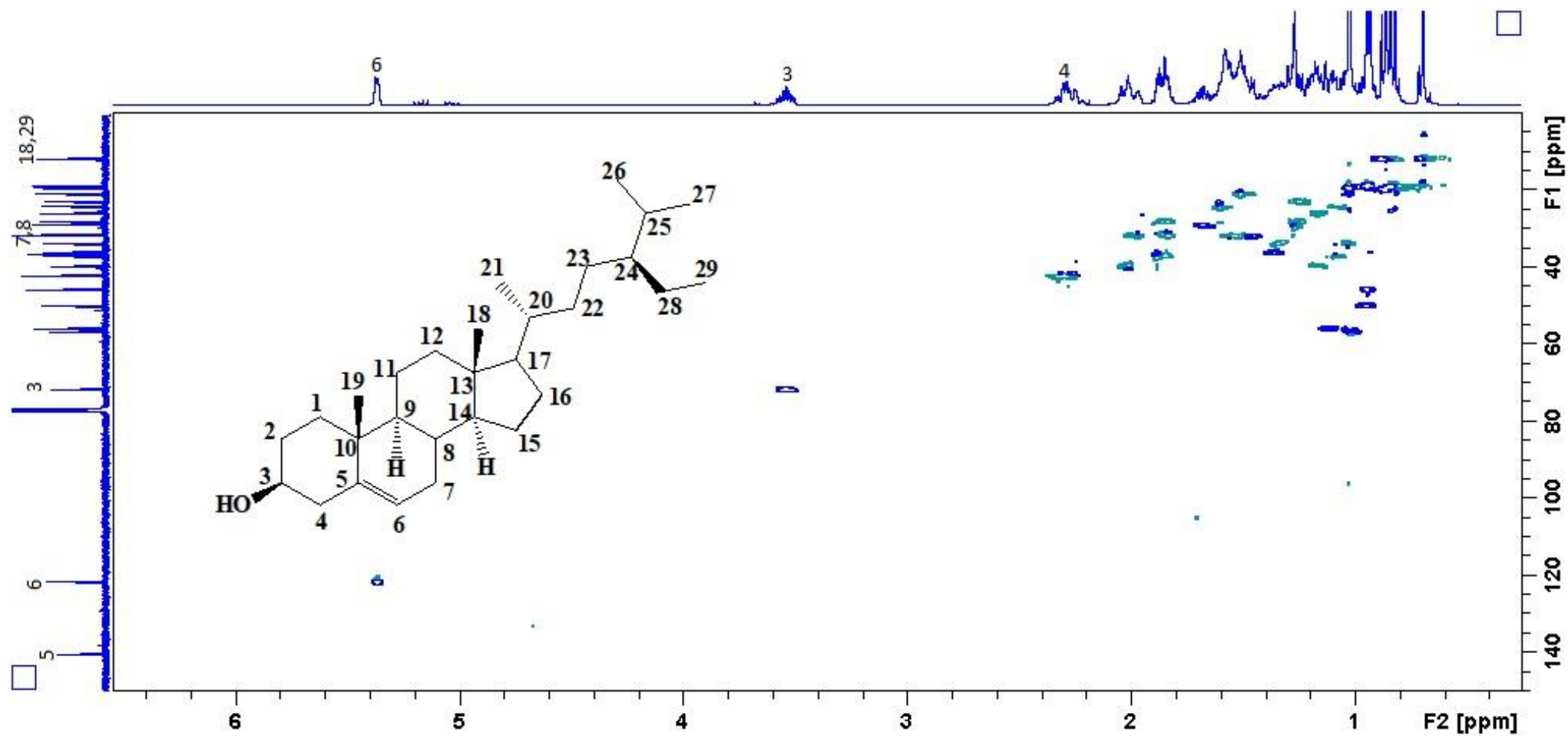
^1H NMR spectrum of β -sitosterol



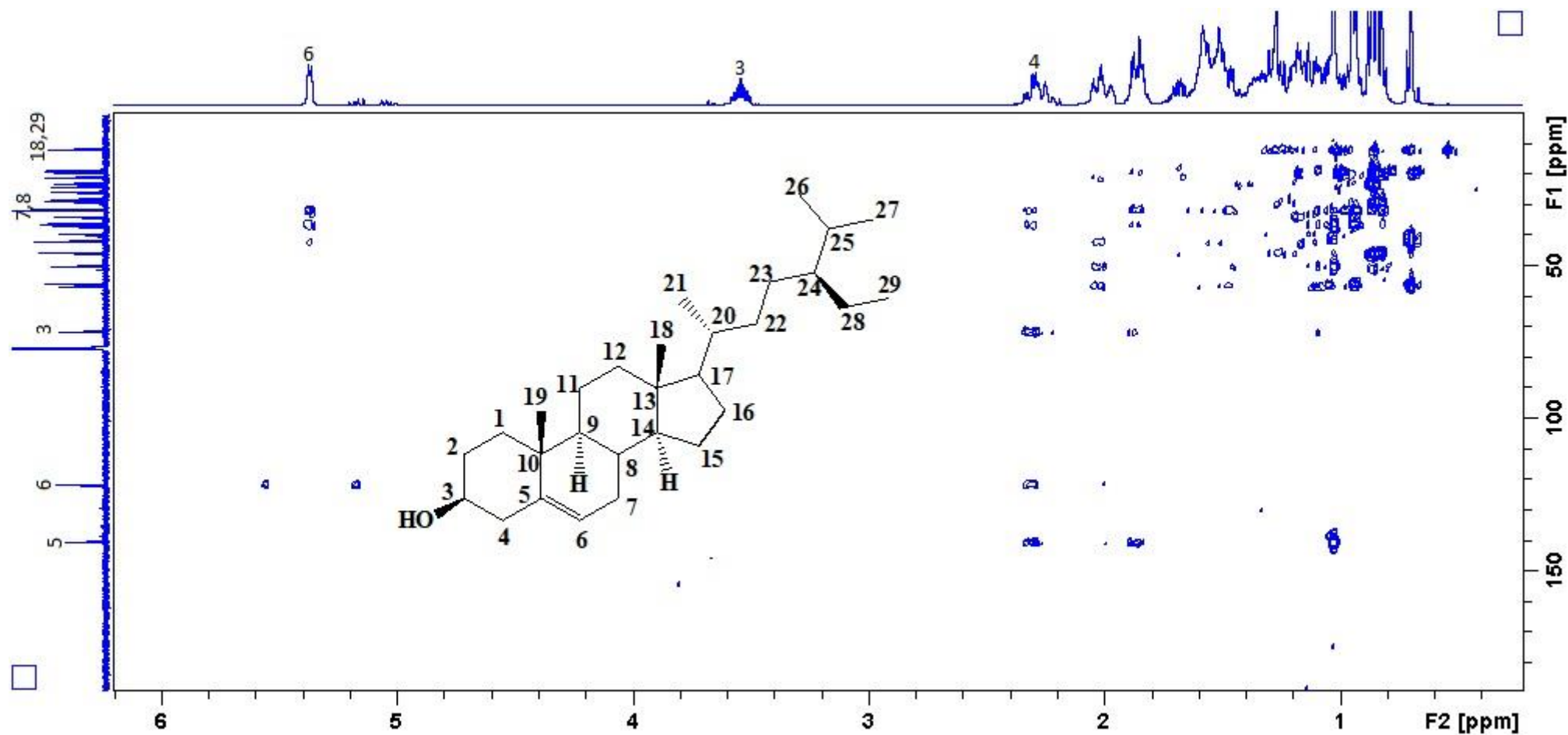
^{13}C NMR spectrum of β -sitosterol



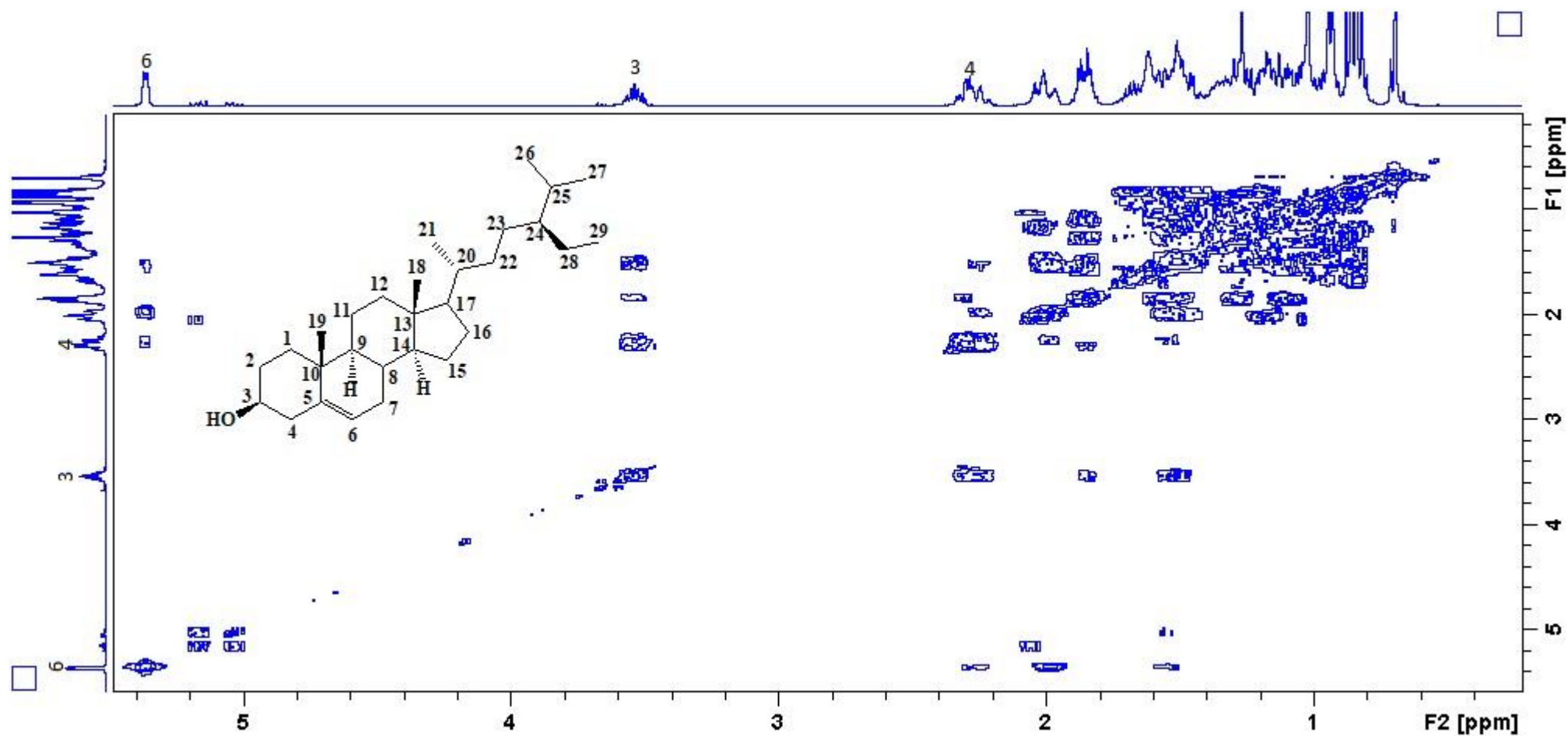
DEPT spectrum of β -sitosterol



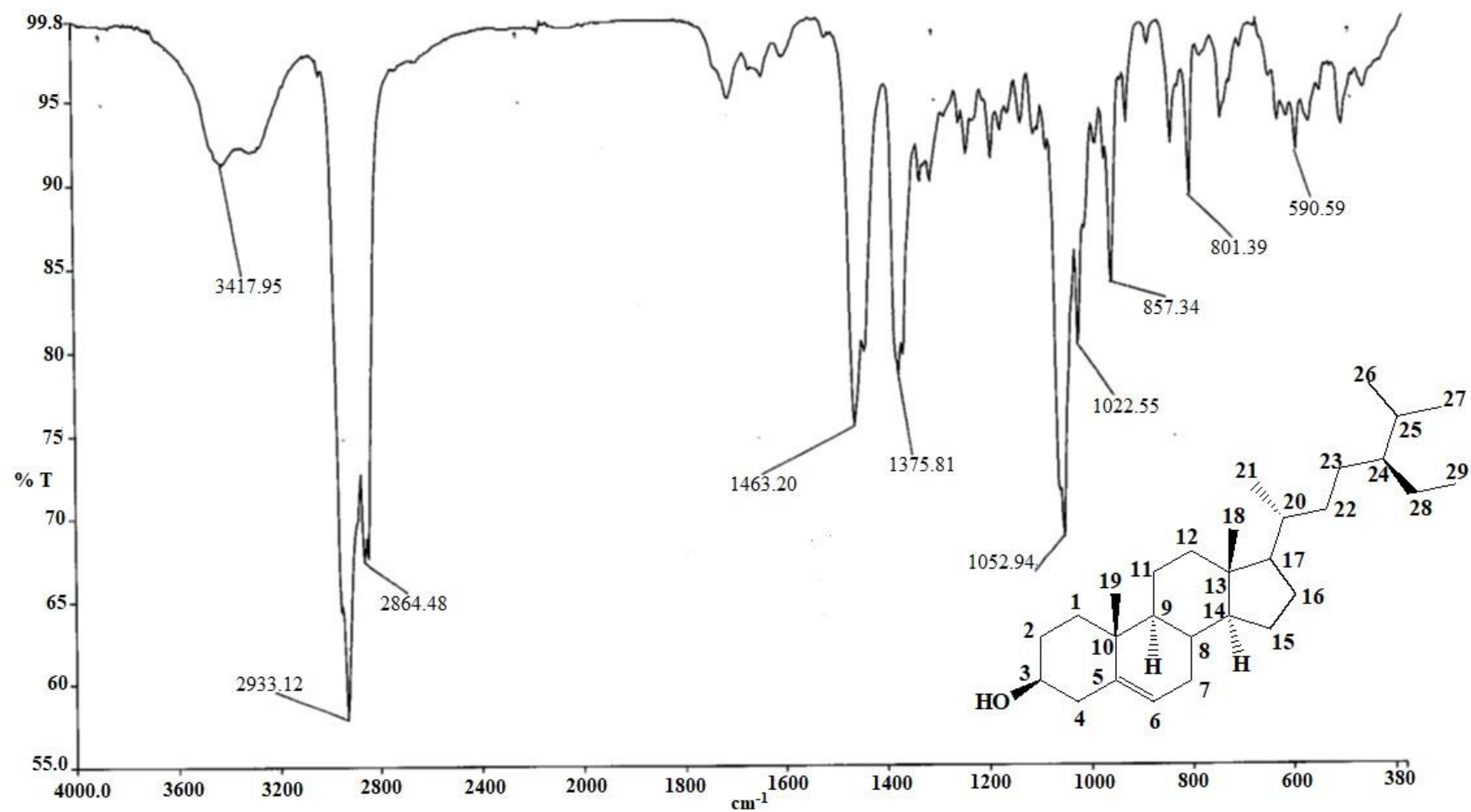
HSQC spectrum of β -sitosterol



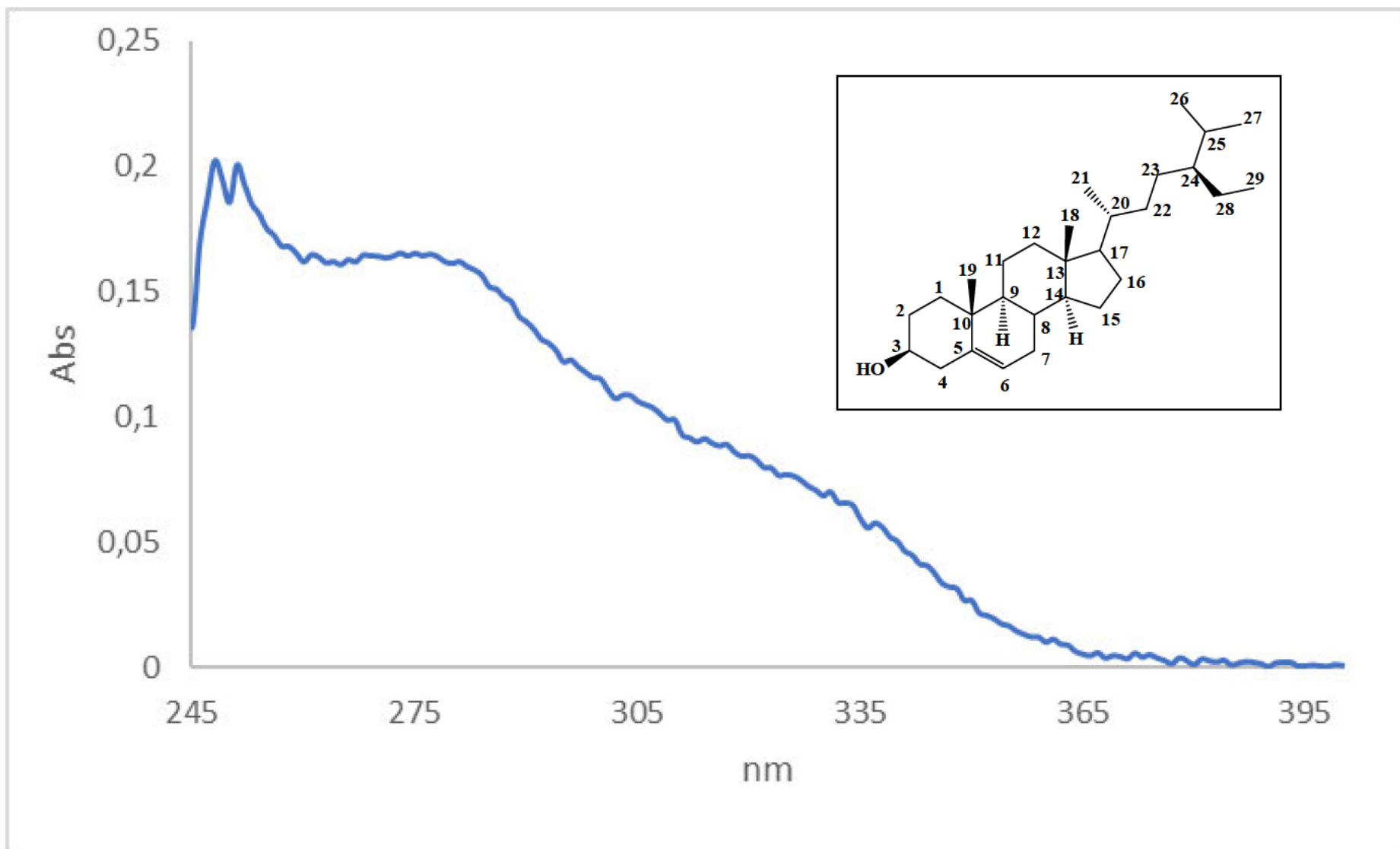
HMBC spectrum of β -sitosterol



COSY spectrum of β -sitosterol

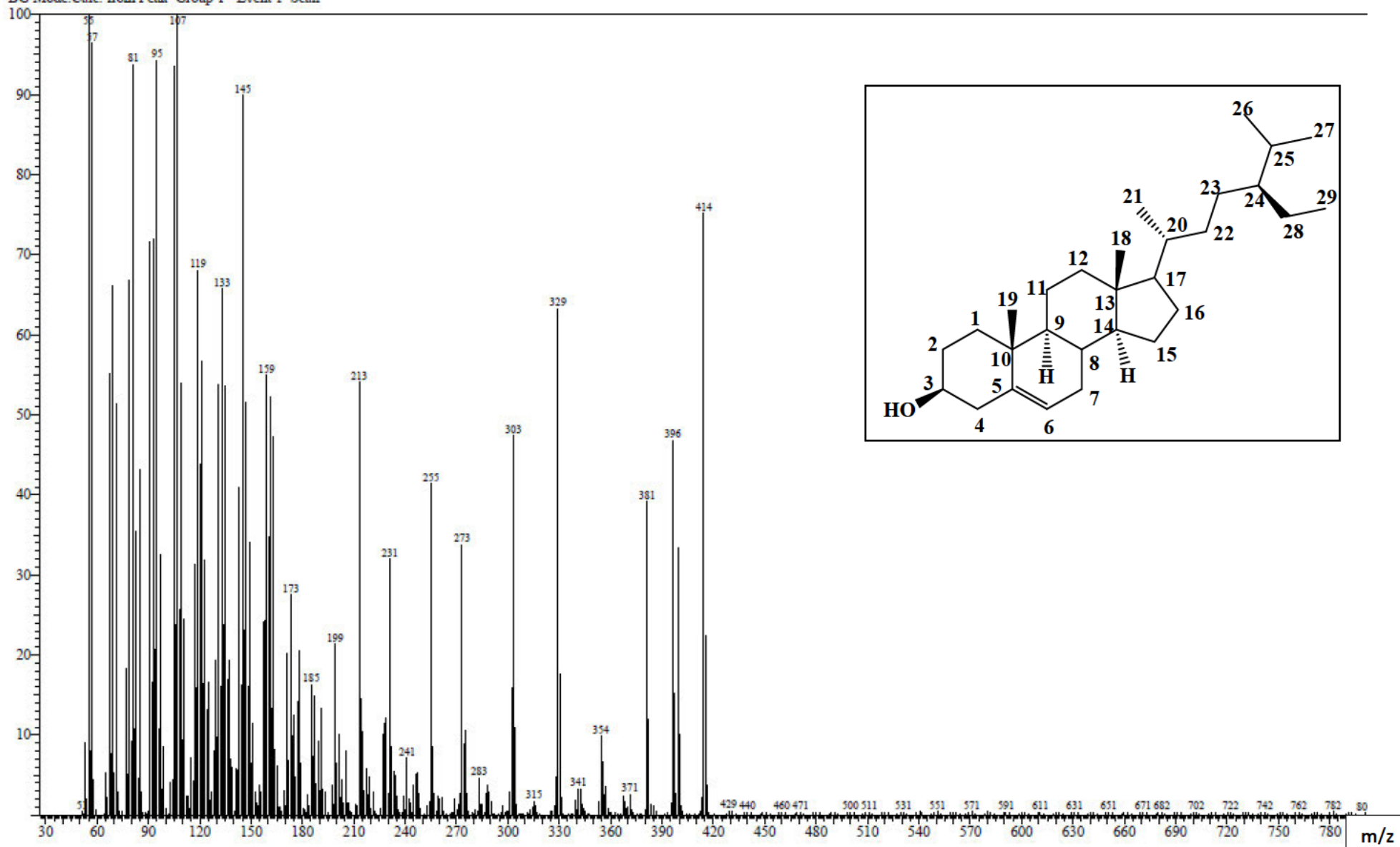


IR spectrum of β -sitosterol

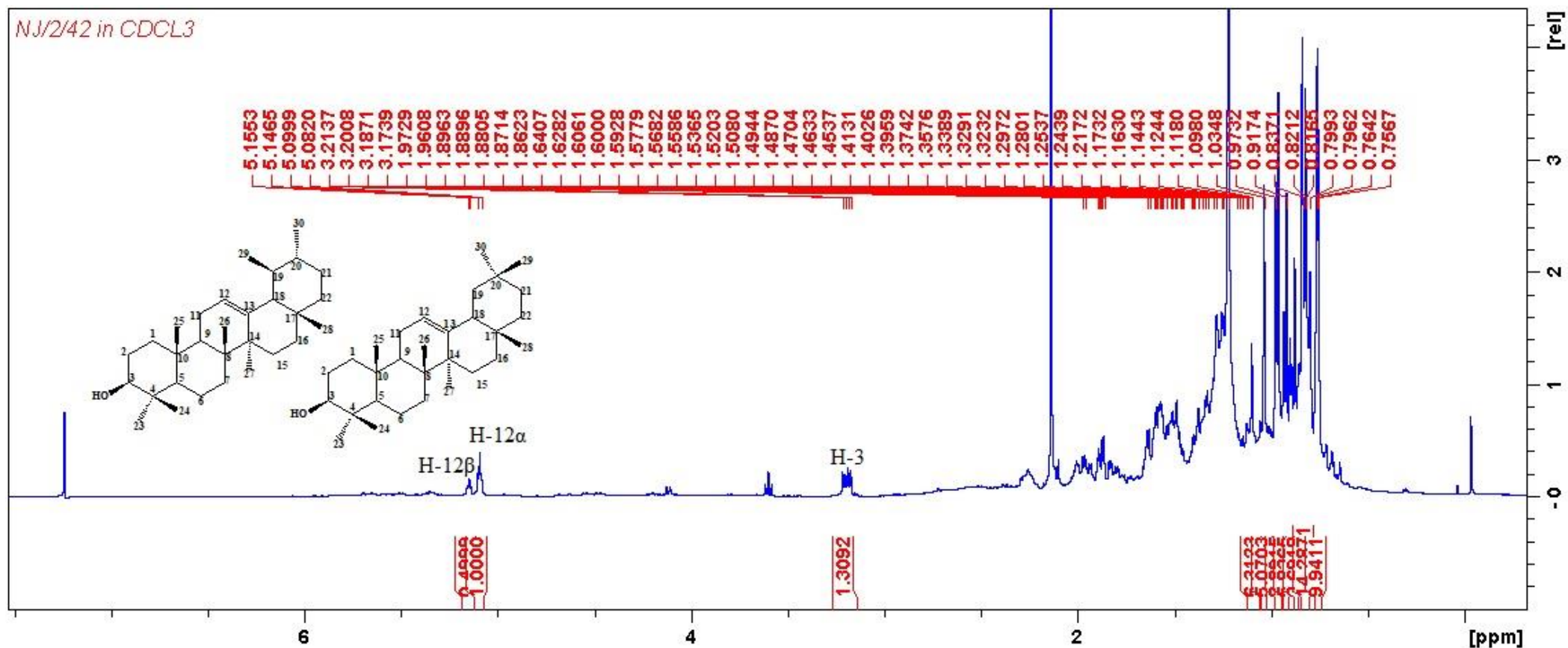


UV spectrum of β -sitosterol

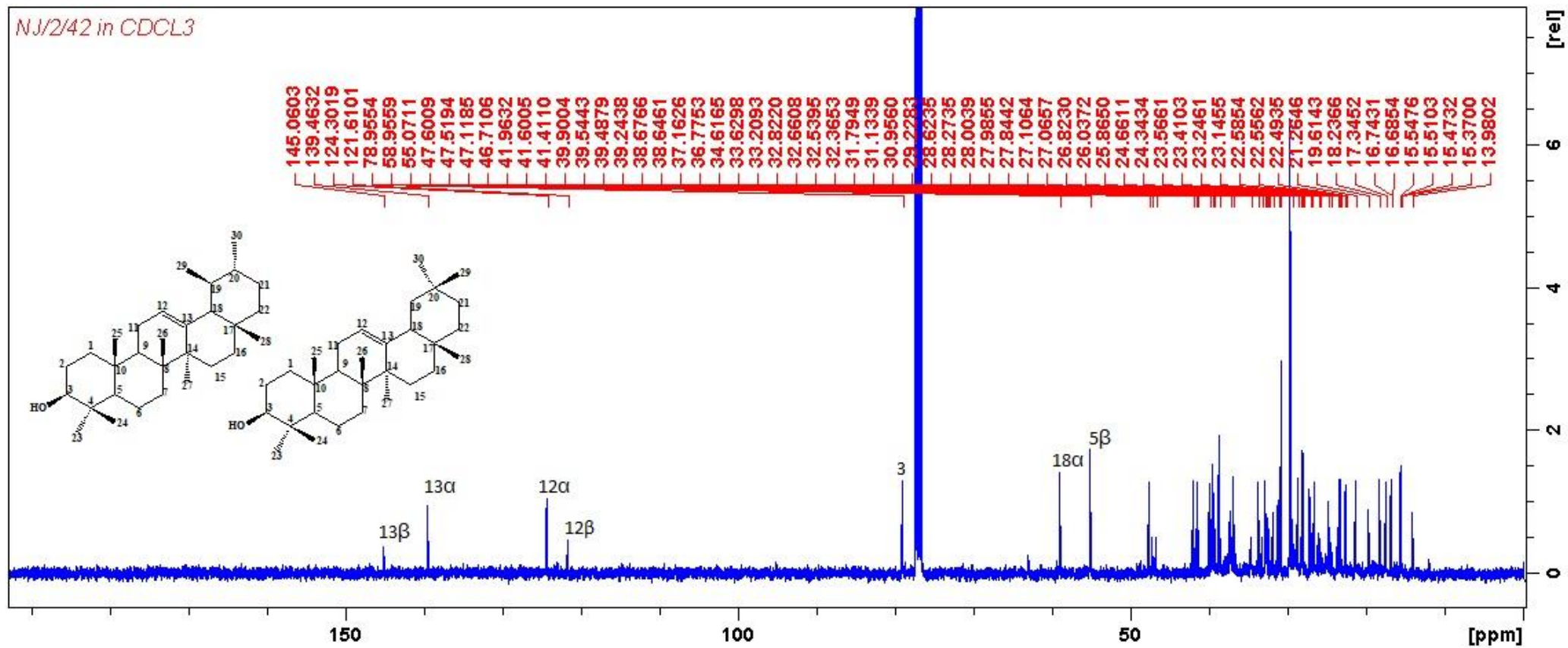
Line#:18 R.Time:30.085(Scan#:5118)
 MassPeaks:484
 RawMode:Averaged 30.080-30.090(5117-5119) BasePeak:55(267953)
 BG Mode:Calc. from Peak Group 1 - Event 1 Scan



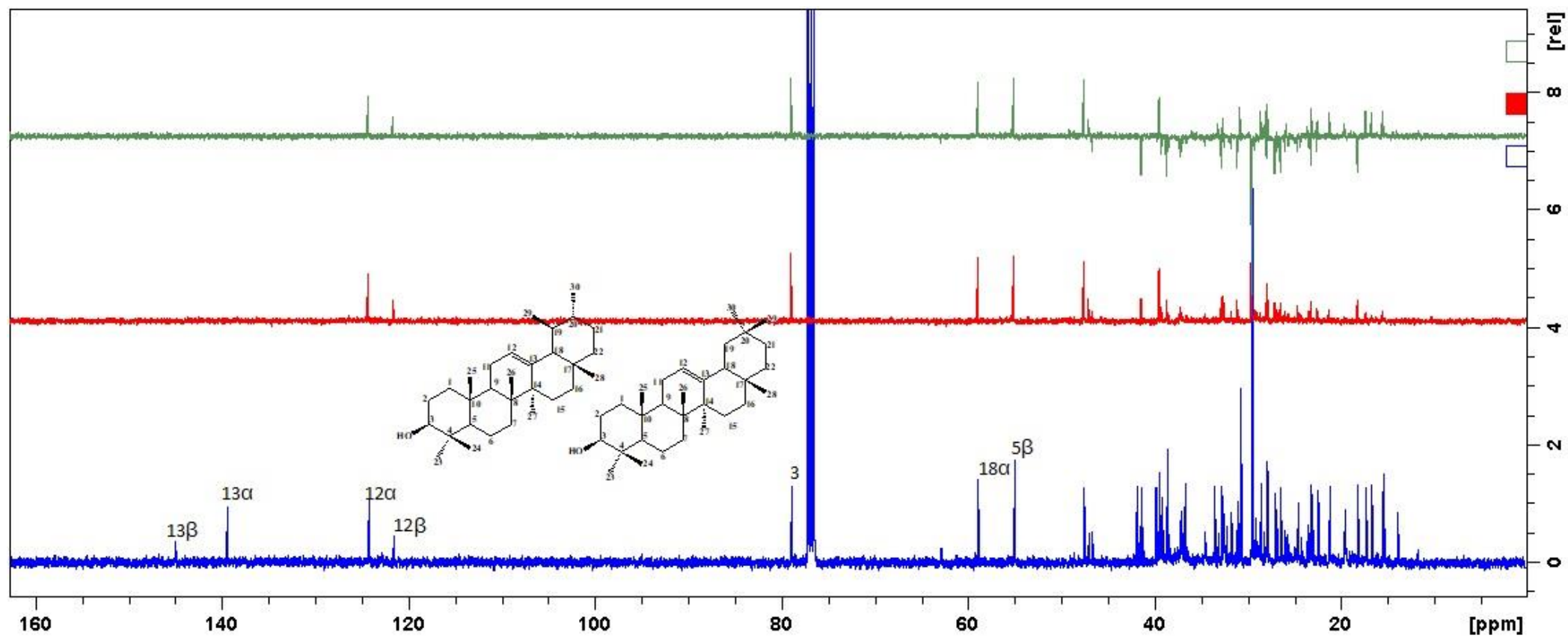
Mass spectrum of β -sitosterol



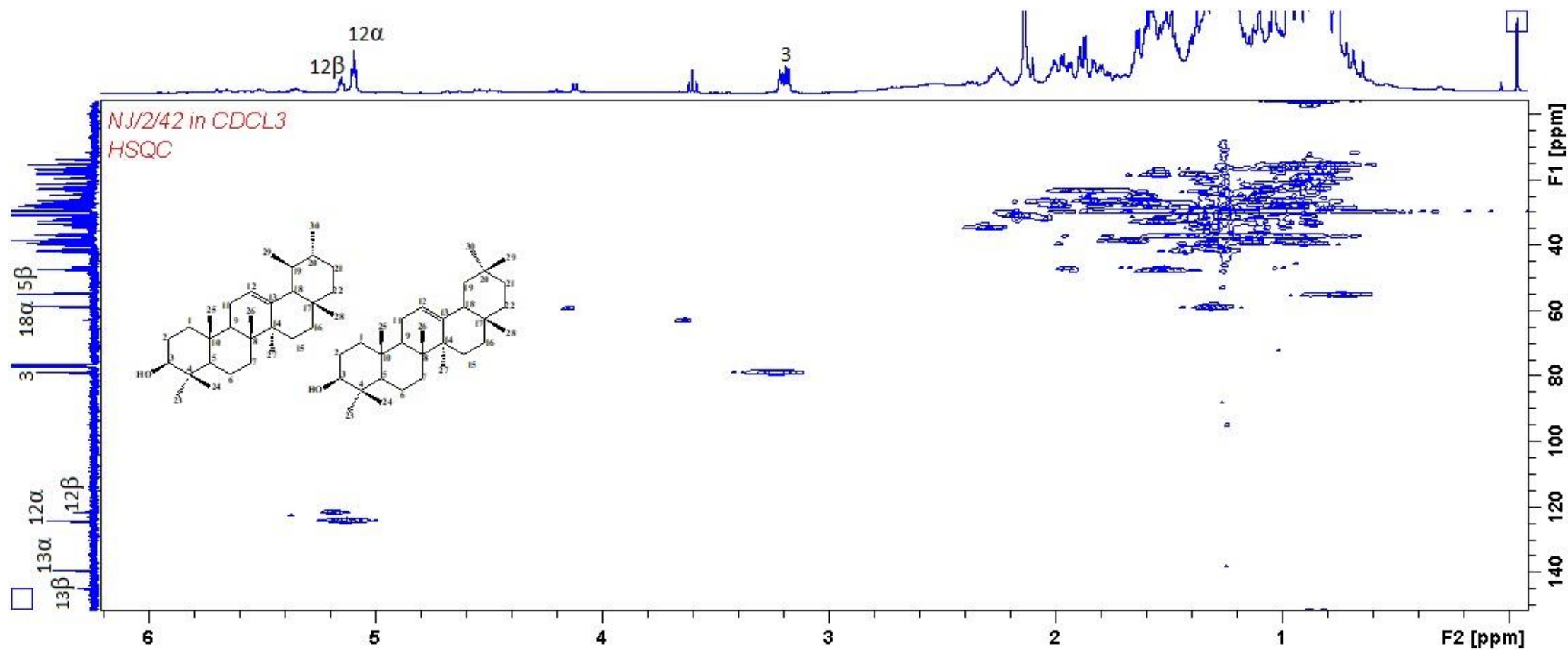
^1H NMR spectrum of α - β amyrin



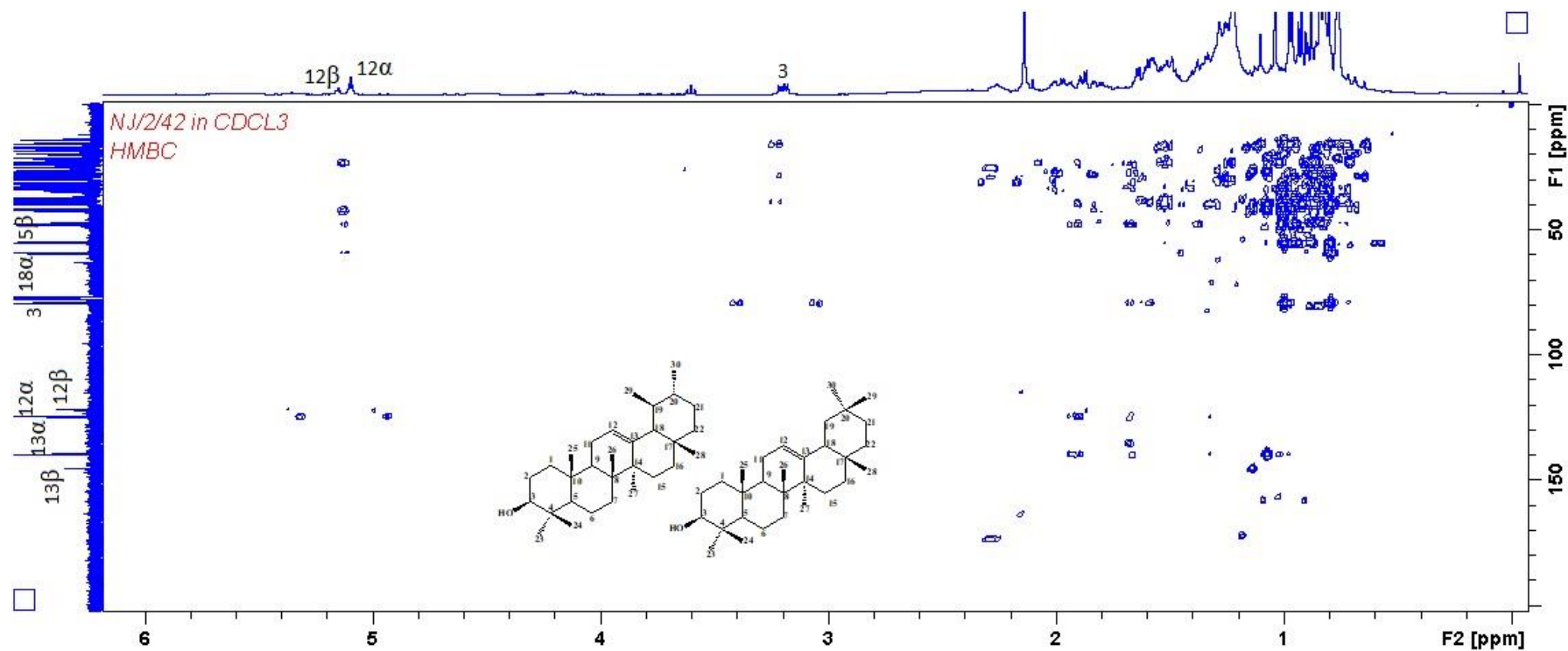
^{13}C NMR spectrum of α - β amyrin



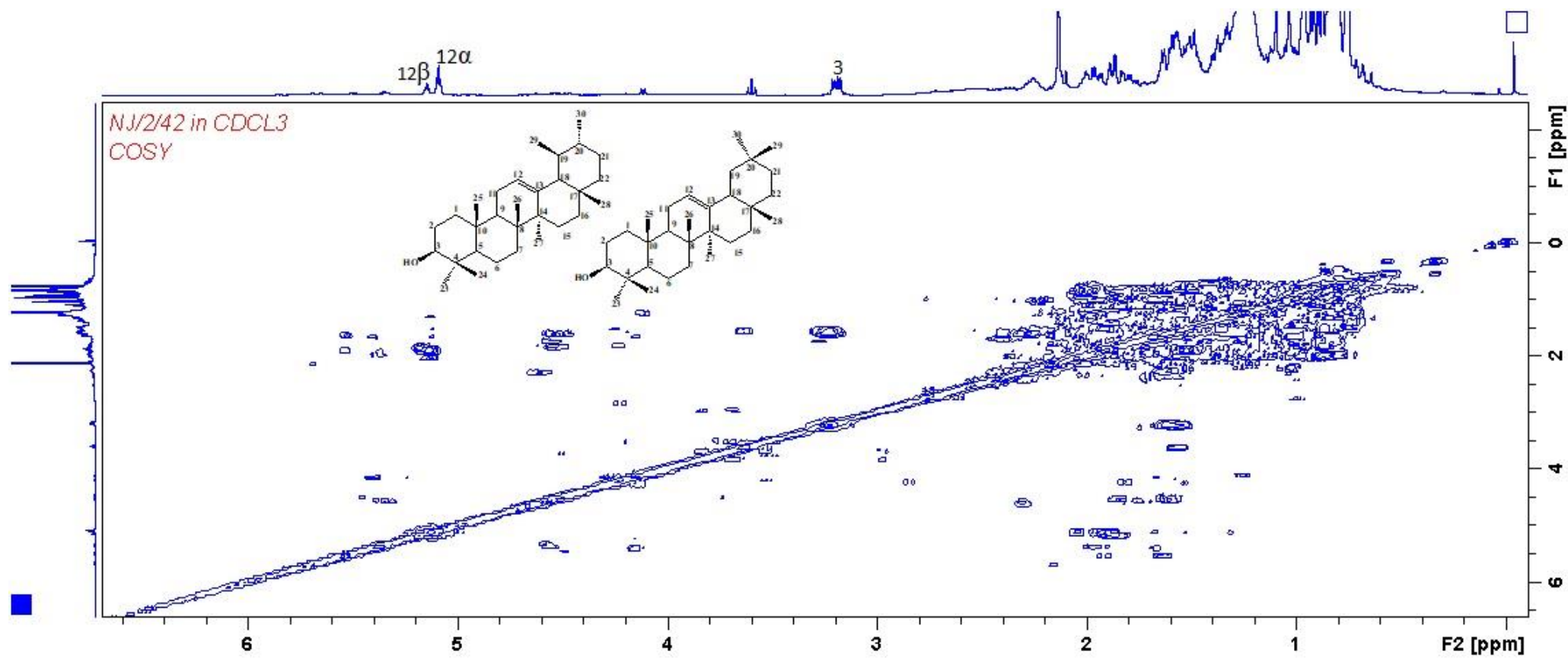
DEPT spectrum of α - β amyrin



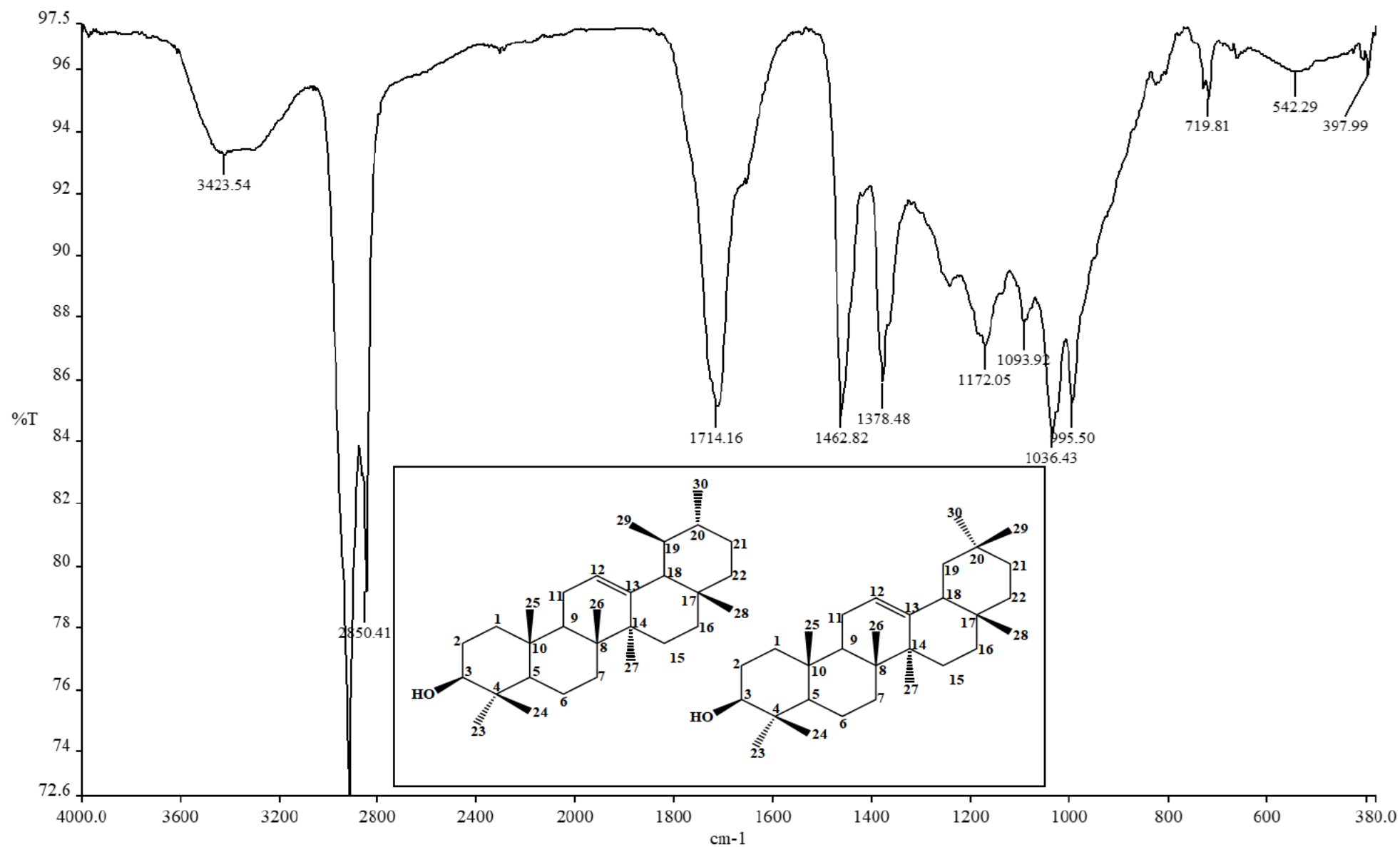
HSQC spectrum of α - β amyrin



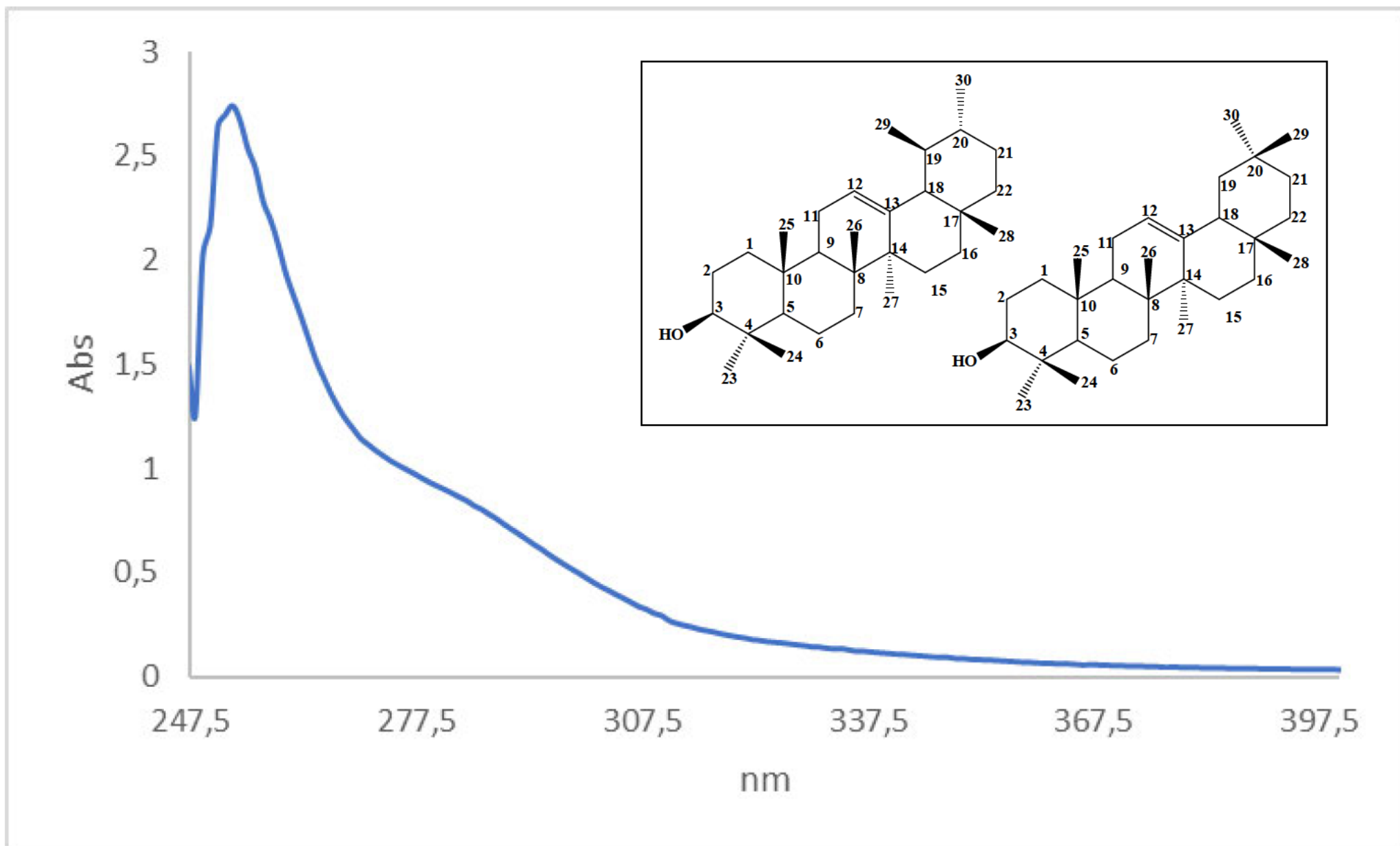
HMBC spectrum of α - β amyrin



COSY spectrum of α - β amyrin



IR spectrum of mixture of α - β amyrin



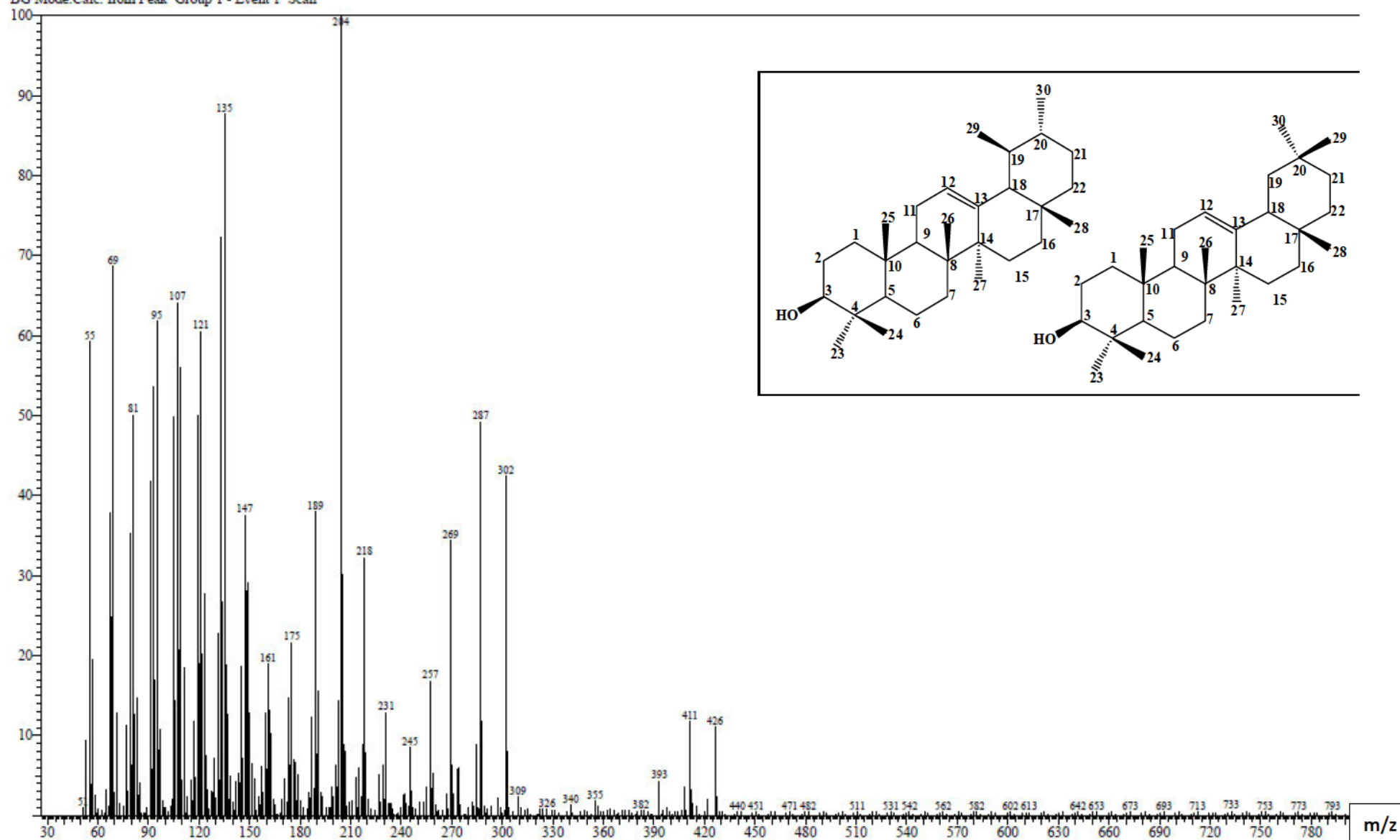
UV spectrum of α - β amyrin

Line#:67 R.Time:30.335(Scan#:5168)

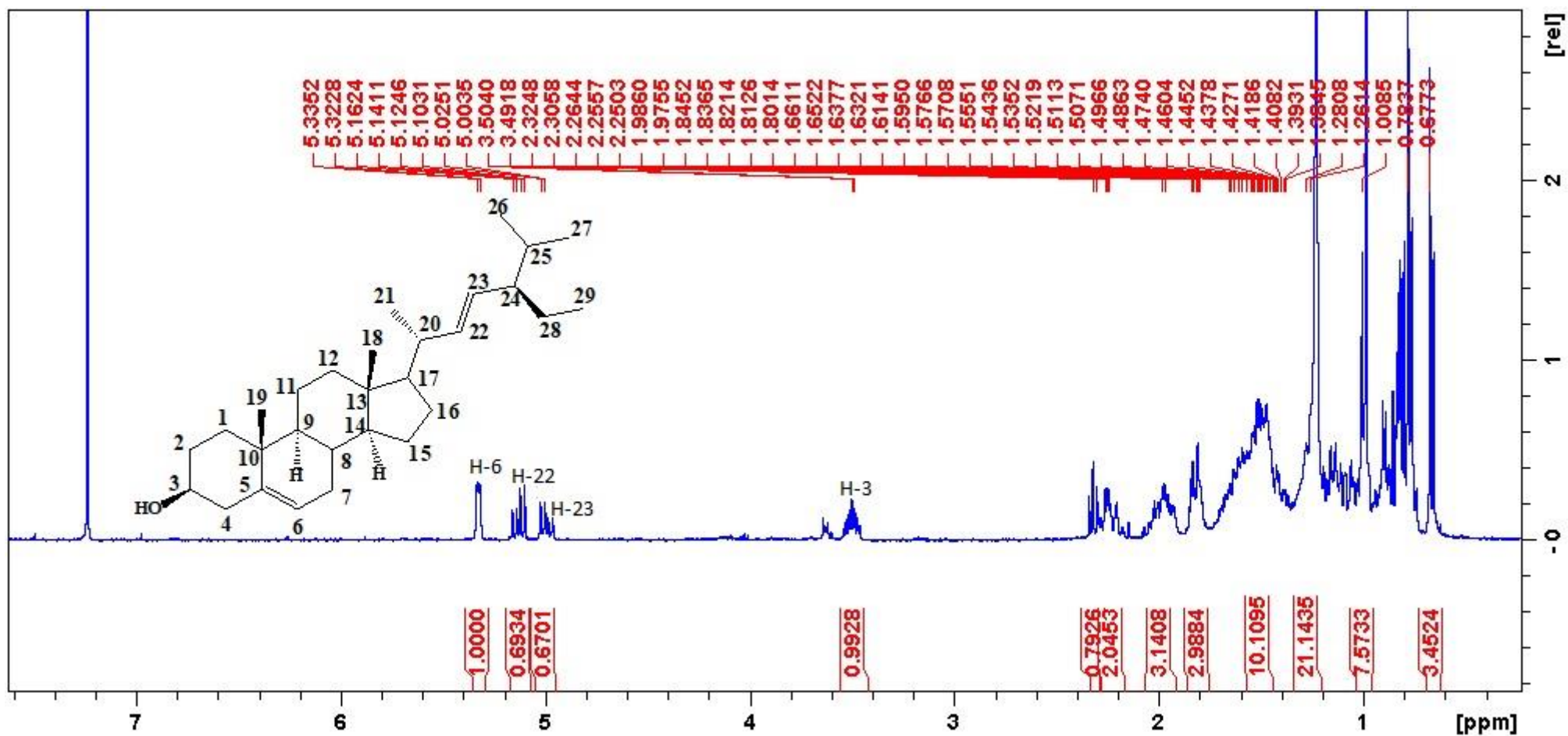
MassPeaks:406

RawMode:Averaged 30.330-30.340(5167-5169) BasePeak:204(112175)

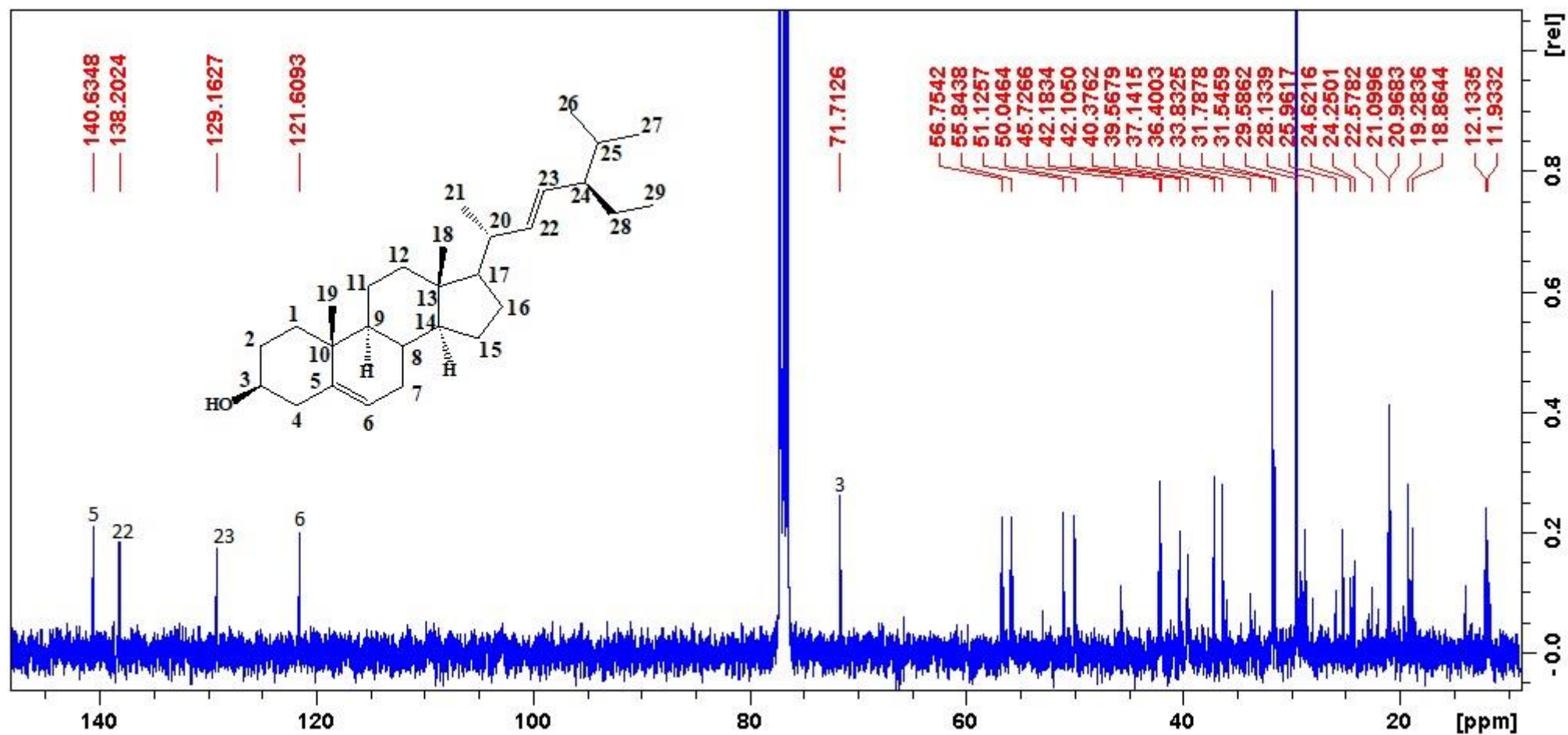
BG Mode:Calc. from Peak Group 1 - Event 1 Scan



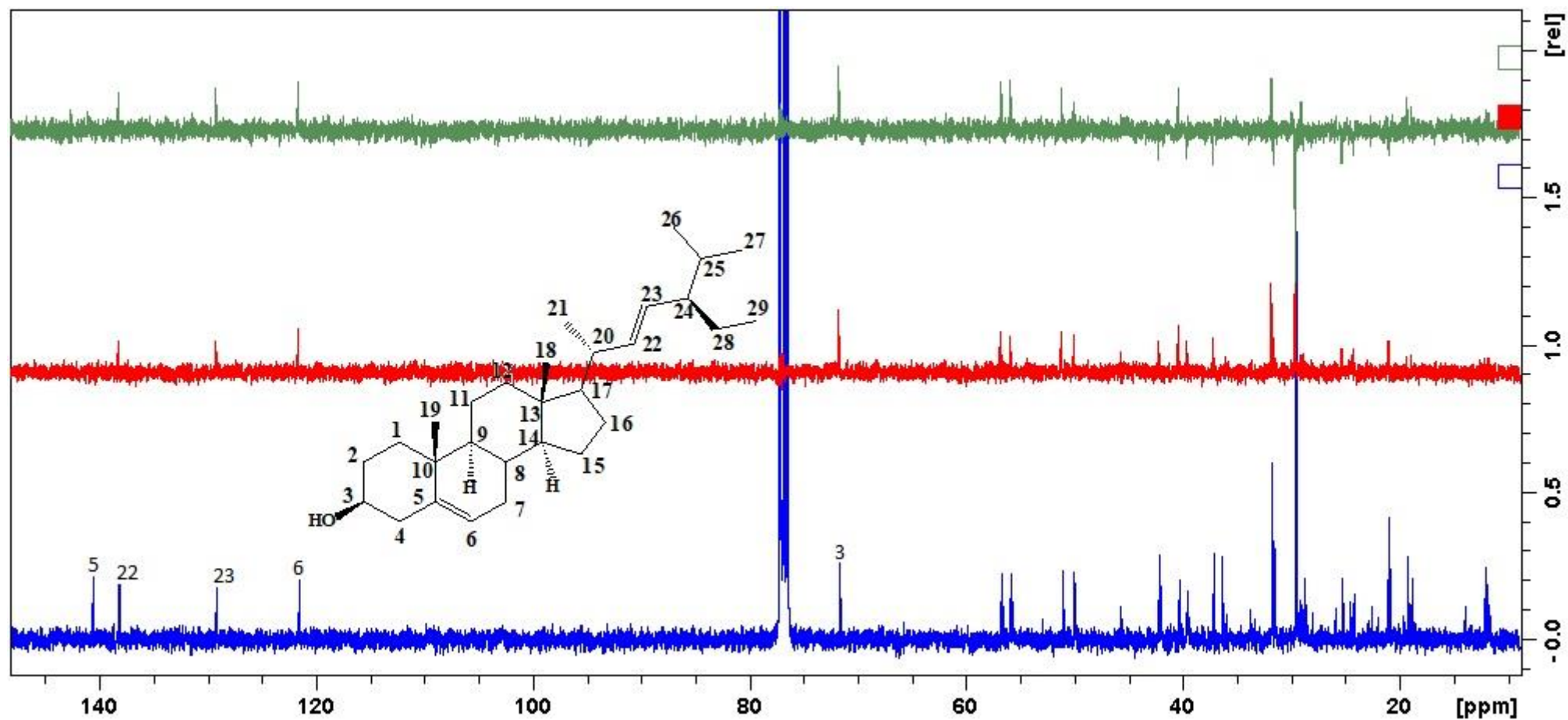
Mass spectrum of α - β amyrin



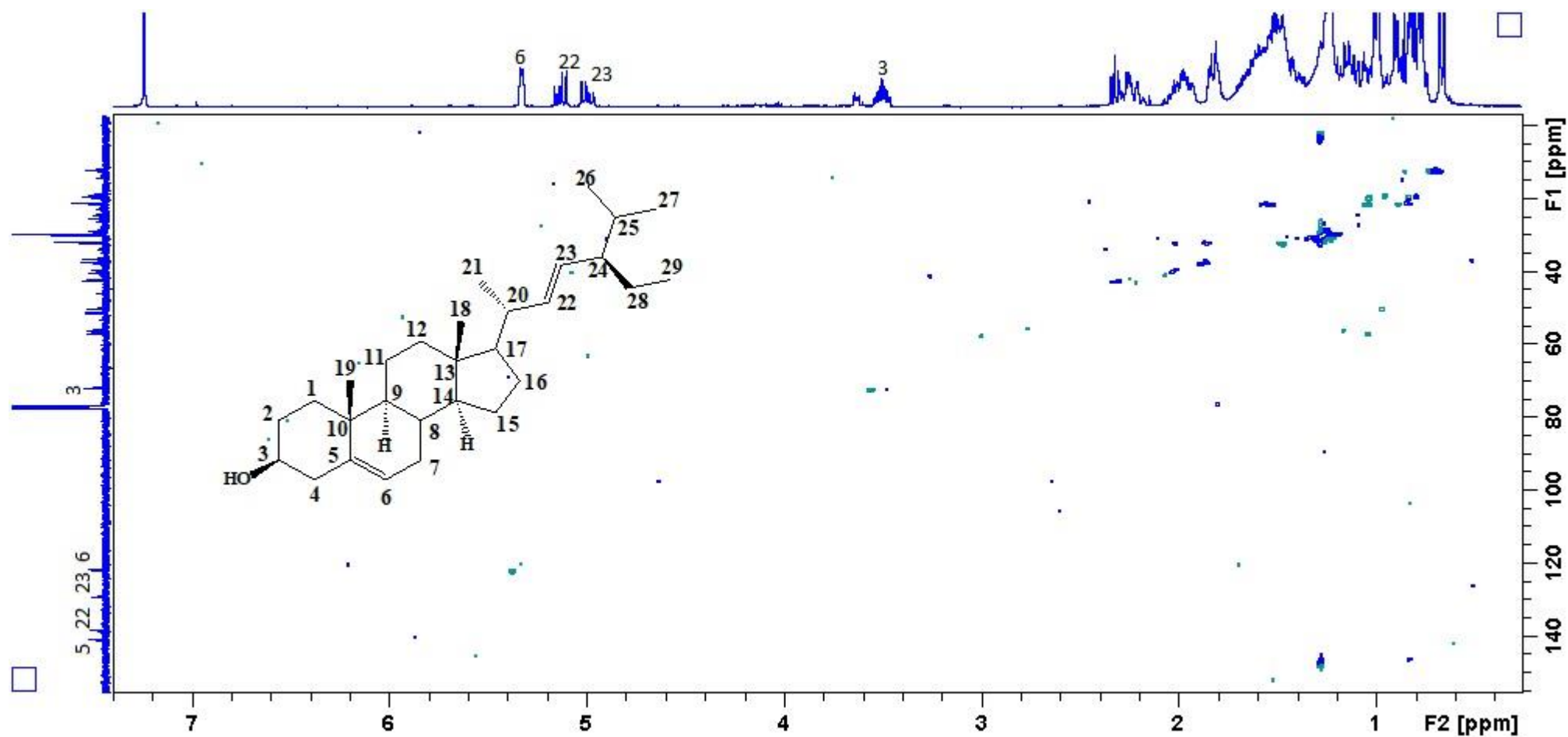
^1H NMR spectrum of stigmasterol



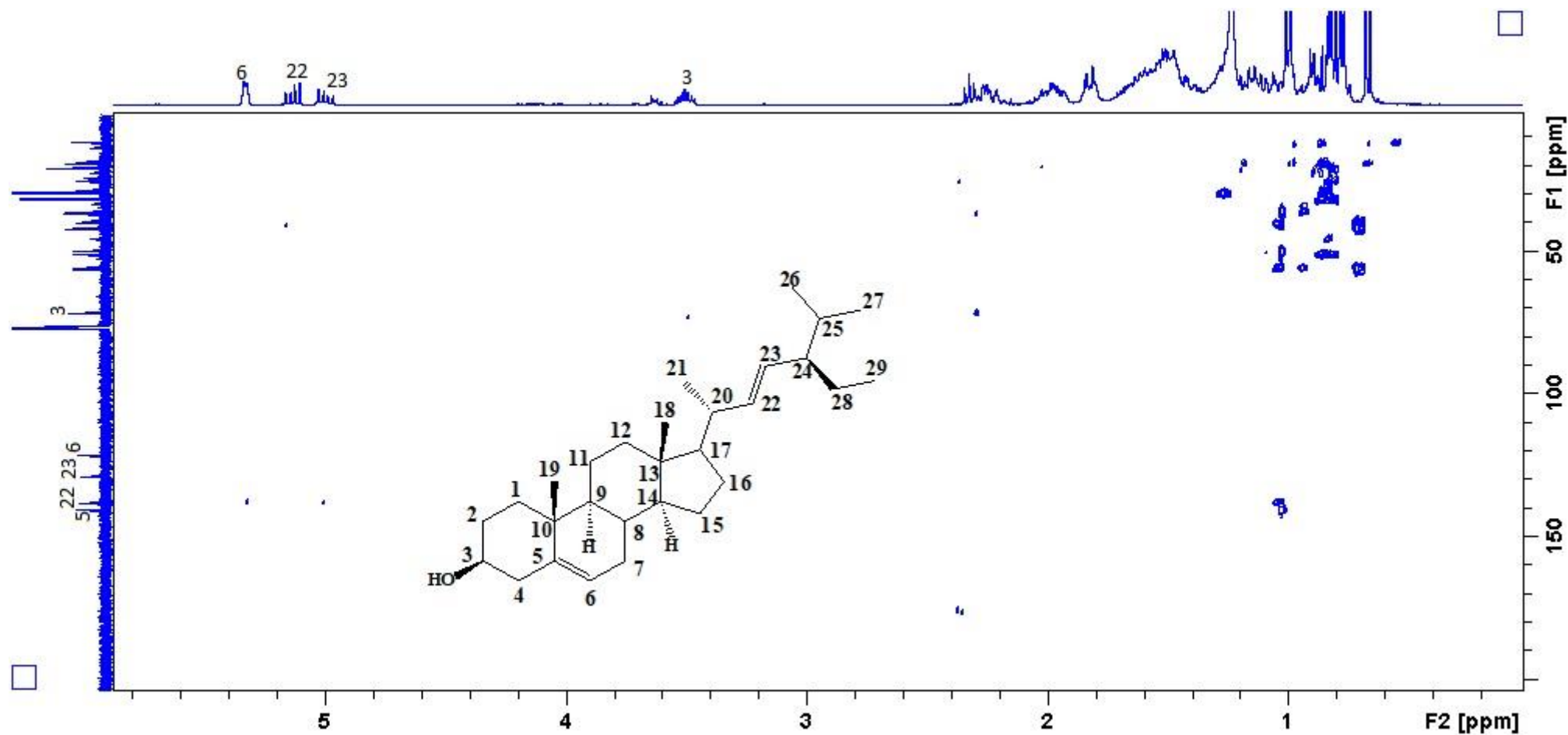
^{13}C NMR spectrum of stigmasterol



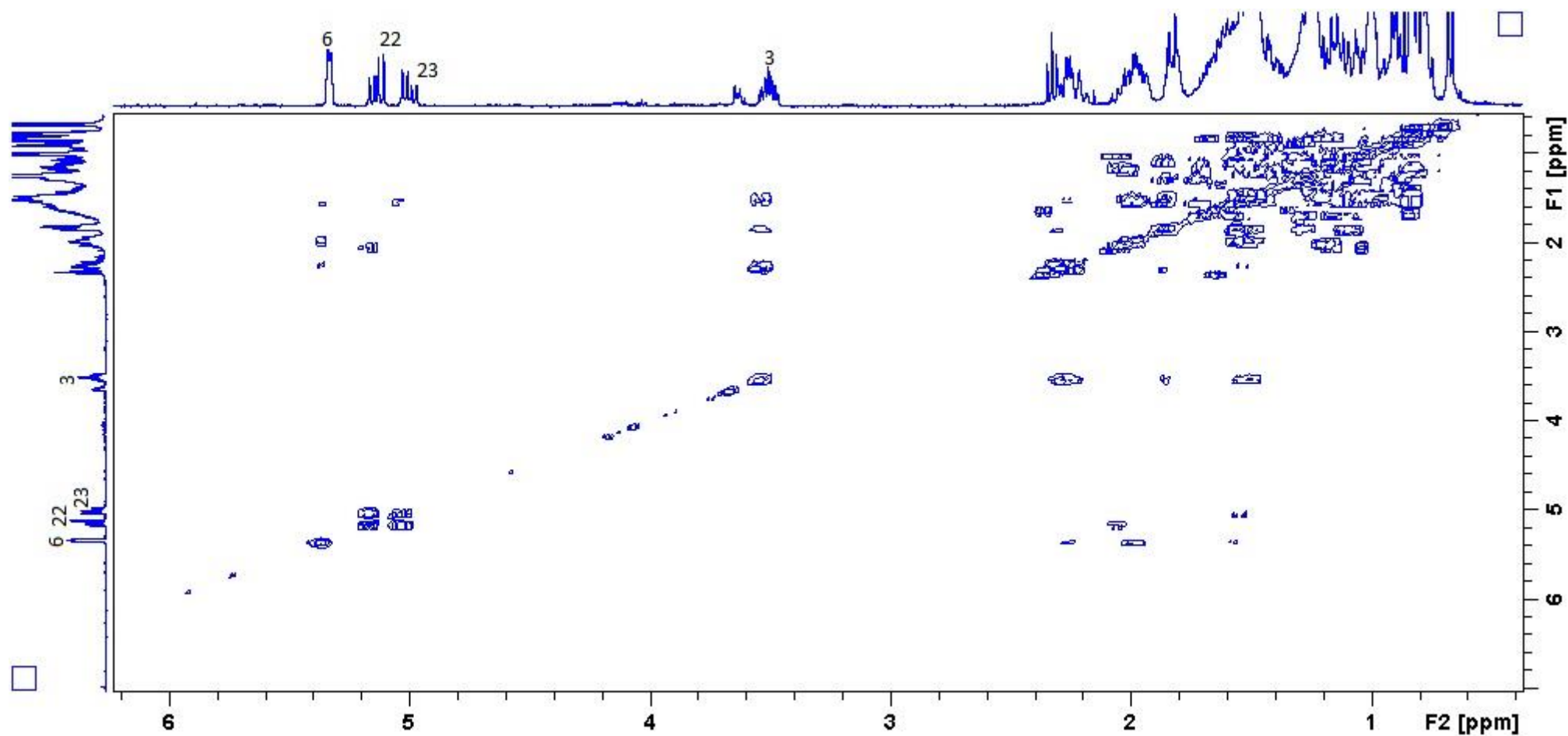
DEPT spectrum of stigmasterol



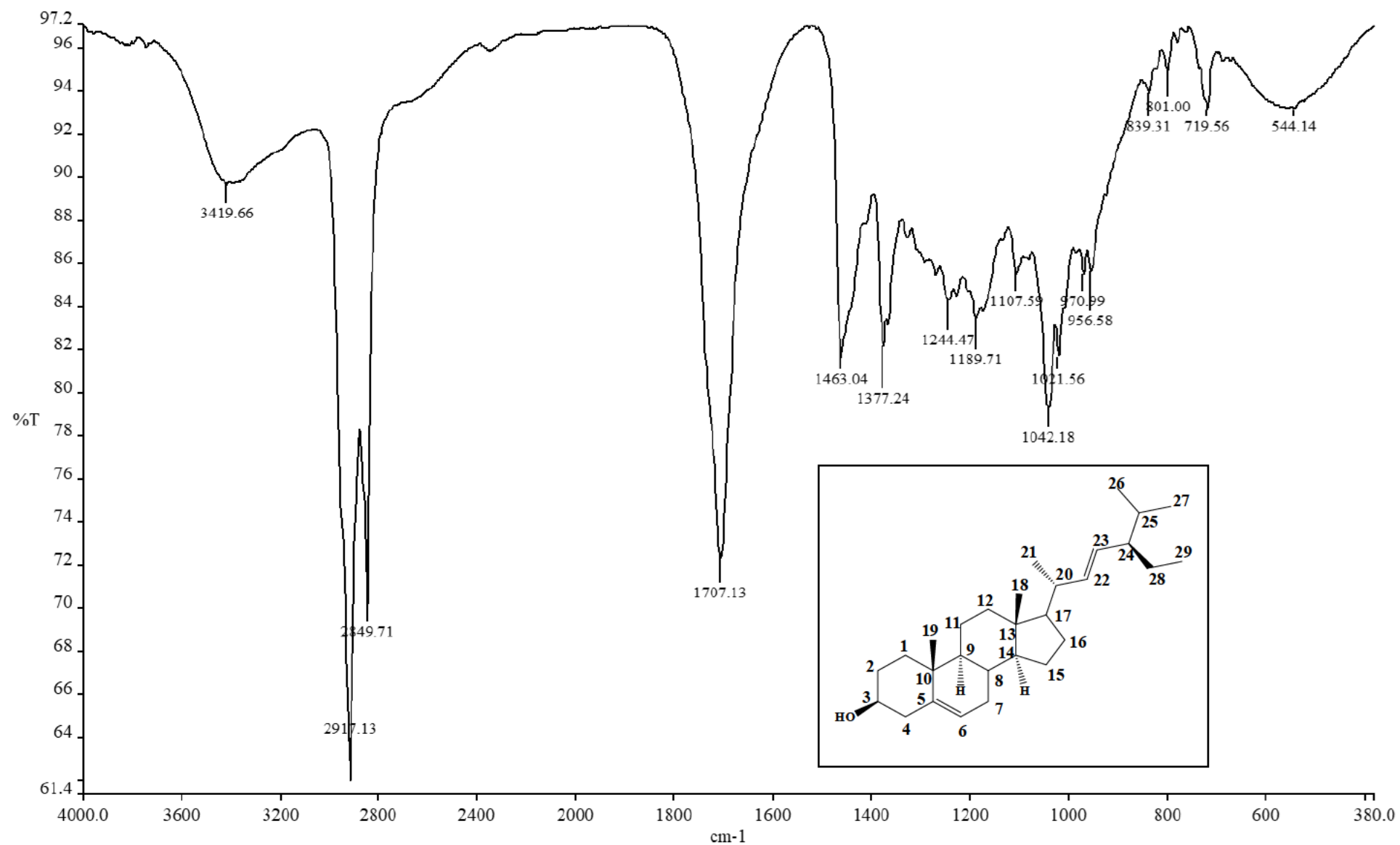
HSQC spectrum of stigmasterol



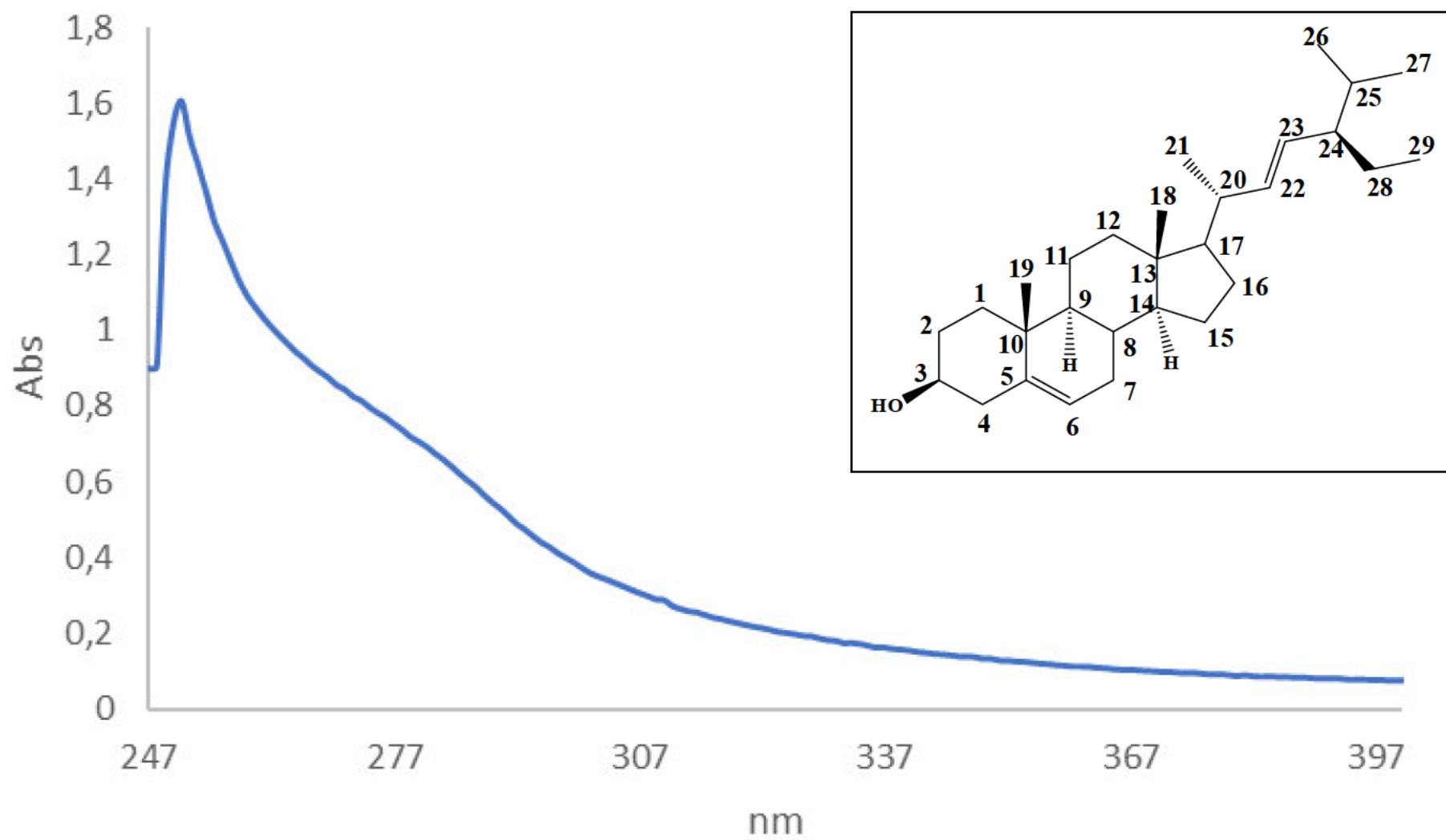
HMBC spectrum of stigmasterol



COSY spectrum of stigmasterol

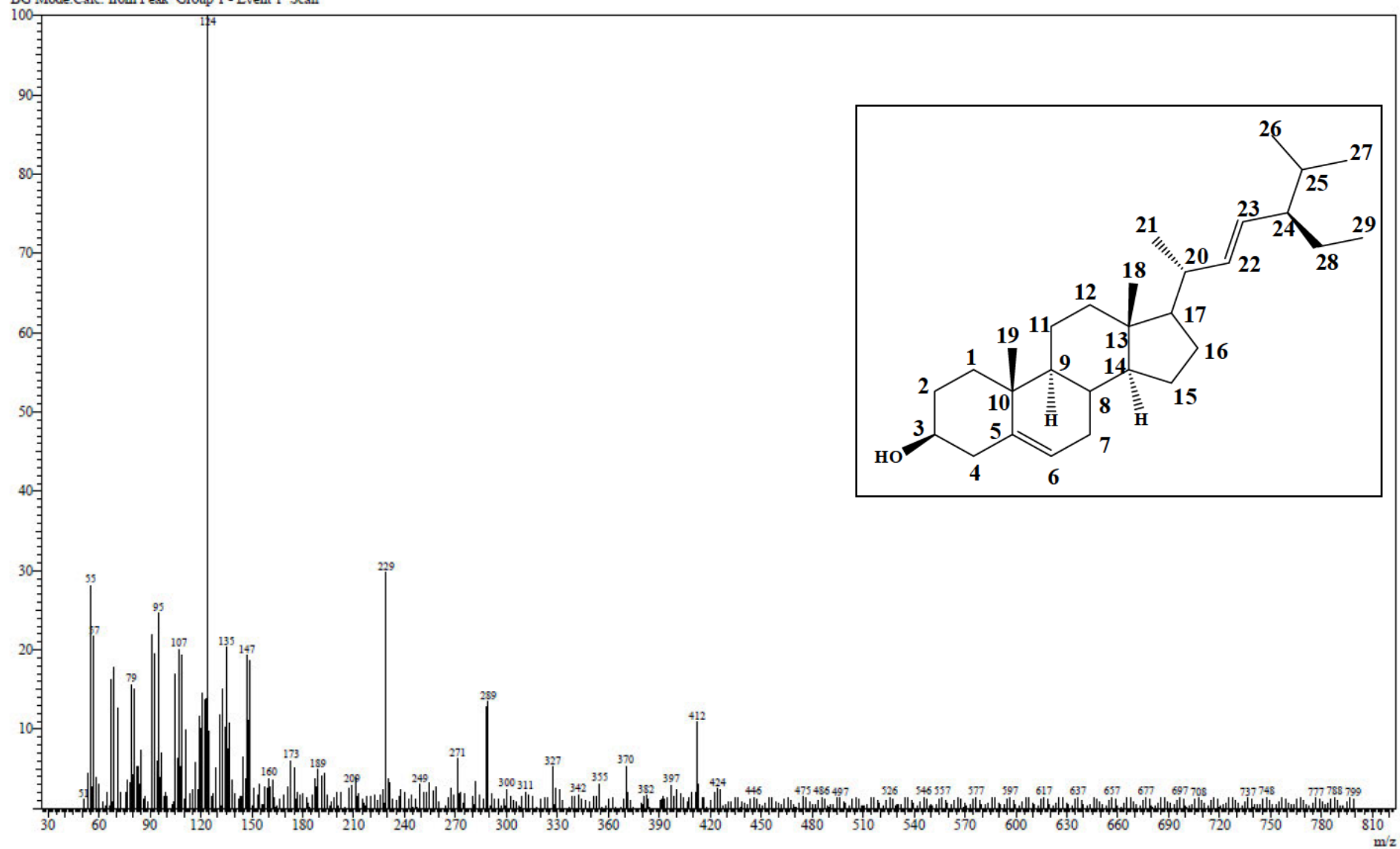


IR spectrum of stigmasterol

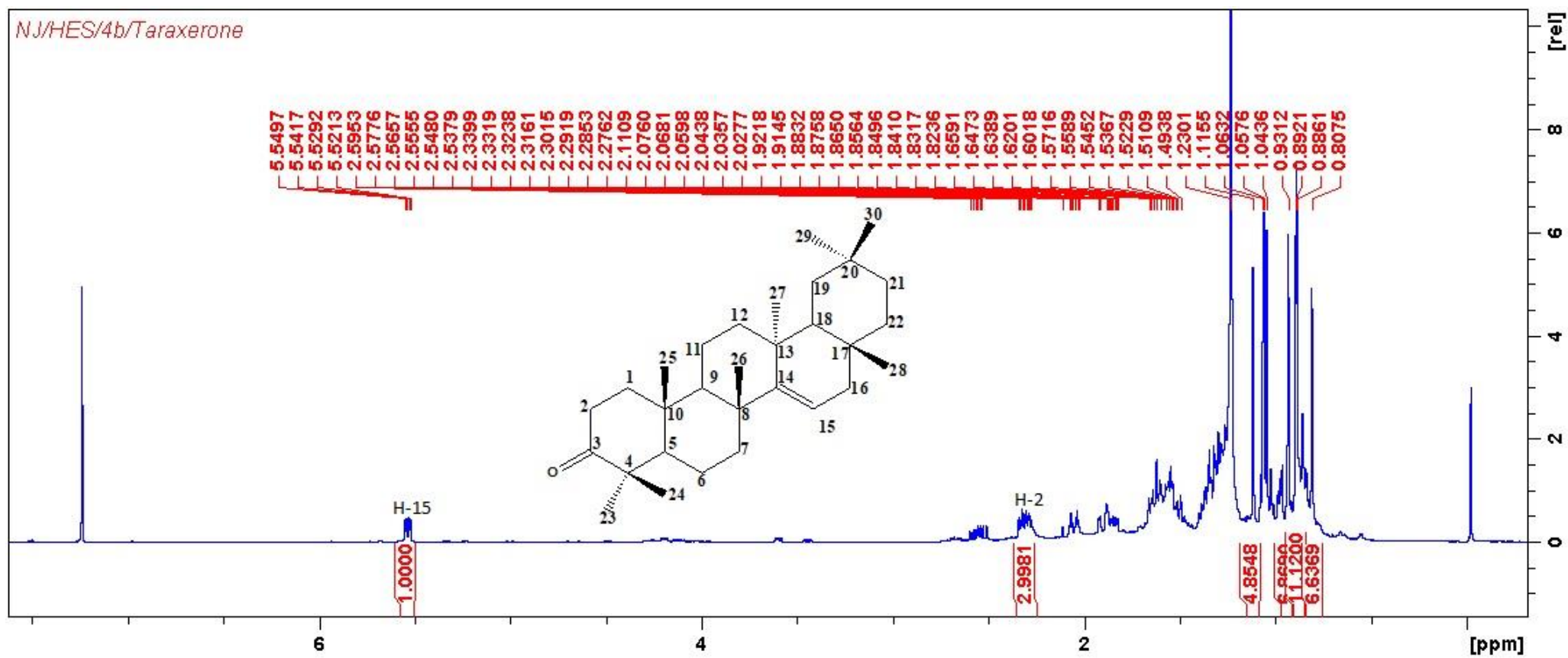


UV spectrum of stigmasterol

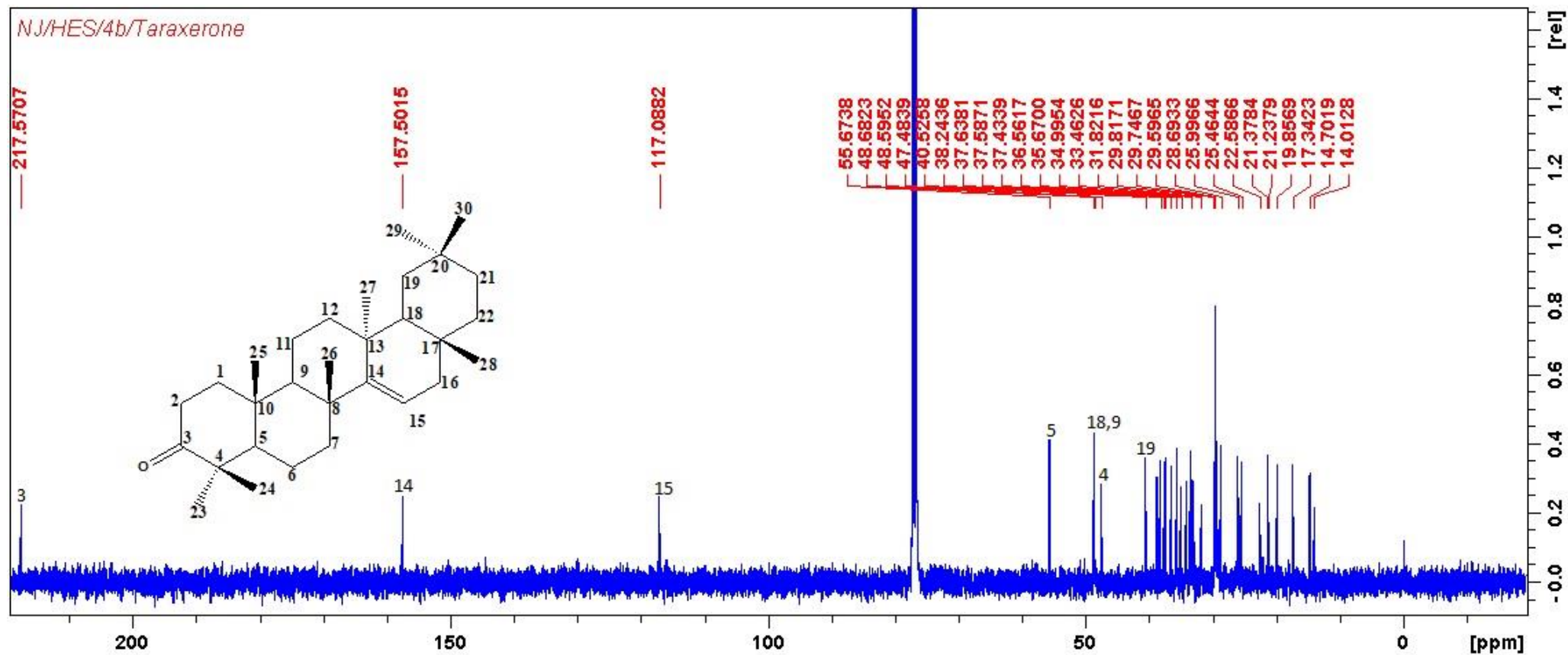
Line#:45 R.Time:31.425(Scan#:5386)
MassPeaks:474
RawMode:Averaged 31.420-31.430(5385-5387) BasePeak:124(46288)
BG Mode:Calc. from Peak Group 1 - Event 1 Scan



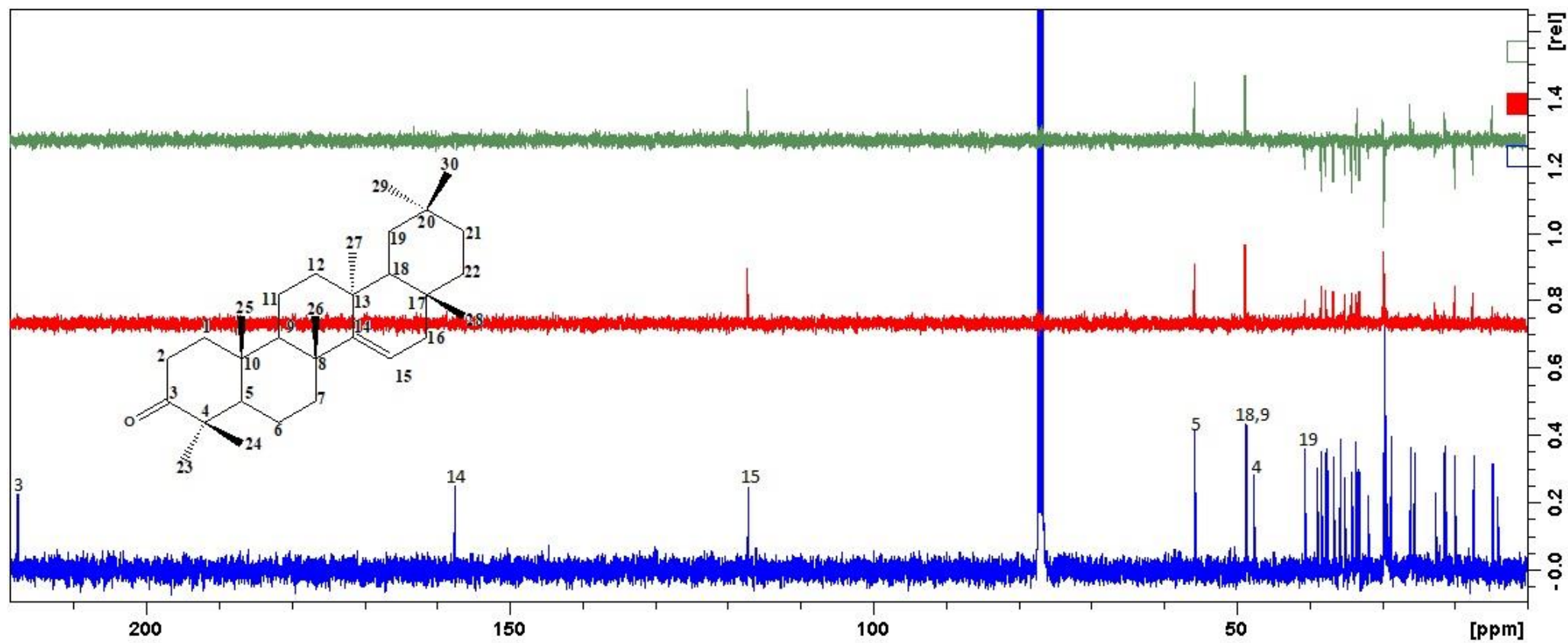
Mass spectrum of stigmasterol



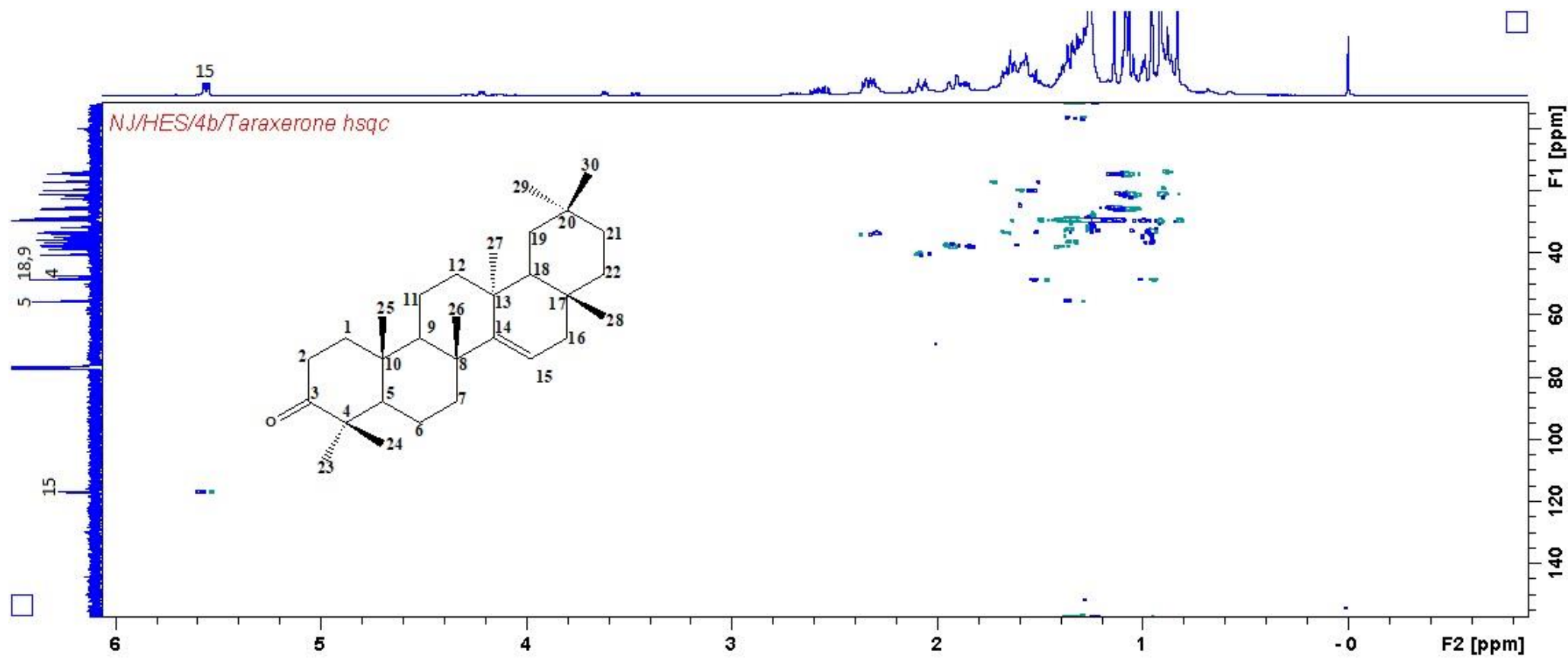
^1H NMR spectrum of taraxerone



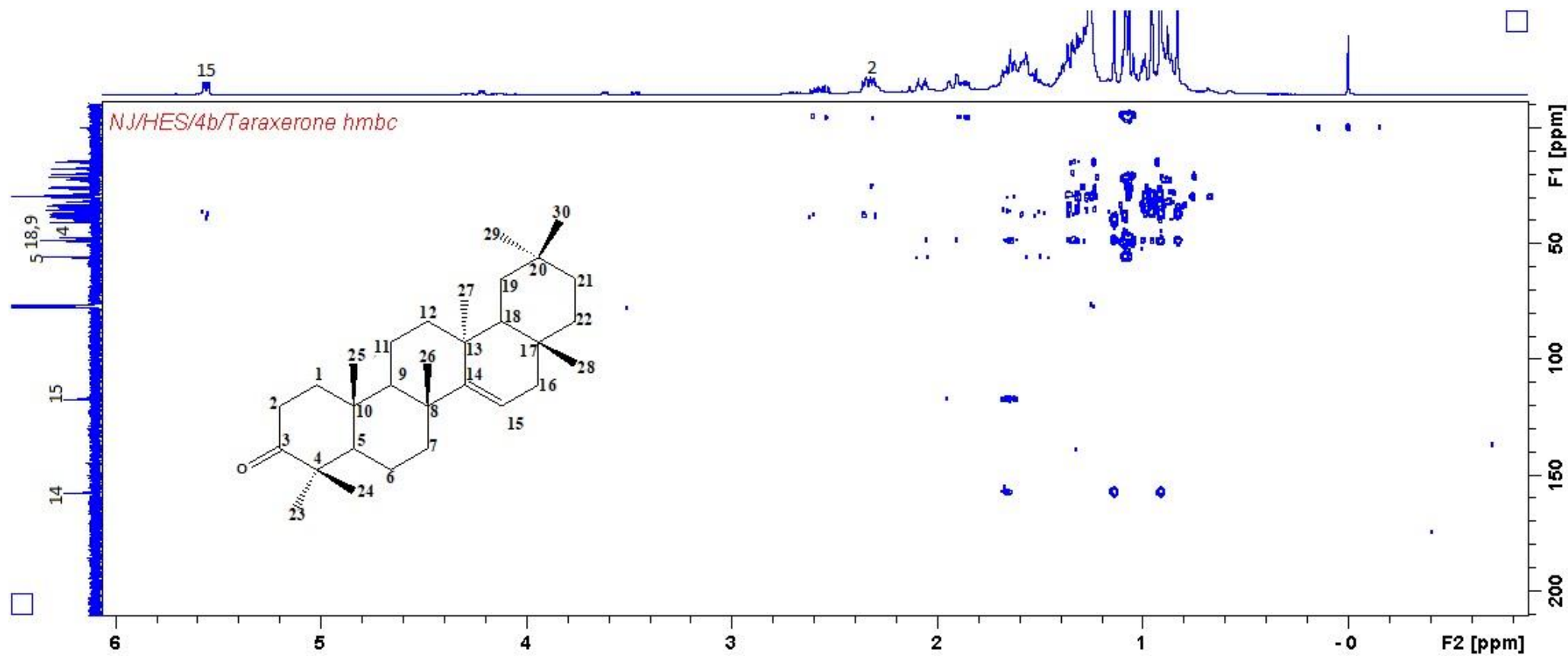
^{13}C NMR spectrum of taraxerone



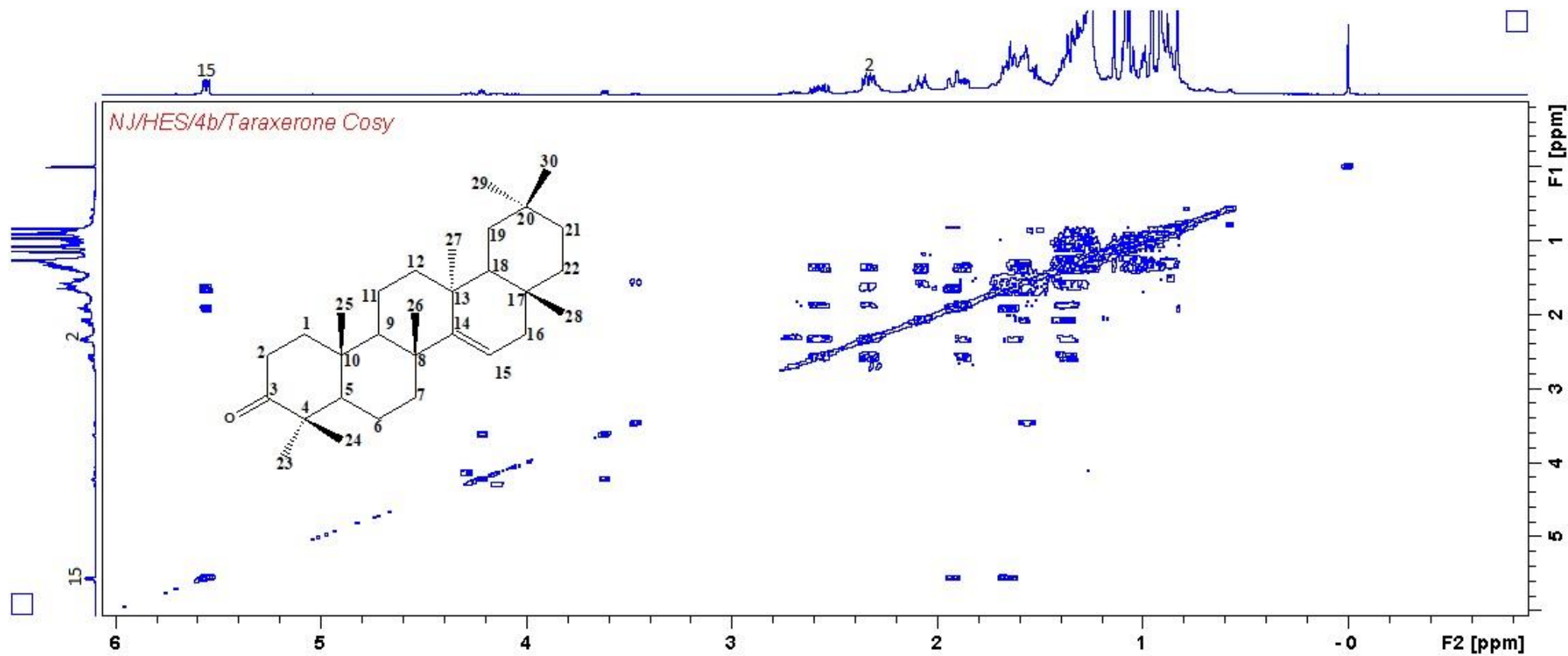
DEPT spectrum of taraxerone



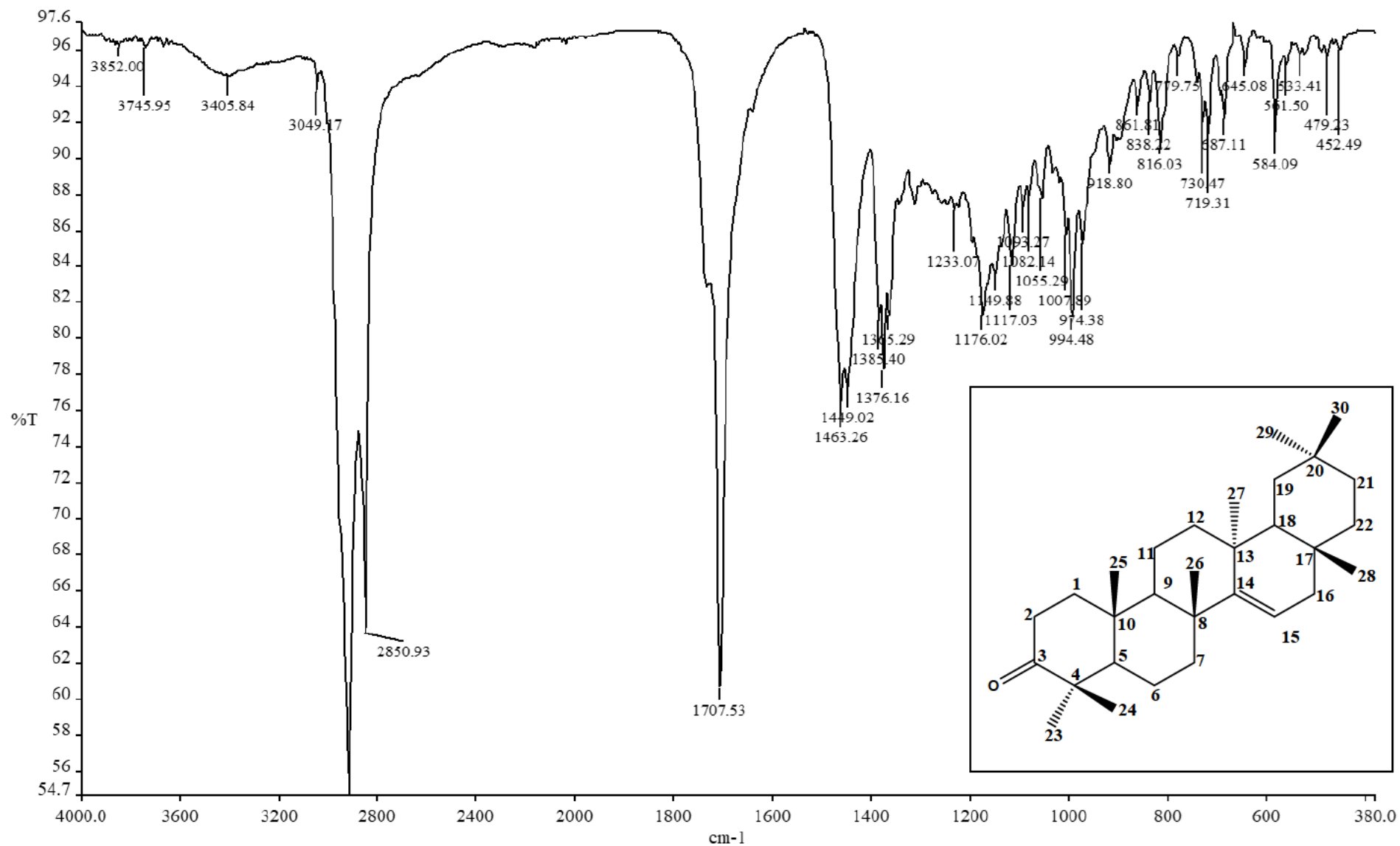
HSQC spectrum of taraxerone



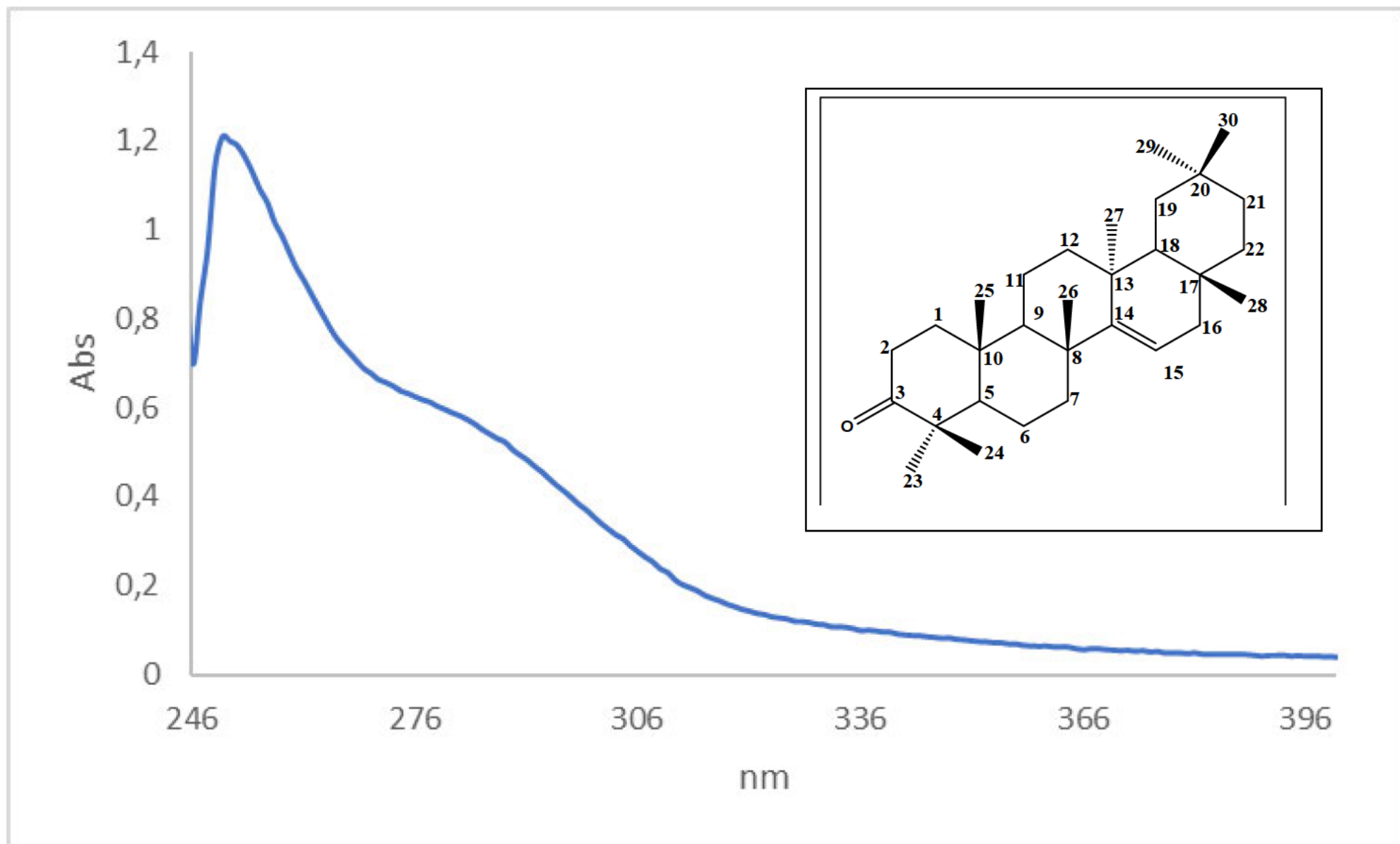
HMBC spectrum of taraxerone



COSY spectrum of taraxerone



IR spectrum of Taraxerone



UV spectrum of taraxerone

Single Mass Analysis

Tolerance = 5.0 PPM / DBE: min = -1.5, max = 50.0

Element prediction: Off

Number of isotope peaks used for i-FIT = 2

Monoisotopic Mass, Even Electron Ions

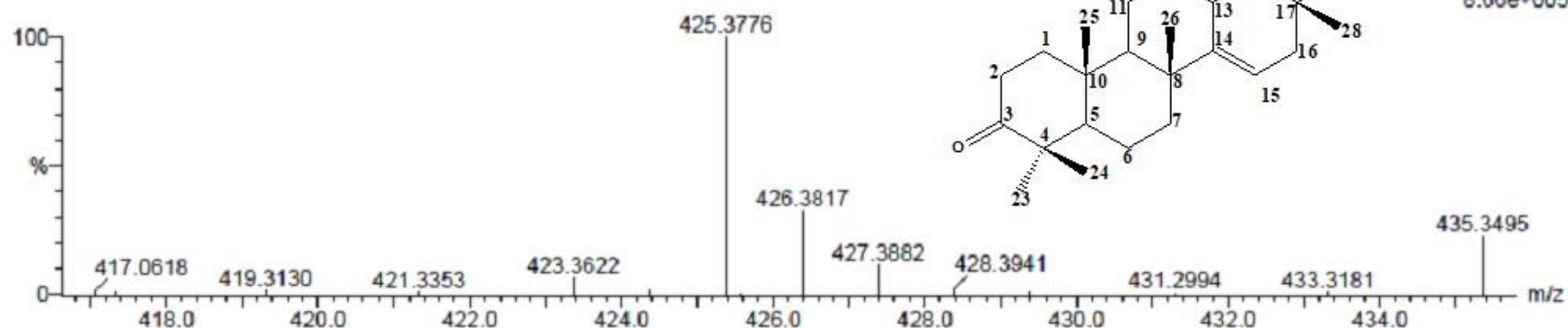
2 formula(e) evaluated with 1 results within limits (up to 20 closest results for each mass)

Elements Used:

C: 30-35 H: 45-50 O: 0-5

3.45 (1.484) Cm (1:61)

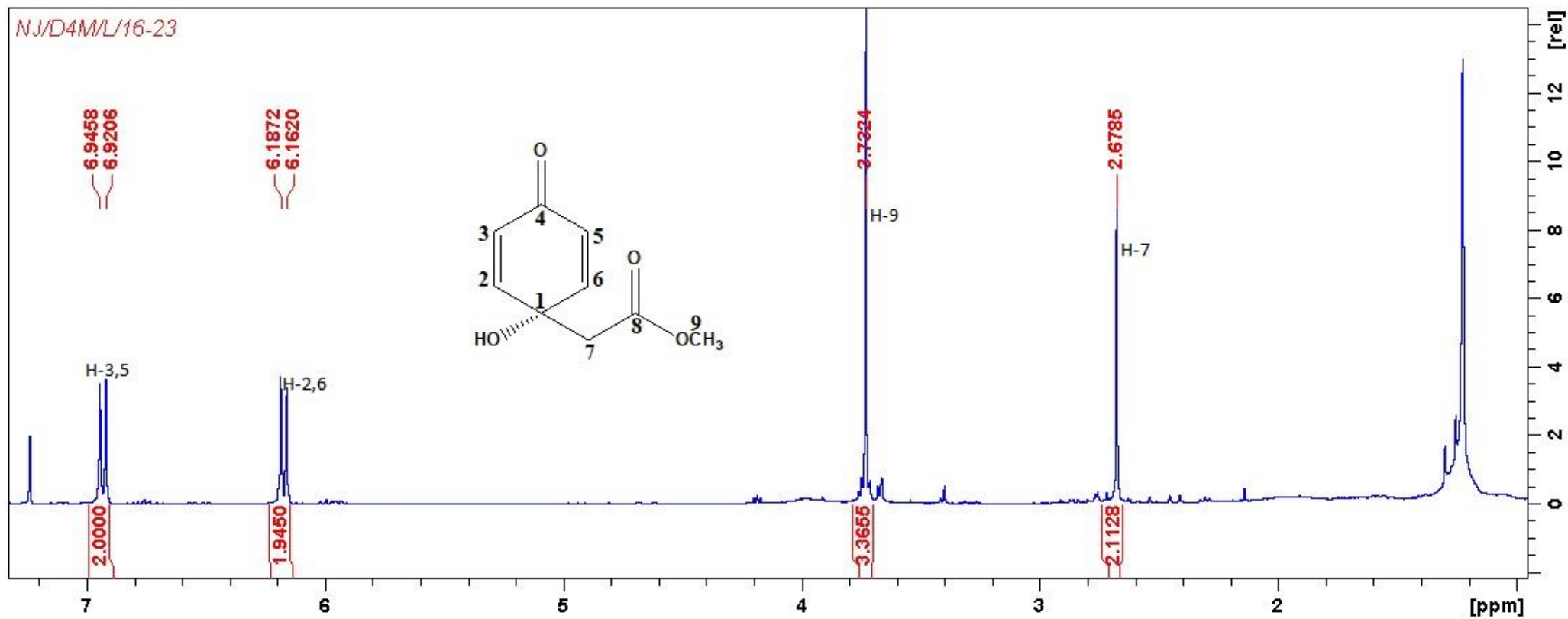
TOF MS AP+



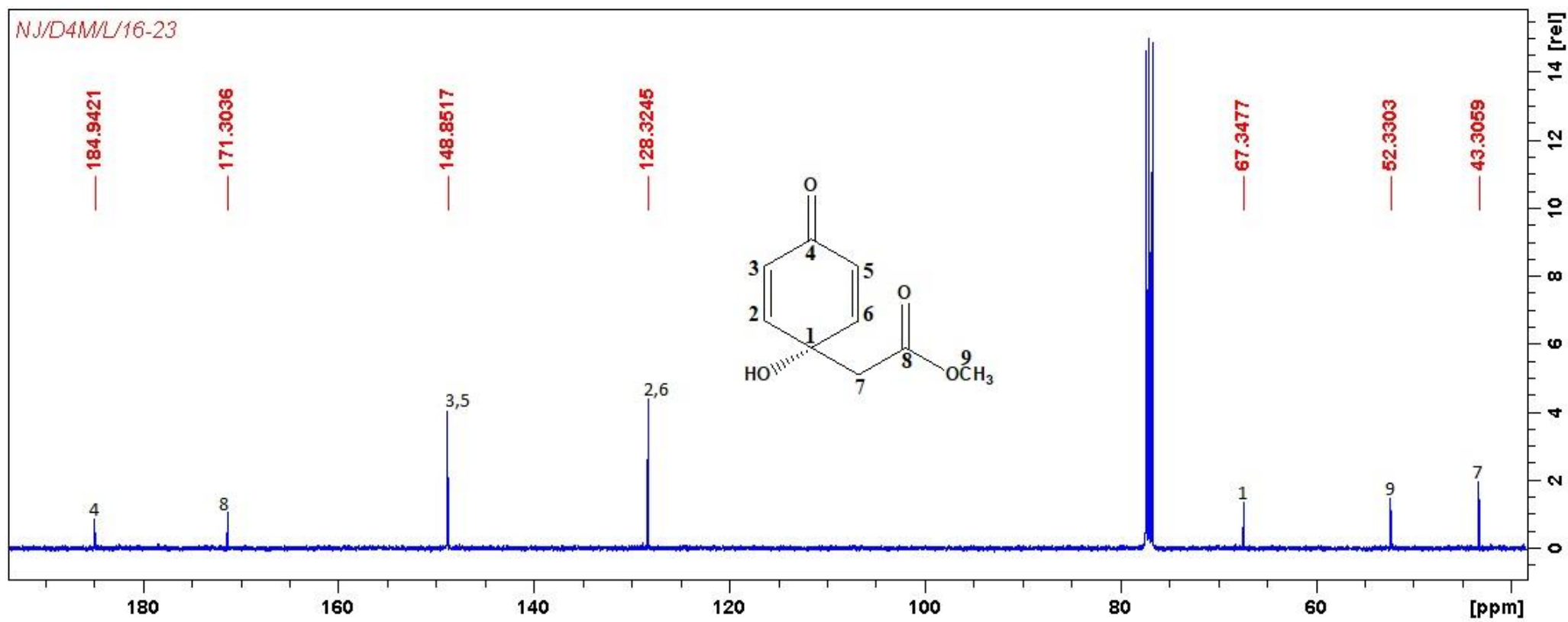
Minimum: -1.5
Maximum: 5.0 5.0 50.0

Mass	Calc. Mass	mDa	PPM	DBE	i-FIT	i-FIT (Norm)	Formula
425.3776	425.3783	-0.7	-1.6	6.5	33.5	0.0	C30 H49 O

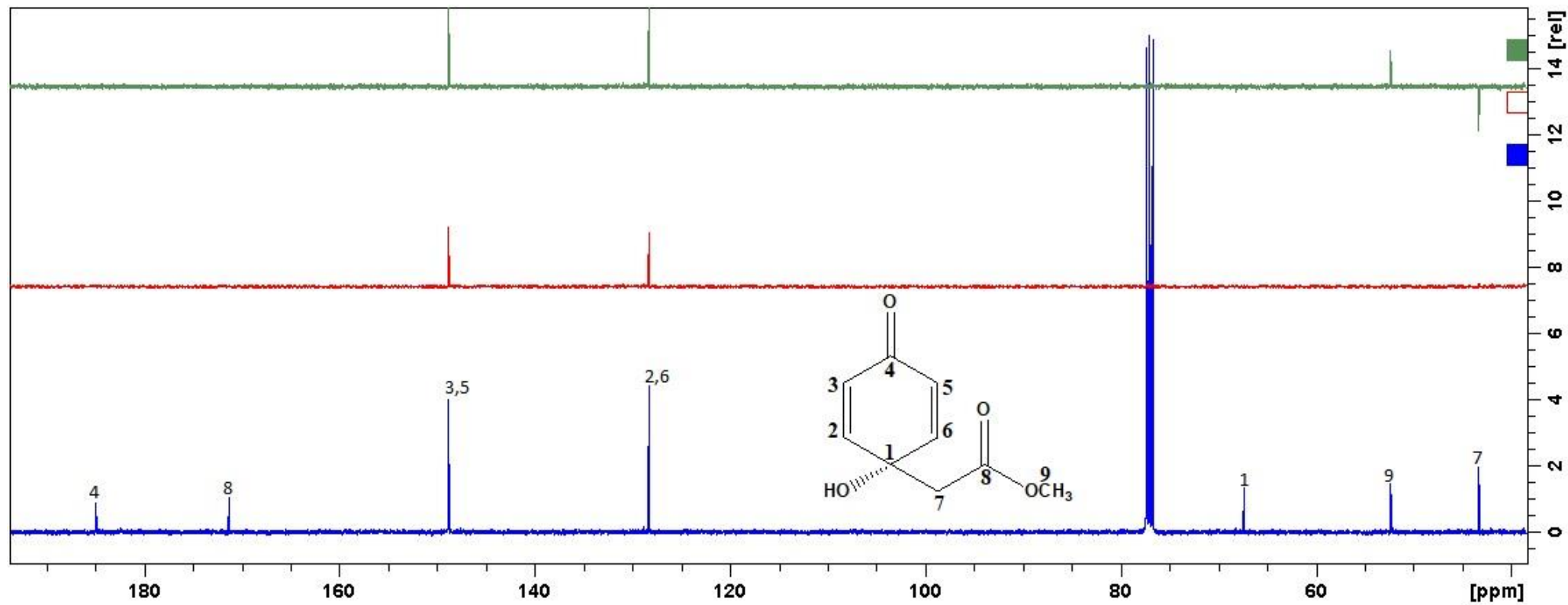
Mass spectrum of taraxerone



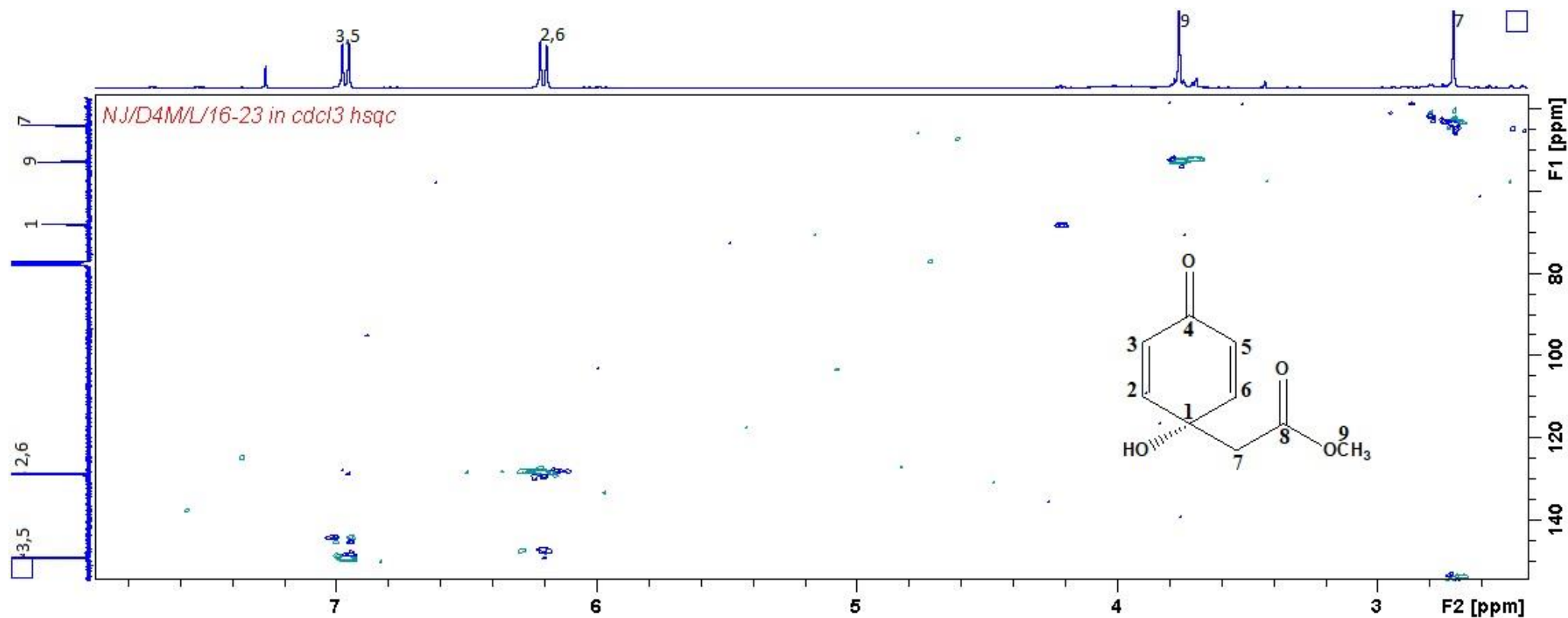
^1H NMR spectrum of jacaranone



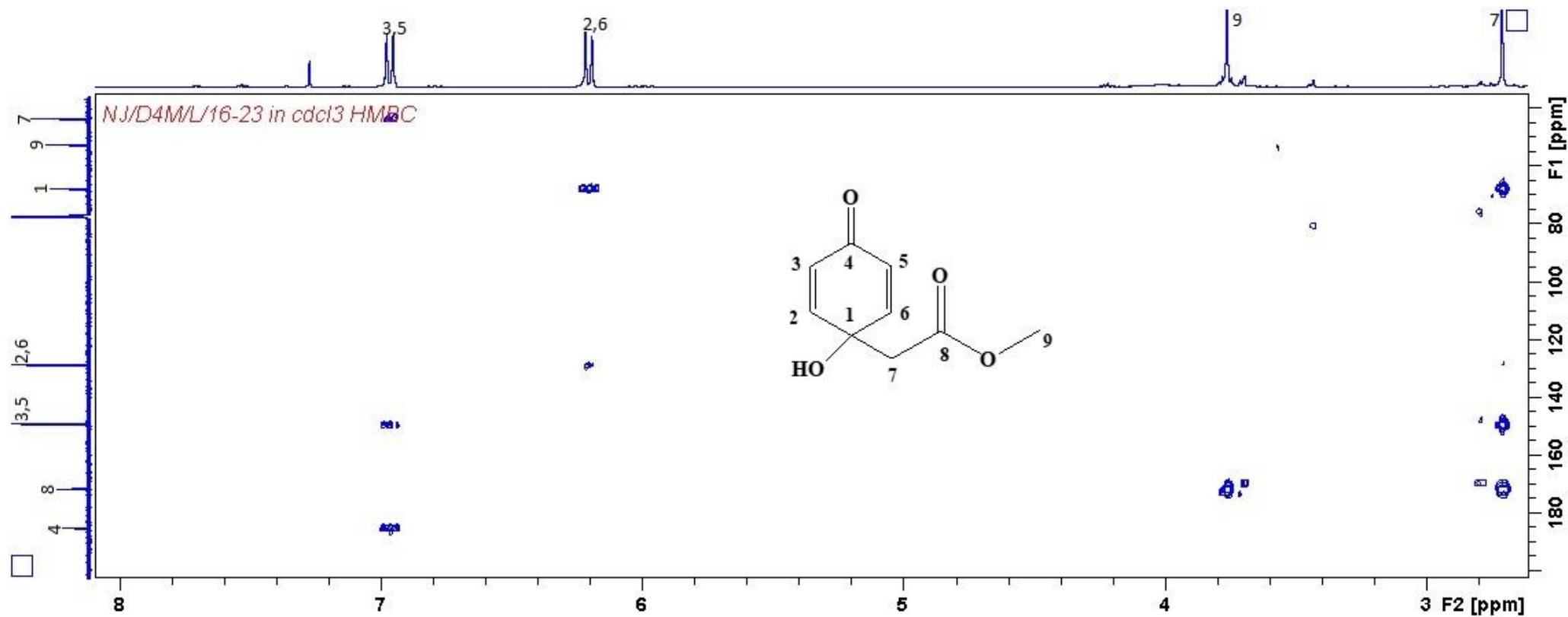
^{13}C NMR spectrum of jacaranone



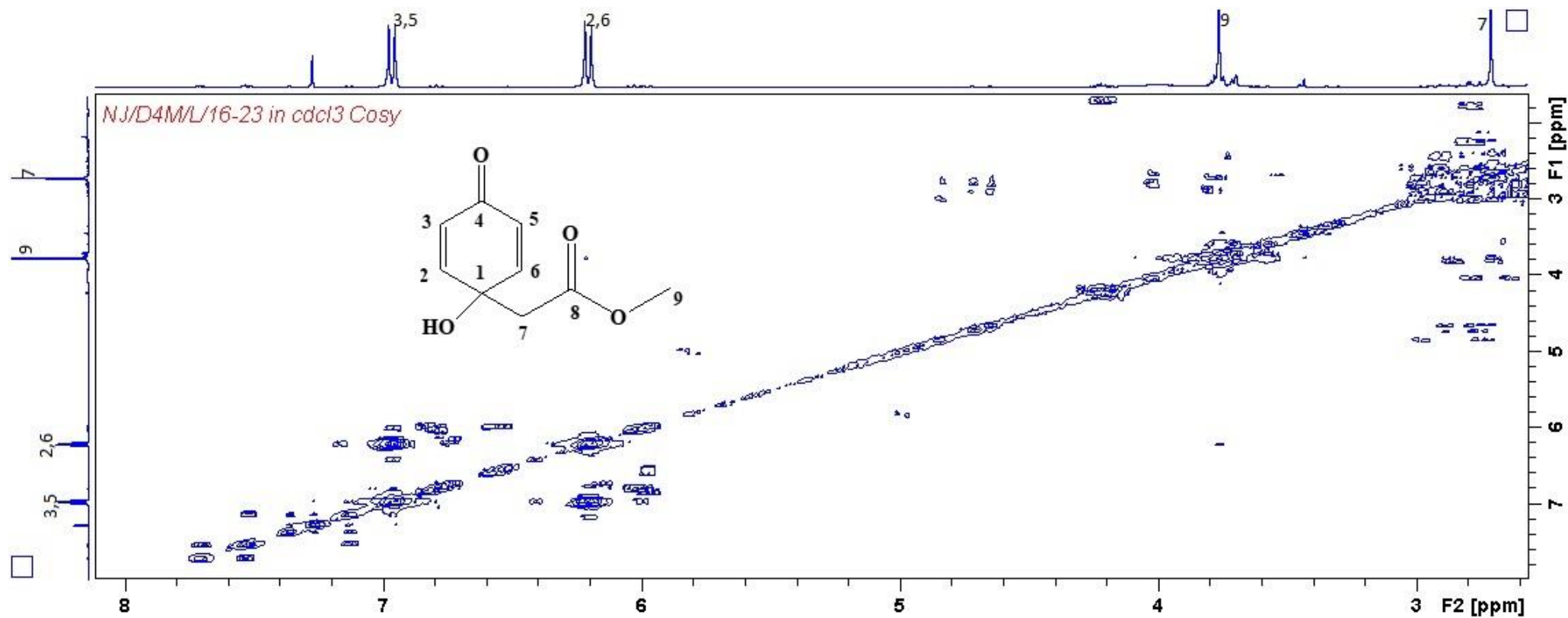
DEPT spectrum of jacaranone



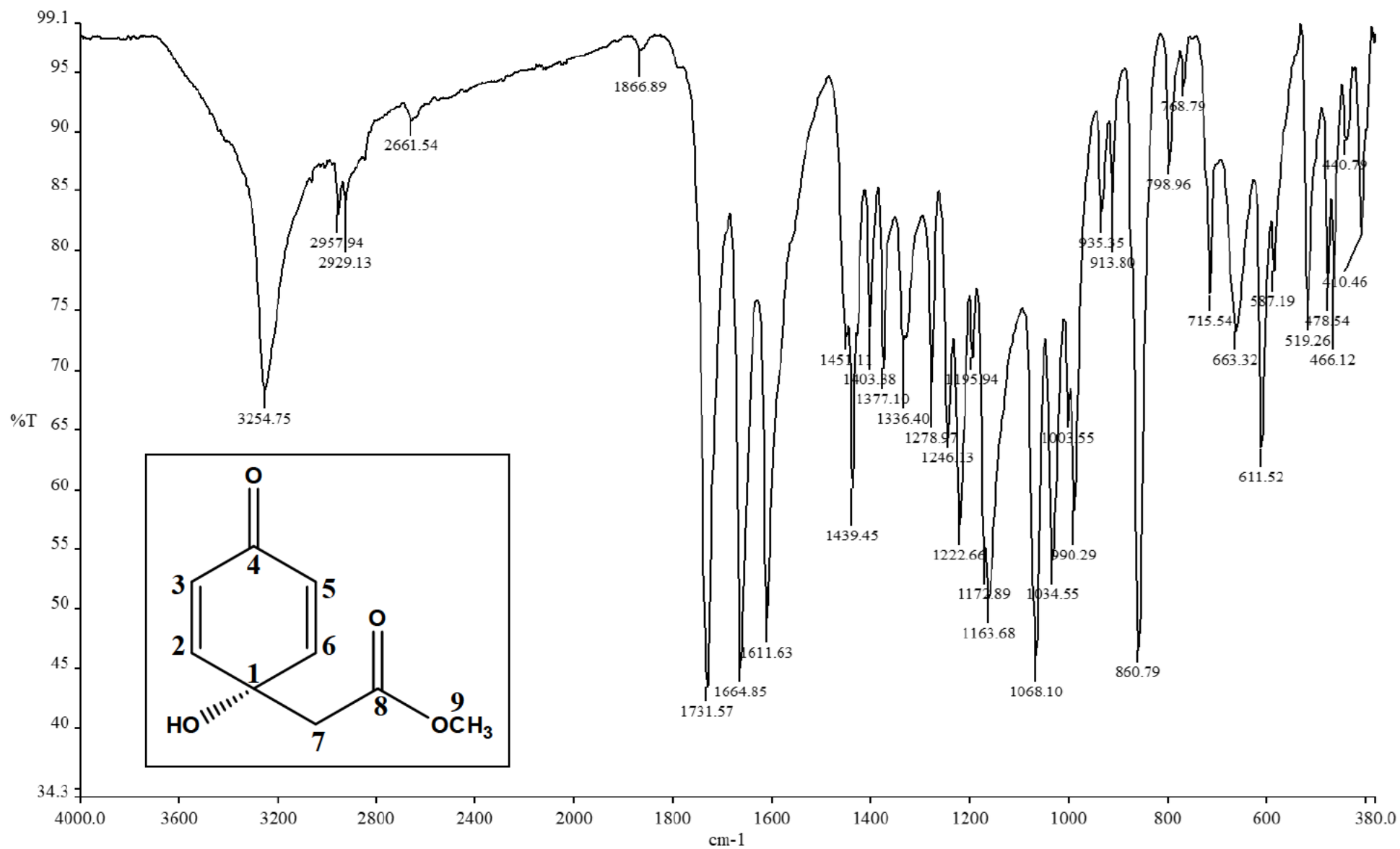
HSQC spectrum of jacaranone



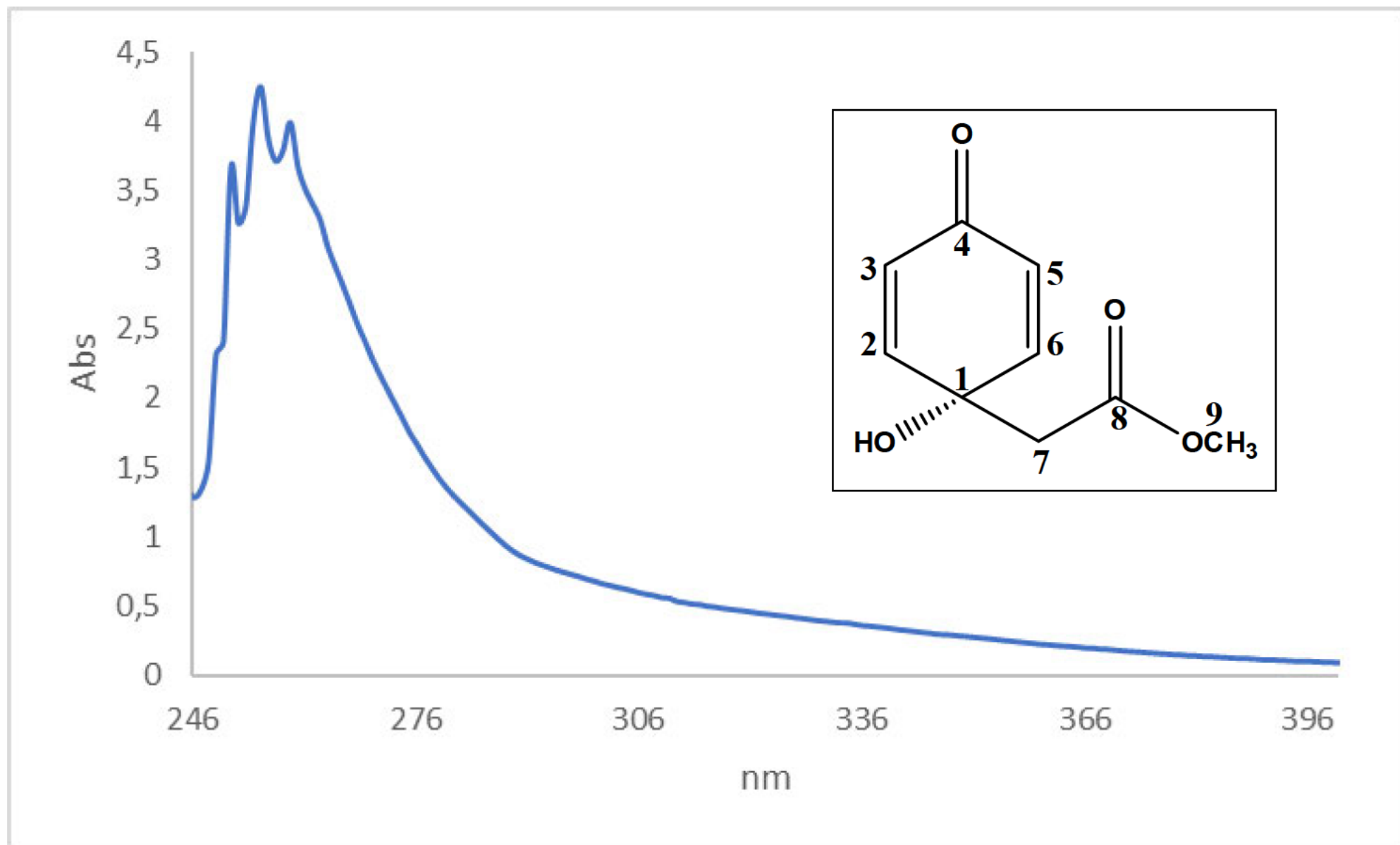
HMBC spectrum of jacaranone



COSY spectrum of jacaranone



IR spectrum of Jacaranone



UV spectrum of jacaranone

Single Mass Analysis

Tolerance = 5.0 PPM / DBE: min = -1.5, max = 50.0

Element prediction: Off

Number of isotope peaks used for i-FIT = 2

Monoisotopic Mass, Even Electron Ions

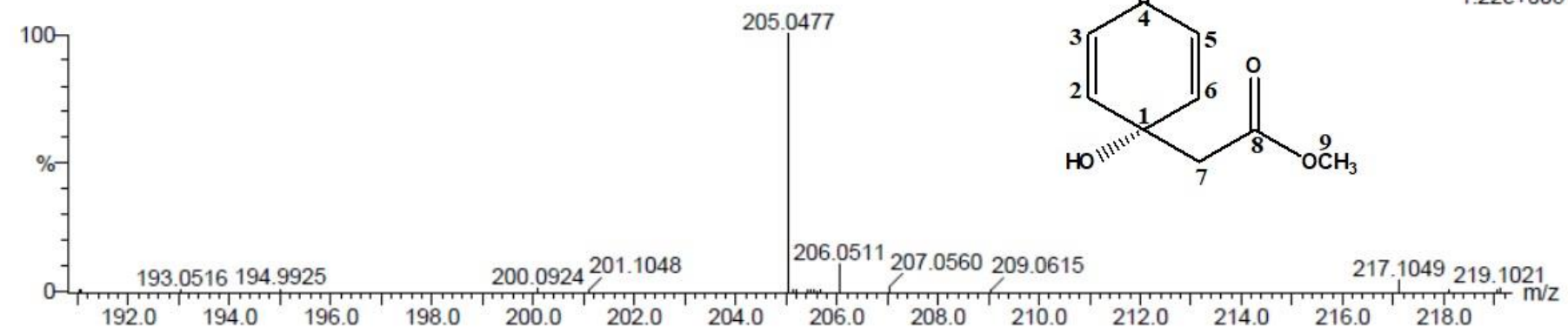
4 formula(e) evaluated with 1 results within limits (up to 20 closest results for each mass)

Elements Used:

C: 5-10 H: 10-15 O: 0-5 Na: 1-1

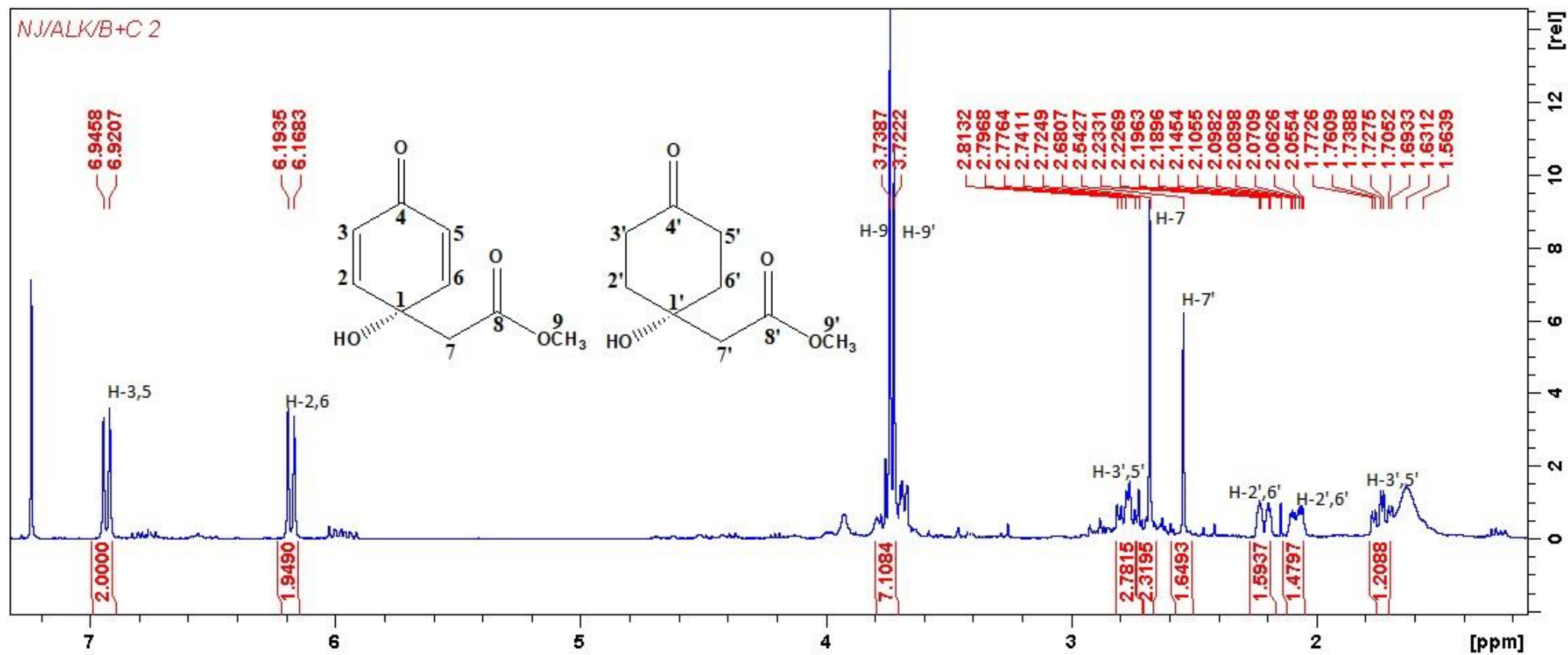
4 14 (0.439) Cm (1:61)

TOF MS ES+

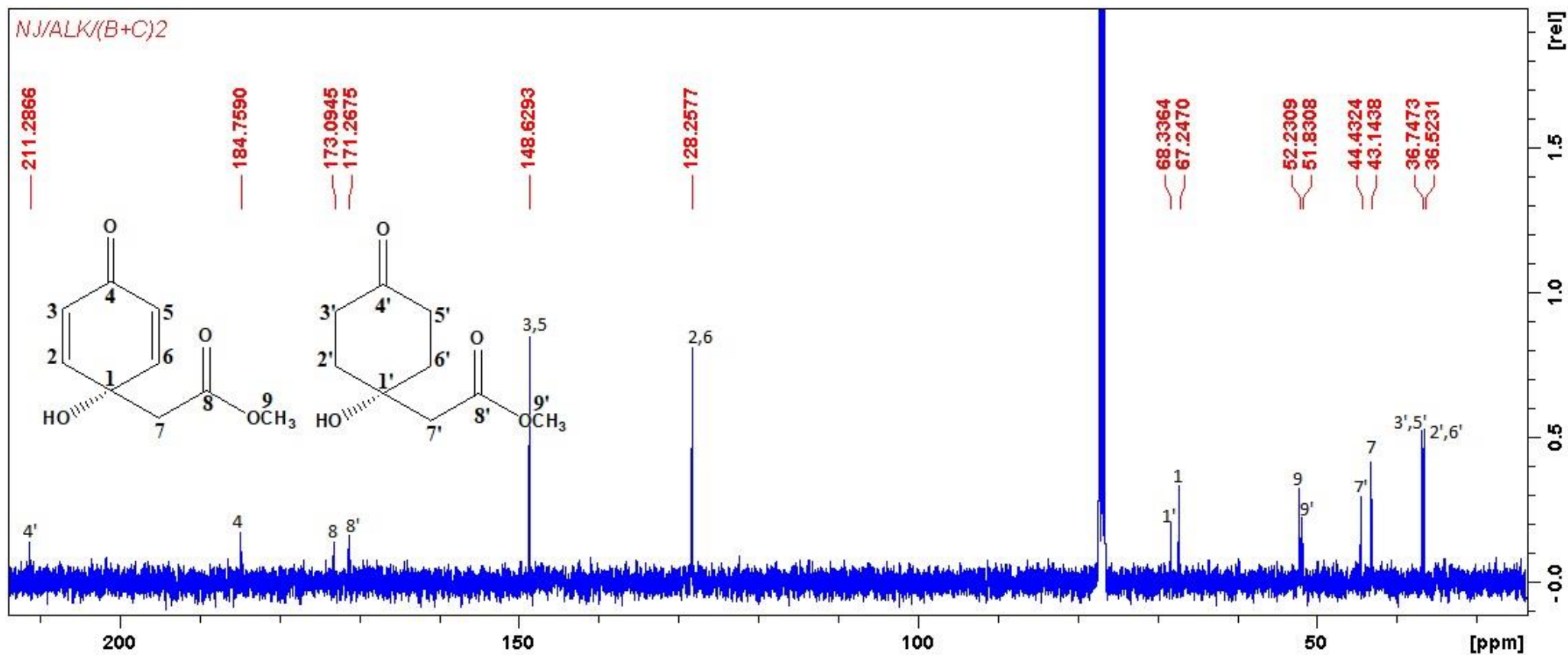


Minimum:				-1.5			
Maximum:		5.0	5.0	50.0			
Mass	Calc. Mass	mDa	PPM	DBE	i-FIT	i-FIT (Norm)	Formula
205.0477	205.0477	0.0	0.0	4.5	94.3	0.0	C9 H10 O4 Na

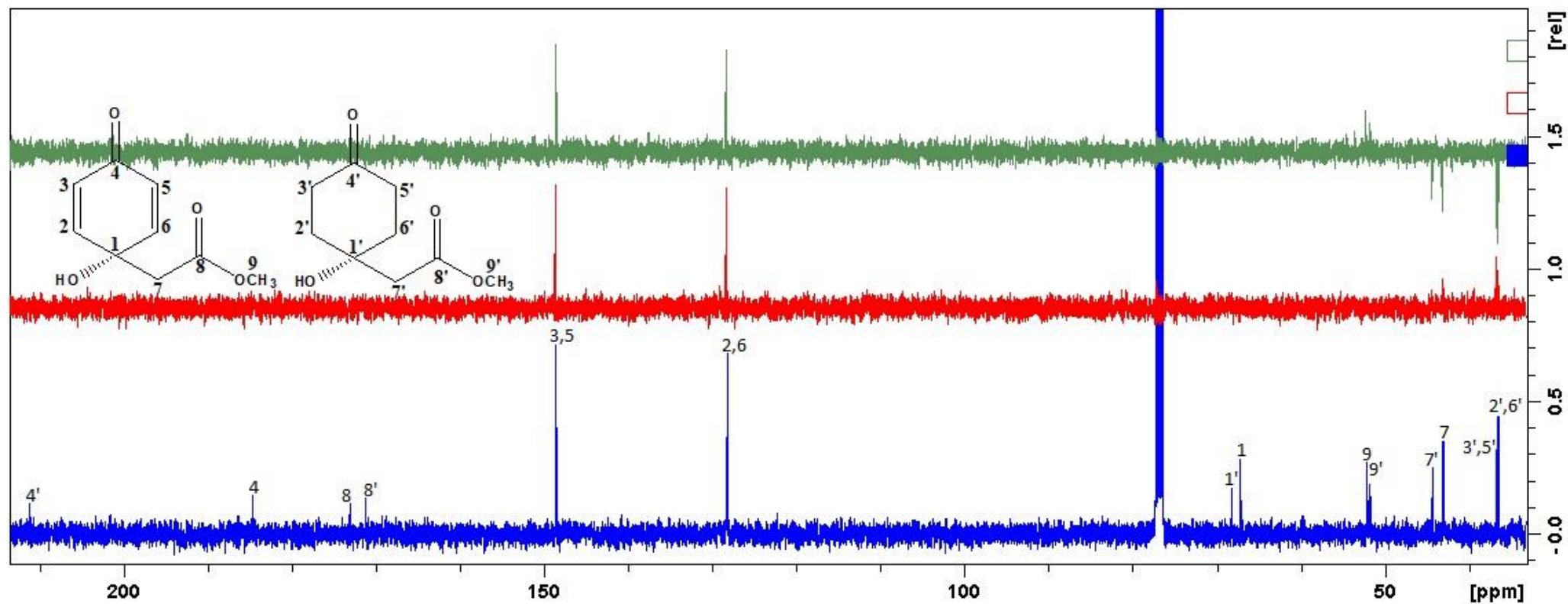
Mass spectrum of jacaranone



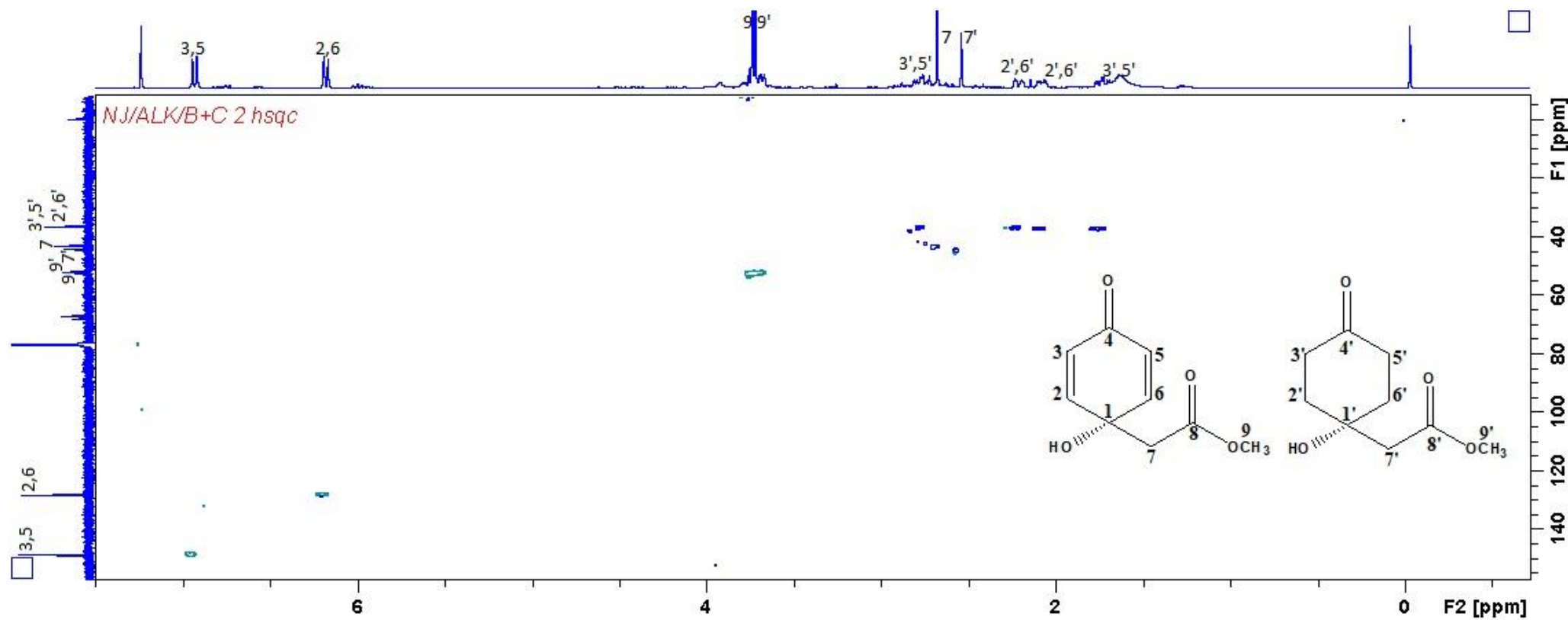
^1H NMR spectrum of mixture of jacaranone methyl ester and methyl-1-hydroxy-4 oxocyclohexylacetate



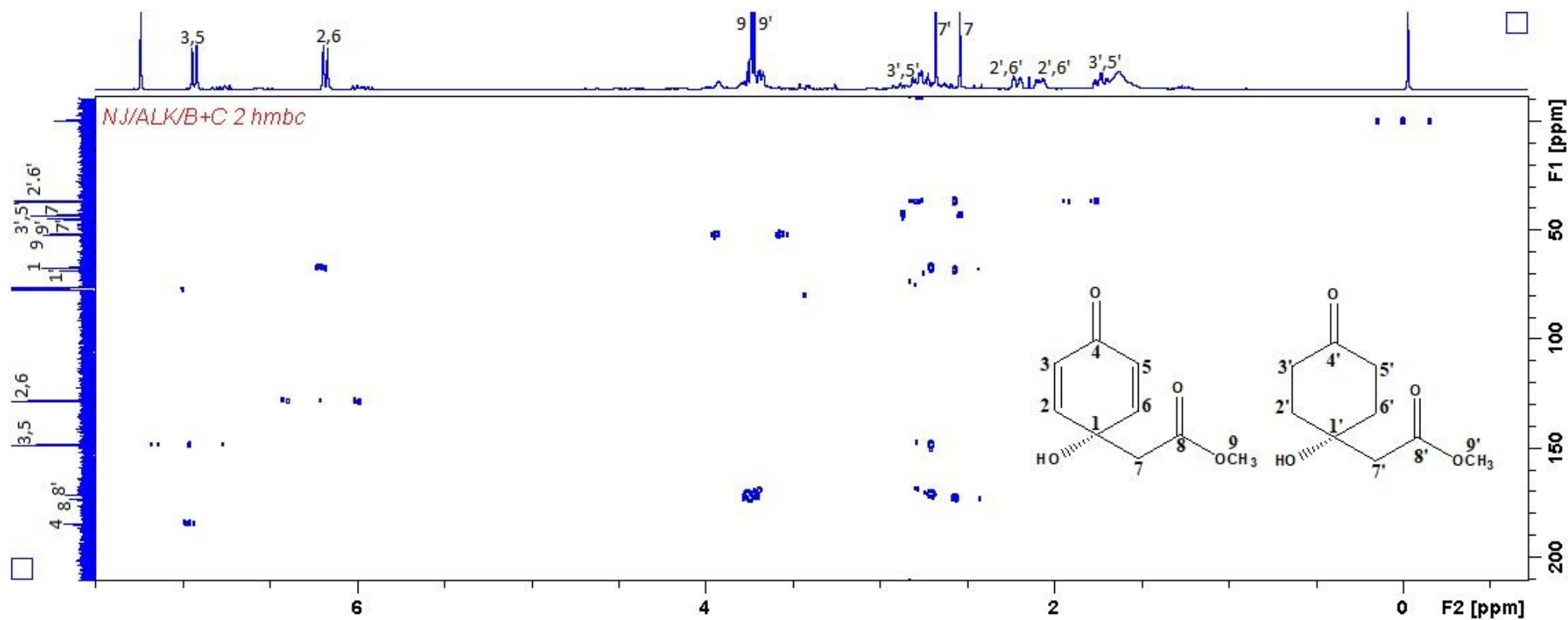
¹³C NMR spectrum of mixture of jacaranone methyl ester and methyl-1-hydroxy-4 oxocyclohexylacetate



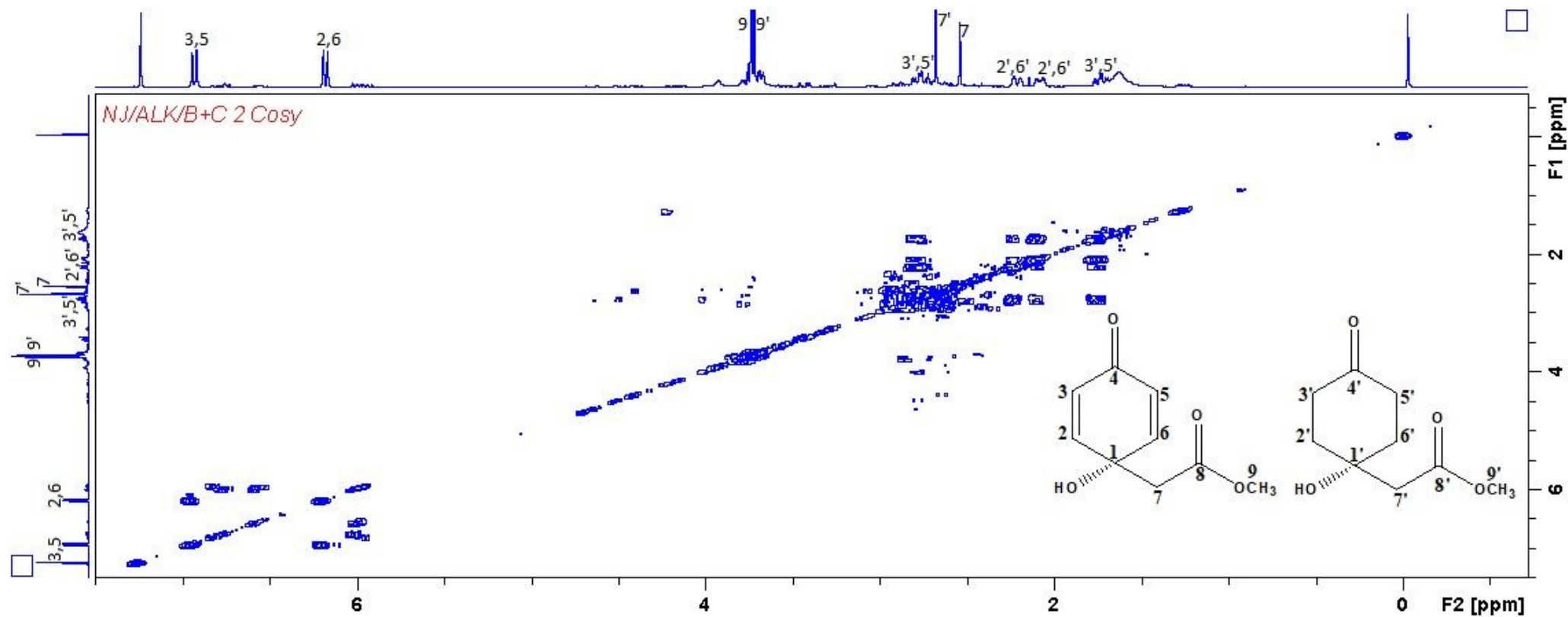
DEPT spectrum of mixture of jacaranone methyl ester and methyl-1-hydroxy-4 oxocyclohexylacetate



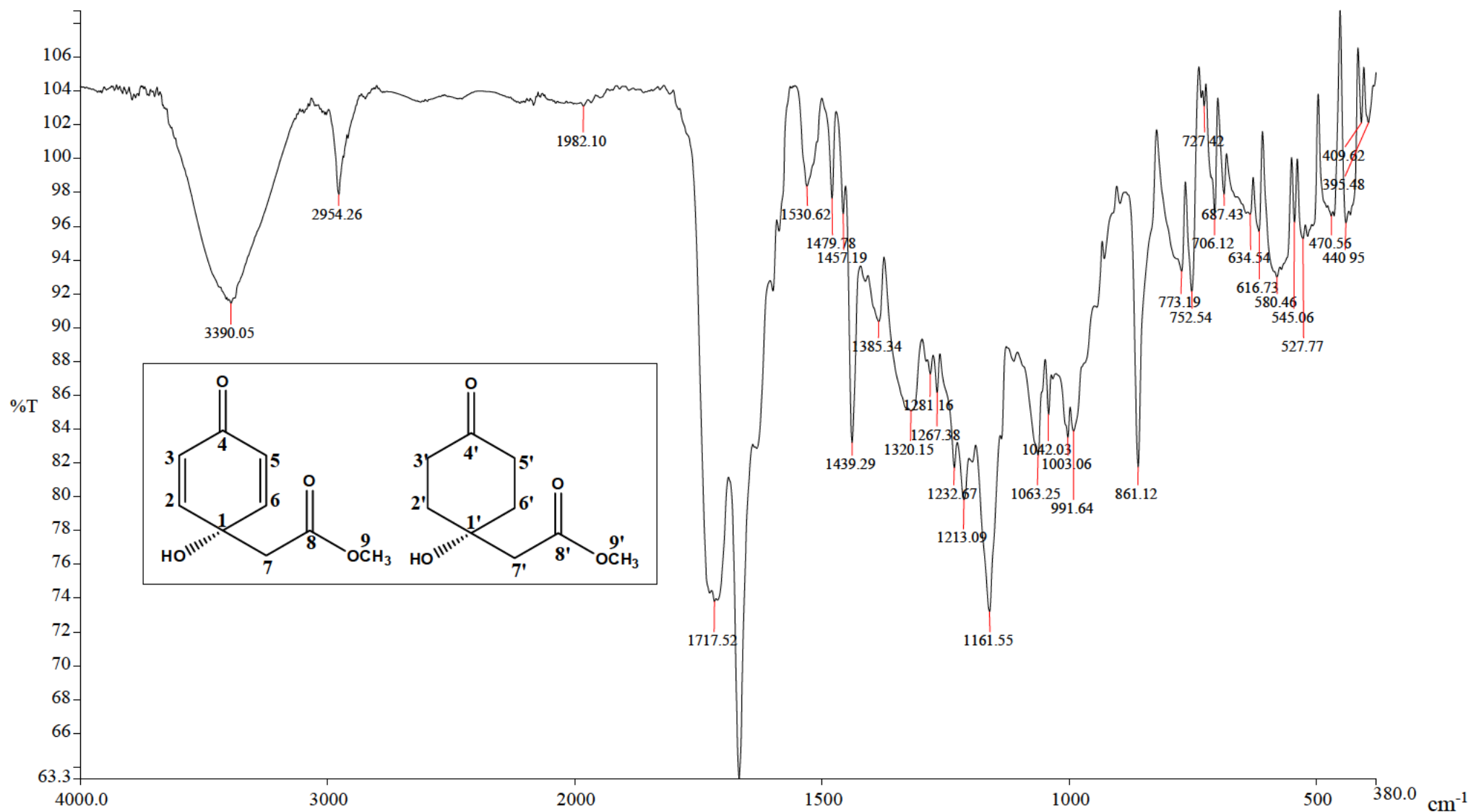
HSQC spectrum of mixture of jacaranone methyl ester and methyl-1-hydroxy-4 oxocyclohexylacetate



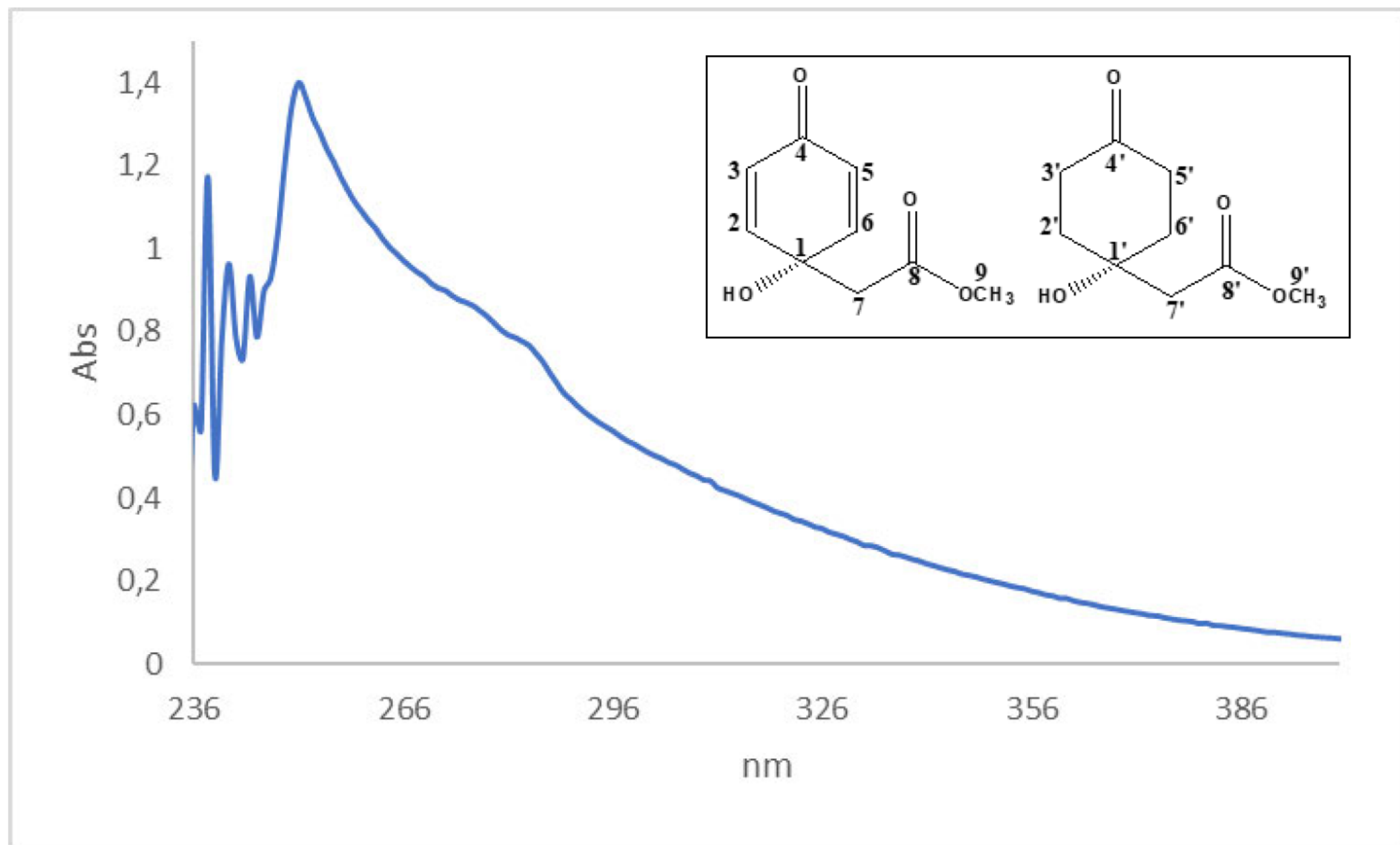
HMBC spectrum of mixture of jacaranone methyl ester and methyl-1-hydroxy-4 oxocyclohexylacetate



COSY spectrum of mixture of jacaranone methyl ester and methyl-1-hydroxy-4 oxocyclohexylacetate



IR spectrum of jacaranone methyl ester and methyl-1-hydroxy-4 oxocyclohexylacetate



UV spectrum of jacaranone methyl ester and methyl-1-hydroxy-4 oxocyclohexylacetate

Single Mass Analysis

Tolerance = 5.0 PPM / DBE: min = -1.5, max = 50.0

Element prediction: Off

Number of isotope peaks used for i-FIT = 2

Monoisotopic Mass, Even Electron Ions

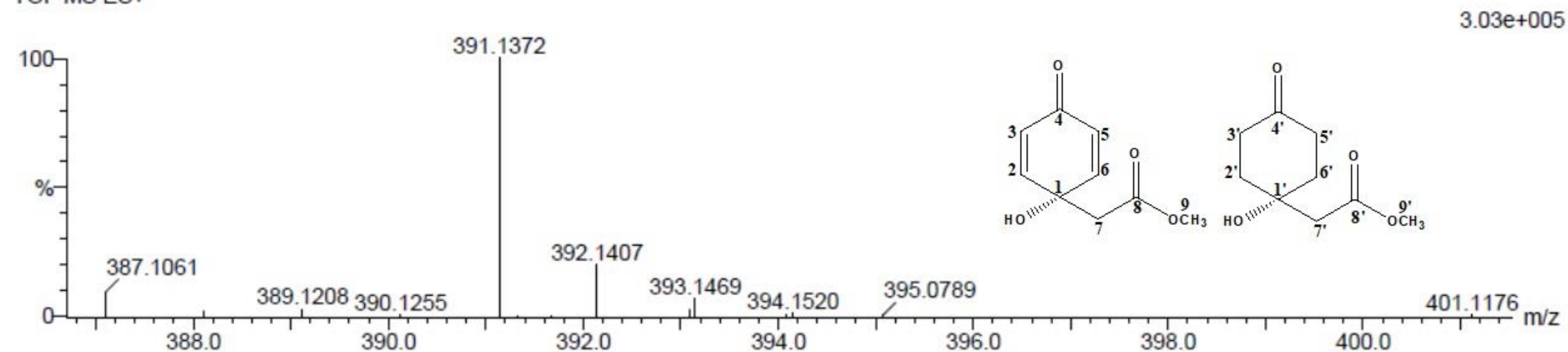
2 formula(e) evaluated with 1 results within limits (up to 20 closest results for each mass)

Elements Used:

C: 15-20 H: 20-25 O: 5-10 Na: 1-1

1 4 (0.101) Cm (1:61)

TOF MS ES+

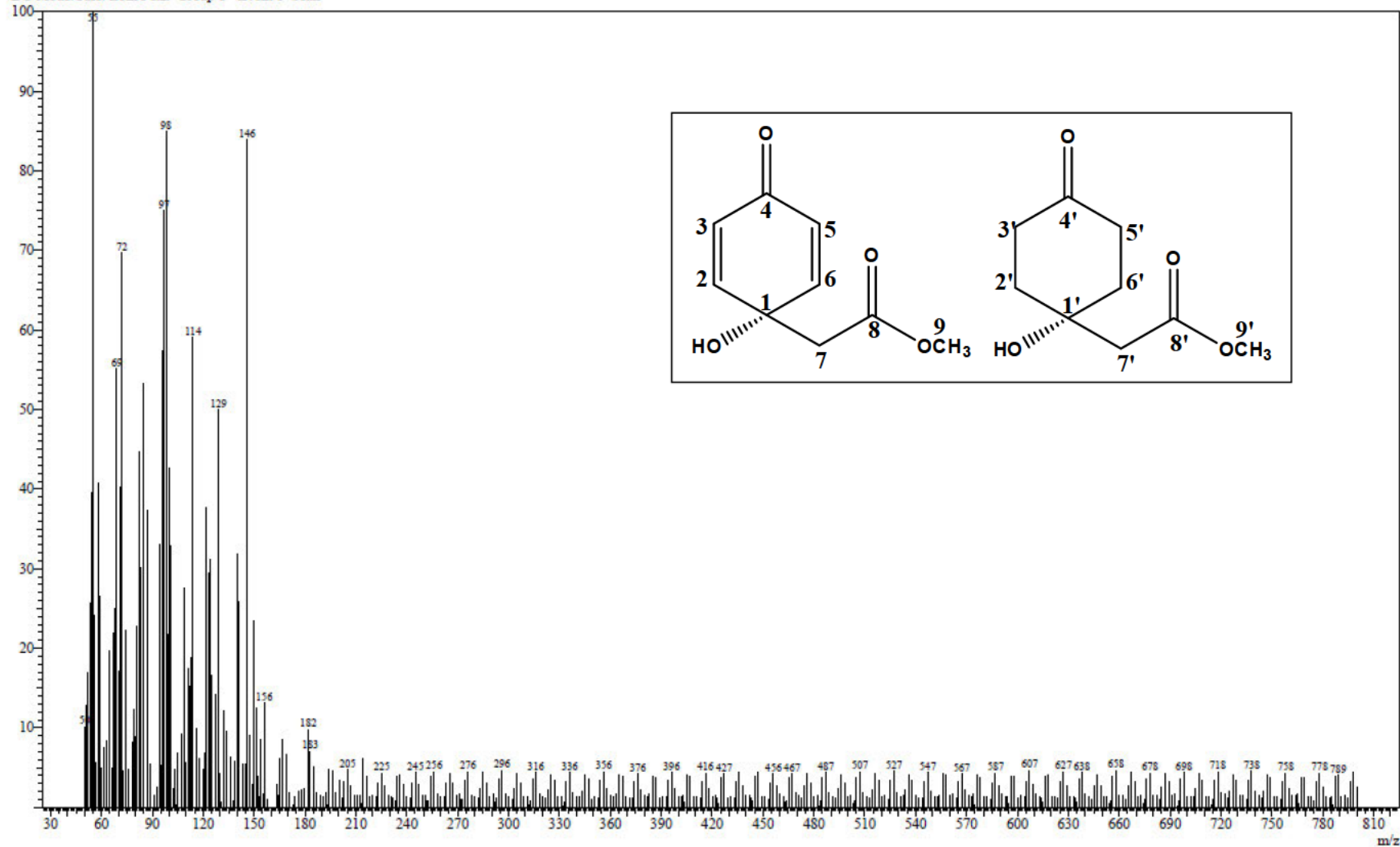


Minimum: -1.5
Maximum: 5.0 5.0 50.0

Mass	Calc. Mass	mDa	PPM	DBE	i-FIT	i-FIT (Norm)	Formula
391.1372	391.1369	0.3	0.8	6.5	40.5	0.0	C ₁₈ H ₂₄ O ₈ Na

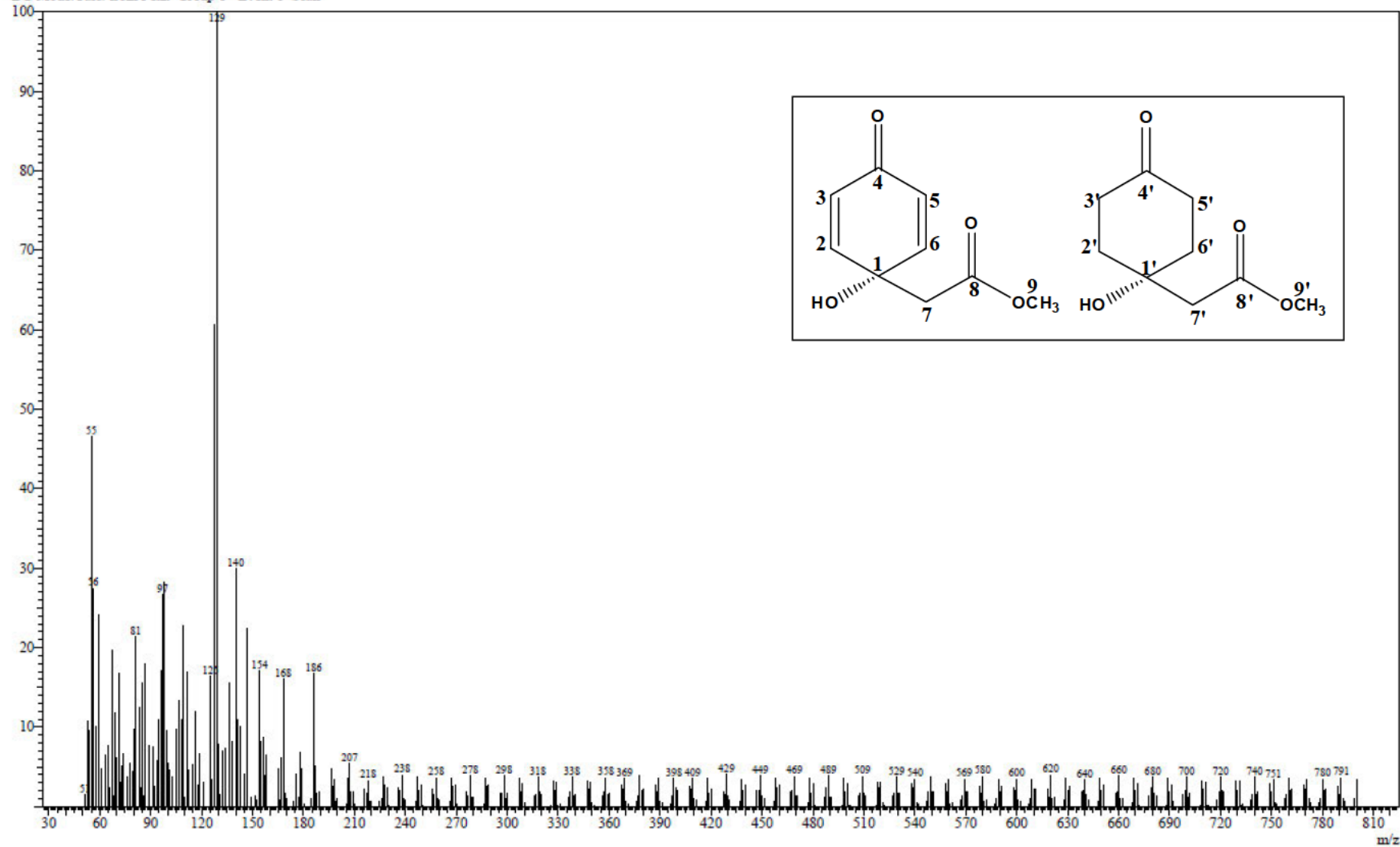
Mass spectrum of jacaranone methyl ester and methyl-1-hydroxy-4 oxocyclohexylacetate

Line#:20 R.Time:15.840(Scan#:2269)
 MassPeaks:463
 RawMode:Averaged 15.835-15.845(2268-2270) BasePeak:55(19846)
 BG Mode:Calc. from Peak Group 1 - Event 1 Scan



Mass spectrum of jacaranone methyl ester and methyl-1-hydroxy-4 oxocyclohexylacetate

Line#:24 R.Time:16.750(Scan#:2451)
MassPeaks:397
RawMode:Averaged 16.745-16.755(2450-2452) BasePeak:129(15345)
BG Mode:Calc. from Peak Group 1 - Event 1 Scan



Mass spectrum of jacaranone methyl ester and methyl-1-hydroxy-4 oxocyclohexylacetate